THE UNIVERSITY
of EDINBURGH

This thesis has been submitted in fulfilment of the requirements for a postgraduate degree (e.g. PhD, MPhil, DClinPsychol) at the University of Edinburgh. Please note the following terms and conditions of use:

This work is protected by copyright and other intellectual property rights, which are retained by the thesis author, unless otherwise stated.
A copy can be downloaded for personal non-commercial research or study, without prior permission or charge.
This thesis cannot be reproduced or quoted extensively from without first obtaining permission in writing from the author.
The content must not be changed in any way or sold commercially in any format or medium without the formal permission of the author.
When referring to this work, full bibliographic details including the author, title, awarding institution and date of the thesis must be given.

Investigating glucocorticoids as mediators of increased bone marrow adiposity and bone loss

Andrea Lovdel

Doctor of Philosophy

The University of Edinburgh

2020

Declaration

I declare that this thesis has been composed solely by myself and that it has not been submitted, in whole or in part, in any previous application for a degree. Except where stated otherwise by reference or acknowledgment, the work presented is entirely my own.

_____

Andrea Lovdel

Edinburgh, January 2020

Acknowledgements

I would like to thank my supervisors, Dr. Will Cawthorn and Prof. Karen Chapman, for their extraordinary support throughout my PhD. I am exceedingly grateful to Will for guiding me through all the experiments and writing, as well as encouraging me through the many hours of ongoing experimental optimisations, animal work and dissections throughout the last three years. Also, most importantly, for introducing me to the wonderful field of bone marrow fat, where I have met many other amazing, brilliant and kind scientists. I am also extremely grateful to Karen for her continual inspiration and support from the very beginning and for offering her expertise on all glucocorticoid-related aspects of the project. I could not have completed this PhD without the support of both of my supervisors.

I am also especially thankful to Dr. Karla Suchacki, my one and only postdoc, who has helped me so much throughout my PhD with regards to everything I could have ever asked about. I will especially miss sharing rooms on conferences abroad and our silly conversations. As well as our 'promenade' of far too many kilometres around Barcelona to find the perfect paella and sangria restaurant, where we also had the same dinner for three nights in a row; or not wanting to miss our conference bus so accidentally turned up half an hour too early. Not to forget other past and current members of the lab including Richard Sulston, Ben Thomas, Iris Cervera, Rachel Bell and many more for all their help with animal and experimental work. Especially Iris and Rachel who have contributed to the ageing part of my thesis, thank you.

I would also like to thank my thesis committee members, Prof. Margarete Heck and Dr. Cecile Benezech, for their support and advice. A very special thank you to other members of the department that have helped me complete this research, especially Jon Henderson for his continuous support with the animals and our enjoyable chats in the animal house; to Dr. Natalie Homer and Scott Denham for all their support with regards to mass spectrometry; to Prof. Nik Morton for allowing me to use the TD-NMR, and also to Dr. Rob Wallace for trusting me to use the very expensive μCT for the many hours required.

To all the wonderful and brilliant people that I met and became friends with, thank you for your moral support and for being a huge part of why I loved my time in Edinburgh so much.

Finally, I would like to express my gratitude to my family back in Sweden as well as my Scottish family for always believing in me and cheering me on. Also, to my very supportive partner, Calum Middleton, for always trying to keep me calm, although when that did not work, he always knew what to do next, and that was to bring out the G&T! I would also like to thank Murphy, Finn and Freddie – the dogs of my dreams, for never having a dull day while writing my thesis up North and for keeping me in shape by running away from me chasing pheasants, and me following in hot pursuit to make sure I did not lose a dog, or three.

Table of Contents

Abstract

In addition to white and brown adipose tissue (WAT and BAT, respectively), there is a third major adipose depot, called bone marrow adipose tissue (BMAT), the formation and function of which is poorly understood. In healthy adults, BMAT accounts for up to 70% of bone marrow (BM) volume and further increases during various conditions, such as ageing, osteoporosis, obesity, oestrogen deficiency, glucocorticoid (GC) therapy and, most surprisingly, during caloric restriction (CR) in animals and anorexia nervosa (AN) in humans. Furthermore, such BMAT expansion often coincides with bone loss. However, the mechanisms regulating BMAT expansion in these adverse conditions remain incompletely understood.

One possibility is that GCs contribute to BMAT expansion and bone loss during CR and ageing. Long-term GC treatment can induce bone loss and BMAT expansion. One recent study found that CR is associated with elevated circulating GCs in mice, but not in rabbits; the mice also have increased BMAT, whereas the rabbits do not. Furthermore, GCs have been reported to increase during starvation or AN in humans, followed by BMAT expansion. Tissue regeneration of GCs is regulated by 11β-hydroxysteroid dehydrogenase (11β-HSD1), which generates active cortisol in humans and corticosterone in rodents, from inactive cortisone and 11-dehydrocorticosterone (11-DHC), respectively. Notably, 11β-HSD1 KO mice resist the Cushingoid effects of GC excess. Thus, the hypothesis for this thesis is that GC excess contributes to BMAT expansion and bone loss during CR and ageing, and that 11β-HSD1 KO mice would therefore resist these effects. Herein, I addressed this hypothesis by characterising the BMAT and bone phenotypes of control and 11β-HSD1 KO mice in response to CR and ageing.

To investigate the effects on BMAT and bone remodelling during CR, male and female C57BL/6J mice lacking 11β-HSD1 (KO) or littermate controls (WT) were fed *ad libitum* (AL) or 70% of AL intake (CR) from 9-15 weeks of age. Whereas, to investigate the effects of ageing on BMAT and bone remodelling, KO and WT mice of both sexes were characterised at 15, 42 and 70 weeks of age.

Following CR, all mice had decreased body mass and increased plasma and BM corticosterone concentrations. Cortical bone loss was present with CR in all mice, and CR significantly increased BMAT in WT males and females, and in KO females. However, KO males resisted CR-induced BMAT expansion. Unexpectedly, the KO males also had significantly increased circulatory and BM progesterone, suggesting that this hormone might be a potential candidate. The aged mice exhibited increased circulating corticosterone and BMAT, and decreased bone mass, compared to young mice. However, unlike during CR, KO males did not resist age-related BMAT expansion, suggesting that the mechanisms for this differ to those responsible for BMAT expansion during CR. Correlation data between BMAT, bone parameters and GCs suggest these factors may be linked, but do not inform cause and effect. Although 11β-HSD1 may play a role in BMAT expansion, the physiological significance remains unknown.

These findings suggest that local corticosterone regeneration might mediate BMAT expansion during CR in males only. However, another possibility is that progesterone might influence the blockade of BMAT, since progesterone is the precursor to oestradiol, and oestradiol blocks BMAT formation. Given the sexual dimorphism, in females other mechanisms likely influence BMAT expansion during CR. Bone loss was observed in all mice, suggesting a limited role for 11β-HSD1 in bone formation. Results in the aged mice suggest that 11β-HSD1 does not influence BMAT expansion in this context. However, ageing-associated corticosterone and BMAT expansion did demonstrate a correlation with bone loss, while corticosterone was positively associated with BMAT volume in aged females.

To conclude, 11β-HSD1 activity is required for CR-induced BMAT expansion in males, and GC excess might contribute to ageing-associated BMAT expansion in females. Considering the broad physiological and pathological implications of BMAT, it will be important for future studies to further dissect the relationship between GC excess, BMAT expansion and bone loss.

Lay summary

Fat is a complex tissue whose main role is to store energy. The ability of our bodies to store fat is important, because it acts as an energy reserve in times of food scarcity. However, in modern times, the ready availability of energy-rich food has driven the increased prevalence of obesity. This disease is defined by the excessive accumulation of fat. Because of the health burden of obesity, there has been much interest in better understanding the functions of fat in normal health and disease.

Mammalian fat is classed as two distinct subtypes, white and brown fat. It is the white fat that is specialised for fat storage and that accumulates excessively in obesity; in contrast, brown fat is specialised for generating heat. There is also a third fat subtype, called bone marrow fat (BMAT), which is present within the bone marrow. BMAT also expands during various clinical conditions such as ageing, bone loss, obesity, cancer treatment, oestrogen deficiency, and following treatment with glucocorticoids (GCs). GCs are a class of hormones that control stress responses. Most surprisingly, BMAT accumulates during caloric restriction (CR) in animals and anorexia nervosa (AN) in humans. CR has many health benefits, such as increased lifespan and decreased risk of diseases, but it can also promote bone loss. Thus, one possibility is that BMAT contributes to these beneficial and detrimental effects of CR. Similarly, BMAT expansion has been suggested to promote bone loss with ageing and in osteoporosis. Therefore, BMAT could be used as a potential drug target to prevent age-induced bone loss. However, there is a lack of knowledge in this field, and the factors responsible for the expansion of BMAT remain incompletely understood.

One factor that might cause BMAT expansion and bone loss during CR and ageing is GCs. Patients on long-term GC treatment often have bone loss and BMAT expansion. A recent study revealed that CR-fed mice have increased BMAT as well as GCs; while CR-fed rabbits had neither of these. Furthermore, GCs and BMAT both increase during starvation or AN in humans, as well as during ageing; each of these conditions is also often accompanied by bone loss. These findings suggest that increases in GCs are required for BMAT accumulation during CR and might also contribute to BMAT expansion and bone loss as we age.

GCs are released by the same glands that produce adrenaline; however, GCs can also be regenerated inside tissues by an enzyme called 11β-hydroxysteroid dehydrogenase 1 (11β-HSD1). This enzyme amplifies GC action by converting inactive GCs into their active forms. The effects of this enzyme have been studied by analysing mice that lack this enzyme, known as 11β-HSD1 knock out (KO) mice, and comparing these to normal, 'wild-type' (WT) mice, that retain this enzyme's function. Such studies have shown, importantly, that KO mice resist the effects of excess amounts of GCs. Therefore, the hypothesis for my thesis is that GC excess controls BMAT expansion and bone loss during CR and ageing, and that 11β-HSD1 KO mice will resist these effects.

To investigate the effects of CR on BMAT and bone, WT and KO male and female mice were fed either a control diet or 70% of control intake (CR) from 9-15 weeks of age. The mice on CR had decreased body mass but increased circulatory and BM GC concentrations. CR also caused bone loss and increased BMAT in female WT and KO mice, and in WT males; however, KO males did not have BMAT expansion. The KO males also had significantly increased levels of progesterone in their BM and blood. Progesterone is a hormone that influences fertility in females, while in men it regulates sperm formation. This finding suggests that progesterone might be involved in BMAT formation, but this new possibility remains to be further investigated.

To determine the effects of ageing on BMAT and bone, KO and WT mice of both sexes were examined at 15, 42 and 70 weeks of age. Older mice had increased BMAT and greater GC levels in their blood, along with decreased bone compared to young mice. GC levels were positively associated with BMAT volume in aged females, while BMAT was associated with bone loss in both males and females. Therefore, it remains possible that BMAT accumulation contributes to ageing-associated bone loss. To conclude, 11β-HSD1 activity is necessary for CR-induced BMAT expansion in males only, whereas GC excess might contribute to BMAT expansion in aged females. Considering the role of BMAT in health and disease, it will be important for future studies to further understand the relationship between GC excess, BMAT expansion and bone loss during various adverse conditions.

Abbreviations

11-DHC	11-dehydrocorticosterone
11β-HSD1/2	11β-hydroxysteroid dehydrogenase type 1/2
ACTH	Adrenocorticotropic hormone
AN	Anorexia nervosa
Apoe	Apolipoprotein E
AR	Androgen receptor
AT	Adipose tissue
AVP	Arginine vasopressin
BAT	Brown adipose tissue
BM	Bone marrow
BMAds	Bone marrow adipocytes
BMAT	Bone marrow adipose tissue
BMD	Bone mineral density
BMI	Body mass index
cAMP	Cyclic adenosine monophosphate
cBMAT	Contitutive bone marrow adipose tissue
CR	Caloric restriction
CRF	Corticotroping-releasing factor
CS	Cushing's syndrome
Ethylenediaminetetraacetic acid	EDTA
FA	Fatty acid
FABP4	Fatty-acid-binding protein 4
FFA	Free fatty acid
FKBP5	Fk506 binding protein 5
GC	Glucocorticoid
GIO	Glucocorticoid-induced osteoporosis
GPCR	G protein-coupled receptor
GR	Glucocorticoid receptor
GRE	Glucocorticoid response element
HFD	High fat diet
HPA	Hypothalamic–pituitary–adrenal axis
HSL	Hormone sensitive lipase
HSP	Heat shock protein
IGF-1	Insulin-like growth factor 1
IL	Inerleukin
iWAT	Inguinal white adipose tissue
MR	Mineralocorticoid receptor
MSCs	Mesenchymal ste cells
mWAT	Mesenteric white adipose tissue
ND	Non-detectable
NR3C1/2	Nuclear receptor subfamily 3 group c member 1/2

Osx	Osterix
Pparγ	Peroxisome proliferator-activated receptor γ
PR	Progesterone receptor
Pref-1	Preadipocyte factor-1
rBMAT	Regulated bone marrow adipose tissue
SNPs	Single nucleotide polymorphisms
StAR	Steroidogenic acute regulatory protein
SVF	Stromal vascular fraction
T1D	Type 1 diabetes
T2D	Type 2 diabetes
TNF-α	Tumour necrosis factor α
UCP-1	Uncoupling protein-1
WAT	White adipose tissue

Chapter 1. Introduction

1.1. Adipose tissue

Adipose tissue (AT) is a complex tissue with profound effects on physiology and pathophysiology. Mammalian AT is generally classed into three distinct subtypes, white AT (WAT), brown AT (BAT) and beige/brite AT (Petrovic *et al.*, 2010; Berry *et al.*, 2013). AT is primarily composed of adipocytes, cells that are specialised for storing energy as fat. Besides adipocytes, AT also contains the stromal vascular fraction (SVF) consisting of cells such as pre-adipocytes, fibroblasts, vascular endothelial cells and also numerous immune cells (Ahima and Flier, 2000; Coelho, Oliveira and Fernandes, 2013). AT also serves mechanical and protective functions, for example in the heel fat pad and around the kidneys, and provides insulation from heat and cold (Rosen and Spiegelman, 2014).

The most abundant human fat, WAT, plays a vital role in energy homeostasis: in times of a positive energy balance (i.e. energy intake > energy expenditure) WAT stores the excess energy as triacylglycerol, whereas in times of negative energy balance (e.g. fasting, starvation) WAT releases fatty acids (FAs) and glycerol to be used for beta-oxidation or gluconeogenesis, respectively. WAT is now also established as a major endocrine organ (Rosen and Spiegelman, 2014). This concept originated with the discovery of adipose-derived circulating factors, called “adipokines”, which include hormones and cytokines such as leptin (Zhang *et al.*, 1994), TNF-α and IL-6 (Cianflone, Xia and Chen, 2003), adiponectin (Scherer *et al.*, 1995; Hu, Liang and Spiegelman, 1996; Maeda *et al.*, 1996; Nakano *et al.*, 1996) and adipsin (Cianflone, Xia and Chen, 2003). Through release of these adipokines, WAT can exert diverse systemic effects, not only on energy homeostasis but also on other aspects of physiology such as blood pressure, immune function, and fertility (Michalakis *et al.*, 2013). Thus, WAT performs many essential physiological functions beyond energy storage and release.

Much of the interest in WAT has been motivated by the increasing prevalence of obesity and associated metabolic diseases, such as type 2 diabetes (T2D), and dysregulated WAT function contributes to the pathogenesis of these diseases. WAT

is found viscerally as well as subcutaneously. Visceral WAT build-up is associated with increased cardio-metabolic risk (Grauer *et al.*, 1984), while subcutaneous WAT build-up has fewer deleterious effects on health (Snijder, Dekker, Visser, Bouter, *et al.*, 2003; Snijder, Dekker, Visser, Yudkin, *et al.*, 2003). Therefore, understanding the mechanisms that influence the development of different AT depots may identify new strategies to treat metabolic diseases.

In contrast to white adipocytes, which store energy, brown adipocytes burn it (Cannon and Nederfaard, 2004). This process is called non-shivering thermogenesis, i.e. the production of heat. This is possible with the help of a BAT-specific protein located within the mitochondria, uncoupling protein-1 (UCP-1) (Aquila, Link and Klingenberg, 1985). Adults have increased BAT activity if exposed to chronic cold, as shown in Scandinavian outdoor workers (Huttunen, Hirvonen and Kinnula, 1981). Furthermore, since BAT burns energy, it has been considered a potential target to treat obesity and associated metabolic dysregulation (Dong *et al.*, 2018; Moonen, Nascimento and van Marken Lichtenbelt, 2019). Prolonged cold exposure in rodents can also alter white adipocytes by causing them to develop a brown-fat-like morphology. These cells have been named “beige” adipocytes and have overlapping but distinct gene expression patterns compared to BAT, as well as having distinct developmental origins to brown adipocytes (Wu *et al.*, 2012; Shan *et al.*, 2013). Brown adipocytes have higher expression of UCP-1 and a greater capacity for uncoupled respiration than beige fat (Wu *et al.*, 2012). In addition, beige AT can also increase energy expenditure, and therefore there has been a large interest in targeting adipocyte ‘beiging’ as another potential strategy to treat obesity (Wu *et al.*, 2012; Shabalina *et al.*, 2013; Phillips, 2019). However, the development of these adipocytes and their mechanism of thermogenic stimulation needs to be better understood.

In addition to WAT, BAT and beige AT, there is also a fourth major depot, called bone marrow adipose tissue (BMAT). BMAT is altered in various physiological and pathological conditions, but, compared to WAT, BAT and beige AT, the formation and function of BMAT is poorly understood. Unlike the other adipose depots, BMAT research has been relatively limited. Therefore, an overarching goal of my PhD research has been to elucidate the mechanisms that regulate BMAT formation, and the implications of this for skeletal function.

1.2. BMAT

Whilst WAT and BAT have received much research focus, BMAT has been largely ignored. Nonetheless, since mid 2000, the interest in BMAT research has expanded (Bravenboer *et al.*, 2019). BMAT accounts for up to 70% of bone marrow (BM) volume and about 10% of total fat mass in healthy lean humans (Fazeli *et al.*, 2013; Cawthorn *et al.*, 2014). Furthermore, BMAT expands during various conditions including in ageing (Griffith *et al.*, 2005, 2006; Yeung *et al.*, 2005; Di Iorgi *et al.*, 2008, 2010; Shen *et al.*, 2012; Schwartz *et al.*, 2013), in mice fed a high-fat diet (HFD) (Doucette *et al.*, 2015; Tencerova *et al.*, 2018), obesity in humans (Bredella *et al.*, 2011; Ambrosi and Schulz, 2017; Ambrosi *et al.*, 2017), osteoporosis (Yeung et al., 2005; Rosen and Bouxsein, 2006; Zhao et al., 2008; Fazeli et al., 2013), in animal models of type 1 diabetes (T1D) (Botolin *et al.*, 2005; Botolin and McCabe, 2007; Slade *et al.*, 2012), oestrogen deficiency (Syed et al., 2008; Veldhuis-Vlug et al., 2015), chronic kidney disease (Woods *et al.*, 2018) and with glucocorticoid (GC) treatment (Vande Berg et al., 1999; J. Li et al., 2013). Perhaps most surprisingly, BMAT also expands during caloric restriction (CR) in animals (Devlin *et al.*, 2010; Cawthorn *et al.*, 2014) and anorexia nervosa (AN) in humans (Bredella *et al.*, 2009, 2014; Ecklund *et al.*, 2010), conditions in which WAT is depleted. The function of BMAT is still to be completely understood, although it is now clear that BM adipocytes (BMAds) are not just space fillers. Naveiras *et al.,* showed that BMAds are negative regulators of the BM microenvironment, suppressing haematopoiesis. Whereas, the lack of BMAds accelerates haematopoietic recovery post-BM transplantation (Naveiras *et al.*, 2009). In addition, just like WAT, BMAT has been identified as a source of adiponectin, highlighting its potential as an endocrine organ with systemic effects (Cawthorn *et al.*, 2014). Furthermore, BMAT expansion is associated with bone loss, increasing the risk of developing osteoporosis (Devlin and Rosen, 2015; Veldhuis-Vlug and Rosen, 2018). These examples underscore the need to better understand BMAT formation and function, issues that are discussed further in the following sections. In addition to the association between bone and BMAT, bone remodelling is also highly regulated by hormones, including leptin (Karsenty, 2006), osteocalcin (Lee *et al.*, 2007; Oury *et al.*, 2011) and sex hormones (Khosla *et al.*, 2001; Nakamura *et al.*, 2007) (Figure 1.1). Leptin, an adipose-derived hormone acts on osteoblasts to regulate bone remodelling (Karsenty, 2006). Besides bone regulation, osteocalcin, an osteoblast specific protein also regulates metabolic functions (Figure 1.2). Uncarboxylated

(active) osteocalcin acts as a hormone to promote β-cell proliferation, insulin secretion and sensitivity as well as energy expenditure (Lee *et al.*, 2007). Carboxylated (inactive) osteocalcin directly binds calcium and resides in the bone. This inactivation is regulated by a different gene expressed in osteoblasts; *Esp* (Ferron, Wei, Yoshizawa, Del Fattore, *et al.*, 2010; Fulzele *et al.*, 2010). In addition to osteocalcin metabolic and bone functions, it was revealed that it also regulates male fertility (Oury *et al.*, 2011). Undercarboxylated osteocalcin directly acts on Leydig cells to produce and secrete testosterone, a steroid hormone required for testicular function and fertility (Figure 2). In contrast, osteocalcin does not affect female fertility. Testosterone itself can also regulate bone remodelling by directly promoting osteoblast differentiation. Similarly, oestrogen also aids bone formation (further reviewed (Mohamad, Soelaiman and Chin, 2016)). This highlights osteocalcin as an endocrine factor from bone. Research regarding osteocalcin effect on BM adiposity or vice versa is yet to confirmed.

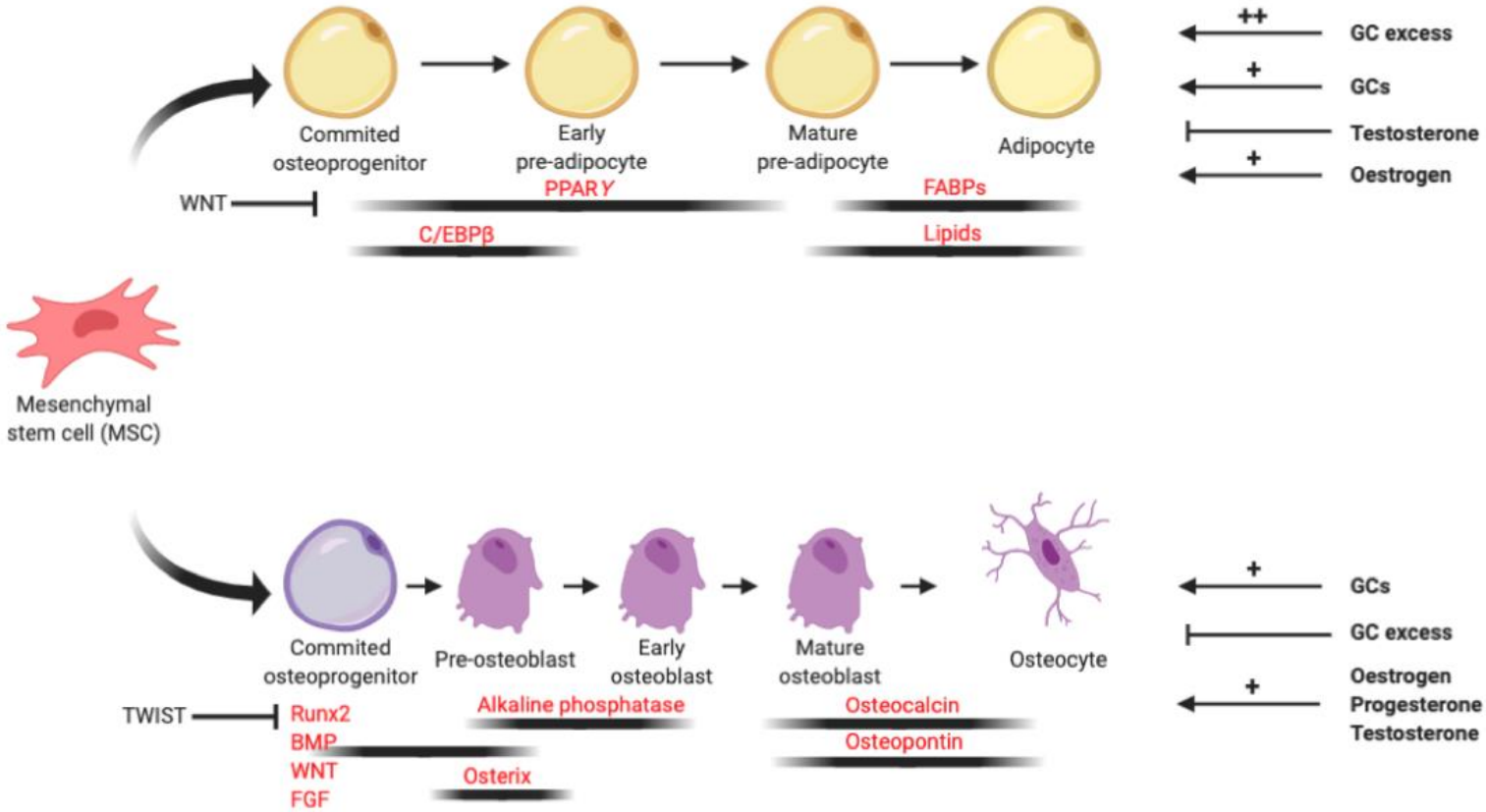

Figure 1.1. The differentiation mechanisms of adipogenesis and osteoblastogenesis. Mesenchymal stem cells (MSCs) can differentiate towards adipocytes and osteoblast. The master regulators of adipogenesis and osteoblastogenesis differ as seen in the figure. GCs can directly affect both pathways. GCs can promote adipogenesis and osteoblastogenesis. Although, excessive GCs leads to increased differentiation towards adipocytes rather than osteoblasts. Furthermore, sex hormones, such as progesterone, oestrogen and testosterone can promote bone formation. However, oestrogen can also promote adipogenesis, whereas, testosterone inhibits it. WNT signalling pathway also inhibits adipogenesis, whereas TWIST, a transcription factor, inhibits osteoblastogenesis. The "+" indicates promotion. The "++" indicates excessive promotion of the effect of a certain hormone. The blunted arrows indicate inhibition. Adapted from Wagner *et al.*, 2010.

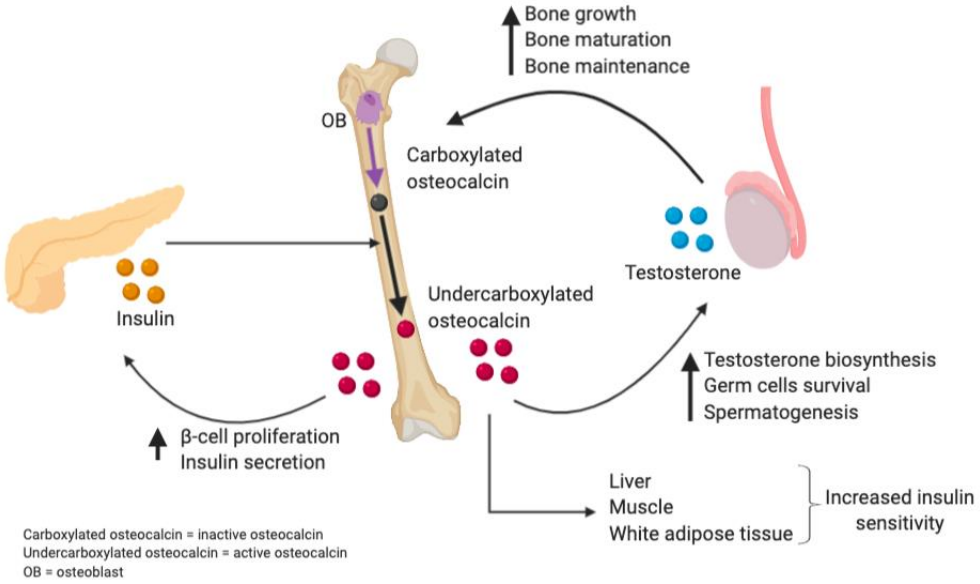

Figure 1.2. Effects of osteocalcin on metabolic functions. Osteocalcin, an osteoblast secreted bone protein can induce endocrine regulation of energy metabolism and male reproduction. Osteocalcin can promote β-cell proliferation and insulin secretion, which further promotes osteocalcin. Furthermore, osteocalcin also promotes male reproductive function by stimulating testosterone production. In addition, testosterone, just like insulin, promotes osteocalcin release and supports bone growth, maturation and maintenance. Adapted from Karsenty and Oury, 2014.

1.2.1. Origins, development and subtypes of BMAT

The observation that BMAT expands during CR/AN is striking due to the fact that WAT decreases under the same conditions, suggesting that these two fat depots are developmentally and/or functionally distinct. Like WAT, BMAds gather lipid that accumulates into a unilocular droplet (Fazeli *et al.*, 2013). WAT is derived from Myf5^{-}/Pax7^{-} progenitor cells, whereas BAT derives from Myf5^{+}/Pax7^{+} progenitor cells (Lepper and Fan, 2010). However, BMAds have developmental origins distinct to WAT and BAT. One of these distinctions relates to the expression of osterix (Osx), a transcription factor implicated in osteoblast development (Chen *et al.*, 2014). Apart from lineage-tracing to osteoblasts and osteocytes, Osx-Cre also targets stromal cells, adipocytes and perivascular cells explicitly within the BM. This indicates a different origin of BMAds compared to white or brown adipocytes which are not traced by Osx-Cre (Chen *et al.*, 2014). An independent study also revealed similar results using a different approach, where sorted stromal cells from BM cultures from pups of Osterix-EGFPCre/Ai9 matings were shown to be able to differentiate into not only

osteoblasts, but also adipocytes (Liu *et al.*, 2013). These results further suggest that BMAds can be derived from cells expressing Osx.

Besides lineage tracing, BMAd progenitors in mice recently have been characterised by flow cytometry using cell markers within the BM (*CD45*$^{-}$*, CD31*$^{-}$*, Sca1*$^{+}$ and *CD24*$^{+}$) and identifying progenitor populations that have adipogenic potential (CD45^{-}CD31^{-}Sca1^{+}CD24^{-}). These adipocytic lineages further respond to diet and age: the expression of the adipogenic marker *Pparg* is increased with age (25-month-old mice), whereas the osteogenic marker *Osx/Sp7* is decreased. Moreover, aged mice on 10-day HFD have an increased proportion of the adipogenic *CD45*$^{-}$*, CD31*$^{-}$*, Sca1*$^{+}$ and *CD24*$^{+}$ population, associated with increased BMAT (Ambrosi *et al.*, 2017). These findings suggest that age-and obesity-related BMAT accumulation is related to effects on progenitors in mice; however, the lineage development of BMAT is complex and additional studies are necessary to uncover it further, including in humans.

1.2.1.1. BMAT development in humans

In humans, at birth, the BM mostly contains haematopoietic cells, and is therefore referred to as red marrow due to its colour from erythroid cells. During postnatal growth, between 4 and 8 weeks of age, BMAds increase in number, resulting in less red marrow and more adipocyte-rich 'yellow' marrow (Scheller and Rosen, 2014). With ageing, the size of the BMAds also increases (Allen *et al.*, 1995). Marrow conversion from red to yellow occurs from distal to proximal BM sites, with the adipocytes in the distal bone developing more rapidly in comparison to the proximal bone. By the mid-20s, the red marrow in the appendicular/distal skeleton of humans is almost entirely converted into yellow marrow; however, in the axial/proximal skeleton, the red marrow persists into adulthood (Kricun, 1985; Scheller *et al.*, 2015), with a slower conversion throughout the rest of life (Justesen *et al.*, 2001). The proximal bones display this slow conversion towards an increase in BMAds throughout life and therefore contains a greater proportion of haematopoietic red marrow compared to distal bone (Scheller *et al.*, 2015). As a result of a slower conversion towards BMAds, the existing BMAds are more interspersed within the haematopoietic BM compared to distal BMAds. BMAT development further differs between men and women. Compared to premenopausal women, postmenopausal women have a sharp increase in BMAT volume, resulting in 10% more BMAT volume

than age-matched men (Griffith *et al.*, 2012; Pansini *et al.*, 2014). This highlights the influence of sex hormones on BMAT development and will be reviewed in more detail in Section 1.2.2.1.

1.2.1.2. BMAT development in rodents

Although it has been assumed that all BMAds are equivalent, a study in 1976 proposed that the characteristics of adipocytes within the proximal bones differ to those within the distal skeleton (Tavassoli, 1976). In rodents, the differences between distal and proximal BMAds are more readily observed than in humans. Distal BMAds have an increase in unsaturated FAs and the adipocytes are larger (Scheller *et al.*, 2015). Just like in humans, these adipocytes develop soon after birth. By light microscopy, distal BMAds appear morphologically similar to WAT, storing lipid in large, unilocular droplets. Once the distal skeleton is accumulated with these mature BMAds there is less haematopoietic activity, owing to displacement of the haematopoietic red marrow. Following this initial stage, BMAds continue to form throughout life within the hematopoietic marrow, i.e. the proximal BMAds within the red marrow in the axial/proximal skeleton (Kricun, 1985). Proximal BMAds are characterised by an increased proportion of saturated FA and are smaller in size compared to the distal BMAds (Scheller *et al.*, 2015). Other vertebrate species, like rabbits, have a similar pattern of BMAT development (Bigelow and Tavassoli, 1984).

1.2.1.3. BMAT subtypes

These observations in humans and other mammals reveal that BMAT is present throughout the skeleton and that BMAds properties show site-specific differences. This suggests that the function and/or formation of BMAds differ based on their location within the skeleton. Indeed, it has been proposed that two subtypes of BMAT exist, designated regulated and constitutive BMAT (rBMAT and cBMAT, respectively) (Scheller *et al.*, 2015; Craft *et al.*, 2018) (Figure 1.3). The anatomical location within the BM, development, morphological, molecular and functional characteristics differ between rBMAT and cBMAT (Craft and Scheller, 2017). cBMAds are larger than rBMAds and exist as contiguous clusters of adipocytes, similar to adipocytes within WAT. They also develop early in life and are resistant to expansion and breakdown. Whereas, rBMAds are present as smaller, discrete adipocytes that are interspersed within the haematopoietic environment. In rodents, cBMAT and rBMAT are more

readily distinguished by their anatomical location (distal-to-proximal), whereas in humans these two subtypes can exist adjacent to each other at a given BM site (Scheller *et al.*, 2015; Craft *et al.*, 2018). However, both rodents and humans display molecular and developmental differences between these subtypes. For example, compared to cBMADs, rBMAds have a greater proportion of saturated FAs and develop later in life. The rBMAds also further increase under different circumstances, including the adverse conditions described at the beginning of section 1.2; this will be further reviewed in Section 1.2.2 (Scheller *et al.*, 2015, 2016, 2019; Craft *et al.*, 2018). Additional molecular and functional distinctions have been found between these two subtypes (reviewed in (Craft *et al.*, 2018)); however, further work is necessary to define how cBMAds and rBMATds relate to the impact of BMAT in health and disease.

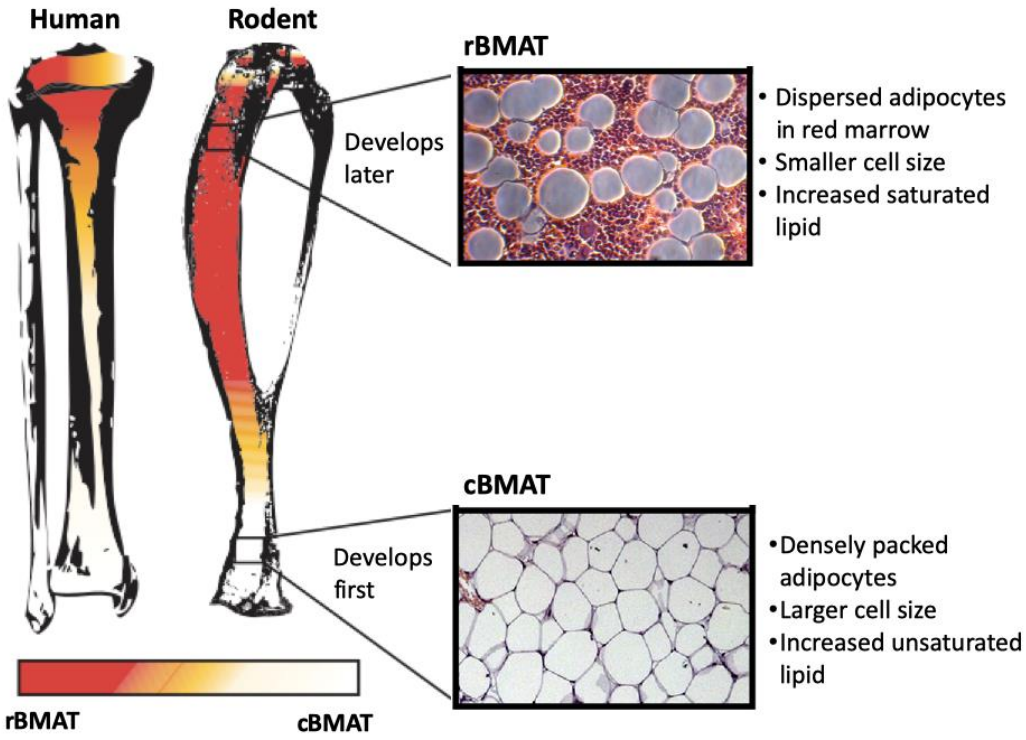

Figure 1.3. Subtypes of BMAT: rBMAT versus cBMAT. rBMAT = regulated BMAT. cBMAT = constitutive BMAT. Adapted from Scheller *et al.*, 2015.

1.2.2. BMAT expansion in health and disease

1.2.2.1. Ageing, osteoporosis and sex hormones

Osteoporosis, i.e. the loss of bone tissue, is commonly observed with ageing. Numerous publications report an inverse correlation between bone mass and BMAT in young and old men and women (Griffith *et al.*, 2005, 2006; Yeung *et al.*, 2005; Di Iorgi *et al.*, 2008, 2010; Shen *et al.*, 2012; Schwartz *et al.*, 2013) (Figure 1.4). A different study did not find the same association, but instead suggested that increased BMAT could be used to diagnose bone weakness and fragility almost as well as measurements of bone mineral density (BMD) (Schellinger *et al.*, 2004). Cross-sectional results have revealed that associations between bone and BMAT expansion differ by sex. Increased BMAT volume is associated with lower trabecular, but not cortical bone mass in older women, but not in men. Furthermore, higher BMAT is instead negatively associated with BMD in men only (Schwartz *et al.*, 2013). Beyond bone morphology, BMAT accumulation also differs between men and women and this relationship differs pre- vs post-menopause. Premenopausal women have lower BMAT volume than age-matched men whereas, post-menopause, BMAT volume sharply increases, such that postmenopausal women have 10% more BMAT compared to age-matched men (Griffith *et al.*, 2012; Pansini *et al.*, 2014). These sex differences are explained by the decrease of oestrogen post menopause, resulting in BMAT expansion (Syed *et al.*, 2008; Limonard *et al.*, 2015). Oestrogen therapy in women can also prevent the increased BMAds (Syed *et al.*, 2008). Although men also have oestrogen, it is not their main reproductive hormone and is therefore likely to have less influence over BM adiposity in males. In addition, ovariectomised rats are more obese, have decreased bone mass and increased BMAT (Sottile, Seuwen and Kneissel, 2004). Although, similarly to humans, oestrogen replacement can reverse BMAT expansion in ovariectomised young and aged female mice (Elbaz, Rivas and Duque, 2009). Besides oestrogen, the ovaries also secrete testosterone and progesterone, suggesting that lack of oestrogen might not be the sole mediator of BMAT expansion post-ovariectomy. Indeed, testosterone administration in female rats decreases fat content in the BM (Tamura *et al.*, 2005), supporting the possibility that other sex steroids influence BM adiposity. A recent cross-sectional study showed a negative association in aged men and women between BMAT and oestrogen/testosterone (Mistry *et al.*, 2018). Besides BMAT, androgens can also regulate bone remodelling as previously mentioned in Section 1.2. Undercarboxylated

osteocalcin secreted from bone directly regulates the production on testosterone in men, but not in females. However, if osteocalcin regulates in/directly the formation of BMAT is unknown. Recent preprint publication shows that the global deletion of *Bglap* and *Bglap2*, meaning an osteocalcin KO mouse, does not have a different bone phenotype compared to control mice (Diegel *et al.*, 2019). This would suggest that it might not affect BMAT either, although it cannot be excluded. Indeed with ageing, osteocalcin levels decrease (Vanderschueren *et al.*, 1990; Obri *et al.*, 2018) but it is yet to be revealed if this is associated with other hormones such as oestrogen, which is known to impact BMAT formation. These findings suggest that sex hormones do play a role in regulating BM adiposity with ageing. It therefore important to further understand the regulation of age-induced BMAT expansion, as BMAT may be a potential target for preventing bone loss.

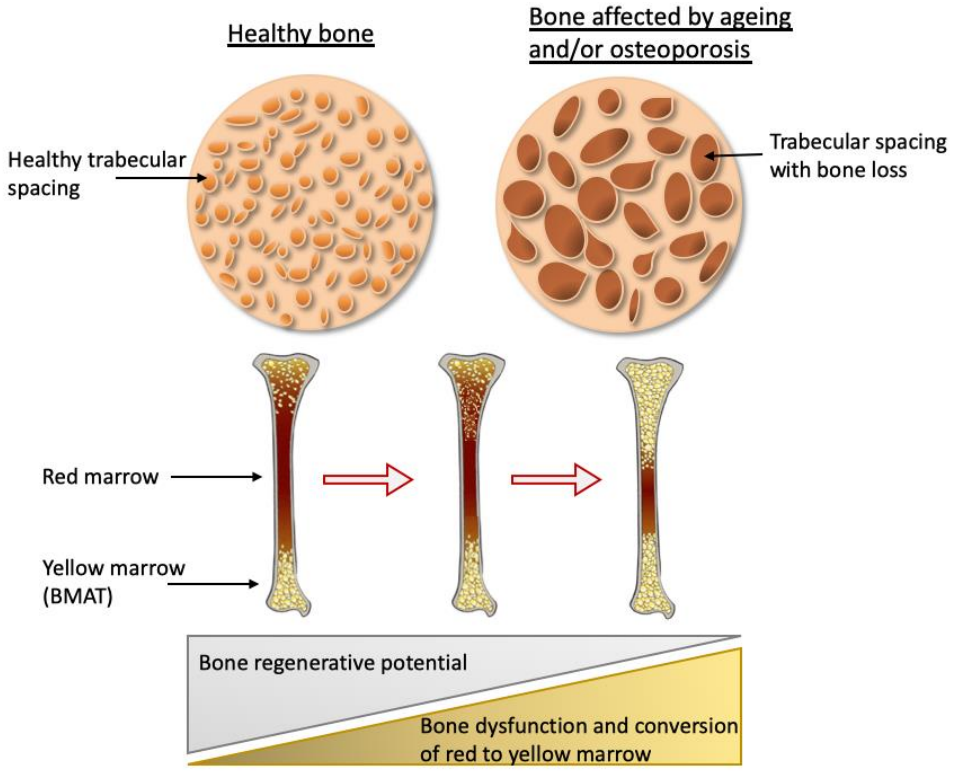

Figure 1.4. The outcome of ageing/osteoporosis on bone morphology and BMAT. Comparison between healthy and aged/osteoporosis trabecular bone. Bone morphology worsens as trabecular spacing increases and the bone formation decreases. BMAT subsequently expands as the bone regenerative potential decreases. Adapted from (Ambrosi *et al.*, 2017).

1.2.2.2. Obesity and HFD-induced obesity

BMAT accumulation does not occur only with ageing, but also with obesity and HFD. A positive association between BMAT and visceral AT was found in obese premenopausal women (Bredella *et al.*, 2011). Similar association was found in healthy women (18-88 years old), with positive but not statistically significant association between BMAT and total body fat. BMAT was instead significantly associated with visceral WAT, but not after adjusting for age and menopause (Shen *et al.*, 2007). In a different study, a positive and significant association was found between BMAT and visceral WAT in premenopausal women (Bredella *et al.*, 2011). These observations show that BMAT can increase in human obesity, although the associations are complex and may depend on age and sex.

Obesity can also increase the risk of developing diabetes in humans, and the association between BMAT and adiposity in diabetic patients has shown contradicting results. Past publications have found a positive association between BMAT and subcutaneous and abdominal AT in T2D postmenopausal women compared to healthy age-matched controls (Baum *et al.*, 2012). However, BMAT significantly increases post menopause; hence, the elevated BMAT volume could have resulted from reduced oestrogen. Men with T2D also exhibit increased BMAT compared to age-matched controls, but overall adiposity was not included in the study (Sheu *et al.*, 2017). However, no significant differences in BM adiposity were found between healthy and diabetic patients in regard to body weight and body mass index (BMI). A past publication reported that BMAT positively correlated with body adiposity in control and diabetic women (Baum *et al.*, 2012), whereas a different publication found no correlations between these parameters (de Araújo *et al.*, 2017). In rodent models, T1D markedly increases BMAT but this is not observed in T1D patients (Slade *et al.*, 2012). Instead, in T1D humans the variation in BMAT is associated with changes in blood lipid levels. The lack of increase in BMAT in T1D humans may be due to insulin treatment, given that animal models of T1D go untreated. However, further research is necessary to understand the mechanism of BMAT expansion in diabetes.

Mice on HFD exhibit a sharp increase in BMAT, with one study showing no changes in trabecular nor cortical bone parameters (Doucette *et al.*, 2015). However, a more recent publication showed that HFD induced not only BMAT expansion, but also bone

loss (Tencerova *et al.*, 2018). With diet-induced obesity, BMAds in young (6 months) and aged (14 months) mice had altered gene expression at each age, but the effects of obesity on the transcriptome were even greater in white adipocytes (Liu *et al.*, 2013). This demonstrates that obesity exerts differential effects on BMAds and white adipocytes, raising the possibility that BMAds may play distinct roles in obesity-related metabolic dysfunction.

Overall, these results demonstrate an association between whole-body adiposity and BMAT. However, it is yet to be confirmed if overall adiposity with obesity initiates BMAT expansion, or if other factors are involved.

1.2.2.3. Iatrogenic BMAT expansion

Besides the above-mentioned conditions, BMAT can also increase in iatrogenic contexts. For example, following thiazolidinedione treatment (antidiabetic drugs), chemo/radiotherapy, GC therapy and beyond.

BMAT significantly increases following chemo/radiotherapy in rodents (Georgiou *et al.*, 2012; Fan *et al.*, 2016; Horowitz *et al.*, 2017; Wang *et al.*, 2018; Lee *et al.*, 2019) and humans (Georgiou, Hui and Xian, 2012; Cawthorn *et al.*, 2014; Mostoufi-Moab *et al.*, 2015; Veldhuis-Vlug and Rosen, 2018). Increased BMAT and bone loss is also evident following thiazolidinedione treatment in mice (Schwartz and Sellmeyer, 2007; Piccinin and Khan, 2014; Sulston *et al.*, 2016; Tencerova and Kassem, 2016) and humans (Grey *et al.*, 2012; Pop *et al.*, 2017). Although one study in humans showed the opposite results, with decreased bone loss and BMAT in the spine (Harsløf *et al.*, 2011), the balance of evidence shows that thiazolidinediones increase BMAT in rodents and humans. GCs are frequently used as anti-inflammatory drugs (Coutinho and Chapman, 2011). However, long-term usage often results in bone loss and increased risk of osteoporosis (LoCascio *et al.*, 1990; Kim *et al.*, 2006). Another outcome of increased GC action with drugs or hormones is BMAT expansion (Vande Berg *et al.*, 1999). GCs are a key subject of this thesis as potential regulators of BMAT, and will therefore be further discussed in Section 1.3.

Overall, these iatrogenic conditions result in increased BMAT in rodents and humans, suggesting that BMAT may contribute to other side effects of these therapeutic interventions. However, in each case the mechanism behind this effect remains to be identified.

1.2.2.4. CR and AN

As mentioned above, during CR in animals (Devlin *et al.*, 2010, 2016; Cawthorn *et al.*, 2016) and AN in humans (Bredella *et al.*, 2009, 2014; Ecklund *et al.*, 2010), BMAT surprisingly increases. This is odd, as other adipose depots simultaneously decrease. This is also in stark contrast to obesity, when both overall body adiposity and BMAT increase (Shen *et al.*, 2007; Bredella *et al.*, 2011; Baum *et al.*, 2012; L. Liu *et al.*, 2013; Doucette *et al.*, 2015). This suggests that, unlike for WAT, the increase in BMAT does not always require excess calories and is likely mediated by different mechanisms in these two adverse conditions. CR without malnourishment, in which there is provision of adequate vitamins and minerals, has been shown to have beneficial effects on the ageing process and can extend lifespan in numerous species (Masoro, Yu and Bertrand, 1982; Lin, Defossez and Guarente, 2000; Houthoofd *et al.*, 2002; Bodkin *et al.*, 2003). With CR, a decrease in body mass, blood pressure, insulin, fasting glucose and serum total cholesterol levels are also observed compared to healthy age-matched controls (Fontana *et al.*, 2004; Meyer *et al.*, 2006). Besides these beneficial metabolic effects of CR, it is also of interest as potential therapeutic strategy to prevent and treat other chronic diseases, including Alzheimer's, asthma, arthritis and cancer. Whether CR-induced BMAT expansion plays a role in these conditions remains to be determined.

In contrast to CR, AN is an eating disorder that is characterised by malnourishment (lack of nutrition), resulting in weight loss and WAT depletion. However, unlike CR, AN has adverse health effects, including bone loss, increased fracture risk, immunosuppression and increased risk of mortality. For both AN and CR, why or how reduced food intake mediates BMAT expansion still remains indefinite. Past publications have demonstrated that women with AN have increased lumbar and femoral BMAT compared to age-matched controls. Moreover, increased BMAT in AN women was inversely correlated with BMD (Bredella *et al.*, 2009, 2014). Adolescent women (between 13 and 18 years old) with AN have a greater risk of developing osteoporosis. By analysing the distal femur and proximal tibia from MRI scans of adolescent women with AN, it was revealed that they exhibit premature replacement of haematopoietic to adipose cells in the marrow. This is most likely owing to the increase of adipogenesis at the expense of osteoblast differentiation (Ecklund *et al.*, 2010). Furthermore, GCs are not only elevated during CR in animals (Sabatino *et al.*,

1991; Chacón *et al.*, 2005; Levay *et al.*, 2010; Pankevich *et al.*, 2010; Cawthorn *et al.*, 2016) but also in AN patients (Boyar *et al.*, 1977; Walsh *et al.*, 1978; Misra *et al.*, 2004; Lawson *et al.*, 2009). This suggests an association between increased GC and BMAT expansion in these conditions.

It is still debatable whether BMAT expansion with CR is good or bad. As CR results in increased BMAT and often bone loss, bone biologists see BMAT expansion as detrimental. However, BMAT has been shown to secrete the adipose-derived hormone adiponectin at higher concentrations than WAT, such that BMAT expansion contributes to hyperadiponectinaemia during CR (Cawthorn *et al.*, 2014). This suggests potential beneficial effects of BMAT, because adiponectin can promote insulin sensitivity and exert other health benefits (further reviewed in section 1.2.3.3). Furthermore, BMAT-derived adiponectin has been implicated with CR-associated metabolic adaptations in skeletal muscle, suggesting that BMAT might have systemic effects (Cawthorn *et al.*, 2014). It is therefore important to understand what regulates CR-induced BMAT expansion, as this understanding may further allow us to comprehend the functions of BMAT in normal physiology and disease. In addition, understanding what regulates CR-induced BMAT expansion, and the role of BMAT during CR, can aid out understanding if BMAT contributes to the health benefits of CR. For example, if and/or how BMAT expansion during CR contributes to the enhanced breakdown of visceral adiposity and the lower risk of developing cardiovascular disease. As of now, this still remains to be revealed.

1.2.3. Functions of BMAT

In section 1.2.2, different conditions were reviewed where BMAT expands in both health and disease. In the present section I focus on the proposed functions of BMAT during these conditions and in normal physiological contexts.

1.2.3.1. BMAT and bone remodelling

As mentioned in Section 1.2.2.1, BMAT expands in conditions such as ageing, which is also accompanied by bone loss. This has led to the concept that BMAT expansion occurs at the expense of bone formation, but this is not always the case. For example, during postnatal development in rabbits, BMAds accumulate as soon as the third to fourth weeks of life, which occurs at the same time as bone growth (Sabin *et al.*,

1936). Bone formation and BMAT accumulation also coincide in armadillos (Weiss and Wislocki, 1956). A similar finding has been observed in young girls (4-10 years of age) (Newton *et al.*, 2013), suggesting that BMAT accumulation is important for bone growth. However, other human studies have found negative associations between BMAT and bone (boys and girls, 5-17/18 years of age) (Shen *et al.*, 2014; Gao *et al.*, 2015). The variance in the results could be due to the age and sex of the children and to the skeletal sites analysed; indeed, inverse associations between BMAT and bone mass are often observed in the proximal BMAT, but not in the distal BMAT.

BMAT volume and bone mass also differ in different mouse strains. For example, in C3H/HeJ mice, bone mass and BMAT volume are greater than in C57BL/6J mice (Scheller *et al.*, 2015). Moreover, in C57BL/6J mice trabecular bone loss is apparent around 8 weeks of age, but BMAT volume does not increase until much later in life (Devlin and Rosen, 2015). Altogether, these observations suggest that BMAT accumulation and bone loss are not always inversely associated, and although increased BMAT is associated with bone loss in some pathological conditions, this likely does not reflect the physiological role of BMAds in healthy bone. Further insights are gained from the observation that, in bony fish, haematopoiesis occurs outwith the skeleton, and yet BMAds are still present (Craft and Scheller, 2017). This suggests that BMAds have physiological functions that are independent of haematopoietic regulation and instead relate to bone remodelling and function (Craft and Scheller, 2017).

While the above findings provide insights into the physiological interplay between BMAds and bone, further data support the concept that BMAds may play detrimental roles in skeletal pathologies. One such context is metastatic bone disease. For example, breast cancer cells spread preferentially to BMAT-rich regions of BM (Templeton *et al.*, 2015). Moreover, mice fed a HFD with prostate tumours have increased tumour growth, and the increased BMAT promotes the proliferation and invasion of these tumour cells (Herroon *et al.*, 2013). In addition, the anatomical location of BMAds also seems to matter, as tumour cells prefer to metastasize to the proximal part of the bone (Kricun, 1985). rBMAds are also more lipolytic compared to cBMAds (Scheller *et al.*, 2019), with an increased supply in FA possibly further aiding tumour cell growth/survival.

The interactions between BMAds and tumours also extend to haematological malignancies, such as multiple myeloma and acute myeloid leukaemia. As previously mentioned, chemo/radiotherapy often results in increased BMAT, suggesting that BMAds could either promote and/or inhibit metastasis and/or tumour progression within bone. Previous research showed that BMAT expansion during multiple myeloma interacts with tumour cells in the BM, promoting tumour cell growth and survival (Trotter *et al.*, 2016). BMAds can act as energy sources for tumour cells. The release from BMAds of growth factors (IL-6, TNF-α, insulin-like growth factor 1 (IGF-1), etc.), free FAs (FFAs) and numerous hormones, including adiponectin and leptin, may promote tumour cell survival and protect the tumour cells from chemotherapy-induced apoptosis (further reviewed (Falank, Fairfield and Reagan, 2016). Altogether, the increase in BMAT is not aiding health in these conditions. Suppressing BMAT expansion might be an alternative to diminish the consequences of these conditions.

Many studies have shown that osteoporotic patients have increased BMAT (Meunier *et al.*, 1971; Justesen *et al.*, 2001; Verma, 2002; Griffith *et al.*, 2005; Yeung *et al.*, 2005; Tang *et al.*, 2010; Devlin and Rosen, 2015; Cordes *et al.*, 2016; Veldhuis-Vlug and Rosen, 2018). Patients with increased BMAT also tend to have a decrease in BMD compared to healthy age-matched controls (Griffith *et al.*, 2012). Furthermore, increased BMAT is associated with higher risk of vertebral fracture in men, independent of BMD (Schwartz *et al.*, 2013), and potentially with bone weakening (Schellinger *et al.*, 2004).

Due to bone loss often occurring with CR in animals and AN in humans, alongside BMAT expansion, studies have often focused on the supplementation of vitamin D. Furthermore, vitamin D is an important regulator of calcium absorption, hence the effects of vitamin D supplementation often include its effects on calcium, or vice versa, as well as the effects on PTH. CR reduced calcium absorption, however urinary calcium does not differ between postmenopausal women on a diet compared to age-matched controls. Nonetheless, PTH decreases with vitamin D treatment. The decrease in calcium absorption could be a contributor to bone loss associated with weight loss during CR, hence calcium supplementation might be necessary alongside vitamin D (Shapses *et al.*, 2013). A different study further showed that vitamin D supplementation and CR affect serum osteocalcin concentrations followed by enhanced insulin sensitivity. Although, in this study, PTH was unaltered between the

groups (Sukumar, Shapses and Schneider, 2015). Although, vitamin D is decreased with obesity, it increases with weight loss (further reviewed (Himbert *et al.*, 2017)). Healthy non-obese volunteers underwent 25% CR for two years, and compared to age-matched controls, PTH did not differ at any point throughout the study. The CR group had significantly increased vitamin D, cortisol and adiponectin (Villareal *et al.*, 2016). Although patients with AN have reduced nutrient intake, one study showed that it most likely does not contribute to the low bone mass. Misra *et al.,* (2006) published that girls with AN consume more calcium and vitamin D via supplements compared to normal-weight girls (Misra *et al.*, 2006). Similar results were published for adolescent girls with AN (Misra *et al.*, 2006; Haagensen *et al.*, 2008; DiVasta *et al.*, 2011). PTH concentration was however decreased in adolescents with AN (Haagensen *et al.*, 2008; Lenherr-Taube *et al.*, 2020). Overall, these results show that with CR there is an increase in vitamin D, but not during AN. Calcium remains unaltered during 25% CR, but it decreases during AN. How vitamin D and calcium are associated with BMAT expansion and bone loss during these conditions is still to be revealed. Although many studies have focused on the effect of vitamin D and calcium on bone, none have yet to include BMAT as a factor. Overall, these pathological functions of BMAT are not aiding health. However, it is vital to understand the mechanisms and pathways behind this for potential treatments. Additional research is also necessary to understand and determine the relevance of BMAds to not only these diseases, but also other bone diseases.

1.2.3.2. BMAT and haematopoiesis

The BM niche is the primary site of haematopoiesis. Changes to the BM, such as those that occur with increased adiposity, affect haematopoietic maintenance and differentiation (Adler, Kaushansky and Rubin, 2014). Furthermore, BMAds act as negative regulators of the BM niche in mice (Naveiras *et al.*, 2009). However, a more-recent publication found that human BMAds exhibit a positive regulation on the haematopoietic system (Mattiucci *et al.*, 2018). Similar results were found in mouse BM, where mice lacking BMAds had slow haematopoietic regeneration post-irradiation (Zhou *et al.*, 2017). In addition, besides adiponectin, BMAds also express stem cell factor which aids the regeneration of the haematopoietic stem cells post-irradiation (Zhou *et al.*, 2017). Thus, the precise function of BMAds in regenerative haematopoiesis remains inconclusive.

Additional insights are provided by studies of BMAT in AN, obesity and ageing. As previously discussed, BMAT accumulates in patients with AN (Section 1.2.2.4). However, in severe cases of AN, BMAT actually decreases and this is associated with decreased haematological function; post recovery, BMAT accumulates and the haematopoietic system regains its normal function (Geiser *et al.*, 2001; Abella *et al.*, 2002; Fazeli and Klibanski, 2019). This further suggests that the presence of BMAT is beneficial for the haematopoietic system.

With obesity and ageing, mesenchymal stem cells (MSCs) are mostly committed to the adipogenic linage (Tencerova *et al.*, 2018), which does not only inhibit bone formation, but it also reduces the haematopoietic reconstitution in mice (Ambrosi *et al.*, 2017). These results suggest that BMAT expansion contributes to age-and obesity-related dysfunctions of the BM microenvironment, which can potentially be involved in numerous other processes that interfere with the maintenance of bone and the haematopoietic system (Ambrosi *et al.*, 2017). The number of haematopoietic stem cells also decreases with ageing in humans, and this is correlated with increased BMAT (Tuljapurkar *et al.*, 2011). Iatrogenic expansion of BMAT following chemo/radiotherapy in rodents and humans can also alter the haematopoietic environment, as previously mentioned in section 1.2.2.3.

Although HFD increases BMAT, BMAds do not exhibit a pro-inflammatory nor an insulin resistance phenotype, compared to white adipocytes (Tencerova *et al.*, 2018). This suggests that although BMAds have a deleterious effect on the skeleton and can reduce haematopoietic reconstitution, obesity-induced BMAT expansion might not be entirely detrimental.

Overall, the literature presents contradictory findings regarding the interplay BMAds and the haematopoietic system. Accordingly, more research is necessary to understand the association between BMAT and the haematopoietic system in various adverse conditions.

1.2.3.3. BMAT metabolism and endocrinology

BMAds are capable of secreting adipokines, such as adiponectin and leptin (Laharrague *et al.*, 1998; Cawthorn *et al.*, 2014), suggesting that BMAT may have endocrine functions similar to WAT (Scherer *et al.*, 1995). The circulatory

concentration of adiponectin is decreased with obesity (Hu, Liang and Spiegelman, 1996; Arita *et al.*, 1999) but increased with CR (Zhu *et al.*, 2004). Similarly, in patients with AN, adiponectin is often increased compared to age-matched controls (Bosy-Westphal *et al.*, 2005; Dolezalova *et al.*, 2007; Modan-Moses *et al.*, 2007); however, this increase is not always observed (Iwahashi *et al.*, 2003; Tagami *et al.*, 2004) and may depend on the duration and severity of the disease. Why circulating adiponectin concentrations increase in CR and AN still remains incompletely understood. A study showed that although adiponectin expression is increased with CR in WAT, adiponectin protein is decreased (Wiesenborn *et al.*, 2014). Whereas, a different study in humans showed that circulating adiponectin is not associated with adiponectin secretion from WAT during CR (Wang *et al.*, 2015). These findings motivated studies of other possible sources of adiponectin secretion, such as BMAT.

As previously mentioned, both adiponectin and BMAT increase during CR in animals and AN in humans, suggesting an association between BMAT and circulating adiponectin concentrations. It has also been reported that adiponectin transcripts and protein are expressed in whole BM of long bones in mice (Berner *et al.*, 2004; Shinoda *et al.*, 2006; DiMascio *et al.*, 2007), as well as in cultured BMAds derived from human femurs (Modan-Moses *et al.*, 2007). BMAT from the rodent caudal vertebrae expresses adiponectin protein at similar levels as WAT (Cawthorn *et al.*, 2014), whereas other adipocyte markers such as PPARγ, fatty-acid-binding protein 4 (FABP4), hormone-sensitive lipase (HSL) and perilipin A are expressed at much lower levels in the BMAds compared to WAT (Liu *et al.*, 2011; Cawthorn *et al.*, 2014). This suggests that, relative to other adipocyte markers, BMAds have greater adiponectin production than white adipocytes. To test if BMAT directly contributes to circulating adiponectin, studies were done in Ocn-Wnt10b mice, which resist BMAT expansion during CR. These mice were also found to resist CR-associated increases in circulating adiponectin, despite unaltered expression and protein in WAT (Cawthorn *et al.*, 2014).

This suggests that the differences in circulating adiponectin concentrations were not a result of altered adiponectin production from WAT and instead resulted from suppressed BMAT expansion. This was further confirmed during CR in rabbits, which decreased adiposity but did not cause BMAT expansion or hyperadiponectinemia (Cawthorn *et al.*, 2016). These observations suggest that BMAT expansion is

necessary for hyperadiponectinaemia during CR, underscoring the conclusion that BMAT is an endocrine organ (Cawthorn *et al.*, 2016).

Besides adiponectin, leptin is also an adipose-derived hormone regulating food intake and energy expenditure (Hussain and Khan, 2017). Circulating leptin concentrations are associated with total AT mass, such that concentrations are increased with obesity (Heymsfield *et al.*, 1999; Ahima, 2008) and decreased with CR/AN (Zgheib *et al.*, 2014; Cawthorn *et al.*, 2016). It has previously been reported that, as in WAT, leptin expression in BMAT is inhibited in response to CR (Cawthorn *et al.*, 2016). Thus, while WAT and BMAT differ during CR in terms of their amount and effects on adiponectin, in terms of leptin expression they may share a common endocrine function. However, whether BMAT contributes to circulatory leptin concentration, and thereby influences downstream functions of leptin, still remains to be defined.

1.2.4. Candidate regulators of BMAT formation

BMAT increases and decreases in numerous adverse physiological and clinical conditions. For this reason, many studies have investigated possible regulators that might promote BMAT development. Prominent candidates include preadipocyte factor-1 (Pref-1), ghrelin, leptin, sex hormones and GCs (Figure 1.5).

Pref-1 is a skeletal stem cell regulator (Abdallah *et al.*, 2004). AN women in recovery have decreased BMAT, but also decreased Pref-1 levels (Fazeli *et al.*, 2012). A positive association was also found between Pref-1 and proximal femur BMAT (Fazeli *et al.*, 2010). This suggests that Pref-1 might have distinct effects during AN compared with nutritional abundance.

Another hormone that might mediate CR/AN-induced BMAT expansion is ghrelin. Ghrelin is secreted by enteroendocrine cells in the stomach and is significantly elevated in AN individuals compared to normal weight subjects (Misra *et al.*, 2005; Germain *et al.*, 2007; Monteleone *et al.*, 2008). BMAT was measured in women administrated ghrelin receptor agonist, and although the results were not significant, there was a trend for a decrease in BMAT. Whereas, in rodents, infusion of ghrelin in tibial BM promotes BMAT accumulation (Thompson *et al.*, 2004). These findings suggest that ghrelin is playing an important role in BMAT development, but more

research is necessary to understand the mechanism behind it and the role of ghrelin in regulating physiological and pathological BMAT formation.

Decreased leptin is correlated with increased BMAT in leptin deficient mice (Hamrick *et al.*, 2004). However, leptin administration decreases BMAT volume in mice and rats (Hamrick *et al.*, 2005, 2006; Devlin *et al.*, 2016). Furthermore, decreased concentrations of leptin are associated with CR-induced BMAT expansion (Devlin, 2011). Conversely, a different publication showed that decreased concentrations of leptin are neither necessary nor sufficient for CR-induced BMAT expansion (Cawthorn *et al.*, 2016). Thus, it seems that hypoleptinaemia is not a critical regulator of BMAT formation in this context.

As previously reviewed in section 1.2.2.1, BMAT expansion is associated with decreased oestrogen and ovariectomy in humans (Wáng *et al.*, 2015) and animals (Elbaz, Rivas and Duque, 2009; Lecka-Czernik *et al.*, 2017). Besides oestrogen, other sex hormones might also influence BMAT development. Administrated testosterone in female rats decreased BMAT (Tamura *et al.*, 2005). Moreover, aged men with low testosterone and oestrogen concentrations have increased BMAT volume (Mistry *et al.*, 2018). These findings suggest that sex hormones do play a role in regulating BMAT, but further research is required to establish the roles of these hormones and others such as progesterone in different conditions of altered BMAT. Whether sex steroids also influence BMAT expansion during CR or AN also remains to be determined.

In addition to the above-mentioned potential regulators, there are many other factors that have been researched, including GCs. GCs can increase BMAT, and GC excess occurs in many conditions in which BMAT accumulates, including ageing, CR/AN, and Cushing's syndrome (CS). CS can lead to increased visceral adiposity, decreased muscle mass and insulin resistance (Lönn, Kvist , Ernest, 1994; Tomlinson *et al.*, 2002). Since GC therapy (Vande Berg *et al.*, 1999) and increased GCs with CR/AN are associated with increased BMAT, one would expect for patients with CS to also have increased BMAT due to excess GCs. One earlier study did not find any increase in BMAT in CS patients, compared to age-matched controls (Mayo-Smith *et al.*, 1989); however, this negative finding may reflect limitations in the techniques available to measure BMAT at the time, as the measurements of BMAT were highly variable.

Indeed, two very recent publications did find increased BMAT volume in CS patients, which was also associated with hypercortisolism (Maurice *et al.*, 2018; Ferraù *et al.*, 2019), compared to age-matched controls. Thus, along with the coincidence of BMAT expansion and GC increases during ageing and CR/AN, these findings in CS patients further support an association between increased GCs and BMAT accumulation. CS patients in remission have decreased BMAT, similar to age-matched controls (Geer *et al.*, 2012; Maurice *et al.*, 2018). Similar results would be expected for patients with AN in remission, and by changing the diet of CR mice to AL, although it has yet to be confirmed.

For this thesis, I am especially interested in the GC excess that occurs during CR and ageing. This is because of the possibility, discussed above in Sections 1.2.2 and 1.2.3, that BMAT expansion may not only contribute to the beneficial effects of CR, but also to bone loss and other detrimental effects of ageing. Therefore, the overarching goal of my PhD research has been to determine if GC excess contributes to BMAT expansion during CR and ageing. I discuss this possibility further in Section 1.3.2; however, before doing so I first summarise the properties and functions of GCs in normal physiology and disease, focusing on CR and AN, and the regulation of GC action by 11β-hydroxysteroid dehydrogenase (11β-HSD1).

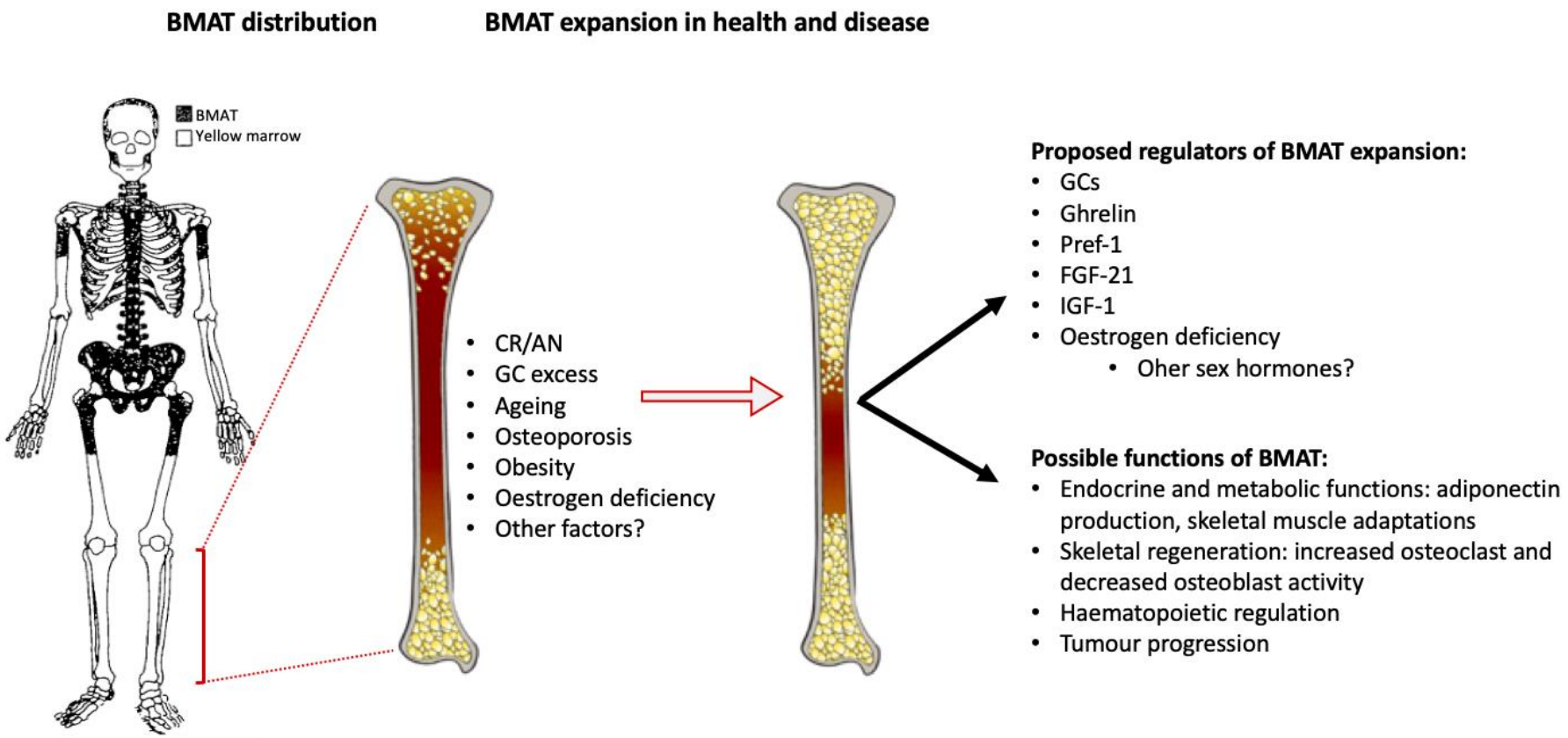

Figure 1.5. Distribution, clinical associations and possible causes and functions of BMAT. Schematic representation of the distribution of BMAT shown by the human skeleton, adapted from Kricun (1985). BMAT expands in various conditions, such as during caloric restriction (CR), anorexia nervosa (AN), ageing, osteoporosis, obesity, oestrogen deficiency and many more. The expansion could potentially be caused by glucocorticoids (GCs), ghrelin, preadipocyte factor 1 (Pref-1), fibroblast growth factor 21 (FGF-21), insulin-like growth factor 1 (IGF-1), oestrogen deficiency and possibly other hormones. Possible functions of BMAT include endocrine and metabolic functions, skeletal regeneration, haematopoietic regulation and tumour progression.

1.3. HPA axis and GCs

In response to stress, GCs are synthesised and secreted by the adrenal gland. GCs are a class of steroid hormones that are used pharmacologically to treat inflammation; however, they can also cause immunosuppression. The release of circulating GCs, predominantly cortisol, but also 10% corticosterone in humans and corticosterone in rodents is centrally regulated by the hypothalamic-pituitary-adrenal (HPA)-axis. Although, most rodents also have cortisol, besides rats and mice because they lack adrenal expression of Cyp17a1. With stress or circadian rhythm, corticotropin-releasing factor (CRF) (Spiess *et al.*, 1981) and arginine vasopressin (AVP) are released from the paraventricular nucleus in the hypothalamus. In turn, these neuropeptides bind to the CRF and vasopressin receptors (1B) in the anterior pituitary, resulting in the release of adrenocorticotropic hormone (ACTH). CRF has been revealed to be the main regulator of ACTH release by the anterior pituitary (Rivier and Vale, 1983). ACTH then binds to receptors in the adrenal cortex, specifically the melanocortin receptor 2 that belongs to the G protein-coupled receptor (GPCR) superfamily, which upregulates intracellular cyclic adenosine monophosphate (cAMP). As a result, the steroidogenic acute regulatory protein (StAR) (Clark *et al.*, 1994) will increase and up-regulate cholesterol transfer within the mitochondria (Simpson and Waterman, 1988). Cholesterol is the precursor to steroids; therefore, it is vital for GC synthesis and secretion into the circulation (Figure 1.6).

Treatment with GCs can lead to visceral obesity, osteoporosis, T2D, increased risk of cardiovascular disease, hypertension and atherosclerosis (Van Staa *et al.*, 2000; Souverein, 2004; de Vries *et al.*, 2007; Amiche *et al.*, 2018). All of these are themselves, to some extent, inflammatory conditions. To exert their effects, GCs bind to intracellular nuclear hormone receptors, which results in the translocation of the receptor and its bound GC to the nucleus. GCs act via two intracellular receptors, glucocorticoid (GR) and mineralocorticoid (MR) receptors. The GR is encoded by the *NR3C1* gene (Nuclear Receptor Subfamily 3 Group C Member 1) while the MR is encoded by the *NR3C2* gene (Nuclear Receptor Subfamily 3 Group C Member 2). Unbound GR resides in the cytoplasm complexed with particular heat shock proteins (HSP), notably HSP90 and HSP70, and chaperone complexes such as FK506 binding protein 5 (FKBP5) (reviewed in ((Grad and Picard, 2007)). GCs can directly enter cells

by diffusing through the membrane and binding to the GR, thereby inducing conformational changes in this receptor. These changes allow the GR to dissociate from the multi-protein complex and translocate to the nucleus where it can transactivate or transrepress gene transcription. Transactivation occurs once the GC-GR binds to the glucocorticoid response element (GRE) and up-regulates the production of regulatory cells with anti-inflammatory properties (e.g. GILZ). Transrepression occurs when the GC-GR complex binds to pro-inflammatory factors (e.g. NF-kB), reducing their expression. The anti-inflammatory properties of GCs can therefore result from both transactivation and transrepression (Coutinho and Chapman, 2011).

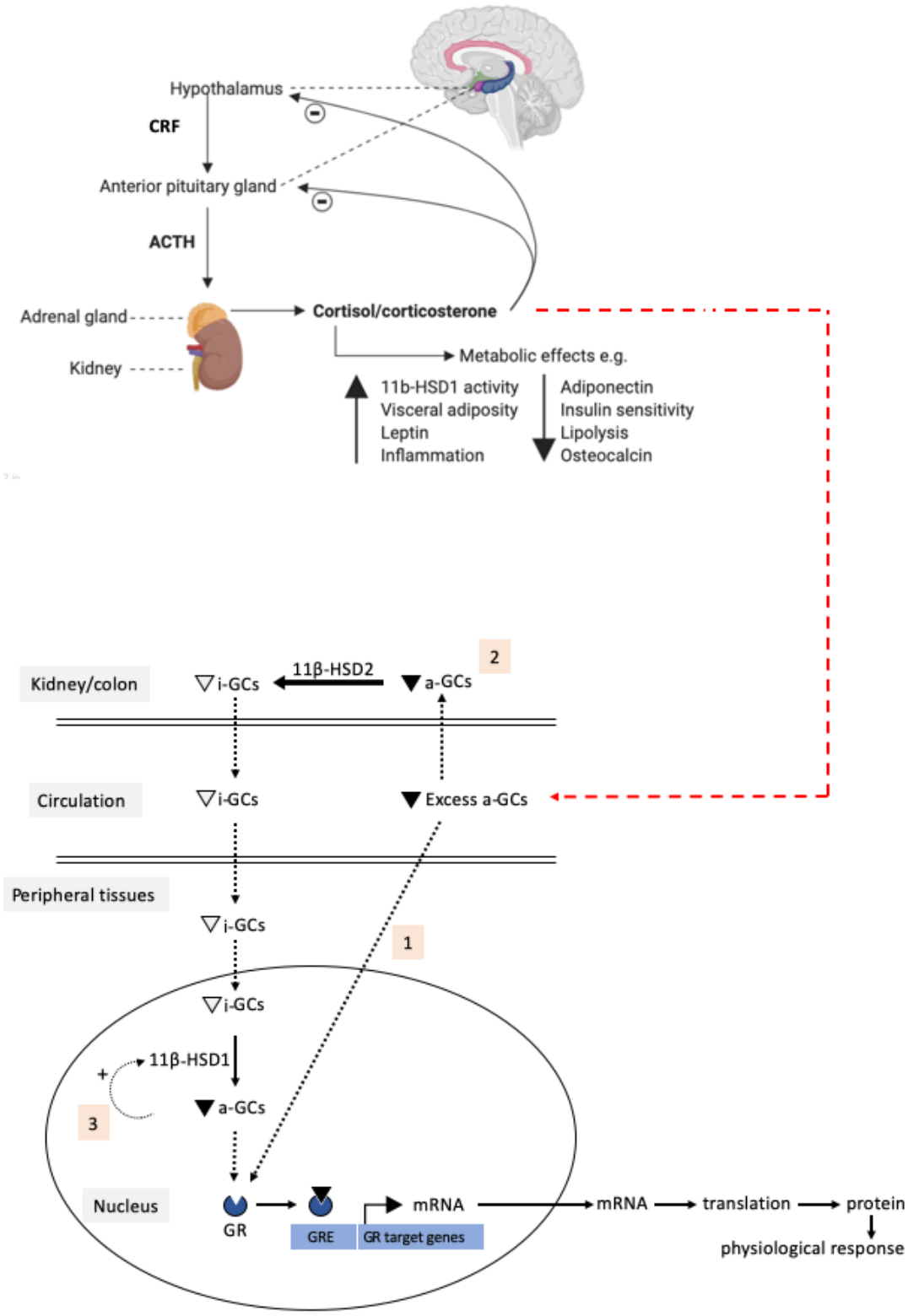

Figure 1.6. Schematic representation of the HPA axis and GC mechanism of action. The hypothalamus secretes corticotrophin-releasing factor (CRF) upon stress, which stimulates the pituitary gland to secrete adrenocorticotrophic hormone (ACTH). The adrenal glands are then influenced by ACTH, resulting in the synthesis and secretion of GCs (cortisol in humans, corticosterone in rodents) which can induce various metabolic effects. The minus signs (-) represent a negative feedback signal,

maintaining homeostasis. GCs can then induce gene expression by three different mechanisms: (1) circulating active GCs (cortisol/corticosterone, a-GCs (a: active)) (red line with dashes) can enter peripheral tissues and directly bind to the glucocorticoid receptor (GR) and transactivate or transrepress gene transcription; (2) inactivation of a-GCs by 11β-HSD2 in the kidneys, followed by inactive GCs (cortisone/11-dehydrocorticosterone, i-GCs (i: inactive)) entering the peripheral tissue where it is reactivated by 11β-HSD1; and (3) the activation of the GR increases 11β-HSD1 activity, further amplifying intracellular a-GCs. Adapted from (Morgan *et al.*, 2014; Morgan, Hassan-Smith and Lavery, 2016; Spencer and Deak, 2017).

1.3.1. 11β-hydroxysteroid dehydrogenase

11β-HSDs are enzymes that catalyse the interconversion of inactive cortisone/11-dehydrocorticosterone (11-DHC) and active cortisol/corticosterone. 11β-HSD1 catalyses the generation of cortisol/corticosterone whereas 11β-HSD2 drives this reaction in the opposite direction, thereby producing cortisone/11-DHC from the active GCs.

11β-HSD1 is a NADPH-dependent enzyme, highly expressed in the liver relative to other tissues, with lower expression in AT and other tissues. In contrast, 11β-HSD2 is a NAD^+-dependent enzyme, highly expressed in mineralocorticoid target tissues such as the placenta, kidney, colon, adrenal cortex and ovary (Condon *et al.*, 1997). In the tissues in which it is expressed, the main role of 11β-HSD2 is to protect the MR from excessive activation by GCs, by converting active to inactive GCs (Figure 1.7). This way, 11β-HSD2 allows for access of aldosterone to the receptor instead (Holmes *et al.*, 2006; Chapman, Holmes and Seckl, 2013). While the HPA axis determines circulatory GC levels, the intracellular GCs are regulated by the activity of 11β-HSD1 and 11β-HSD2. The former can act bi-directionally *in vitro*, however, *in vivo* it predominantly catalyses intracellular regeneration of active GCs (Lakshmi and Monder, 1988) (Figure 1.5). The *Hsd11b1* gene has 3 promoters: P1 (Bruley *et al.*, 2006) in the lung and kidney; P2 (Bruley *et al.*, 2006) in liver, AT and brain; and P3 (Moisan, Edwards and Seckl, 1992) in the kidney. Mice lacking this enzyme cannot convert 11-DHC to corticosterone *in vivo*, supporting the fact that 11β-HSD1 is the only 11β-reductase enzyme in mice (Kotelevtsev *et al.*, 1997).

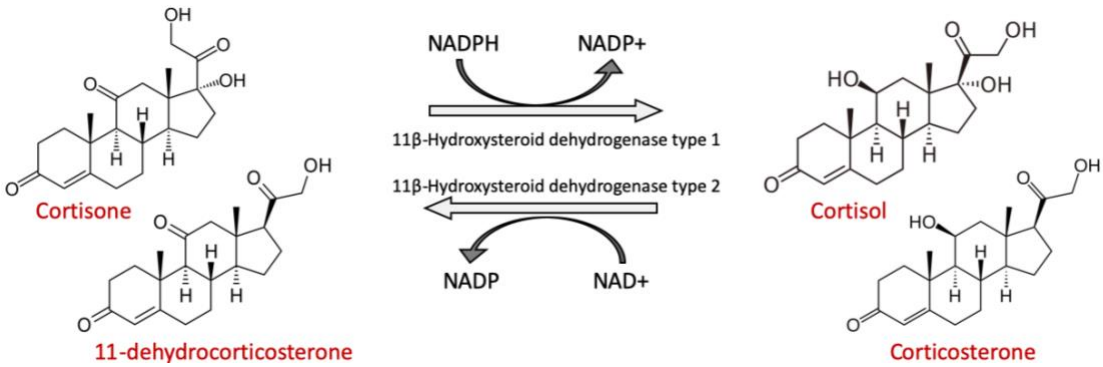

Figure 1.7. Reaction catalysed by 11β-Hydroxysteroid dehydrogenase type 1 and 2. 11β-HSD1, primarily a reductase in intact cells and *in vivo*, catalyses NADPH-dependent reduction of cortisone in humans and 11-dehydrocorticosterone in rodents to active cortisol and corticosterone, respectively. 11β-HSD2, an oxidising enzyme, converts the NAD_+-dependent inactivation of cortisol and corticosterone to cortisone and 11-dehydrocorticosterone, respectively (Griffiths and Wang, 2019). Adapted from (Chapman, Holmes and Seckl, 2013).

1.3.1.1. Regulation of 11β-HSD1

11β-HSD1 regulation is influenced by numerous factors such as metabolic conditions, pro-inflammatory cytokines, sex hormones, insulin, thyroid hormone and other endocrine mediators. However, the effects of these factors are tissue-specific and also vary between species (further reviewed by (Tomlinson *et al.*, 2004)). 11β-HSD1 is also regulated by GCs themselves, both in primary cells *in vitro* (Jamieson, 1995; Whorwood *et al.*, 2001) and *in vivo* (Hundertmark *et al.*, 1994; Jamieson, Chapman and Seckl, 1999; Michailidou, Coll, *et al.*, 2007). Indeed, 11β-HSD1 expression in mice is up-regulated by GCs in both AT (Michailidou *et al.*, 2007) and in the liver (Morgan *et al.*, 2014). HFD-fed mice overexpressing 11β-HSD1 in AT are not only obese, but they also have increased 11β-HSD1 activity in AT (Masuzaki, 2001). Whereas in obese rats, 11β-HSD1 is unaltered in subcutaneous AT but increased in omental AT and decreased in liver, compared to lean rats (Livingstone *et al.*, 2000). A different study further confirmed the decrease in 11β-HSD1 mRNA in the liver of obese mice (Liu *et al.*, 2003). In contrast, a later publication showed an increase in 11β-HSD1 mRNA and activity in obese compared to lean mice (Morton *et al.*, 2005). In obese humans compared to lean counterparts, 11β-HSD1 activity is increased in subcutaneous AT (Rask *et al.*, 2001, 2002; Paulmyer-Lacroix *et al.*, 2002; Wake *et al.*, 2003; Desbriere *et al.*, 2006). However, at least one contradictory study suggests otherwise (Tomlinson *et al.*, 2002). In contrast, in visceral AT, both increased

(Desbriere *et al.*, 2006) and unchanged (Goedecke *et al.*, 2006) expression of 11β-HSD1 mRNA concentration have been reported in obese subjects compared to healthy age-matched controls. This contradiction could be due to the fact that in the first mentioned study, lean vs obese women were examined (23 – 50 years of age), whereas, in the second study, premenopausal women (24 – 53 years of age) were examined. Thus, age and obesity may influence the relative expression of 11β-HSD1 in visceral vs subcutaneous AT. In contrast to obesity, only one study has examined 11β-HSD1 activity and mRNA expression during CR (Loerz *et al.*, 2017). This study incorporated a porcine and a mouse model and revealed that 11β-HSD1 regulation following CR and re-feeding is species-dependent (Loerz *et al.*, 2017). Thus, in the mouse liver, mRNA was not changed between the AL-and CR-fed mice but it was increased in the CR-fed mice following re-feeding. However, protein levels showed the opposite results, while 11β-HSD1 activity was significantly increased post-CR and re-feeding. Moreover, in the porcine model 11β-HSD1 was unaltered in liver, AT and skeletal muscle following CR and re-feeding (Loerz *et al.*, 2017). These results further confirm that regulation of 11β-HSD1 is species-dependent. However, for better comparison between the two models, mouse AT should have been included.

It is unknown if the effects of obesity and CR on activity and expression of 11β-HSD1 are similar between WAT and BMAT. Given that both of these adipose depots increase with obesity and HFD, it is possible that they also share similar responses in terms of 11β-HSD1 function. However, considering the divergent effects of CR on WAT and BMAT, a key question is whether CR elicits differential effects on 11β-HSD1 function, and indeed GC action, in WAT and BMAT. This is important to establish considering the insights that may be revealed from better understanding the formation and function of BMAT during CR.

1.3.1.2. 11β-HSD1 deficiency

Intracellular GCs are not only determined by systemic levels within the plasma, but also by intracellular levels that are regenerated from inert-11 keto forms by 11β-HSD1. To further understand the importance of this enzyme *in vivo*, a 11β-HSD1 knockout mouse model was first created in 1997, with exons 3 and 4 of the *Hsd11b1* gene replaced with a neomycin-resistance cassette (Kotelevtsev *et al.*, 1997).

However, this KO model proved to be hypomorphic (partial loss of gene function) and continues to express *Hsd11b1* in lung and kidney (Yang, 2010). Hereinafter, this KO model will be referred to as the 'hypomorphic' 11β-HSD1 KO. An improved model was later created, with Cre-LoxP deletion of exon 3 in a C57BL/6 genetic background, completely lacking activity of 11β-HSD1 (Vandermosten *et al.*, 2017; Zhang *et al.*, 2017; Verma *et al.*, 2018). Indeed, these improved 11β-HSD1 KO mice did not regenerate corticosterone from 11-DHC, and 11β-HDS2 was not affected by the knock out. This further confirmed 11β-HSD1 as the predominant or sole 11β-reductase in the body. Hereinafter, this improved KO model will be referred to as the 'null' 11β-HSD1 KO. In addition to the null 11β-HSD1 KO model, a third 11β-HSD1 KO model was generated by Semjonous *et al.,* (2011). Compared to the hypomorphic and null 11β-HSD1 KO model, this model was generated by removing exon 5 with LoxP sites (Semjonous *et al.*, 2011). This model will be referred to as the 11β-HSD1 'exon 5' KO.

Previously, the hypomorphic 11β-HSD1 KO male mice on a MF1/29 background were used to investigate HPA axis regulation compared to age-matched controls. Overnight, circulatory corticosterone and ACTH concentration were significantly increased in the KO mice. Upon stress, corticosterone and ACTH concentrations were further increased, with an extended fall in concentration post stress. These observations implied that the KOs had increased basal HPA axis activity with reduced GC feedback, presumably to make up for the lack of intracellular regeneration of corticosterone (Harris *et al.*, 2001). In addition, in a different strain of KOs, C57Bl/6J, these results differed. Plasma corticosterone and ACTH concentrations were not increased as in the MF1/29 strain. Furthermore, C57Bl/6J 11β-HSD1 KOs have an increase in plasma corticosterone at only 10 min post restraint, whereas at 45-and 90-minutes, no genotype differences were present. ACTH concentration was increased in both genotypes post 10 minutes of restraint, but returned to baseline levels after 45 and 90 minutes, with no genotype differences at any time point (Carter *et al.*, 2009).

The hypomorphic KO model was also shown to be protected from obesity, hyperglycaemia and dyslipidaemia induced by HFD (Kotelevtsev *et al.*, 1997; Morton *et al.*, 2004). However, in the newer, null KO model, this finding was not reproducible (K. Chaman, personal communication). In addition, pharmacological inhibition of 11β-

HSD1 in Apolipoprotein E (*Apoe*) KO mice prevented atherosclerosis progression, as well as further improving glucose tolerance and lowered triglycerides and FFA (Hermanowski-Vosatka *et al.*, 2005). Furthermore, a different publication also treated Apolipoprotein E KO mice with an 11β-HSD1 inhibitor, which reduced atherosclerosis by 74-76% but without influencing lipids or glucose (Kipari *et al.*, 2013). A double knockout of Apolipoprotein E KO and 11β-HSD1 KO mice was generated and showed a greater reduction in atherosclerosis compared to the inhibition of 11β-HSD1 only. Transplantation of BM cells from the double knockout to the Apolipoprotein E KO mice further reduced atherosclerosis by 51%. These results suggest that 11β-HSD1 inhibitors could have beneficial effects on atherosclerosis, especially via effects on BM cells (Kipari *et al.*, 2013). However, the 11β-HSD1 KO model used in the publication was the original, hypomorphic KO; it remains to be investigated if the improved KO model has the same effects. A different study looked at metabolic consequences of the lack of 11β-HSD1, specifically focusing on lipid and lipoprotein profile (Morton *et al.*, 2001). Plasma triglyceride levels were decreased in AL-fed hypomorphic 11β-HSD1 KO mice compared to WT controls. The KOs also had increased HDL cholesterol, with increased liver mRNA and serum concentrations of apolipoprotein A1 (protein component of HDL). Moreover, AL-fed KOs had significantly increased circulating corticosterone concentration, but with neither fasting nor re-feeding, the concentration in the KOs did not vary compared to the WTs, suggesting a deficiency in intracellular GCs in times of stress (Morton *et al.*, 2001).

These effects of 11β-HSD1 on cardiovascular risk and metabolic function also extend to situations of systemic GC excess. Thus, Tomlinson *et al.,* revealed that a 20-year old student with CS did not exhibit the classic phenotypes of this syndrome and instead had normal adipose distribution, lacked muscle weakness and had ideal blood pressure (115/70 to 122/82 mm Hg). In addition, she had mildly increased circulating cortisol but highly increased urine cortisol. Furthermore, cortisol to cortisone ratio was low, suggesting a partial defect of 11β-HSD1 activity (Tomlinson *et al.*, 2002). Likewise, a later publication showed similar results from a patient lacking the CS phenotype with a defect in 11β-HSD1 activity (Arai *et al.*, 2008). These studies suggest that deficiency and/or a defect in 11β-HSD1 activity could improve the side effects of CS. More recently, 11β-HSD1 has been revealed to be a regulator of tissue-specific effects of circulating GC excess in mice (Morgan *et al.*, 2014). Global 11β-

HSD1 exon 5 KO mice were protected from glucose intolerance, hyperinsulinemia, hepatic steatosis, adiposity and further symptoms of CS compared to age-matched controls. In addition, hepatocyte-specific 11β-HSD1 exon 5 KO male mice developed a full CS phenotype, but adipocyte-specific KO male mice did not (Morgan *et al.*, 2014). In humans, 11β-HSD1 inhibitor INCB13739 has shown to increase morning plasma ACTH and DHEAS levels in T2D patients. Four weeks in the treatment, the hormones increase, but they do not exhibit a further increase at week twelve, not even with the highest concentration treatment. ACTH and DHEAS concentrations return to baseline three weeks post the final treatment. Morning cortisol was unaltered by the inhibitor throughout the treatment, suggesting that the increase in ACTH might have been a compensatory response. Androstenedione, an androgen steroid hormone showed a dose-related increase in morning fasting serum. Testosterone was unaltered in male patients, but increased in a dose-related manner in the females (Rosenstock *et al.*, 2010). Overall, this treatment improved the patient's hyperglycaemia and it also indicates a functional HPA axis function post treatment. A different 11β-HSD1 inhibitor, MK-0916, showed similar results in T2D patients with increases in androstenedione, DHEA and DHEAS concentrations (Feig *et al.*, 2011). However, female patients did not have an increase in testosterone as they did with the INCB13739 inhibitor. Testosterone concentrations were not reported for men (Feig *et al.*, 2011). Overall, these data from animal and human research further support that concept that inhibition of 11β-HSD1, systemically or within adipose tissue only, may be a potential approach to treat CS and protect against metabolic disease. Whether it can also modulate GC action in other conditions of increased GCs, such as ageing or CR, remains to be determined.

1.3.1.3. Role of 11β-HSD1 in bone cells

The latter point is of interest in the context of bone loss and BMAT expansion. Firstly, a short description about bone remodelling. The formation of bone can be regulated by two different ways. Firstly, the conversion of MSCs into bone (intramembranous ossification) which primarily occurs in the skull. Secondly, endochondral ossification, the formation of a cartilage intermediate followed by being converted into bone by osteoblasts (further reviewed Berendsen and Olsen, 2015; Katsimbri, 2017; Klar, 2018). Throughout life, bone is further remodelled and regenerated by the interplay of osteoblasts (bone forming cells) and osteoclasts (bone resorption cells). Cortical

bone remodelling is more complex than trabecular but it not remodelled as often as trabecular. Bone remodelling consists of three stages: resorption, reversal and formation. During resorption, osteoclasts produce irregular cavities on the bone surface, followed by reversal where the osteoclasts enter apoptosis and mononuclear cells emerge on the surface. Thereafter, numerous proteoglycans are deposited on the surface, allowing the differentiation and proliferation of osteoblasts. Finally, during formation osteoblasts deposit osteoid that is transformed into mineralised bone (Berendsen and Olsen, 2015; Katsimbri, 2017; Klar, 2018). Bone metabolism is controlled by numerous signalling pathways. FGF, BMP and the Wnt signalling pathway are vital for osteoblast differentiation. Transcription factors such as RUNX2 and osterix are also important for osteoblast differentiation (Javed, Chen and Ghori, 2010; Lin and Hankenson, 2011). To maintain healthy bone mass and strength, bone must be continuously replaced.

The effects of GCs on bone are well described, both for negative and positive outcomes. The negative outcomes include decreased osteoblast differentiation, apoptosis of osteoblasts/osteocytes and increased osteoclastic bone resorption, resulting into GC-induced osteoporosis (GIO). In contrast, the positive outcome is the increased differentiation of osteoblasts, resulting in greater bone formation. This was also shown by transgenic 11β-HSD2 mice (Sher *et al.*, 2004). Different strains of mice have been shown to be affected differently by excess GCs. GIO was induced in both C57Bl/6J and CD1 mice over 56 days, however, the C57Bl/6J mice osteoclast and osteoblast were not as responsive to GCs as CD1 mice. Furthermore, C57Bl/6J mice were not susceptible to bone changes associated with GIO (Ersek *et al.*, 2016). GIO is the consequence of reduced osteoblast differentiation and osteocyte function, and increased osteoclast differentiation, resulting in decreased bone mass which further increases the risk of fractures. GC administration in mice has shown that GCs directly act on osteoclasts by increasing their lifespan, resulting in bone loss (Jia *et al.*, 2006; Henneicke *et al.*, 2011; Zhou, Cooper and Seibel, 2013). However, the suppression of osteoblasts and osteocytes plays a bigger role in GIO, as shown in both clinical and experimental data (O'Brien *et al.*, 2004; Zhou, Cooper and Seibel, 2013). 11β-HSD1 exon 5 KO mice treated with corticosterone for four weeks showed almost a complete protection against bone loss compared to WT mice, who had decreased bone volume. Compared to the above-mentioned study regarding strain difference, this study treated the mice with 100μg/ml corticosterone (Fenton *et al.*, 2019). Therefore, it is worth acknowledging that the dose, duration and strain are all

important factors. Further effects of GCs on bone cells and GIO models are reviewed by Wood *et al.,* (2018). Briefly described, most GIO models are in mice as they share more than 95% of the human genome and have been identified as appropriate pre-clinical models of GIO (Wood *et al.*, 2018). Osteoblasts and osteocytes are the main bone cells in humans that express 11β-HSD1, although osteoclasts can also express it (Cooper *et al.*, 2000). Besides increased levels of circulatory GCs, 11β-HSD1 expression and activity has also been reported to be up-regulated in *ex vivo* cultured human osteoblasts with ageing and with GC administration (Cooper *et al.*, 2002) and in mouse bones (Weinstein *et al.*, 2010). Bone expression of 11β-HSD1 is significantly up-regulated in aged (25-31 months old) compared to young (4 months old) male and female mice (Weinstein *et al.*, 2010). Moreover, in aged humans (61 – 73 years of age) a negative association was indeed revealed between circulatory cortisone concentration and serum osteocalcin (Cooper *et al.*, 2005). No correlations were found between cortisol and bone markers. However, a different study showed that in response to ACTH, a positive association was found between cortisol and the loss of mineral density in the spine of men (Reynolds *et al.*, 2005). In women, cortisol was associated with increased femoral bone loss rate. As GC concentration and bone expression of *Hsd11b1* both increase with ageing, it suggests age-induced bone loss is associated with increases in GCs.

Cooper *et al.,* investigated the role of 11β-HSD1 activity in predicting GC effects on bone. Healthy men on 5 mg prednisolone for seven days showed decreased bone formation but unaltered bone resorption markers. The decreased bone formation was strongly correlated with increased 11β-HSD1 activity, suggesting that the enzyme activity could predict susceptibility to GIO (Cooper *et al.*, 2003).

Genome-wide association studies have further implicated 11β-HSD1 in age-associated bone loss (Hwang *et al.*, 2009; Feldman *et al.*, 2012). A polymorphism in the *HSD11B1* gene is associated with reduced BMD and an increased risk of fractures in postmenopausal women (Hwang *et al.*, 2009). A different study examined whether *HSD11B1* gene polymorphisms could affect bone in healthy and postmenopausal osteoporotic women. One of twelve single nucleotide polymorphisms (SNPs) showed an association with higher BMD in the spine in both groups. Further *in vitro* work on this SNP showed suppression of 11β-HSD1, suggesting a beneficial effect of the SNP to reduce the regeneration of GCs and their detrimental effects on bone (Feldman *et al.*, 2012).

Several 11β-HSD1-selective inhibitors have been proposed to protect against GIO, with one of them being BVT.2733 (Wu *et al.*, 2013). Overexpression of 11β-HSD1 in mouse osteoblast precursor cells resulted in increased 11β-HSD1 activity and decreased osteogenic differentiation. However, the addition of the inhibitor *in vitro* returned the osteogenic genes to normal levels, suggesting bone formation may also be restored in the face of GC excess *in vivo.*

Up until now, several studies have addressed the function of 11β-HSD1 in bone (Tomlinson *et al.*, 2004; Gathercole *et al.*, 2013; Zhou, Cooper and Seibel, 2013; Fenton *et al.*, 2019) but very little is known about its function in the BM and BMAT. Gathercole *et al.,* (2013) published a review about translational and therapeutic aspects of 11β-HSD1 in metabolism, bone, cardiovascular diseases, inflammation, ageing and nervous system, and only mentioned BM as one of many stromal cell types in which 11β-HSD1 expression and activity are increased with inflammation. Justesen *et al.,* (2004) investigated BMAT as well as the bone phenotype in the hypomorphic 11β-HSD1 KO mice. They reported that these KO mice lack BMAT but do not exhibit any other obvious bone phenotype. These results could infer that the lack of BMAT is not necessary for normal bone development and remodelling. However, Coutinho *et al.,* (2012) later demonstrated histologically that the hypomorphic KO mice do not lack BMAT (Coutinho *et al.*, 2012). Subsequently, our lab has also shown that, on a normal diet, the null 11β-HSD1 KO mice have a normal BMAT phenotype; this latter finding is based on osmium tetroxide staining, which, as described in the Methods (Section 2.6), allows BMAT quantification in intact whole bones, *ex vivo,* and is emerging as the gold-standard for BMAT quantification. It is important to reiterate that the data from Coutinho *et al.,* (2012) and Justesen *et al.,* (2004) used the hypomorphic KO model, whereas in our lab, we used the more-robust null 11β-HSD1 KO model.

Beyond these studies, there is no other direct evidence for a role of 11β-HSD1 in BMAT. On balance, these data show that lack of 11β-HSD1 does not robustly influence BMAT development, at least in a normal developmental and physiological context. However, a key goal for my thesis was to determine the basis for BMAT formation during CR and ageing, which, as discussed below, are conditions often characterised by GC excess.

1.3.2. Glucocorticoids: Possible mediators of BMAT expansion and bone loss during CR and ageing

As briefly mentioned in Section 1.2.4, GCs have been postulated to regulate BMAT expansion. In terms of the association between GCs and BMAT, several studies show effects of GCs in a therapeutic context. For example, CR has been reported to elevate circulating GCs (cortisol in humans, corticosterone in rodents) (Sabatino *et al.*, 1991; Patel and Finch, 2002; Chacón *et al.*, 2005; Levay *et al.*, 2010; Pankevich *et al.*, 2010; Tomiyama *et al.*, 2010; Cawthorn *et al.*, 2016; Fontana *et al.*, 2016). In addition, besides increased GCs and BMAT volume, CR has been well established to slow the ageing process and to prolong lifespan. Although increased longevity is a positive outcome of CR, negative outcomes of ageing, such as physical, mental and cognitive impairment are common (Kehler, 2019). This means poor health with ageing, including bone loss, increased BMAT and the risk of fractures, as previously discussed in Section 1.2.2.1. Indeed, ageing-related chronic disease is currently a major burden on public health worldwide (James *et al.*, 2018). It is therefore important to understand the association between bone loss and increased BMAT with ageing, and if GC action contributes to these outcomes. Besides CR in animals and humans, AN in humans is strongly associated with circulatory (Boyar *et al.*, 1977; Walsh *et al.*, 1978; Misra *et al.*, 2004; Lawson *et al.*, 2009) and salivary (Putignano *et al.*, 2001; Oskis *et al.*, 2012; Paszynska *et al.*, 2016) hypercortisolaemia (Luz Neto *et al.*, 2019). Hypothalamic CRF secretion has been reported to decrease with CR (Brady *et al.*, 1990; Lindblom *et al.*, 2005), whereas ACTH was shown to either be reduced (Chacón *et al.*, 2005) or unaltered (Levay *et al.*, 2010) with CR. This could mean that the HPA axis responses could also be attenuated. A different study examined the responses of CR and stress on the HPA axis in rats, and besides increased circulatory corticosterone concentration, no other changes were detected (Kenny *et al.*, 2014). This suggests a beneficial effect of CR to retain stress responses.

A study in humans showed similar responses compared to rodents. Obese volunteers underwent 30% CR for 12 weeks, and although they lost significant weight, the restriction did not influence the HPA axis. For example, basal cortisol and 11β-HSD1 activity were not changed compared to at the end of the 12 weeks (Ho *et al.*, 2007). In contrast to CR, obesity has been shown to dysregulate the HPA axis (further reviewed in more detail (Seimon *et al.*, 2013)), with increased ACTH and cortisol

concentration. However, both short-and long-term food restriction in obese men and women has shown either no change (Ho *et al.*, 2007; Tomlinson *et al.*, 2008), decrease (Giovannini *et al.*, 1990; Hainer *et al.*, 1992; Vilà *et al.*, 2001; Espelund *et al.*, 2005; Pasiakos *et al.*, 2011) or an increase (Johnstone *et al.*, 2004) in cortisol concentration. One limitation to the above studies is that they focus on CR as a weight loss intervention in obese individuals: although this brings health benefits, it is distinct from CR in normal-weight subjects, in which CR is of interest to further improve health span. In this regard, one study investigated food restriction in non-obese men and women and showed a significant increase in circulatory cortisol concentration (Fontana *et al.*, 2016). Moreover, patients with AN do not only exhibit increased BMAT, but also hypercortisolaemia (Boyar *et al.*, 1977; Walsh *et al.*, 1978; Misra *et al.*, 2004; Lawson *et al.*, 2009). These observations confirm that the BMAT and GC relationship extends to conditions of energy deficit in humans, and not just in animal models. The obese subjects showed contradicting effects in response to fasting, whereas the non-obese and AN subjects showed increased circulating cortisol concentrations. These disparate findings might therefore be due to age, sex and body mass differences in the individuals studied.

To summarise, evidence from non-obese subjects, AN patients and CR-fed animals presents a similar finding: that GC excess and BMAT accumulation coincide in these conditions. Other evidence for this relationship in humans is based on MRI-scanned GC-treated pre-menopausal women. The patients presented BMAT expansion, bone loss and higher risk of developing osteoporosis, suggesting an association between increased BMAT volume and GC exposure (Vande Berg *et al.*, 1999). To add to this conclusion, one *in vivo* study further elucidated these relationships in CR-fed mice and rabbits (Cawthorn *et al.*, 2016). Here, circulating corticosterone and BMAT were elevated in male and female mice during CR, whereas neither corticosterone, cortisol nor BMAT was altered during CR in rabbits. This supports the possibility that GC excess is required for BMAT expansion during CR. Further *in vitro* experiments support this association between GCs and BMAT expansion. *In vitro* treatment of human femoral head BM MSCs with dexamethasone increased BM adipogenic differentiation as well as enlarging adipocyte size (Kitajima *et al.*, 2007), suggesting that GCs do increase BMAd differentiation and lipogenesis. Likewise, dexamethasone treatment of rat and mouse BM MSCs resulted in similar findings, with an increase in BM adipogenic differentiation and target genes, and reduced bone transcription factors (Yin, Li and Wang, 2006; Lin, Dai and Fan, 2010). Progressive

changes in BMAds were reported in GIO and osteonecrosis in rabbits. Small-sized BMAds were significantly increased in the early stage of the treatment, with the total volume increasing later on (Li *et al.*, 2013; Sheng *et al.*, 2013). Overall, the *in vivo and vitro* results show that GCs can directly promote BMAT expansion. The hypercortisolaemia that occurs alongside CR-induced BMAT expansion could be associated with changes in the HPA axis that have yet to be explored. The previous findings of Morgan and colleagues (2014) shows that lack of 11β-HSD1 can block the effects of GC excess (Morgan *et al.*, 2014), even if it does not prevent BMAT formation in normal conditions (Coutinho *et al.*, 2012). Based on the presented evidence, further and more in-depth research is necessary to comprehend the regulation behind CR-induced BMAT expansion. For this reason, my PhD research focused on GCs as potential mediators of CR-induced BMAT expansion. My rationale for addressing this hypothesis was that, by understanding the formation and function of BMAT during CR, we might further understand if/how BMAT contributes to the health benefits of CR; we might be able to treat CR-and age-related bone loss by preventing BMAT expansion, or by targeting BMAT to improve other adverse conditions such as obesity; and, finally, that understanding the association between increased GCs and BMAT might aid the development of new treatments for conditions involving bone disease and excess GCs, such as CS.

1.4. Hypothesis and aims

1.4.1. Hypothesis

Based on the preceding evidence, my hypothesis is:

11β-HSD1 contributes to GC excess that mediates BMAT expansion and bone loss during CR and ageing.

BMAT and bone morphology have not previously been investigated in null 11β-HSD1 KO mice in conditions of GC excess. Since CR/AN, ageing and GC therapy are associated with increased BMAT and circulating GC concentration, and mice deficient in 11β-HSD1 can resist the consequences of excess GCs, I investigated if null 11β-HSD1 KO mice could resist CR-and age-induced BMAT expansion and bone loss.

My specific hypotheses are as follows:

1. CR contributes to increased GC action within AT and BM
2. 11β-HSD1 KO mice resist CR-induced BMAT expansion
3. 11β-HSD1 KO mice resist CR-induced bone loss
4. Age-associated GC excess contributes to BMAT expansion and bone loss.

1.4.2. Aims

My PhD research aimed to test the above-mentioned hypotheses, by determining if GC excess mediates BMAT expansion and bone loss during CR and ageing. I sought to address this aim by using null 11β-HSD1 KO and WT male and female mice. My rationale for using this model is that these KO mice also resist the effects GC excess in the context of exogenous corticosterone administration (Morgan *et al.*, 2014).

My specific aims were as follows:

1. Firstly, to identify if GC action is increased in BM and AT during CR in WT mice.

2. Secondly, determine if the lack of intracellular regeneration of corticosterone (KO of 11β-HSD1) prevents BMAT expansion.
3. Thirdly, to identify if the lack of intracellular regeneration of corticosterone (KO of 11β-HSD1) prevents bone loss with CR.
4. Finally, to establish if the lack of intracellular corticosterone regeneration (KO of 11β-HSD1) prevents bone loss and BMAT expansion with ageing.

To test the hypotheses, quantification of GCs in the circulation and within BM, as well as analysis of GC target gene expression in BM and AT, were performed. Moreover, BMAT and bone morphology were also analysed in the younger mice undergoing CR (and *ad libitum*-fed controls), and in *ad libitum*-fed older mice.

Chapter 2. Methods

2.1. Animal care and caloric restriction

2.1.1. Animals

The mice were kept and experimented under humane conditions in accordance to the Animal (Scientific Procedures) Act UK 1986, with the 3Rs (replacement, reduction and refinement) implemented wherever possible.

Global HSD11β1$_{Del1/Del1}$ (KO) mice were received by Karen Chapman (University of Edinburgh) within the same animal facility, Bioresearch and Veterinary Services (BVS), Little France, Edinburgh, UK. The KO mice are carrying a null allele of *Hsd11b1*, generated by Cre-LoxP deletion of exon 3 in a C57BL/6JOlaHsd genetic background, completely lacking activity of 11β-HSD1 (Vandermosten *et al.*, 2017; Zhang *et al.*, 2017; Verma *et al.*, 2018). The KO mice were generated by mating heterozygous males and females. The experiment used KO male and female mice with age-matched C57BL/6J mice as controls (WT). The mice were housed individually or in groups of 2-5 mice per cage and kept under controlled conditions (7:30am to 7:30pm light/dark cycle, 21°C) with *ad libitum* (AL) access to water and regular rodent chow (Special Diet Services, UK), unless stated otherwise.

2.1.2. Caloric restriction

At 8 weeks of age, the mice were single-housed and the diet changed from standard chow to a low-fat control diet (Research Diets D12450B) to allow them to get used to the different food. The mice were weighed daily (Figure 2.1.A) to prevent loss either due to stress from being single-housed or due to adaptation to the new food. Daily AL-food intake was also recorded (Figure 2.1.B), firstly to ensure the mice were eating, and secondly, to identify the average food intake for calculating out the CR diet.

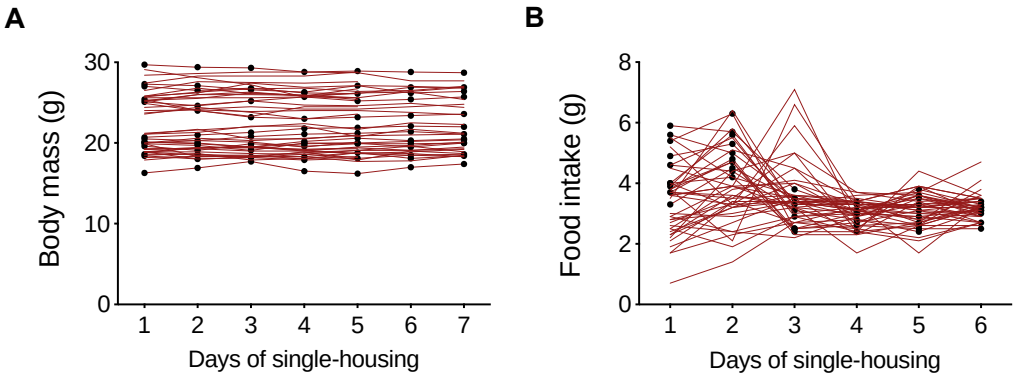

Figure 2.1. Body mass progression and food intake during the first week of diet change. (A) Body mass progression over the first week of single-housing. **(B)** Daily AL food intake during the first week of single-housing. Each point represents the weighed food mass eaten per day.

Post the first week of single-housing, the mice were randomly assigned to two equally sized groups, consisting of both males and females, for the time of one or six weeks. One group was assigned to AL food intake (Research Diets D12450B); the other group was assigned to a CR diet (Research Diets D10012703) at 70% of the previously calculated AL food intake (2.1g). Previous experiments (Devlin *et al.*, 2010; Cawthorn *et al.*, 2014), found that 70% of the AL food intake was sufficient to drive BMAT expansion and bone loss in mice. Therefore, it was a clear-cut decision to choose this method. The CR diet was enriched to prevent deficiency of micronutrients. Further details about the caloric information on the diets is described in Table 2.1.

Diet	***Ad libitum* control diet (D12450B)**		**Caloric restriction diet (D10012703)**	
Food group	grams	% (kcal)	grams	% (kcal)
Protein	19.2	20	18.9	20
Carbohydrate	67.3	70	66	70
Fat	4.3	10	4.2	10
kcal/gram	3.85		3.77	

Table 2.1. Caloric information on *ad libitum* control and caloric restriction diet.

Throughout the one or six-week period, all mice were monitored and weighed daily for the first two weeks (mice on six-week CR) or for the entire one week (mice on one-week CR) of the CR experiment, ensuring their body weight did not exceed loss of 30% of their current body weight. Afterwards, the mice were still monitored daily, but weekly weighed only. If their body weight did not exceed loss of 30% of their starting

body mass in the first two weeks, it meant they were maintaining a suitable body weight.

2.1.3. Weakly measurements

Post the weekly body weights, blood glucose was also weekly measured to monitor the mice for hypoglycaemia, by a blood glucose meter (OneTouch Verio® meter or OneTouch Verio® IQ meter). Blood sampling was weekly collected in the morning, approximately 09:00, before feeding the CR mice. Blood was collected from the tail vein in Ethylenediaminetetraacetic acid (EDTA)-lined capillary tubes (Sarstedt, 16.444) and placed on ice until centrifuged down at 2000 rcf for 10 minutes at 4°C. Plasma was then collected and stored at -80°C until required.

Body composition was also weekly measured and recorded using time domain nuclear magnetic resonance (TD-NMR, Bruker). The TD-NMR measurement provided details regarding the mice body fat, lean mass and free fluid. It allows to measure body composition without harming the mice, using radio-frequency energy, allowing non-destructively analysing the entire sample volume. The mice are inserted in plastic tubes that are provided by Bruker, followed by gently pushing the mice at the end of the tube with the inserter which will then lock onto the tube to keep the mice safely inside. The tube will then be inserted into the TD-NMR machine for approximately 20-30 seconds. Once the scanning is complete, the values for body fat, lean mass and free fluid are provided as absolute mass. The tube will then be removed from the TD-NMR, and opened above the cage to release the mouse.

2.2. Genotyping

Initially, I started performed the genotyping myself. However, to save time, I provided these primers and amplicon details to Transnetyx so that subsequent genotyping could be done by sending ear clips to them. Genotype was then further confirmed after euthanasia by qPCR measurement of *Hsd11b1* mRNA in adipose depots (iWAT and gWAT, figure 4.8) and the BM (Figure 4.12.A-B). The genotyping protocol is described below.

Primers

Flox 1F: CTTGCATGTGTTTGGTGTTGG

Flox 1R: AATGTTTCCAAATGCATTGTGGG

DEL 1F: GTGATGTCAGATCTACAGAAGG

Two reactions were used due to uncertainty of the results, as sometimes the bands were too weak to distinguish between the WT and KO: one using Flox 1F + Flox 1R primers, and the second one using DEL 1F + Flox 1R. The cycling conditions are the same for each reaction. DNA was extracted from the ear clips by adding them to 75µl of solution 1 (100ml dH_2O, 40µl of 0.5M EDTA, 0.1g NaOH), followed by incubation at 95°C for 30 minutes in a thermal cycler. Afterwards, 75µl of solution 2 (96ml dH_2O, 4ml 1M TRIS, adjust to pH 5.5) was added to neutralise the solution. Thereafter, it was kept on ice or stored at -20°C until use.

PCR reaction mix

Reagents	**Flox 1F + 1R reaction (µl)**	**DEL 1F + Flox 1R reaction (µl)**
5xQ solution (Qiagen Taq PCR Core Kit, 201225)	10	10
10x Buffer (Qiagen Taq PCR Core Kit, 201225)	5	5
dNTP (10mM) (Qiagen Taq PCR Core Kit, 201225)	1	1
Flox 1F primer (25µM)	2	-
Flox 1R primer (25µM)	2	2
DEL 1F primer (25µM)	-	2
Qiagen Taq (Qiagen Taq PCR Core Kit, 201225)	0.24	0.24
H_2O (VWR, SH30538.03)	26.8	26.8
Total Volume	47.04	47.04
DNA (from the earclip)	3	3

PCR cycling conditions

Cycle 1 (1 cycle)	95°C, 10 min
Cycle 2 (35 cycles)	95°C, 30 sec 63.2°C, 30 sec 72°C, 90 sec
Cycle 3 (1 cycle)	72°C, 10 min
Cycle 4 (1 cycle)	Hold at 4°C

2.3. Euthanasia and tissue sampling

2.3.1. Young mice on CR

At the end of the CR experiment, the day before termination, a final body composition measurement was performed using TD-NMR. The evening prior to termination, the mice on the six-week CR experiment were fasted. The AL fed mice had their food removed, and were given half a portion of the 70% of food that they were daily consuming (1.5 g). The CR fed mice were also given half a portion (1.05 g) of their 30% CR diet. Thereafter, they were fasted approximately 12 hours before dissections. The mice on the one-week CR experiment were not fasted prior to termination. They were equally scanned by TD-NMR the day prior to termination, but they were not fasted nor re-fed in the evening.

The morning of dissections, between 08:00 – 09:00, blood glucose was measured and tail vein blood collected. The mice were then transferred over to the department's *ex vivo* room, where they were culled between 09:00 – 11:00 by cervical dislocation, followed by decapitation to confirm death. Core blood was then collected from the site of decapitation and organs were harvested. Half of the tissues of the liver, both kidneys', both adrenal glands and the WAT, such as inguinal WAT (iWAT), gonadal WAT (gWAT), mesenteric WAT (mWAT) and BAT, were collected and placed in Eppendorf tubes containing 10% formalin (Sigma Life Science, HT501320-9.5L), and the other halves of tissues were placed in empty Eppendorf tubes stored on dry ice. The spleen and thymus were placed in 1x PBS (Gibco, 14190-094) in preparation for flow cytometry analysis. The heart, caudal and lumbar vertebrae were merely collected for storage in 10% formalin. One of each of the long bones collected, two tibiae, two femurs, two humeri and two forearms, were placed in 10% formalin, and the others on dry ice.

2.3.2. Aged mice

At approximately 42-and 70-weeks of age, the WT control and 11β-HSD1KO mice were the appropriate age for the ageing experiment. Throughout the 42-and 70-weeks, the mice were seldom handled. When they reached the appropriate age, the mice were weighed and also scanned for body composition, specifically for the fat mass, by TD-NMR.

Prior to dissections, the mice were fasted for one hour. An hour later, blood was collected from the tail vein. Thereafter, the mice were transferred over to the *ex vivo* room of the department where they were culled by cervical dislocation, followed by decapitation to confirm death. Core blood was then collected from the site of decapitation and organs were harvested as previously, apart from the spleen and thymus which were collected for formalin only.

2.4. Transcript quantification

2.4.1. Frozen tissue homogenisation using mortar and pestle

The frozen adipose depots were put on dry ice to remain cold. The mortar and pestle were also put on dry ice and liquid nitrogen was poured over them to accelerate the cooling down process. The frozen AT was put in the mortar and liquid nitrogen was poured over the tissue and grounded up using the pestle. Once the tissue was ground up, a small amount of liquid nitrogen was added while mixing the tissue with a pre-chilled spatula towards one side of the mortar. Half of the tissue was then transferred using the spatula into a new 1.5 mL tube for RNA isolation, and half was transferred to a different 1.5 mL tube for DNA/protein isolation. The top of the tubes were punctured to prevent explosion. Once all AT were ground up, RNA was isolated.

2.4.2. RNA isolation of AT and whole bone

1. 600 μL of Ribozol (VWR chemicals, N580) was added to each tube with the powdered tissue specifically for RNA isolation. It was then mixed using the tip of a 21G needle in a 1.5 mL syringe, and then aspirated into the syringe gradually to dissolve clumps.
2. Further 600 μL of Ribozol was added and resuspended through the needle until a homogenous lysate was produced. Clumps of tissue that did not go through the needle were worn down by scraping between the needle tip and the side of the tube, or removed.
3. Once homogenised, the solution was stored at room temperature for 10 minutes.

4. **For AT**
    a. Due to AT containing high lipid content, a layer of lipid was formed above the homogenate,

b. The lipid layer was removed and replaced with the same volume of fresh Ribozol.

5. The homogenate was moved to a new tube due to having a punctured lid from the grinding stage.
6. 240 μL chloroform (Fisher Scientific, C/4960/17) was then added to the homogenate and shaken for 20 seconds, followed by allowing it to rest at room temperature for 2-3 minutes.
7. Thereafter, it was centrifuged in a microfuge at 4°C for 15 minutes at 15,000 rcf, resulting into an upper aqueous phase (clear), a thin interphase (white solid) and a lower organic phase (pink).
8. The upper aqueous phase was transferred to a new 1.5 mL tube containing 700 μL isopropanol (VWR chemicals, 20842.323). The samples were then mixed by inverting the tubes 4-5 times, then incubated at room temperature for 15 minutes, following centrifugation at 18,000 rcf for 60 minutes at 4ºC.
9. The supernatant was transferred into a labelled tube, in case sample was lost.
10. The pellet was then washed with 75% ethanol (VWR chemicals, 20821.330) (1.5 mL per sample) and gently vortexed so that the pellet floated up in the ethanol, and then centrifuged at 12,000 rcf for 5 minutes at 4°C.
11. The above step (10) was repeated, but the ethanol was discarded in the waste.
12. After the second centrifugation, the ethanol was removed and the tubes were put open on a 55°C heating block until leftover ethanol had evaporated.
13. Thereafter, the pellets were resuspended in 35 μL RNase-free water (Omega BIO-TEK, PD092) and put on ice while quantifying for RNA by NanoDrop. The RNA was then stored in the freezer at -80C° until reverse transcription was performed.

2.4.3. RNA isolation of BM

1. 0.5 ml and 2 ml Eppendorf tubes were prepared ahead. The 0.5 ml tubes had their ends cut off, and the 2 ml tubes contained 100 μl Ribozol and were labelled with the corresponding mouse ID number.

2. **For isolation from bones stored at -80°C**
    a. The tibia was quickly removed off the dry ice, and the ends were cut off using a razor blade. The tibia was then put back on dry ice in its corresponding 0.5 ml tube.
    b. The 0.5 ml tube containing the tibia was then quickly inserted into a 2 ml tube, and put into the centrifuge to spin down the BM into the 2 ml tube.
    c. The BM was centrifuged down into the 2 ml tube at 8000 rcf for 1-2 minutes.

3. **For isolation from freshly dissected bones**
    a. Soft tissue was quickly removed off the tibia. The ends of the tibia were then cut off using a razor blade.
    b. The tibia was then inserted inside the 0.5 ml tube, followed by inserting the 0.5 ml tube in the 2 ml tube that already contained 100 μl Ribozol, and then put into the centrifuge to spin down the BM into the 2 ml tube.
    c. The BM was centrifuged down at 8000 rcf for 1 minute.

4. 500 μL of Ribozol was further added to each tube with the BM. It was then mixed using the tip of a 21G needle in a 1.5 mL syringe, and then aspirated into the syringe gradually to dissolve clumps.
5. Once homogenised, the solution was stored at room temperature for 10 minutes.
6. Thereafter, the solution was stored in the freezer at -80°C until all samples were homogenised and ready for the next stage.

7. Once all samples were homogenised, the 2 ml Eppendorf tubes containing Ribozol and homogenised BM were taken out and allowed to defrost on ice.
8. The samples were then vortexed for approximately 10 seconds each.
9. 120 μL chloroform was then added to the homogenate and shaken for 20 seconds, followed by incubating at room temperature for 2-3 minutes.
10. Thereafter, it was centrifuged at 4°C for 15 minutes at 15,000 rcf.
11. The upper aqueous phase was transferred to a new 1.5mL tube containing 200 μl 70% ethanol, and vortexed. From this step onwards, the RNeasy Mini Kit (QIAGEN, 74106) protocol was followed.

12. The entire sample was transferred to a RNeasy Mini spin column in a 2 ml collection tube, followed by centrifugation for 20 seconds at 10000 rcf. The flow-through was discarded.
13. 700 μl of buffer RW1 was added to the column, and centrifuged as previously mentioned. The flow-through was discarded.
14. 500 μl of buffer RPE was added to the column, and centrifuged as before. The flow-through was discarded.
15. Further 500 μl of buffer RPE was added to the column, and centrifuged for 2 minutes at 10000 rcf.
16. The collection tube was then replaced with a new one, and centrifuged again for 1 minute at 10000 rcf to dry the membrane.
17. The RNeasy spin column was then placed in a new 1.5 ml collection tube, and 40 μl RNase-free water was directly added to the spin column, and left at room temperature for 10 minutes.
18. Thereafter, the tubes were centrifuged for 2 minutes at 10000 crf to elute the RNA.
19. The RNA was then put on ice while quantified and thereafter stored in the freezer at -80°C.

2.4.3.1. Optimisation of frozen BM isolation

The bones collected from the six-week CR mice were either put in formalin for BMAT analysis, or put on dry ice for RNA isolation for a later time. Previously, whole bone was crushed for gene expression. However, it was later realised that separating the bone from the BM would provide more reliable results in regards to what essentially happens in the BM. Since the tibiae were frozen at -80°C, a few tests were implemented to make sure the BM and bone RNA were not degraded throughout the process. A few of those tests incorporated different thawing processes of spare bones (on ice, at room temperature, in cold ribozol and in RNA later (Invitrogen, AM7020) including trying to speed the process up to avoid RNA degradation. Although the RNA isolation was abundant, the RNA was degraded compared to freshly flushed BM RNA (Figure 2.2).

RNA later Ice (Invitrogen, AM7030) is similar to RNA later, but allows frozen tissue/cells to thaw in the solution without RNA degradation. Whole bones were allowed to thaw in the solution, but also bones that had their end cut to allow the

solution to enter the BM straightforwardly. This process was performed a few times, allowing the bone to thaw in the solution for 5-10 minutes, up to 1 hour. The centrifugation of the BM failed when the bones were left in RNA later Ice for longer than 10 minutes due to the BM “drying out” and needing to grind it out of the bone with a needle after cutting through the bone to open it up. It was therefore concluded that RNA later Ice was not adequate. Because of the failed optimisations of obtaining undegraded RNA from the frozen bones, the next step taken was to work with the degraded RNA. The frozen BM was compared to fresh BM RNA, and the results were analysed for comparisons. The BM was isolated from spare frozen and fresh bones (from the same mouse, i.e. left and right tibia), and RNA was isolated as previously described and reverse transcribed as in the next section (Secton 2.3.4). The following housekeeping genes were analysed: *18s, Actb, Gapdh, Ppia* and *Tbp*. *Hsd11b1* and *Fabp4* were used as genes of interest. Average CT values were compared as raw data, but also based on standard curve made from the samples. The fresh samples gave lower CT values (greater amount of target nucleic acid in the sample) compared to the frozen samples that gave approximately 1.5 CT values higher. The frozen samples followed a similar pattern to the fresh ones, suggesting that the results would be marginally reliable, but showing lower amounts of the target nucleic acids. A few examples are shown in Figure 2.3. Based on the comparison to the fresh BM samples, it was decided that the frozen BM would be used anyway, but analysed with caution.

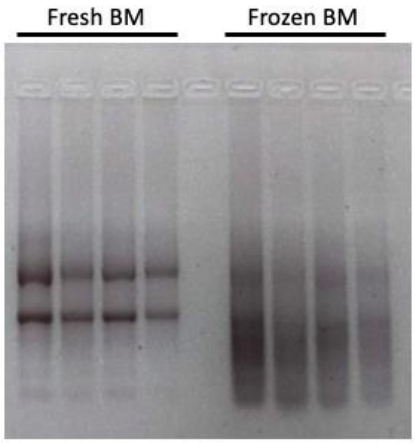

Figure 2.2. Comparison of fresh vs frozen BM RNA on 1% agarose gel. The BM was isolated from spare frozen and fresh bones (from the same mouse, i.e. left and right tibia), followed by RNA isolation and reverse transcription. Thereafter, 1% agarose gel was prepared to run the samples. The two lines below the fresh BM represents the 28/18S intact ribosomal RNA. The RNA below the frozen BM lack the lines, suggesting degraded RNA.

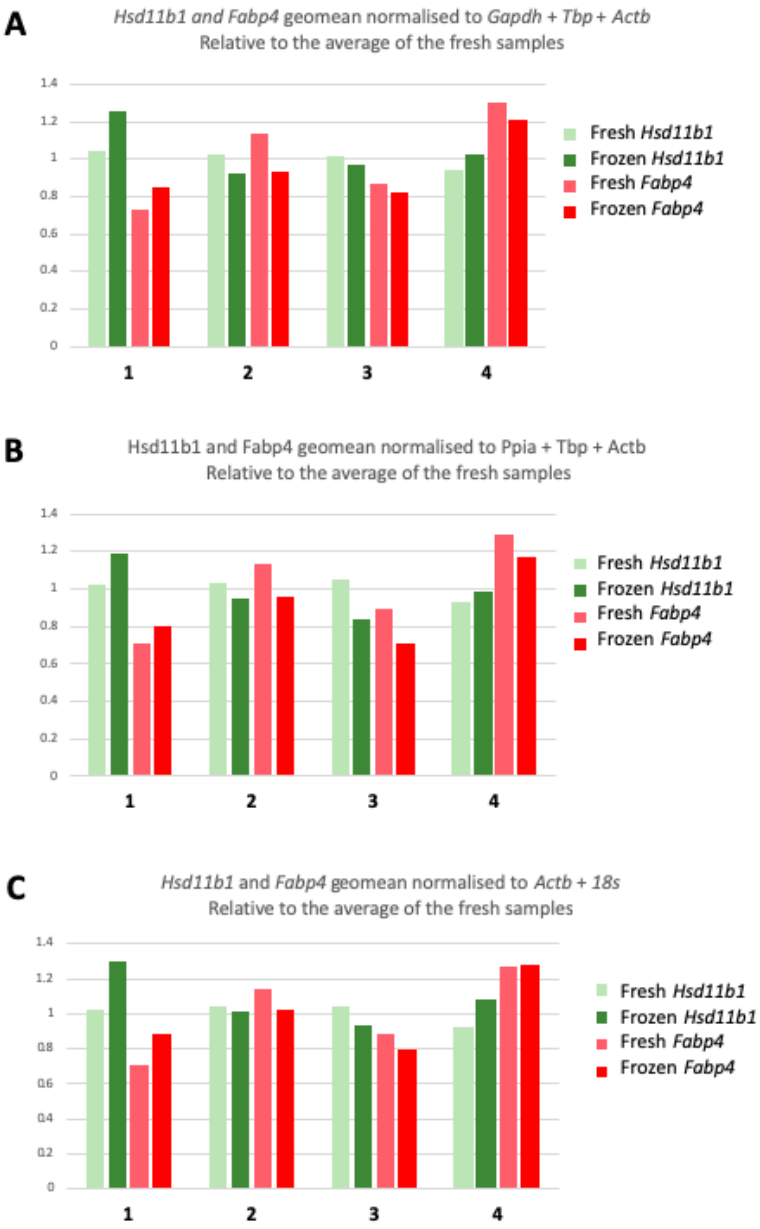

Figure 2.3. Comparison between fresh vs frozen *Hsd11b1* and *Fabp4* mRNA in BM. Fresh (light green/red) vs frozen (dark green/red) BM was evaluated by quantitative polymerase chain reaction (qPCR) of *Hsd11b1* (green) and *Fabp4* (red). **(A)** Combination of housekeeping genes *Gapdh, Tbp* and *Actb*. **(B)** Combination of housekeeping genes *Ppia, Tbp* and *Actb*. **(C)** Combination of housekeeping genes *Actb* and *18s*. The numbers represent the sample numbers, and are matched i.e. tibiae for fresh and frozen from the same animal. n = 4.

2.4.4. Reverse transcription

1 μg (1000 ng) of total RNA was reverse transcribed to cDNA using random hexamers primers. Table 2.2 contains the master mix recipe for reverse transcription of RNA to cDNA, with the cycling conditions in Table 2.3.

RT recipe	**Final concentration**	**# reactions**
		1
10X RT buffer (Applied Biosystems, 4486221)	1x	5
MgCl2 (25mM) (Applied Biosystems, 4486225)	5.5mM	11
dNTPs (10mM; 2.5mM each) (Applied Biosystems, 1710366)	0.5mM each	10
Random hexamers (100μM stock; diluted 1:6 to 16.7μM) (Thermo Scientific, SO142)	0.83μM	2.5
RNase inhibitor (40U/μL) (Thermo Scientific, E00381)	0.8U/μL	1
MultiScribe MMLV reverse transcriptase (50l/μl) (Thermo Scientific, 4311235)	1.25U/μL	1.25
		31.75μL/tube
RNA-H_2O (1μg)	1μg/18.25μL	19.25
31.75μL of the master mix was added to each tube of RNA-H_2O.		
Total		**50μL**

Table 2.2. Master mix recipe for reverse transcription of RNA to cDNA.

Step	**1**	**2**	**3**	**4**
Temperature (°C)	25	37	95	4
Time (minutes)	10	30	5	Hold

Table 2.3. Cycling conditions for reverse transcription.

2.4.5. Quantitative polymerase chain reaction

Quantitative polymerase chain reaction (qPCR) was used to detect a variety of gene expressions from AT, BM and bones from mice. Transcript expression was analysed by qPCR in 10μL duplicate reactions using qPCRBIO SyGreen Blue Mix (PCR Biosystems, PB20.17-50) and/or qPCRBIO Probe Blue Mix Separate-ROX TaqMan (PCR Biosystems, PB20.27-50). The samples were loaded into 384-well plates (Sarstedt, 72.1985.202) and run on a Light Cycler 480 (Roche). Transcript expression

was calculated based on a cDNA titration loaded on each plate and was shown relative to geomean expression of the housekeeping genes (Table 2.4 and 2.5).

2.4.5.1. Primers and probes used

Gene	Protein	Sequence
Fabp4	Fatty acid-binding protein 4	F: TGGAAGCTTGTCTCCAGTGA R: AATCCCCATTTACGCTGATG
Hprt	Hypoxanthine phosphoribosyl-transferase 1	F: TCATTATGCCGAGGATTTGGA R: GCACACAGAGGGCCACAAT
Hsd11b1	Hydroxysteroid 11-beta dehydrogenase 1	F: AGA CCA GAA ATG CTC CAG GG R: ATA AGC ATG TCC AGT CCG CC
Ppia	Peptidyl-prolyl cis-trans isomerase A	F: CACCGTGTTCTTCGACATCA R: CAGTGCTCAGAGCTCGAAAGT
Tbp	TATA box-binding protein	F: ACCTTATGCTCAGGGCTTGG R: GCCGTAAGGCATCATTGGAC
18S	18S Ribosomal RNA	F: CGATGCTCTTAGCTGAGTGT R: GGTCCAAGAATTTCACCTCT
Pparg	Peroxisome Proliferator Activated Receptor Gamma	F: GGAAAGACAACGGACAAATCAC R: TACGGATCGAAACTGGCAC
Cebpd	CCAAT Enhancer Binding Protein Delta	F: CGCCGCAACCAGGAGAT R: GCTGATGCAGCTTCTCGTTCT

Table 2.4. Sybr Green primer sequence for qPCR.

Gene	Protein	Assay ID
Fkbp5	FK506 binding protein 5	Mm00487406_m1
Gapdh	Glyceraldehyde 3-Phosphate dehydrogenase	Mm99999915_g1
TSC22D3 (Gilz)	TSC22 Domain Family Member 3 (Glucocorticoid-induced leucine zipper)	Mm00726417_s1
Per1	Period Circadian Regulator 1	Mm00501813_m1

Table 2.5. Taqman probes for qPCR.

2.4.5.2. Cycling conditions

Sybr Green	**# reactions: x1 (uL)**
2x Sybr Master mix (PCR BIOSYSTEMS, PB20.17-50)	5
Forward + Reverse primers	1
H_2O	2
8uL/tube	
cDNA	2
Total	10 (8uL mix + 2uL cDNA)

Table 2.6. qPCR Master Mix Recipe for SybrGreen primers.

Step	Temperature °C	Time	# Cycles
Pre-incubate	95°	10 minutes	1
Program	95° 60°	10 seconds 30-60 seconds	40
Melt curve	65 to 95 °C (increasing at 0.06 °C/second, 10 acquisitions per °C)	10 seconds	1
Cool	37°	Hold	1

Table 2.7. qPCR cycling conditions for SybrGreen primers.

Taqman	# reactions: x1 (uL)
2x Taq Master mix (PCR Biosystems, PB20.27-50)	5
20x Probe set (gene)	0.25
H_2O	2.75
8uL/tube	
cDNA	2
Total	10 (8uL mix + 2uL cDNA)

Table 2.8. qPCR Master Mix Recipe for Taqman probes.

Step	Temperature °C	Time	# Cycles
Pre-incubate	95°	5-10 minutes	1
Program	95° 60°	10 seconds 30-60 seconds	50
Cool	37°	Hold	1

Table 2.9. qPCR cycling conditions for Taqman probes.

2.5. Corticosterone Enzyme-linked immunosorbent assay

Corticosterone Enzyme-linked immunosorbent assay (ELISA) (Enzo Life Sciences, Famingdale, NYADI-901-097) was used to quantify corticosterone concentration in weekly plasma from the six-week CR and aged mice. The ELISA was performed according to manufacturer's instructions. The ELISA was a colorimetric competitive enzyme immunoassay used to quantify corticosterone levels in the mouse plasma. A polyclonal antibody was used to bind corticosterone, in a competitive manner. The

first step was to prepare the reagents for the assay following manufacturer's instructions.

1. **Assay buffer 15**: The assay buffer was prepared by diluting 10mL of the stock with 90 mL deionised water.
2. **Corticosterone standard**: The 200,000 pg/mL corticosterone standard solution was taken out in advance to warm up to room temperature. Five 12 x 75mm glass tubes were labelled #1 through #5. 1ml of the Assay buffer 15 was added to tube #1, and 800 μL was added into tubes #3 through #5. 200000 pg/ml corticosterone standard was then serially diluted to 20000, 4000, 800, 160, 32 and 0 pg/ml.
3. **Wash buffer**: 5mL of the stock was diluted with 95mL of deionised water.

Next, plasma was prepared according to the small volume protocol, due to inadequate plasma, by mixing 10 μl steroid displacement reagent with 10 μl plasma, followed by diluting it out with 380 μl ELISA buffer (final dilution 1:40).

The protocol:

1. 100 μL of assay buffer 15 was added to the NSB and the B_0 wells, meaning these well did not contain corticosterone concentration (0 pg/mL Standard).
2. 100 μL of each standards #1 through #5, and 100 μL of each sample was added to the appropriate well.
3. Additional 50 μL of assay buffer 15 was added to the NSB well.
4. 50 μL of blue Conjugate was added into each well, apart from the total activity (TA) and blank well.
5. 50 μL of yellow antibody was added into each well, apart from the blank, TA and NSB wells. The plate was then covered with a plate sealer and incubated at room temperature on a plate shaker for 2 hours.
6. Following the 2 hours incubation time, the plate contents were emptied and washed by adding 400 μL of wash solution to every well. This washing step was repeated 2 more times for a total of 3 washes.
7. Post the final wash, the wells were emptied and firmly tapped on a lint free paper towel to remove any leftover wash buffer.
8. 5 μL of blue conjugate was added to the TA well.

9. 200 μl of para-Nitrophenylphosphate substrate was then added to every well and incubated at room temperature for 1h without shaking.
10. After 1h, 50 μL of stop solution was added to every well and the plate was read instantly at 405 nm, with correction at 580 nm.

Plasma corticosterone concentration was calculated from interpolation against absorbance of the standards and correction for initial dilution.

2.6. Steroid analysis by Liquid chromatography-tandem mass spectrometry in murine plasma and bone marrow

Liquid chromatography tandem mass spectrometry (LC-MS/MS) is a sensitive and specific analytical tool and methods can be developed to allow for simultaneous analysis of more than one compound in a single sample. In recent years LC-MS/MS has been adopted for both clinical and pre-clinical studies for accurate quantification of steroids in biological samples such as plasma, serum and tissue. The Journal of Clinical Endocrinology and Metabolism released a position statement in 2013 (Handelsman and Wartofsky, 2013) requiring analysis of sex steroid hormones be carried out by LC-MS/MS.

When developing a quantitative LC-MS/MS method, to ensure that the data generated is accurate and precise, certain bioanalytical guidelines must be followed, such as inclusion of analogous or more preferably isotopically labelled internal standard and calibration standard curves that are appropriate for the expected concentration ranges of the analytes in the samples. The developed method of sample preparation chromatographic separation and mass spectral analysis must be assessed for accuracy, precision, extraction efficiency and matrix effects before its application to biological samples.

2.6.1. Assessment of a Supported Liquid Extraction LC-MS/MS analysis of GCs, testosterone and progesterone in mouse samples

In order to assess steroid concentrations in end-point plasma from both male and female mice that were on one-and six-week CR, an LC-MS/MS method was required for separation and quantitation of the steroid hormones 11-DHC, Corticosterone

(CORT), Testosterone (T) and Progesterone (P) to investigate concentrations in WT and 11β-HSD1 KO mice. The volume of plasma sample available from mice in this study was limited (<100 μL). Previously published methods required 150 μL (Verma *et al.*, 2018) using Liquid Liquid Extraction (LLE) to successfully detect 11-DHC in the samples. As such, the method required re-evaluating to assess whether the volume of mouse plasma available was sufficient to detect steroids in small volumes. Experiments were performed to assess a different sample preparation technique called Supported Liquid Extraction (SLE), aiming to improve the precision of sample preparation while reducing the volume of sample required.

2.6.1.1. Liquid Chromatography tandem Mass Spectrometry settings

An LC-MS/MS method for excellent separation and detection of both GCs and androgens had already been developed and applied to human clinical samples (Gifford *et al.*, 2019). The suitability of this method was assessed in the context of mouse GCs, focussing on 11-DHC, CORT, T and P. Briefly, the LC-MS/MS system consisted of a Sciex 6500+ QTrap tandem quadrupole mass spectrometer used in Multiple Reaction Monitoring (MRM) mode. Automated injection of samples took place using a Shimadzu Nexera uHPLC system. Separation was performed on a Phenomenex Kinetex C18 column (150 mm x 3.0 mm, 2.6 µm particle size) fitted with a Phenomenex KrudKatcher Ultra In-Line Filter 0.5 µm porosity. The column was maintained at a temperature of 40°C. Mobile phase A consisted of formic acid (FA) (0.1%) in LC-MS graded water (VWR, 83645.320), and mobile phase B consisted of FA (0.1%) in LC-MS graded methanol (VWR, 83638.320). A flow rate of 0.5 mL/min was used with the gradient described in Table 2.10.

Time (min)	Composition (%) A	Composition (%) B
Initial	45	55
4.00	45	55
10.00	0	100
12.00	0	100
12.10	45	55
16.00	45	55

Table 2.10. Gradient details for Phenomenex Kinetex C18 (150 x 3.0 mm; 2.6 μm) for steroid separation. A- 0.1% FA in water, B- 0.1% FA in methanol (40°C, 0.5 mL/min).

The mass spectrometer was operated in positive ion MRM mode and monitored for quantitative and qualitative ions for each steroid of interest plus corresponding internal standards (d8B, d4F, (Table 2.11)). Instrument control, data acquisition and integration were achieved using Sciex Analyst software running Version 1.6.3. Chromatographic separation of the steroids of interest are shown in Table 2.12.

Compound ID	Q1 *m/z*	Q3 *m/z*	Expected RT (mins)
11-dehydrocorticosterone (11-DHC) 1	345.1	121.2	3.98
11-dehydrocorticosterone (11-DHC) 2	345.1	91.2	3.98
Corticosterone (B) 1	347.1	121.1	5.98
Corticosterone (B) 2	347.1	90.9	5.98
d4-Cortisol 1 (d4F 1)	367.3	121.1	5.00
d4-Cortisol 2 (d4F 2)	367.3	91.1	5.00
d8-Corticosterone (d8B) 1	369.2	169.0	4.11
Testosterone 1	289.1	97.0	7.75
Testosterone 2	289.1	109.2	7.75
13C3-Testosterone 1	292.2	100.2	7.74
Progesterone 1	315.1	97.1	8.99
Progesterone 2	315.1	109.1	9.00
D9-Progesterone 1	324.1	100.0	9.00

Table 2.11. Corresponding internal standards and analytes of interest. Positive Ion MRM mode, Curtain Gas 40, Collision Gas (medium), Ionspray Voltage 5.5 kV, temperature 600C, Ion source gas 1 and 2, 40 and 60 psi.

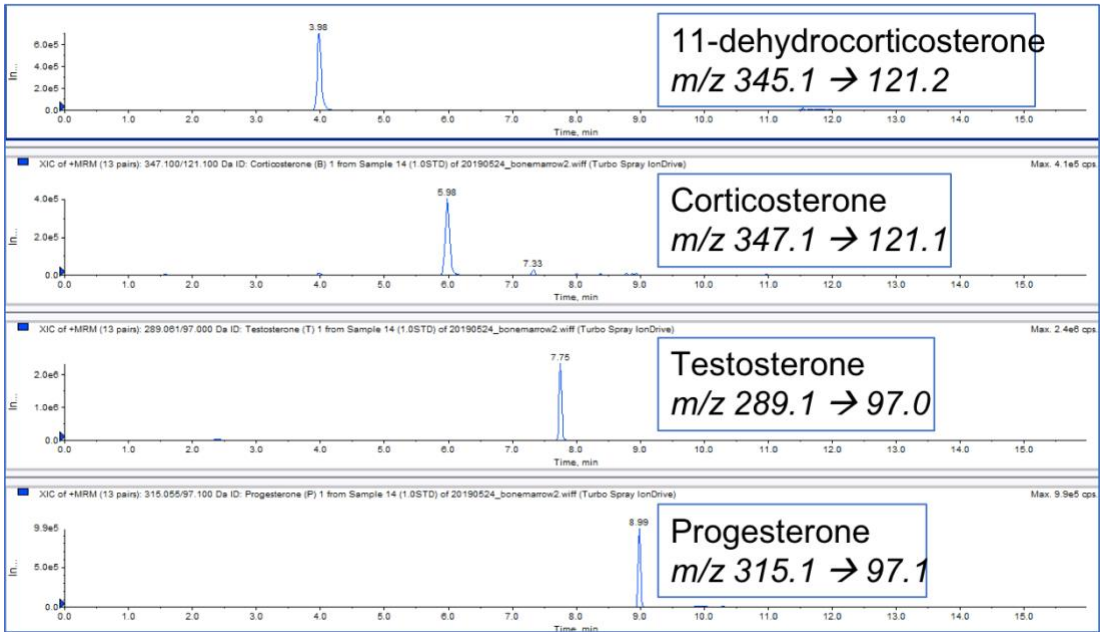

Figure 2.12. Chromatographic separation of the steroids of interest. Extracted Ion Chromatogram showing the major steroids (11-DHC, CORT, T and P) and their separation on the Kinetex C18 (150 x 3 mm; 2.6 um) column using 0.1% FA in water/methanol as a gradient system over 16 minutes at 40C.

2.6.1.2. Assessment of SLE as an alternative to LLE for sample preparation of mouse plasma for steroid analysis

Materials: SLE array cartridges were from Biotage (SLE400 and SLE200 were compared, using an array cartridge vacuum manifold by IST, Sweden). Deep Well collection plates were from Waters, UK. Plate seal films were zone-free plate seals from Waters. Rimless cultured glass tubes 12mm x 75mm (Fisherbrand™, 11517403) were used. Total recovery glass vials from Waters. All solvents used were LC-MS grade water and LC-MS grade Methanol from Fisher Scientific, UK

Stock solutions of steroid hormones: All steroid powders were from Steraloids. 1 mg/mL stock solutions were made up individually in methanol and stored at -20°C. These 1 mg/mL stocks were diluted in methanol on the day of analysis. Combined stock solutions of the analytes were prepared by adding 1 mg/mL 11-DHC (5 μL) and corticosterone (5 μL) up to 1 mL methanol. Further dilutions were prepared to give 500 ng/mL, 50 ng/mL, 5 ng/mL and 0.5 ng/mL solutions in methanol.

Stock solutions of internal standards: d8-corticosterone (d8B) and deuterated cortisol (d4-F) were prepared in methanol at 1 mg/mL from powders from Steraloids

and diluted to give a working internal standard at 250 ng/mL in methanol.

Calibration standard curves were prepared at the following levels: 0, 0.01, 0.025, 0.05, 0.1, 0.25, 0.5, 1, 2, 5, 10, 20, 50 ng (from 0.01 – 50 ng) of both Corticosterone and 11-DHC. Each standard and sample were enriched with 10 μL x 2500 ng/mL of d8B and d4F (2.5 ng).

2.6.1.2.1. LLE (Aqueous calibration and plasma)

Calibration standards were prepared using the calibration solutions above. Water (50 μL) was aliquoted into a glass culture tube and the appropriate amount of calibration standard was added (e.g. 10 μL x 5 ng/mL CORT and 11-DHC to give 0.05 ng standard), enriched with d4F and d8B (2.5 ng) and mixed. Chloroform was added (500 μL), mixed and the top layer was transferred to a clean glass vial, dried down under nitrogen, resuspended in 70:30 water/methanol (100 μl), transferred to an LC-MS total recovery vial and analysed by LC-MS/MS.

A pool of mouse plasma was prepared, mixed thoroughly and an aliquot of 50 μL plasma was added to a glass culture tube and enriched with d4F and epiB (25 ng). 500 μl chloroform was added, the tube was vortexed and the top layer was transferred to a clean glass vial, dried down under nitrogen and resuspended in 70:30 water/methanol (100 μL), transferred to an LC-MS total recovery vial and analysed by LC-MS/MS.

2.6.1.2.2. SLE 400 (Aqueous calibration and plasma)

For each aqueous standard, 50 μl water was aliquoted into a glass culture tube, and the appropriate amount of calibration standard was added (e.g. 10 μL x 5 ng/mL CORT and 11-DHC to give 0.05 ng standard), and internal standard (d4F and eD8B (25 ng)) was added. 150 μl water was added to dilute the sample to final volume of 200 μL.

For each mouse plasma sample, 50 μl mouse plasma was aliquoted into a glass culture tube and internal standard (d4F and epiB (2.5 ng)) was added. 150 μL water was added to dilute the sample to final volume of 200 μL. 200 μl of 0.5 M ammonium hydroxide (Fisher Chemical, 10305170) was added to the sample, vortexed and the

400 μL was transferred to individual SLE400 array cartridges in an IST array holder. Standards and samples were left to soak on cartridges for 5 minutes, followed by careful vacuuming for approximately 2 seconds to absorb onto the cartridge. Samples were left for 5 minutes. 600 μl Dichloromethane/isopropanol (95:5) (VWR, 23373.320; and VWR, 20880.320) was added to each cartridge, vacuumed through into a 96-well deep well collecting plate for 2 minutes. The addition of 600 μL elution solvent was repeated twice. The eluent was dried down in the 96-well deep well collecting plate, under nitrogen and resuspended in 70:30 water/methanol (100 μL), the plate sealed, placed on plate shaker for 5 minutes at 300 rpm, and transferred to the autosampler for analysis by LC-MS/MS.

2.6.1.2.3. SLE 200 (Aqueous calibration and plasma)

For each aqueous standard, 50 μl water was aliquoted into a glass culture tube, and the appropriate amount of calibration standard was added (e.g. 10 μL x 5 ng/mL CORT and 11-DHC to give 0.05 ng standard), and internal standard (d4F and epiB (25 ng)) was added. 50 μL water was added to dilute the sample to final volume of 100 μL.

For each mouse plasma sample, 50 μl mouse plasma was aliquoted into a glass culture tube and internal standard (d4F and d8B (2.5 ng)) was added. 50 μL water was added to dilute the sample to final volume of 100 μL. 0.5 M ammonium hydroxide (100 μL) was added to each sample, vortexed and the 200 μL was transferred to individual SLE200 array cartridges in an IST array holder. Standards and samples were left to soak on cartridges for 5 minutes, followed by careful vacuuming for approximately 2 seconds to absorb onto the cartridge. Samples were left for 5 minutes. Dichloromethane/isopropanol (95:5, 450 μL) was added to each cartridge, vacuumed through into a 96-well deep well collecting plate for 2 minutes. The addition of 450 μL elution solvent was repeated twice. The eluent was dried down in the 96-well deep well collecting plate, under nitrogen and resuspended in 70:30 water/methanol (100 μL), the plate sealed, placed on plate shaker for 5 minutes at 300 rpm, and transferred to the autosampler for analysis by LC-MS/MS

2.6.1.3. Method validation

To validate the SLE LC-MS/MS assay, the recovery, linearity and lower limits of detection and quantitation were determined in accordance with the European Medicines Agency bioanalytical method validation guidelines (European Medicines Agency, 2011)

2.6.1.3.1. Recovery of 11-DHC and corticosterone from water

The absolute recovery was assessed by enriching water with 2.5 ng of 11-DHC and CORT, using the SLE method described (Section 2.5.1.1.3/4). Peak areas of CORT and 11-DHC in these enriched aqueous samples were compared with those from pure water subjected to the extraction procedure and post-spiked with CORT and 11-DHC (2.5 ng).

2.6.1.3.2. Recovery of internal standards, d8B and d4F from plasma

Recoveries of d4F and d8B from pooled control murine plasma (150 μL) enriched with D4F and d8B (2.5 ng) were ascertained using the extraction procedure described in section 2.5.1.1.4. The peak areas of d4F and d8B from these 'pre-spiked' plasma samples were divided by those of plasma that were post-spiked with d4F and d8B (2.5 ng) and the percentage recovery of the internal standards from mouse plasma was calculated. The pre-spiked values were compared to pure-solutions of d4F and d8B (2.5 ng) to calculate the matrix effects on the internal standards.

2.6.1.3.3. Sensitivity and linearity (LOD, LOQ, accuracy and precision)

Six sets of calibration standards (0.01-10 ng) were prepared and extracted by SLE200 and analysed by LC-MS/MS. The detection and quantitation limits (LOD and LOQ respectively) were calculated. Linearity was evaluated in calibration standards generated on six different days, assessing peak area ratios of analyte (CORT and 11-DHC) divided by that of the internal standard (D4F and d8B).

2.6.1.3.4. Reproducibility

Accuracy and precision were determined by assessing calibration standards, following extraction, at the LLOQ and at low, medium and high amounts of 11-DHC and CORT (0.01, 2.5, 10 ng) in replicates of six prepared on the same day (intra) and of three prepared on different days (inter). The amount of steroid was calculated using the calibration curve and accuracy calculated as the relative mean error (RME).

2.6.1.4. Recovery following extraction by LLE, SLE400 and SLE200 of 50 μL murine plasma

LLE using chloroform (10:1) was compared with SLE400 and SLE200 of 50 μL mouse plasma from a pool of mouse plasma. The calculated amounts were related to the corresponding calibration curve. The precision of the calculated amounts in triplicate was compared for each steroid, for each method of preparation – LLE, SLE400 and SLE200. The variability of the calculated amounts (26 % for CORT and 45 % for 11-DHC) was much larger in LLE than that seen in the SLE400 extracts (21 % for CORT and 13 % for 11-DHC) and yet the variability in calculated amounts (10 % for CORT and 2% for 11-DHC) was further improved using the SLE200 (Table 2.5.4.) Therefore, SLE200 (Section 2.5.1.2.3) was considered the acceptable and reliable method of sample preparation for 50 μL mouse plasma (Table 2.13).

	LLE (50 μL)		SLE400+ (50 μL)		SLE200+ (50 μL)	
	11-DHC	**CORT**	**11-DHC**	**CORT**	**11-DHC**	**CORT**
LLOD	0.25	0.5	0.1	0.05	0.1	0.05
ULOD	5	10	10	10	10	10
%RSD in pooled mouse plasma	45.03%	26.25%	13.23%	21.29%	10.18%	2.46%
IntStd Recovery (%)	62% (d4F)	9.1% (d8B)	72% (d4F)	87% (d8B)	76% (d4F)	88% (d8B)

Table 2.13. Comparison of %RSD at limit of detection following extraction of mouse plasma (50 μL) using LLE, SLE400 and SLE200 extraction. LLOD = Lower limit of detection. ULOD = Upper limit of detection. %RSD = percentage relative standard of deviation ((standard deviation/average) * 100). 11-DHC = 11-dehydrocorticosterone. Cort = corticosterone.

2.6.1.4.1. Sensitivity and linearity

1-week CR: 11-DHC = 0.001 and 5 ng; Corticosterone = 0.0025 and 10 ng; Testosterone = 0.001 and 10 ng; Progesterone = 0.0025 and 10 ng.
6-week CR: 11-DHC = 0.01 and 2 ng; Corticosterone = 0.05 and 20 ng; Testosterone = 0.01 and 5 ng.
Based on regression parameters, d4F was consistently found to be the best internal standard for 11-DHC, as they elute close to each other, while d8B was the best internal standard for CORT.

2.6.1.4.2. Method Application of SLE200 for murine plasma steroid analysis

The plasma from 122 individual mice, were analysed using the validated SLE200 protocol for mouse plasma, where the range for the steroids are shown below.

1-week CR: 11-DHC = 0.0338 and 76 ng/mL; Corticosterone = 12.3 and 330 ng/mL; Testosterone = 0.0227 and 0.31 ng/mL; Progesterone = 0.0478 and 10.56 ng/mL

6-week CR: 11-DHC = 1.1 and 60.4 ng/mL; Corticosterone = 44.3 and 364 ng/mL; Testosterone = 0.0035 and 8.96 ng/mL

2.6.2. Optimisation of sample preparation of murine BM for LC-MS/MS analysis of steroids

LC-MS/MS was performed on femoral BM from both male and female mice that were on one-and six-week CR. Analytes of interest; 11-DHC, CORT, T and P were detected and quantified. Prior to performing LC-MS/MS on the experimental frozen femoral BM, prior steps had to be taken to optimise a protocol for extracting the BM from the bone. The sample preparation of the BM was optimised from previous methods (Tobiansky *et al.*, 2018), followed by our SLE200+ protocol (2.5.1.2.3) prior to analysis by LC-MS/MS. Test BM samples were flushed and used to assess the levels of CORT and 11-DHC, T and P in the samples.

2.6.2.1. Optimisation of BM collection from bone

2.6.2.1.1. Assessment of different masses of BM for steroid extraction by SLE200

BM samples were prepared from one, two, four or eight tibiae and femurs to determine what mass of BM is needed to detect the four steroids of interest using our sensitive LC-MS/MS assay previously applied to plasma (50 μL). BM collection was carried out using the same protocol as Tobiansky *et al*., (2018) followed by extraction using SLE200 and LC-MS/MS analysis.

Bones were transferred from dry ice onto wet ice, and ends were cut off using a razor blade. A razor blade was used to remove the base of a 0.5 ml Eppendorf tube. The tube was placed inside an intact Eppendorf tube. The bone was added into the double layer tube and centrifuged at 8000 rcf for 1 minute. The BM pellet was weighed and recorded. 500 μl Acetonitrile (VWR, 20060.320) with 0.01% FA (v/v) was added to the BM pellet. The BM was homogenised with a metal bead in a bead mill homogeniser at 30 Hz for 30 seconds. Samples were incubated for 1h at -20°C, centrifuged for 5 minutes at 16,100 rcf, and the supernatant was transferred to a clean glass vial. A further aliquot of acetonitrile (400 μL, 0.01% FA, v/v) was added to the pellet, vortexed

and centrifuged as before. The supernatant was added to the glass vial containing the initial supernatant. The samples were dried down with nitrogen at 40°C for approximately 30 minutes and resuspended in 200 μl water prior to extraction by SLE200 (like previously from the plasma, same protocol and same calibration curve, Section 2.5.1.2.3), following enrichment with internal standards (2.5 ng). The samples were analysed alongside a calibration curve (0.01 -10 ng) also enriched with internal standards (2.5 ng). 50 μL of BM aliquot used for the extraction.

CORT and T were quantified in the BM from all samples, but the table below (Table 2.14) shows data from 1 femur only. However, 11-DHC and P were not detected, but the recovery of the internal standards was satisfactory (Table 2.14).

	SLE200			
	11-DHC (d4F)	**CORT (d8B)**	**T (13C3T)**	**P (d9P)**
LLOD (ng)	0.01	0.01	0.01	0.01
ULOD (ng)	0.5	1	0.5	0.5
Recovery of internal standard	79%	81%	101%	94%

Table 2.14. Comparison of recovery of internal standards between analytes following extraction of mouse BM. LLOD = Lower limit of detection. ULOD = Upper limit of detection. 11-DHC = 11-dehydrocorticosterone. CORT = corticosterone.

2.6.2.1.2. Assessment of 0.01% and 0.1% FA in acetonitrile (v/v) on steroid recovery from collected BM by SLE400

0.01 % and 0.1 % FA in acetonitrile was compared in BM test samples. The amount of the BM aliquot was increased from 50 μl to 200 μl so that the steroids fell within the detection limit of the method. The final change included decreasing the resuspension volume to 70 μl from 100 μl prior to running it on the LC-MS/MS. The method for BM collection was increased to 200 μl, which resulted in a higher liquid volume and a transfer to SLE400 from SLE200.

For each mouse sample, 200 μl mouse BM was aliquoted into a glass culture tube and internal standard (d4F and epiB (2.5 ng)) was added. 200 μl of 0.5 M ammonium hydroxide was added to the sample, vortexed and the 400 μL was transferred to individual SLE400 array cartridges in an IST array holder. Standards and samples were left to soak on cartridges for 5 minutes, followed by careful vacuuming for approximately 2 seconds to absorb onto the cartridge. Samples were left for 5 minutes. 600 μl Dichloromethane/isopropanol (95:5) was added to each cartridge, vacuumed through into a 96-well deep well collecting plate for 2 minutes. The addition of 600 μL elution solvent was repeated twice. The eluent was dried down in the 96-well deep well collecting plate, under nitrogen and resuspended in 100μl 70:30 water/methanol, the plate sealed, placed on plate shaker for 5 minutes at 300 rpm, and transferred to the autosampler for analysis by LC-MS/MS.

The results obtained from the assessment of the percentage of FA in acetonitrile showed that 0.1 % was not an improvement on 0.01 % FA solution for extraction. Based on the results in table 2.15, it was clear that the % of FA did not impact the quantification of the analytes of interest. Therefore, it was decided to continue with the original 0.01% solution. Further tests were performed to investigate whether the resuspension volume of the BM pellet (400 μl vs 200 μl) and the incubation temperature (-20°C vs -80°C) could alter the results, but no differences were observed (data not shown).

0.01 % FA	11-DHC ng/mg	CORT ng/mg	T ng/mg	P ng/mg		0.01 % FA	11-DHC ng/mg	CORT ng/mg	T ng/mg	P ng/mg
Male 1 - 0.01%	10222.22	1294.44	1266.667	109.44		**Female 1 - 0.01%**	2470.00	6266.67	103	3500.00
Male 2 - 0.01%	13704.55	9068.18	422.7273	<0		**Female 2 - 0.01%**	337.80	2158.54	<0	6646.34
Male 3 - 0.01%	881.48	710.37	178.5185	82.22		**Female 3 - 0.01%**	505.62	2505.62	<0	8786.52
% RSD	80%	126%	92%	20%		**% RSD**	107%	63%	N/A	42%
0.1 % FA	**11-DHC ng/mg**	**CORT ng/mg**	**T ng/mg**	**P ng/mg**		**0.1 % FA**	**11-DHC ng/mg**	**CORT ng/mg**	**T ng/mg**	**P ng/mg**
Male 1 - 0.1%	569.8113208	1971.698	2150.943	364.1509		**Female 1 - 0.1%**	537.7778	4733.333	104.2222	3400
Male 2 - 0.1%	2081.447964	1330.317	78.28054	200.4525		**Female 2 - 0.1%**	590.6977	3465.116	<0	12441.86
Male 3 - 0.1%	3123.222749	319.4313	90.99526	368.7204		**Female 3 - 0.1%**	733.3333	12380.95	378.0952	34000
% RSD	67%	69%	154%	31%		**% RSD**	16%	70%	80%	95%

Table 2.15. Comparison between 0.01 % and 0.1 % FA in acetonitrile in mouse femoral BM samples. %RSD = percentage relative standard of deviation ((standard deviation/average) * 100). 11-DHC = 11-dehydrocorticosterone. CORT = corticosterone. T = testosterone. P = progesterone.

2.6.2.2. Final step: Extension of calibration curve to lower limits for all experimental steroids

The final protocol for quantifying 11-DHC, corticosterone, testosterone and progesterone from femoral BM is described in Section 2.6.2.1.2. No further changes were done to the BM collection. Instead, further lower standards were added to the calibration curve to include the lower limits of steroids, and the higher standards of 5, 10, 20 and 50 ng were excluded. The final calibration curve was the following: 0, 0.001, 0.0025, 0.005, 0.01, 0.025, 0.05, 0.1, 0.25, 0.5, 1, 2 ng (from 0.001 – 2 ng).

2.6.2.3. Method Application of BM extraction by SLE400 for steroid analysis

The BM from 122 individual mice (an aliquot of 200 μl femoral BM per sample), were analysed using the SLE400 protocol (section 2.6.2.1.2), where the range for all steroids for 1-and 6-week CR was 0.001 and 2 ng; comfortably within the validated ranges of the assay: 0.001 – 2 ng. Furthermore, additional lower standards were added to the protocol as described in Section 2.6.2.2.

2.7. Bone morphology and bone marrow adiposity quantification by μCT

2.7.1. Bone preparation

The tibiae of the mice were surgically isolated and all tissue around it removed. To obtain the morphology of trabecular and cortical bone, the tibiae were fixed in 10% formalin (Sigma, HT501380-9.5L) at 4°C for 7 days until embedded in 1% agarose (1g agarose in 100ml deionised water). Six tibiae were arranged in parallel in two layers in the 1% agarose (w/v), in a 30-ml universal tube and then mounted in a Skyscan 1172 desktop micro CT (μCT) (Bruker, Kontich, Belgium).

To further quantify BMAT, following the scanning, the tibiae were removed from the 1% agarose and transferred to 14% EDTA at 4°C for 2 weeks for decalcification. The EDTA solution was replaced every 2 days. Thereafter, the tibiae were washed in Sorensen's Phosphate buffer (81 mM KH2PO4, 19 mM Na2 HPO4 · 7H2 O, pH 7.4) to ensure removal of EDTA.

Once decalcified, the tibiae were stained using osmium tetroxide (2% w/v; Agar Scientific, UK). Firstly, the osmium tetroxide was diluted 1:1 in 0.1M Sorensen's Phosphate buffer. The tibiae were then stained with the 1% osmium tetroxide solution over 48 hours at room temperature. Subsequently, the tibiae were washed and stored in Sorensen's Phosphate buffer at 4°C until embedded in 1% agarose for μCT scanning to quantify BMAT.

2.7.2. μCT scanning for bone and BMAT

The tubes containing the tibiae were then scanned through 360°, using a step of 0.40° between exposures. An isotropic voxel resolution of 6 μm and 12 μm was obtained in the scans, for fixated unstained bones and decalcified osmium-tetroxide stained bones, respectively, using the following settings: 54 source voltage, 185 source current with a filter exposure time of 1767ms for fixated unstained bones and 885ms for osmium stained bones. To further optimise the scan, a 2-frame averaging for fixated unstained bones, and 4-frame averaging for stained bones, was used alongside a 0.5mm aluminium filter. For fixated unstained bones, the minimum and maximum for CS to image conversion was 0.005 and 0.125, while for osmium stained bones it was 0.005 and 0.35. Following scanning, data was reconstructed using Skyscan software NRecon v1.7.3.0 (Bruker, Kontich, Belgium). The reconstruction thresholding window was accustomed to capture all bones within the image. The ring artefact for fixated unstained bones was 5 with the beam hardening set at 40%, while for stained bones it was 10 and 40%, respectively. Bone morphology and BMAT were quantified using CT Analyser v1.16.4.1 (Bruker, Kontich, Belgium).

2.7.3. Bone morphology analysis

Prior to analysing the tibiae for bone morphology, the 6 parallel tibiae on the dataset were separated out and saved each to their own for analysis by CT (computed tomography) Analyser. To obtain the trabecular morphology of the tibiae, the trabecular bone was analysed by counting the inner trabecular part, starting 16 slices away from the growth plate (area of growing tissue at the proximal part of the bone) and then again further 167 slices (Figure 2.13). The area in between was contoured around the trabecular, marked as the "region of interest" (ROI), excluding any cortical bone, with a threshold of 50-255. 3D analysis of the trabecular ROI was then performed, with the following settings: Threshold as 50-255; Despeckle, to remove

white speckles in 2D less than 4 pixels; 3D analysis with basic and additional values added. The threshold of 50-255 refers to the inclusion of the trabecular or cortical bone that will be analysed. Any background noise, meaning anything other than bone will be excluded. To obtain the cortical morphology, the cortical bone was analysed by counting 500 slices away from the growth late, and then again further 83 slices (Figure 2.13). The area in between was contoured around the cortical bone – being the ROI, with a threshold of 50-255. Thereafter, a similar 3D analysis was performed, with the following settings: Threshold as 50-255; Despeckle, to remove white speckles in 2D less than 4 pixels; ROI shrink-wrap for 2D space, stretching over holes with a diameter in 20 pixels; 3D analysis with basic values added; 2D analysis with all results added.

The medullary cavity was also quantified for presenting the BMAT data proportional to the space within the bone cavity. To receive the data for the tibia medullary cavity, the fixated unstained bones were divided in two parts; proximal and distal, by using CT Analyser. The proximal region starts at the growth plate of the tibiae, and ends at the tibia-fibula-junction. While the distal region starts from the tibia-fibula-junction and ends at the bottom of the tibia. Each region was analysed separately. The proximal region was analysed by contouring the tibia, excluding the fibula, from the growth plate to the tibia-fibula-junction. The distal region was analysed by contouring the tibia, including the fibula, from the tibia-fibula-junction to the bottom of the tibia. The settings used to obtain the medullary cavity were the following: Threshold as 50-255; Despeckle, to remove white speckles in 2D less than 5 pixels; Despeckle, to remove black speckles in 2D less than 5 pixels; ROI shrink-wrap for 2D space, stretching over holes with a diameter in 16 pixels; 3D analysis with basic values added.

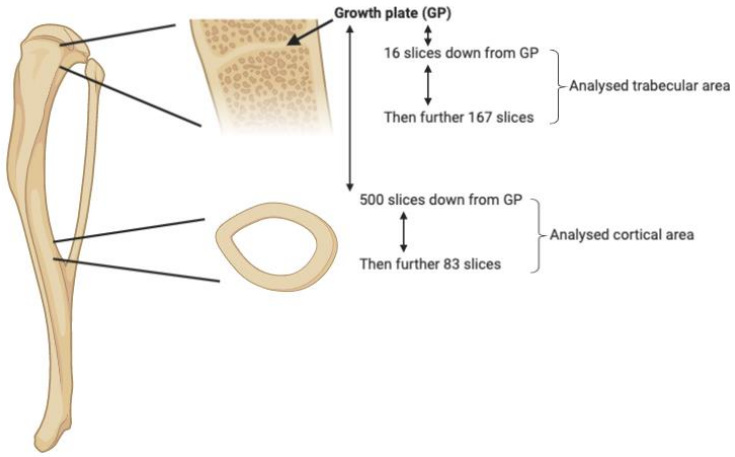

Figure 2.13. Analysis of trabecular and cortical bone. Analysis of 167 slices for trabecular and 83 slices for cortical bone by μCT Analyser.

2.7.4. BMAT analysis

To obtain BMAT quantification, the tibiae were divided into two parts: rBMAT (proximal) and cBMAT (distal), by using CT Analyser. The rBMAT region starts at the growth plate of the tibiae, and ends at the tibia-fibula-junction. While the cBMAT region starts from the tibia-fibula-junction and ends at the bottom of the tibia. Each region was analysed separately. Starting with rBMAT, the BMAT is distinguished as white due to it being stained with osmium-tetroxide and can therefore be contoured around, from top to bottom through every slice. Remaining soft tissue can also be distinguished as white due to the staining, therefore, only white regions within the bone are contoured around, excluding any bits that appear to be outside the cortical bone. The threshold for BMAT quantification was set to 70-255 to exclude background noise. Thereafter, cBMAT was similarly contoured, from the junction to the end of the bone. The settings used to obtain the amount of BMAT present within the bones were the following: 3D analysis with basic values added. BMAT volume in the distinct tibial regions were quantified and presented proportional to total tibial marrow volume.

2.8. Statistical analysis

Statistical analysis was performed using GraphPad Prism 8 software (GraphPad Software). Two-and Three-way ANOVA tests were performed to compare overall interaction between two-and three factors, respectively. In addition, multiple comparisons by Sidak's/Tukey's test were performed to detect specific differences between the groups (male/female, AL/CR, WT/KO). Furthermore, non-parametric Mann-Whitney U-test was also performed between two groups only that were not equally distributed. Distribution was examined by Normal (Gaussian) distribution.

Chapter 3. Sex-specific effects of caloric restriction on glucocorticoid action in adipose tissue and bone marrow

3.1. Introduction

CR without malnourishment decreases the risk of ageing-associated diseases and can extend lifespan in numerous species, including rodents (Masoro, Yu and Bertrand, 1982), rhesus monkeys (Bodkin *et al.*, 2003), yeast (Lin, Defossez and Guarente, 2000) and nematodes (Houthoofd *et al.*, 2002). This highlights CR as a nutritional strategy to combat chronic disease and promote healthy ageing. However, the mechanisms underlying these CR-associated health benefits remain incompletely understood.

With CR, decreased body mass, lower blood pressure and cholesterol levels are evident (Fontana *et al.*, 2004; Meyer *et al.*, 2006; Devlin *et al.*, 2010; Narita *et al.*, 2018), and these may contribute to the health benefits of CR. For example, CR showed improved results on the major atherosclerosis risk factors that would normally increase with age (Fontana *et al.*, 2004). Although decreased blood pressure is not always required for certain health benefits (e.g. protection from stroke or neuron loss (Speakman and Mitchell, 2011)). CR also decreases adiposity, and this is postulated to contribute to the metabolic and lifespan-extending effects of CR (Muzumdar *et al.*, 2008).

In striking contrast to WAT, recent studies have revealed that CR causes increases in BMAT (Devlin *et al.*, 2010, 2016; Devlin, 2011; Cawthorn *et al.*, 2014, 2016; Ghali *et al.*, 2016). During CR, BMAT contributes to increased circulating concentrations of adiponectin, a hormone that exerts beneficial cardiometabolic and anti-inflammatory effects (Cawthorn *et al.*, 2014; Straub and Scherer, 2019). Thus, another possibility is that, by producing adiponectin or through other mechanisms, BMAT expansion contributes to the health benefits of CR. However, the mechanisms through which CR drives BMAT expansion are still incompletely understood. One under-explored possibility is that GCs contribute to these effects of CR. Indeed, CR increases activity

of the HPA axis, resulting in increased circulating GC concentrations (Stewart *et al.*, 1988; Cawthorn *et al.*, 2016). GCs are steroid hormones that regulate gene expression by activating the GR, which is present in almost all cells (de Guia, Rose and Herzig, 2014; Caratti *et al.*, 2015). GCs thereby exert diverse metabolic and immunomodulatory effects. Cortisol is the major circulating GC in humans, whereas in rodents corticosterone is the predominant circulating GC. The intracellular concentrations of these GCs are regulated by the enzymes 11β-HSD1 and 11β-HSD2. 11β-HSD1 is mainly expressed in the liver and AT, where it acts as a reductase, generating corticosterone. In contrast, 11β-HSD2 is mostly expressed in the kidney and generates 11-DHC from corticosterone. Although GCs are anti-inflammatory, chronic elevation of GCs causes CS, where visceral obesity, decreased muscle mass and insulin resistance are common characteristics (Hauner, Schmid and Pfeiffer, 1987; Pantoja, Huff and Yamamoto, 2008). Investigating GCs at a molecular level, it has been shown that GCs are required for adipocyte precursor differentiation (Hauner, Schmid and Pfeiffer, 1987; Pantoja, Huff and Yamamoto, 2008; Velez-delValle *et al.*, 2013). Nonetheless, the effects of CR on GCs at a molecular level are less well known, especially in adipose depots and the BM.

The above observations demonstrate that GCs can have profound effects on WAT biology, often in contrast to those occurring during CR. Whilst CR-induced GCs appear to be anti-inflammatory (Klebanov *et al.*, 1995; Allen *et al.*, 2019), GC excess promotes visceral adiposity and inflammation. However, most of our knowledge of this is based on CS or other states of GC excess, when GCs are compromising adipose function. This raises the question of how CR-associated GC excess influences WAT function. Previous results from our lab also suggest that GC excess may contribute to BMAT expansion during CR. Our previous publication (Cawthorn *et al.*, 2016) revealed that CR-induced BMAT expansion is associated with hyperglucocorticoidaemia. CR and GC therapy have both shown to increase BMAT (Vande Berg *et al.*, 1999; Bredella *et al.*, 2009; Devlin *et al.*, 2010; Ecklund *et al.*, 2010). However, the relationship between CR, BMAT expansion and GC action within BM remains to be addressed. Despite there being an increase in circulatory GCs during CR, is the GC action equally increased in different adipose depots and the BM? The action of GCs specifically during CR in the BM has not been explored. Therefore, in this chapter, 30% CR was implemented in mice to determine if elevated corticosterone concentration affects adipose depots and BM, with the aim to

determine if GC action is increased during CR in young mice. The hypothesis tested was that CR leads to increased GC action within AT and BM. To address this, C57BL/6JOlaHsd male and female mice were fed *ad libitum* (AL) or 70% of *ad libitum* food intake (CR) from 9-10 or 9-15 weeks of age, followed by analysis of corticosterone in the circulation and within BM, as well as analysis of GC target gene expression in these tissues.

3.2. Results

3.2.1. Body mass of young mice decreases with CR

To determine if the CR protocol had functioned as expected, the body weight of the mice was measured over the course of the experiment. It was expected for the mice on CR diet to have a decrease in body weight compared to the mice on AL diet. Figure 3.1 shows the body weight progression of both male and female mice measured weekly for six weeks. Both male and female mice were randomly assigned to AL or CR diet, so both diet groups started at approximately the same body mass. After one week of CR both sexes showed a decrease in body mass, whilst the AL mice continued to gradually increase body mass at the same rate as observed before commencing the diet intervention. The male mice on CR continued to show a decrease in body weight until week four post-dietary intervention, where they reached maximum loss. Meanwhile, the female mice on CR did not lose additional weight after week one. Indeed, three-way ANOVA confirmed a significant interaction between diet and sex, such that the magnitude of the CR effect differed between males and females. Up until week five the CR mice maintained their lower body mass, but by week six they began to regain body weight in comparison to previous weeks. At the end of the experiment, the CR mice still showed reduced body weight compared to the AL mice. These results confirmed that that CR intervention acted as expected.

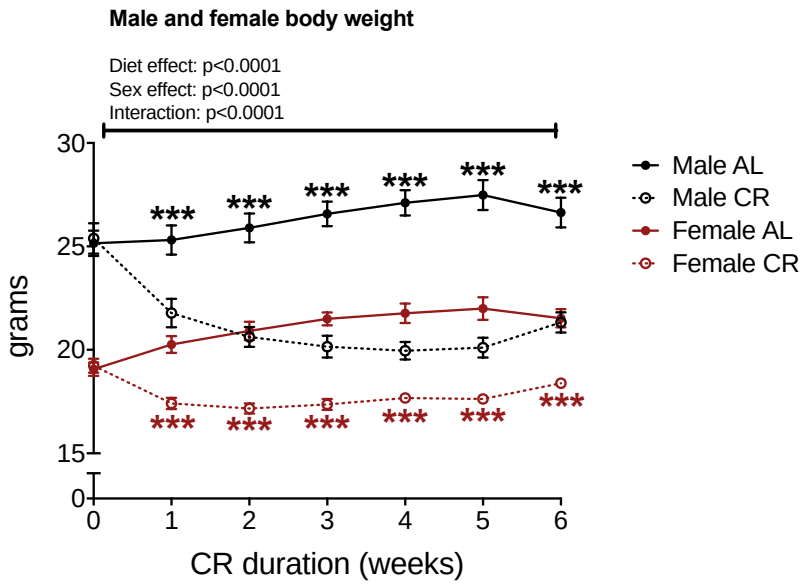

Figure 3.1. Young male and female mice lose body mass with 30% CR diet over six weeks. C57BL/6JOlaHsd male (black) and female (red) mice were fed *ad libitum* (AL, closed symbols, solid line) or 70% of *ad libitum* food intake (CR, open symbols, dotted line) for six weeks, from 9 weeks until 15 weeks of age. The mice were weekly weighed. Data is mean +/- SEM and were analysed by 3-Way ANOVA with Sidak's multiple comparison test. Within each sex, significant differences between AL and CR at each timepoint are indicated by *** ($p<0.001$). n (AL male) = 7. n (CR male) = 11. n (AL female) = 8. n (CR female) = 13.

3.2.2. CR decreases fat mass in male, but not female mice

As discussed in section 3.1, decreased adipose mass may contribute to the health benefits of CR (Muzumdar *et al.*, 2008). Thus, to further characterise the tissue losses and understand the association between diet and body mass, body composition was measured weekly by TD-NMR throughout the six weeks. TD-NMR uses radio-frequency energy, which measure identified fat and lean masses based on the location of protons in the mice. Figure 3.2 shows fat and lean mass of male and female mice, expressed as absolute mass (g) and as a % of total body mass.

Male fat mass showed a significant decrease throughout the six weeks of CR diet, both as absolute mass (Figure 3.2.A) and as a % of body mass (Figure 3.2.B). In contrast, female fat mass as absolute mass (Figure 3.2.A) showed a small diet effect at weeks four and five only. As % of body mass (Figure 3.2.B), female fat mass showed no significant diet effect.

The male lean mass as absolute mass (Figure 3.2.C) showed a significant decrease during CR, from week two onwards. Nonetheless, as % of body mass (Figure 3.2.D), the lean mass was significantly higher in the CR compared to the AL males. In females, absolute lean mass (Figure 3.2.C) significantly decreased with CR. Meanwhile, as % of body mass (Figure 3.2.D), no diet effects were present.

These results show sex differences in changes in body composition in response to CR, suggesting that male mice are mainly losing fat mass but are protecting against loss of lean mass, while female mice are not. Instead, female mice are mainly losing fat and lean mass in proportion to the decrease in body mass; hence, females' % fat and lean mass does not significantly decrease in response to CR.

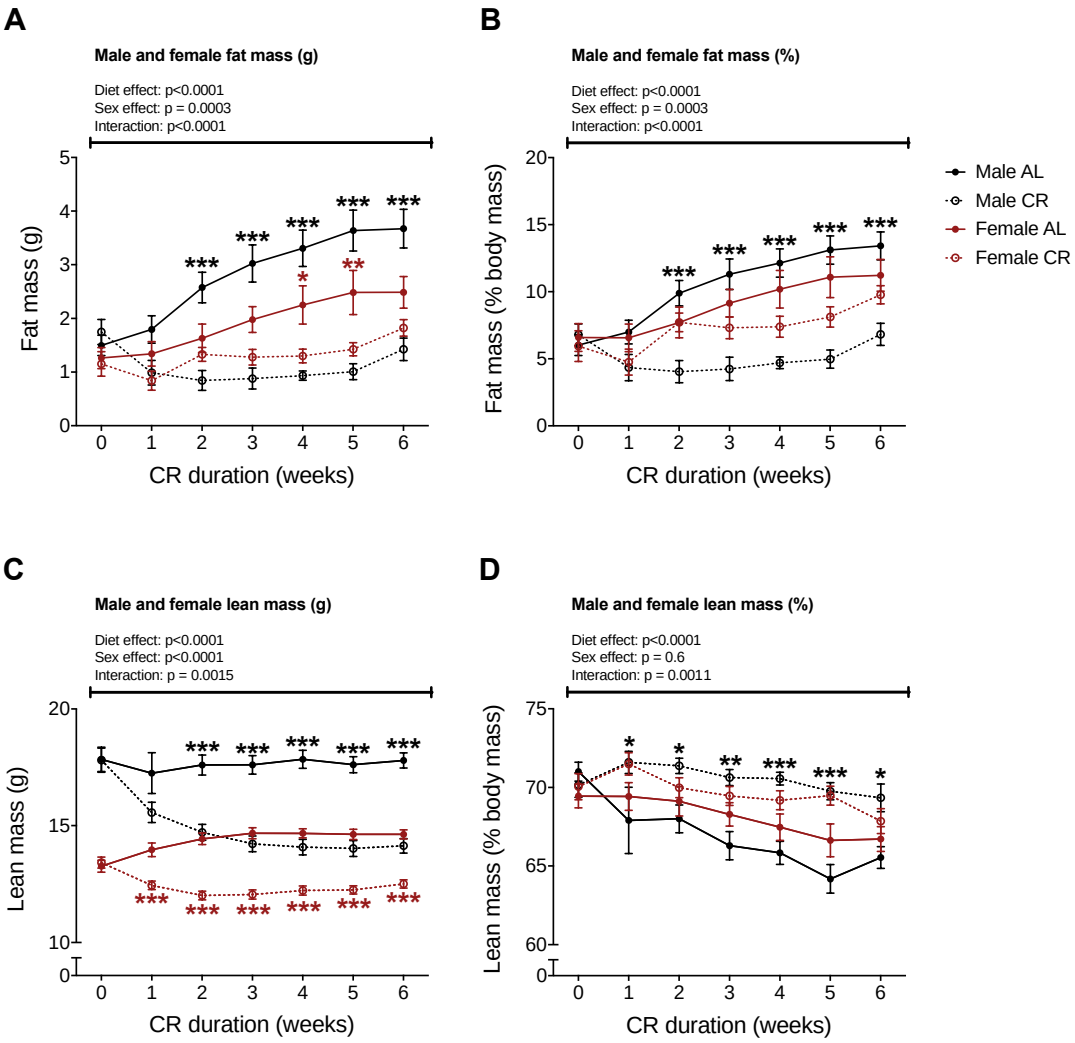

Figure 3.2. Body composition determined by TD-NMR in response to CR. Male and female mice were fed AL or CR diets from 9-15 weeks of age, as described for Figure 3.1 and Methods (2.1.2). Both male and female mice were weekly scanned by TD-NMR. Male and female fat mass shown in grams **(A)** and % of body mass **(B)**. Male and female lean mass shown in grams **(C)** and % of body mass **(D)**. Data is mean +/- SEM and were analysed by 3-Way ANOVA with Sidak's multiple comparison test. Numbers of mice per group, and presentation of statistically significant differences between groups, are as described for figure 3.1. Within each graph, significant differences between AL and CR at each timepoint are indicated by asterisks: *: p<0.05. **: p<0.01 ***: p<0.001.

3.2.3. White adipose depot masses are decreased in male mice in response to CR

To further investigate if specific WAT depots were reflecting the TD-NMR results, after euthanising mice the AT were dissected out and weighed to determine diet differences. Figure 3.3 shows the absolute and relative masses of WAT depots as well as BAT, in both male and female mice subject to CR or AL diets. Inguinal WAT (iWAT) is a subcutaneous AT, whereas gonadal WAT (gWAT) and mesenteric WAT (mWAT) are visceral AT.

Male mice subject to CR lost absolute mass of iWAT (Figure 3.3.A) and gWAT (Figure 3.3.C), whereas the masses of these depots were unaltered by CR in females. As % of body mass, only gWAT in males showed a significant loss with CR (Figure 3.3.D). No mWAT loss was observed in mice subject to CR (Figure 3.3.E, F). This suggests that the loss detected in fat mass with TD-NMR could be from the WAT depots. In females no diet differences were observed, further confirming the lack of loss of fat mass detected by TD-NMR. Overall, these adipose depot masses confirmed the TD-NMR results, showing that males lost fat mass with CR, especially gWAT and to a lesser extent iWAT, whereas females maintained their fat mass. For BAT, a thermogenic adipose depot, both absolute (Figure 3.3.G) and relative mass (Figure 3.3.H) significantly increased with CR across both sexes, although multiple comparisons showed that, within each sex, this CR effect reached statistical significance only for relative BAT mass in males (Figure 3.3.H).

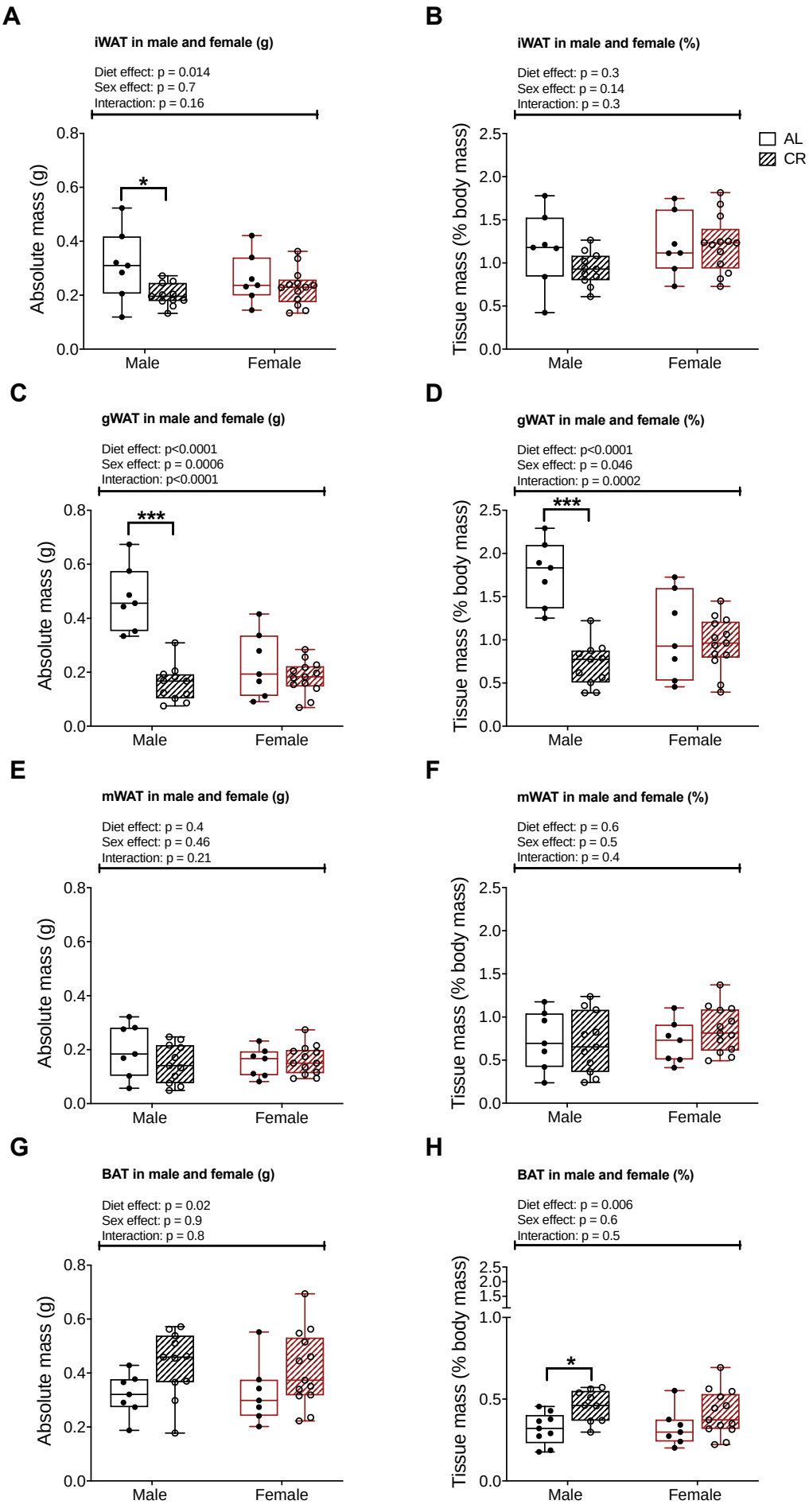
A
iWAT in male and female (g)
Diet effect: p = 0.014
Sex effect: p = 0.7
Interaction: p = 0.16
Absolute mass (g)
0.0
0.2
0.4
0.6
0.8
*
Male
Female
B
iWAT in male and female (%)
Diet effect: p = 0.3
Sex effect: p = 0.14
Interaction: p = 0.3
Tissue mass (% body mass)
0.0
0.5
1.0
1.5
2.0
2.5
AL
CR
Male
Female
C
gWAT in male and female (g)
Diet effect: p<0.0001
Sex effect: p = 0.0006
Interaction: p<0.0001
Absolute mass (g)
0.0
0.2
0.4
0.6
0.8
***
Male
Female
D
gWAT in male and female (%)
Diet effect: p<0.0001
Sex effect: p = 0.046
Interaction: p = 0.0002
Tissue mass (% body mass)
0.0
0.5
1.0
1.5
2.0
2.5
***
Male
Female
E
mWAT in male and female (g)
Diet effect: p = 0.4
Sex effect: p = 0.46
Interaction: p = 0.21
Absolute mass (g)
0.0
0.2
0.4
0.6
0.8
Male
Female
F
mWAT in male and female (%)
Diet effect: p = 0.6
Sex effect: p = 0.5
Interaction: p = 0.4
Tissue mass (% body mass)
0.0
0.5
1.0
1.5
2.0
2.5
Male
Female
G
BAT in male and female (g)
Diet effect: p = 0.02
Sex effect: p = 0.9
Interaction: p = 0.8
Absolute mass (g)
0.0
0.2
0.4
0.6
0.8
Male
Female
H
BAT in male and female (%)
Diet effect: p = 0.006
Sex effect: p = 0.6
Interaction: p = 0.5
Tissue mass (% body mass)
0.0
0.5
1.0
1.5
2.0
2.5
*
Male
Female

Figure 3.3. Dissected adipose depots of male and female mice post six weeks of CR diet. Male and female mice were fed AL or CR diets from 9-15 weeks of age, as described for Figure 3.1 and Methods (2.1.2). iWAT in male and female mice shown in grams **(A)** and as % of body mass **(B)**. gWAT in male and female mice shown in grams **(C)** and as % of body mass **(D)**. mWAT in male and female mice shown in grams **(E)** and as % of body mass **(F)**. BAT in male and female mice shown in grams **(G)** and as % of body mass **(H)**. Data points are presented with median, interquartile range and range shown by box and whisker plot. Data was analysed by 2-Way ANOVA with Sidak's multiple comparison test. n (AL male) = 7. n (CR male) = 11. n (AL female) = 7. n (CR female) = 13. *: $p<0.05$. ***: $p<0.001$.

3.2.4. CR promotes hypercorticosteronaemia and sex-dependent effects on adrenal masses

It has previously been shown that circulating GC concentrations increase during CR (Sabatino *et al.*, 1991; Chacón *et al.*, 2005; Levay *et al.*, 2010; Pankevich *et al.*, 2010; Tomiyama *et al.*, 2010; Cawthorn *et al.*, 2016; Fontana *et al.*, 2016). Therefore, I sought to confirm this in my AL and CR mice. Prior to termination, tail and core blood was collected for plasma. Adrenal glands were dissected and weighed as indicators of increased capacity of corticosterone synthesis.

Figure 3.4 presents plasma corticosterone concentrations throughout the six-week CR. ANOVA confirmed that circulating corticosterone concentration was significantly increased during CR across both sexes, with multiple comparisons revealing that CR males (Figure 3.4 – black dotted lines) had increased corticosterone compared to AL males at each week of CR. CR males also had greater corticosterone than CR females at week two of CR. Meanwhile, multiple comparisons revealed that female mice (Figure 3.4 – red dotted lines) on CR showed a significant increase only at week five of CR. Together, these data show that CR increases plasma corticosterone in male and female mice and that this effect is greater in males.

At week six, corticosterone concentrations in AL female mice were increased compared to the previous week, whereas males and females on CR showed a decrease at week six compared to the previous week. As discussed further in the discussion (Section 3.3), this variability between weeks 5-6 likely resulted from fasting both AL and CR mice for several hours prior to termination. One concern was that these changes in plasma corticosterone might extend to altered GC action within WAT and BM. If so, such tissue-specific readouts of GC action might not be representative of the tissue-level GC effects occurring throughout the remainder of the six-week CR regimen. Therefore, to overcome this, a short-term one-week CR experiment was also done, similarly to the six-week experiment, but without fasting the mice prior to the endpoint.

The short-term one-week CR mice were culled at 10-weeks of age, whereas, the long-term six-week CR mice were culled at 15-weeks of age. Quantification of corticosterone by ELISA was not implemented on the one-week CR mice, as it was

already clear from figure 3.4 that corticosterone would increase prior to termination. Therefore, subsequent analyses will not only compare between sex and diet, but also between the long-term six-week (15-weeks of age) and short-term one-week CR (10-weeks of age) mice.

Figure 3.5 shows the adrenal gland masses. In the 15-week-old males, CR caused a significant increase in absolute mass (Figure 3.5A) and relative mass (Figure 3.5.C) of the adrenal glands. Analysis by ANOVA revealed an overall diet effect in the 15-week-old mice for relative mass of the adrenal glands (Figure 3.5.C). It also revealed an overall sex effect, with heavier adrenal glands in the females (Figure 3.5.A, C). In the 10-week-old mice, diet differences were not detected (Figure 3.5.B, D) although ANOVA revealed an overall sex effect for relative adrenal mass (Figure 3.5.D), with females again having a greater % mass than males.

Figure 3.6 displays plasma corticosterone and 11-DHC concentrations as determined by LC-MS/MS, as well as the ratio between the two. CR was associated with significantly increased plasma corticosterone concentration in the 10-week-old mice (Figure 3.6.B), whereas 15-week-old mice lacked diet effects (Figure 3.6.A). No diet or sex effects were detected for plasma 11-DHC concentrations in the 15-week-old mice (Figure 3.6.C), whereas 10-week-old mice subject to CR showed an increase in plasma 11-DHC (Figure 3.6.D). The ratio of 11-DHC to corticosterone was significantly decreased in 10-week-old male mice on CR (Figure 3.6.F), whereas no changes were detected in 15-week-old mice with CR (Figure 3.6.E).

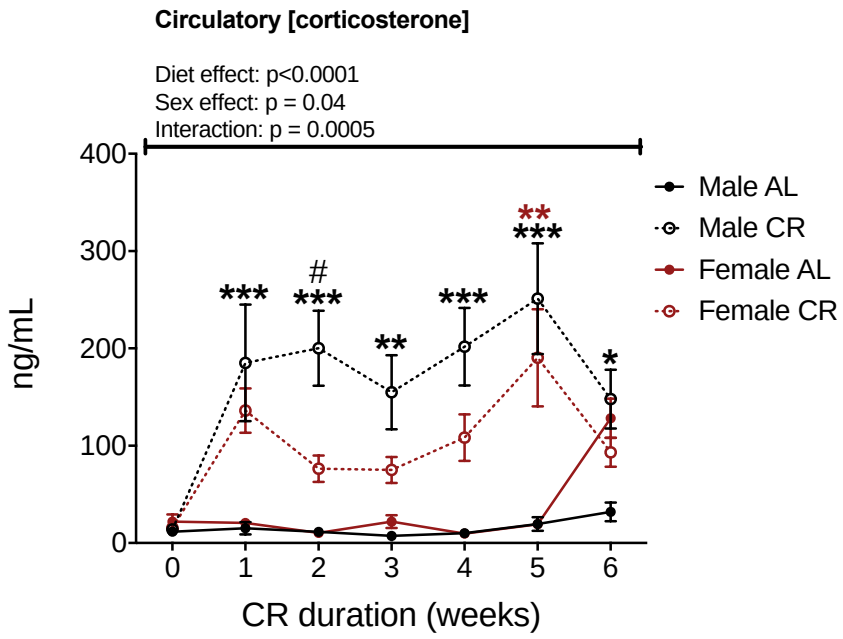

Figure 3.4. Circulating corticosterone concentration is increased in mice subject to CR. Male and female mice were fed AL or CR diets from 9-15 weeks of age, as described for Figure 3.1 and Methods (2.1.2). Throughout the CR experiment, blood was sampled and quantified by ELISA as described in Methods (2.4). Circulatory corticosterone concentration in male and female mice from weekly collected plasma. Data is mean +/- SEM and was analysed by 3-Way ANOVA with Tukey's multiple comparison test. n (AL male) = 7. n (CR male) = 10. n (AL female) = 6. n (CR female) = 9. * (male): p<0.05. ** (male) ** (female): p<0.01. *** (male): p<0.001. # (sex effect): p<0.05.

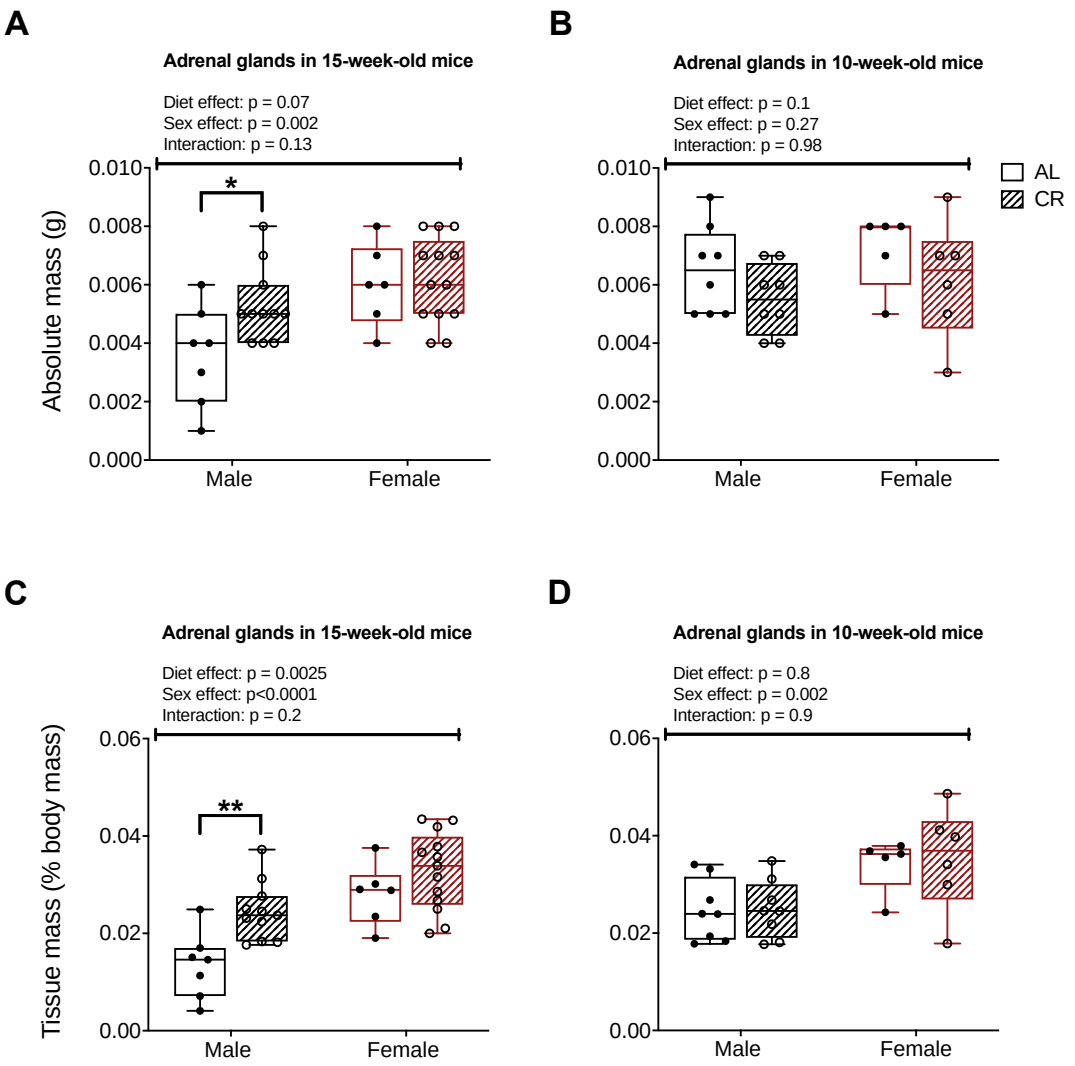

Figure 3.5. Adrenal gland mass is predominantly increased in male mice subject to CR. Male and female mice were fed AL or CR diets from 9-15 (left graphs) and 9-10 (right graphs) weeks of age, as described for Figure 3.1 and Methods (2.1.2). Fasting protocol is described in Methods (2.3.1). Post termination, adrenal glands were dissected and weighed. 15-and **(A)** 10- **(B)** week-old male and female adrenal glands shown in grams. 15-and **(C)** 10- **(D)** week-old male and female adrenal glands shown % of body mass. Data points are presented with median, interquartile range and range shown by box and whisker plot, and were analysed by 2-Way ANOVA with Sidak's multiple comparison test. 15-week-old mice: n (AL male) = 7. n (CR male) = 10. n (AL female) = 7/8. n (CR female) = 9. 10-week-old mice: n (AL male) = 8. n (CR male) = 8. n (AL female) = 5. n (CR female) = 6. *: $p<0.05$. **: $p<0.01$.

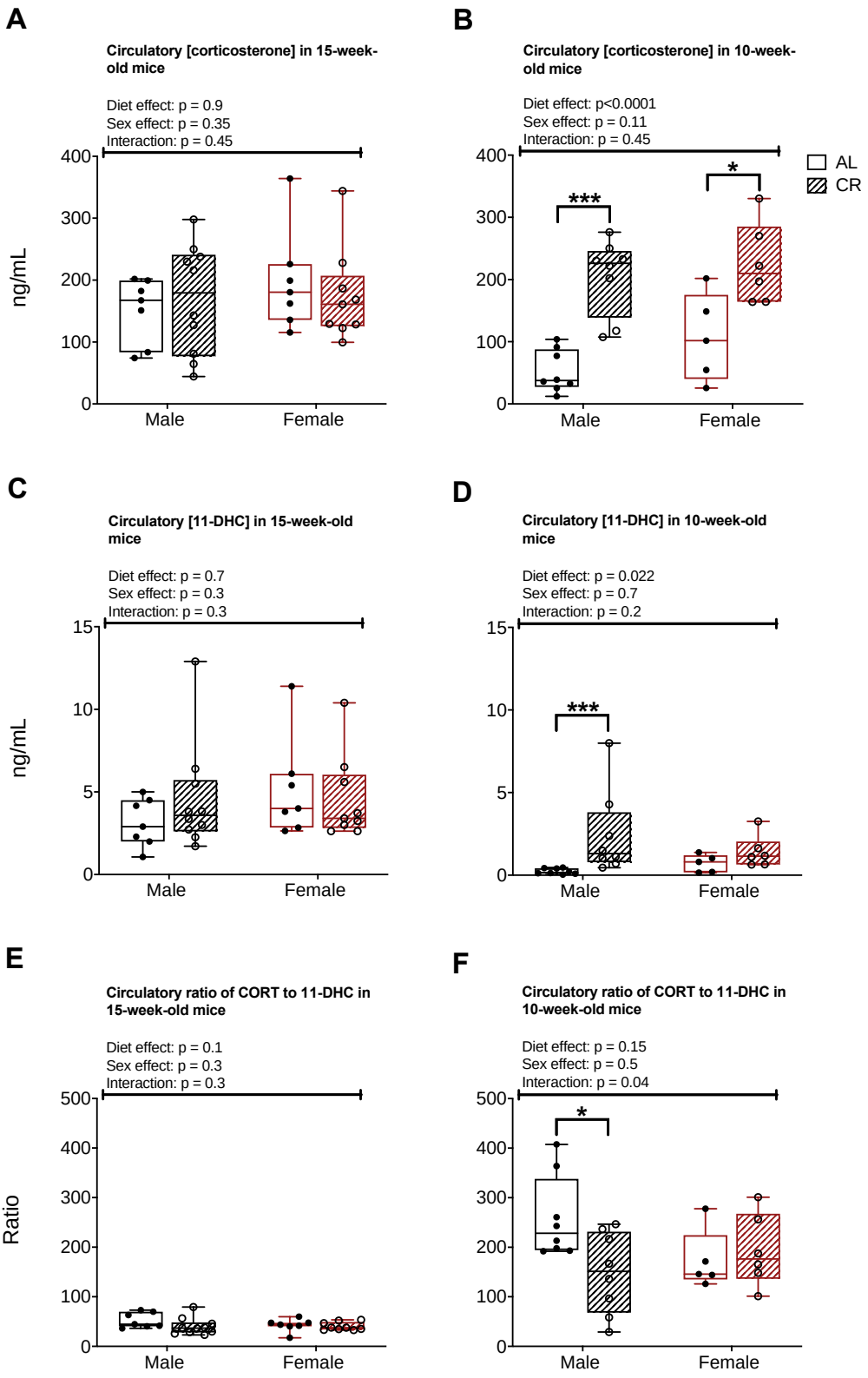

Figure 3.6. End-point GCs are increased in mice subject to CR. Male and female mice were fed AL or CR diets from 9-15 (left graphs) and 9-10 (right graphs) weeks of age, as described for Figure 3.1 and Methods (2.1.2). Fasting protocol is described in Methods (2.3.1). Prior to termination, end-point blood was sampled and quantified by LC-MS/MS as described in Methods (2.5.1). Circulatory corticosterone

concentration in 15-and **(A)** 10- **(B)** week-old mice. Circulatory 11-DHC concentration in 15-and **(C)** 10- **(D)** week-old mice. Ratio of circulatory corticosterone to 11-DHC in 15-and **(E)** 10- **(F)** week-old mice. Data points are presented with median, interquartile range and range shown by box and whisker plot, and were analysed by 2-Way ANOVA with Sidak's multiple comparison test. 15-week-old mice: n (AL male) = 7. n (CR male) = 10. n (AL female) = 7. n (CR female) = 9. 10-week-old mice: n (AL male) = 8. n (CR male) = 8. n (AL female) = 5. n (CR female) = 6. *: $p<0.05$. ***: $p<0.001$.

3.2.5. GC regeneration in the BM is modulated by CR

Due to the differences observed between the circulatory GCs in 15-week-old vs 10-week-old mice, I next sought to determine if CR exerted similar effects on GC concentrations within the BM. Indeed, no previous studies have addressed the impact of CR on BM GC concentrations, underscoring the rationale for this experiment. Post-termination, femurs were collected and stored at -80ºC until LC-MS/MS quantification of GCs within the femoral BM.

Figure 3.7 shows the results obtained from LC-MS/MS for corticosterone, the active GC, and for 11-DHC, the inactive GC, as well as the ratio between the two. Corticosterone (Figure 3.7.A) and 11-DHC (Figure 3.7.C) concentration in 15-week-old mice lacked diet differences. However, in the 10-week-old mice, both corticosterone (Figure 3.7.B) and 11-DHC (Figure 3.7.D) were increased with CR. The ratio of 11-DHC to corticosterone lacked diet differences in the 15-week-old mice (Figure 3.7.E), although an overall sex effect was detected by ANOVA, with higher expression in the female mice. For the 10-week-old mice ANOVA revealed that CR significantly decreased the ratio across both sexes of mice (Figure 3.7.F). Multiple comparisons further confirmed that CR significantly decreased the ratio in females, with a similar but non-significant effect in males (Figure 3.7.F).

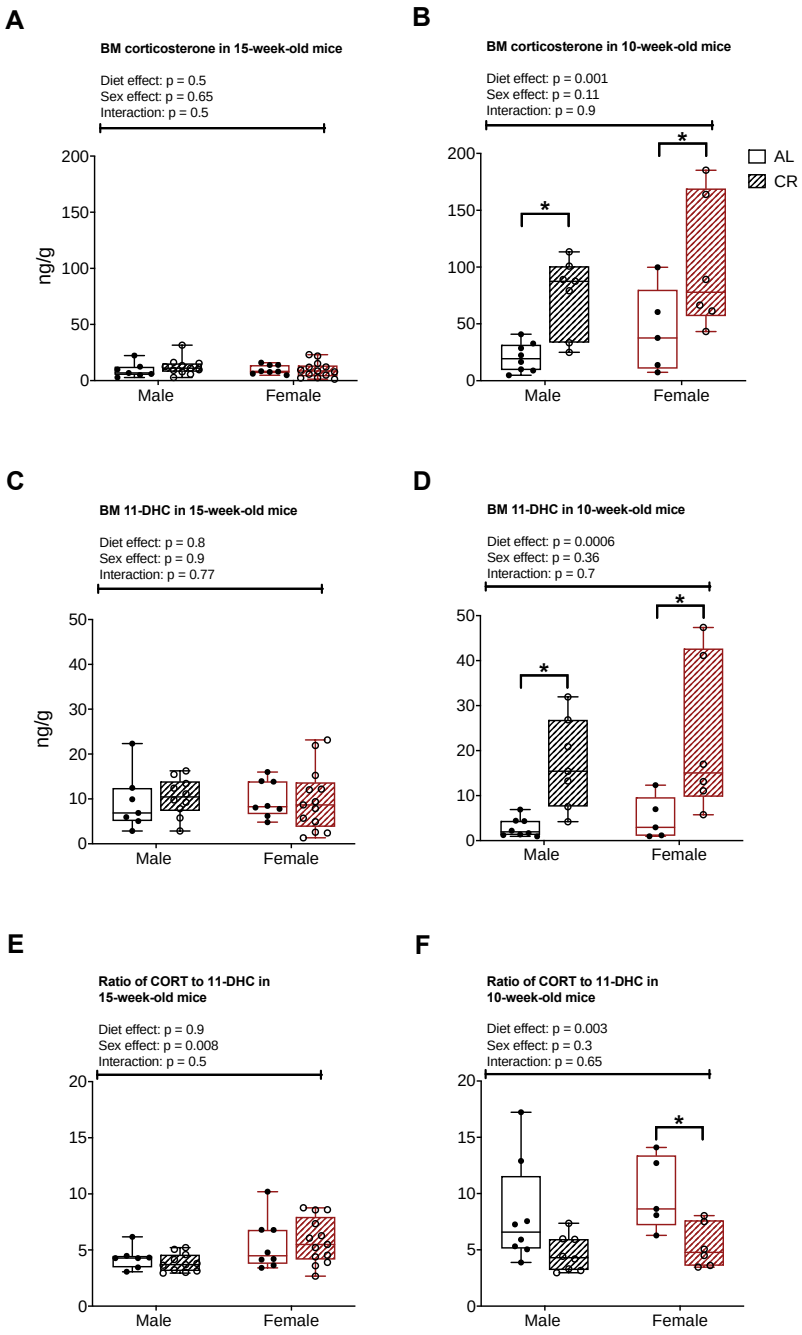

Figure 3.7. BM GCs are increased in mice subject to CR. Male and female mice were fed AL or CR diets from 9-15 (left graphs) and 9-10 (right graphs) weeks of age, as described for Figure 3.1 and in Methods (2.1.2). Fasting protocol is described in Methods (2.3.1). Post termination, femurs were collected and the femoral BM was quantified for 11-DHC and corticosterone by LC-MS/MS as described in methods (2.5.2). BM corticosterone concentration in 15- and **(A)** 10- **(B)** week-old mice. BM 11-DHC concentration in 15- and **(C)** 10- **(D)** week-old mice. Ratio of corticosterone to 11-DHC in 15- and **(E)** 10- **(F)** week-old mice. Data points are presented with median, interquartile range and range shown by box and whisker plot, and were analysed by 2-Way ANOVA with Sidak's multiple comparison test. 15-week-old mice: n (AL male) = 7. n (CR male) = 10. n (AL female) = 8. n (CR female) = 9. 10-week-old mice: n (AL male) = 8. n (CR male) = 8. n (AL female) = 5. n (CR female) = 6. *: $p<0.05$. **: $p<0.01$.

3.2.6. CR is associated with increased GC target gene expression in the BM

As mentioned previously, corticosterone concentration assessed by ELISA in plasma showed increased levels with CR (Figure 3.4). Likewise, the 10-week-old mice cohort showed increased corticosterone in the circulation and the BM. Therefore, to further compare how CR modulates peripheral tissues, and if tissue-specific GC action differed between the 15-week-old vs 10-week-old mice, expression of GC target genes were examined in the BM of both cohorts.

Figure 3.8. shows expression of *Hsd11b1*, a GC target gene in the BM of 15-and 10-week-old mice. *Hsd11b1* expression was increased with CR in the 15-week-old mice (Figure 3.8.A), whereas in the 10-week-old mice, no diet differences were detected (Figure 3.8.B).

Figure 3.9 shows additional GC target genes, *Fkbp5, Gilz* and *Per* in the BM of 15- and 10-week-old mice. *Fkbp5* expression was upregulated with CR in the BM of the 10-week-old mice (Figure 3.9.B), but not in the 15-week-old mice (Figure 3.9.A). *Gilz* (Figure 3.10.C) and *Per1* (Figure 3.10.E) expression was unaltered with CR in the 15-week-old mice, but significantly increased in the 10-week-old mice (Figure 3.10.D, F).

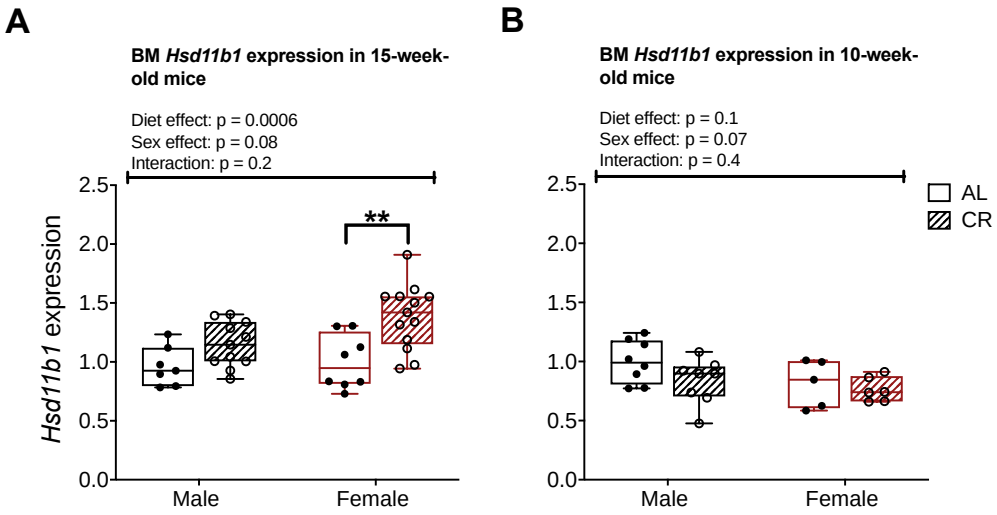

Figure 3.8. *Hsd11b1* expression is increased post six-weeks but not one-week of CR in the BM. Male and female mice were fed AL or CR diets from 9-15 (left graphs) and 9-10 (right graphs) weeks of age, as described for Figure 3.1 and Methods (2.1.2). Fasting protocol is described in Methods (2.3.1). Post termination, the tibiae were collected and snap-frozen on dry ice. The tibia BM was then centrifuged down as described in Methods (2.3.3), followed by RNA extraction and reverse transcription to cDNA. qPCR was performed to quantify expression of *Hsd11b1* in the BM. Genes were normalised to geomean of the following housekeeping genes: *Ppia*, *Tbp* and *Actb*, and presented as relative to the WT AL average of male and female mice together. *Hsd11b1* expression of BM in 15- **(A)** and 10- **(B)** week-old mice. Data points are presented with median, interquartile range and range shown by box and whisker plot, and were analysed by 2-Way ANOVA with Sidak's multiple comparison test. 15-week-old mice: n (AL male) = 7. n (CR male) = 10. n (AL female) = 8. n (CR female) = 9. 10-week-old mice: n (AL male) = 8. n (CR male) = 8. n (AL female) = 5. n (CR female) = 6. **: $p<0.01$.

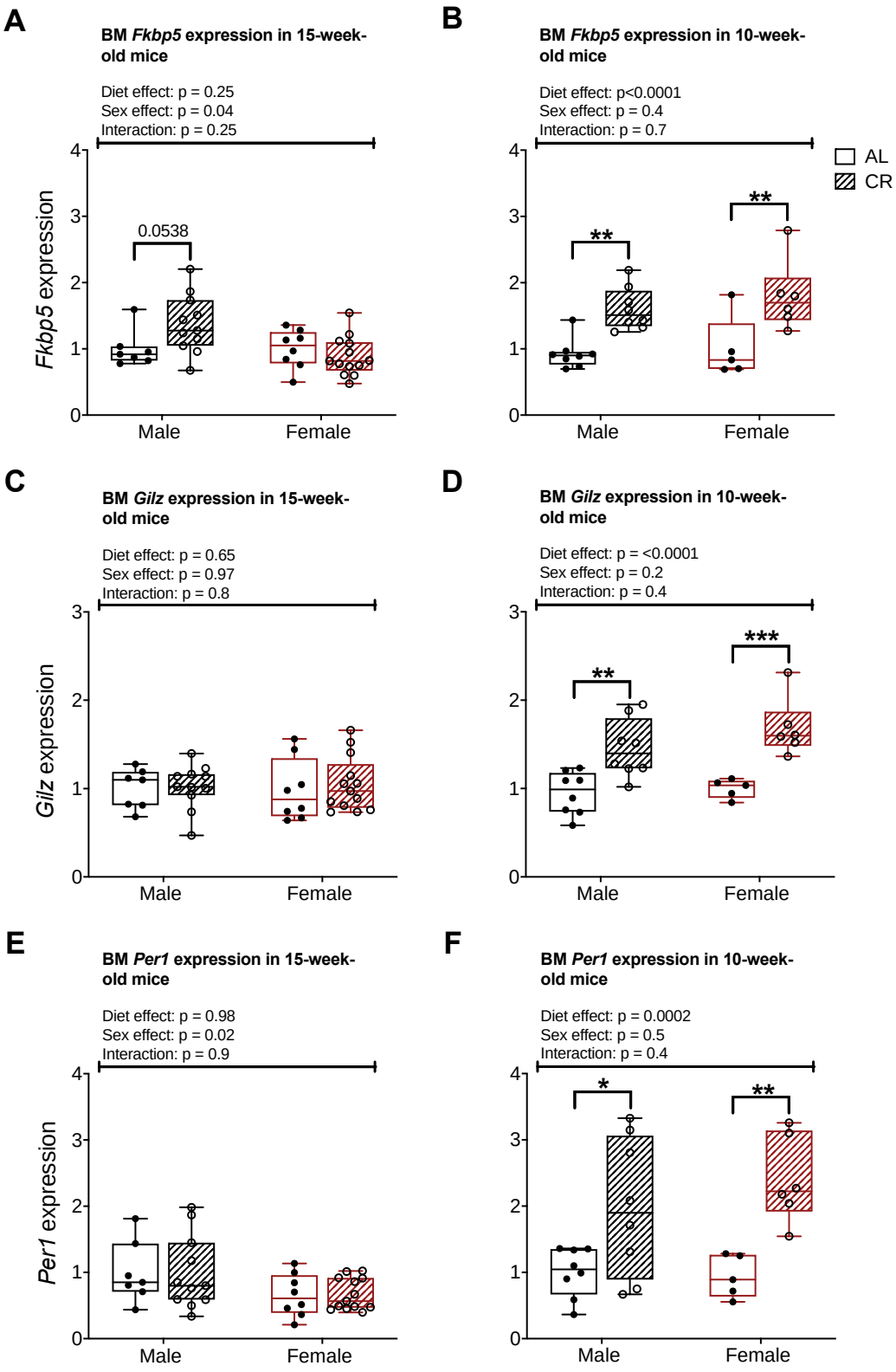

Figure 3.9. GC target genes, *Fkbp5, Gilz* and *Per1*, are increased with CR in BM. Male and female mice were fed AL or CR diets from 9-15 (left graphs) and 9-10 (right graphs) weeks of age, as described for Figure 3.1 and Methods (2.1.2). Fasting protocol is described in Methods (2.3.1). Post termination, the tibiae were collected and snap-frozen on dry ice. The tibia BM was then centrifuged down, followed by RNA

extraction and reverse transcription to cDNA. qPCR was performed to quantify expression of *Fkbp5, Gilz and Per1* in the BM. Genes were normalised to geomean of the following housekeeping genes: *Ppia*, *Tbp* and *Actb*, and presented as relative to the WT AL average of male and female mice together. *Fkbp5* expression of BM in 15- **(A)** and 10- **(B)** week-old mice. *Gilz* expression of BM in 15- **(C)** and 10- **(D)** week-old mice. *Per1* expression of BM in 15- **(E)** and 10- **(F)** week-old mice. Data points are presented with median, interquartile range and range shown by box and whisker plot, and were analysed by 2-Way ANOVA with Sidak's multiple comparison test. 15-week-old mice: n (AL male) = 7. n (CR male) = 10. n (AL female) = 8. n (CR female) = 9. 10-week-old mice: n (AL male) = 8. n (CR male) = 8. n (AL female) = 5. n (CR female) = 6. *: $p<0.05$. **: $p<0.01$. ***: $p<0.001$

.

3.2.7. CR alters expression of GC target genes in WAT

As shown in sections 3.2.2 and 3.2.3, male mice subject to CR had significantly decreased fat mass whereas female mice resisted this effect of CR. More specifically, CR significantly decreased the masses of iWAT and gWAT in male mice only (Figure 3.3). Moreover, plasma corticosterone concentrations were significantly increased throughout CR in males, but less so in the females (Figure 3.4). Therefore, one possibility is that sex differences in GC excess contribute to the sex differences in adipose mass during CR, perhaps through molecular mechanisms induced by GCs. To further address this, transcript markers were used to assess the effects of CR on expression of GC target genes in adipose depots.

Figure 3.10 shows expression of the GC target genes *Hsd11b1*, *Gilz*, *Per1* and *Fkbp5* in iWAT and gWAT of both CR cohorts. *Hsd11b1* was significantly increased in 15-week-old male mice subject to CR (Figure 3.10.A), with females showing a similar but non-significant trend; however, ANOVA detected overall diet effects across both sexes. In the 10-week-old mice, no diet differences were detected with CR (Figure 3.10.B). Overall sex effects by ANOVA was detected in both cohorts, with females having lower *Hsd11b1* expression than males. *Gilz* expression was upregulated in iWAT of 15-week-old male mice subject to CR (Figure 3.10.C), and in iWAT of 10-week-old females subject to CR (Figure 3.10.D). Overall diet effects by ANOVA were detected in all groups, apart from gWAT of 15-week-old mice. *Per1* expression was significantly increased in 10-week-old iWAT females and gWAT males, with CR (Figure 3.10.F) Overall diet effects by ANOVA for *Per1* expression were detected in iWAT of both cohorts, and gWAT of the 10-week-old mice. The overall diet effects for iWAT of the 15-week-old cohort reflected a decrease with CR in males only, whereas in the 10-week-old cohort, it revealed the opposite. *Fkbp5* expression was significantly decreased in iWAT of 15-week-old male mice subject to CR (Figure 3.10.G). However, in the 10-week-old males, an overall diet effect by ANOVA suggested an increase in *Fkbp5* expression (Figure 3.10.H). gWAT in the 10-week-old mice on CR showed increased *Fkbp5* expression (Figure 3.10.H), but no diet differences were detected in the 15-week-old mice (Figure 3.10.G).

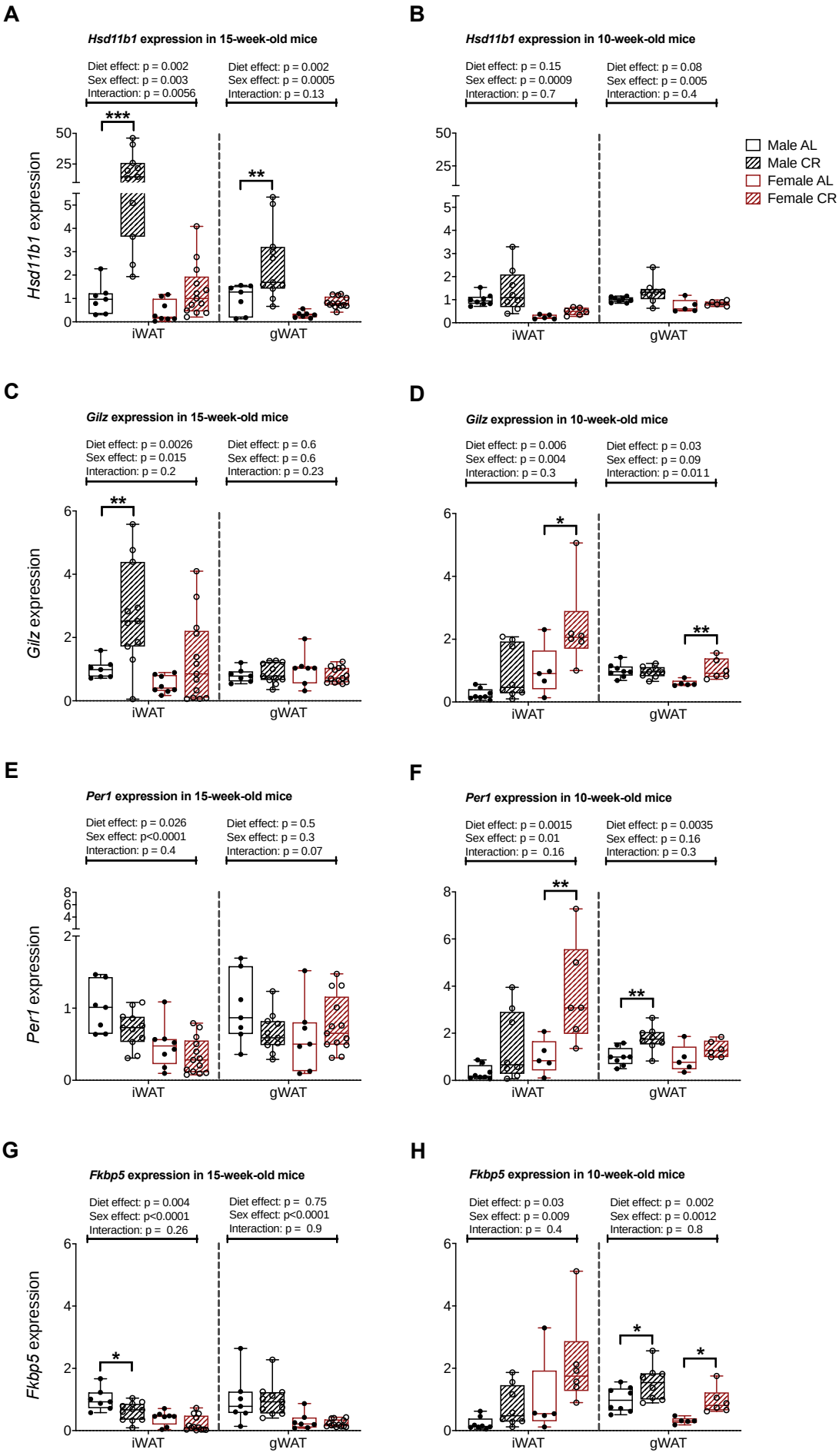
A
Hsd11b1 expression in 15-week-old mice
Diet effect: p = 0.002
Sex effect: p = 0.003
Interaction: p = 0.0056
Diet effect: p = 0.002
Sex effect: p = 0.0005
Interaction: p = 0.13
Hsd11b1 expression
iWAT
gWAT
B
Hsd11b1 expression in 10-week-old mice
Diet effect: p = 0.15
Sex effect: p = 0.0009
Interaction: p = 0.7
Diet effect: p = 0.08
Sex effect: p = 0.005
Interaction: p = 0.4
Male AL
Male CR
Female AL
Female CR
C
Gilz expression in 15-week-old mice
Diet effect: p = 0.0026
Sex effect: p = 0.015
Interaction: p = 0.2
Diet effect: p = 0.6
Sex effect: p = 0.6
Interaction: p = 0.23
Gilz expression
D
Gilz expression in 10-week-old mice
Diet effect: p = 0.006
Sex effect: p = 0.004
Interaction: p = 0.3
Diet effect: p = 0.03
Sex effect: p = 0.09
Interaction: p = 0.011
E
Per1 expression in 15-week-old mice
Diet effect: p = 0.026
Sex effect: p<0.0001
Interaction: p = 0.4
Diet effect: p = 0.5
Sex effect: p = 0.3
Interaction: p = 0.07
Per1 expression
F
Per1 expression in 10-week-old mice
Diet effect: p = 0.0015
Sex effect: p = 0.01
Interaction: p = 0.16
Diet effect: p = 0.0035
Sex effect: p = 0.16
Interaction: p = 0.3
G
Fkbp5 expression in 15-week-old mice
Diet effect: p = 0.004
Sex effect: p<0.0001
Interaction: p = 0.26
Diet effect: p = 0.75
Sex effect: p<0.0001
Interaction: p = 0.9
Fkbp5 expression
H
Fkbp5 expression in 10-week-old mice
Diet effect: p = 0.03
Sex effect: p = 0.009
Interaction: p = 0.4
Diet effect: p = 0.002
Sex effect: p = 0.0012
Interaction: p = 0.8

Figure 3.10. Effects of CR on GC target genes in WAT. Male and female mice were fed AL or CR diets from 9-15 (left graphs) and 9-10 (right graphs) weeks of age, as described for Figure 3.1 and Methods (2.1.2). Fasting protocol is described in Methods (2.3.1). Post termination, iWAT and gWAT depots were dissected and snap-frozen on dry ice. The depots were homogenised in liquid nitrogen, followed by RNA extraction and reverse transcription to cDNA. qPCR was performed to quantify expression of *Hsd11b1, Gilz*, *Per1* and *Fkbp5*. Genes were normalised to geomean of the following housekeeping genes: *Ppia*, *Tbp* and *Hprt*, and presented as relative to the WT AL average of male and female mice together. *Hsd11b1* expression of iWAT and gWAT in 15- **(A)** and 10- **(B)** week-old mice. *Gilz* expression of iWAT and gWAT in 15- **(C)** and 10- **(D)** week-old mice. *Per1* expression of iWAT and gWAT in 15- **(E)** and 10- **(F)** week-old mice. *Fkbp5* expression of iWAT and gWAT in 15- **(G)** and 10- **(H)** week-old mice. Data points are presented with median, interquartile range and range shown by box and whisker plot, and were analysed by 2-Way ANOVA with Sidak's multiple comparison test. 15-week-old mice: n (AL male) = 7. n (CR male) = 10. n (AL female) = 8. n (CR female) = 9. 10-week-old mice: n (AL male) = 8. n (CR male) = 8. n (AL female) = 5. n (CR female) = 6. *: $p<0.05$. **: $p<0.01$. ***: $p<0.001$.

3.3. Discussion

3.3.1. Sexual dimorphism in body composition

A surprising observation from the quantification of body composition was that female mice did not lose fat mass during CR. Further analysis of the adipose depots confirmed the lack of loss in fat mass in female mice. This suggests that female mice are resistant to fat mass loss, most likely due to adiposity being fundamental for reproductivity, for example the release of leptin from WAT. Leptin is essential for maintaining pregnancy, as it is increased throughout pregnancy, and only declines postpartum (Hardie *et al.*, 1997; Schubring *et al.*, 1998). Furthermore, leptin-deficient females are infertile (Ahima *et al.*, 1997; Chehab, 1997; Ewart-Toland *et al.*, 1999), and the fall in leptin is why females can become amenorrhoeic if they become too thin as in AN or in female athletes. However, during CR, leptin is decreased (Cawthorn *et al.*, 2016) in male mice only, suggesting that female mice on CR maintain their leptin and fat mass for possible reproduction. Moreover, mild 5% CR has shown to induce fat accumulation in female mice (Li *et al.*, 2010). Porter *et al.,* investigated mild (5%) to moderate (29%) CR in male and female rats and found that females preserved adipose fat cells, but the fat cell volume was shrunken (Porter *et al.*, 2004). Meanwhile, male rats showed the opposite results. Although a stricter CR diet was implemented in my mice, it is confirming the lack of loss in fat mass in female mice (Li *et al.*, 2010). Previous research has compared gluteal vs abdominal adipocytes and found that both noradrenaline-and catecholamine-induced lipolysis is greater in abdominal than gluteal, and more so in women than men (Wahrenberg, Lönnqvist and Arner, 1989; White and Tchoukalova, 2014). This further highlights the resistance of gluteal fat loss in women. However, a limitation of my study is that adipocyte size was not quantified and can therefore not be commented on for the sex difference.

It is also common in humans for women to have higher adiposity relative to men. The adipose distribution varies between men and women, with men having more visceral adipose, whereas women have more gluteal adiposity (Machann *et al.*, 2005; Camhi *et al.*, 2011). It has also been shown that although women can lose fat mass to a similar extent as men while subject to 25% CR for six months, they lose significantly less visceral adiposity compared to men (Redman *et al.*, 2007). It is however important to notice that the study was performed on obese, but healthy volunteers.

Moreover, the starting points between men and women did vary as the men were heavier and fatter at baseline. Meanwhile, a 20% CR study was performed on non-obese healthy men and women, where body weight and composition were significantly lost with CR, but no sex differences were investigated (Racette *et al.*, 2006). Furthermore, previous publication reported that GCs are dependent on insulin and adrenalin to induce lipolysis in subcutaneous AT; visceral AT resisted the lipolytic effects (Stimson *et al.*, 2017). These findings could point towards the characteristics of central adipose accumulation with chronic GC excess. The males in this study lost subcutaneous and visceral adiposity, suggesting that insulin and/or adrenaline could have been involved with CR, or other factors that are yet to be revealed. In addition, correlation data between plasma corticosterone and absolute fat mass was negatively associated, although not significant (data not shown). However, the females which resisted the loss of fat could have potentially also resisted the insulin and/or adrenaline, or their insulin and/or adrenalin levels could have been significantly lower to have had an impact.

In the present study, CR mice were given their food portion approximately at 9:00. From approximately 10:00 until 9:00 the following day, the mice underwent short-term fasting between daily feeds, which could have increased the males' metabolism to burn fat mass, while female mice resisted lipolysis (Mauriège *et al.*, 1999). Another reason the female mice are resisting fat loss could be due to being fed more food per body mass. The CR food mass was decided on how much the mice ate daily during their first single-housed week, and that was averaged at the end of the week, for male and female mice together, suggesting the female mice might receive less than 30% CR. To test this out, we investigated the association between their food intake and changes in fat mass (data not shown), and no associations were evident enough that the feeding affected the fat mass. However, to understand this further, data from all animal studies could be collected to look separately in AL-and CR-fed males and females.

These data show that sexual dimorphism, especially during CR, ought to be considered when researching AT. By doing so, better diagnosis and treatments will become available for various adiposity conditions, where sex-specific treatments might be required.

3.3.2. Diet effects – to fast or not to fast

Excluding possible sex differences, a diverse reason for not observing any diet differences between GC target genes and BM corticosterone concentration, in the 15-week-old six-week CR cohort, could be due to the previously mentioned fasting of the AL mice and re-feeding of the CR mice prior to termination. If the mice were culled without fasting, the AL mice would be culled in a fed state, whereas the CR mice would be in a fasted state. The aim with six-weeks of CR was to look at the effects of GC action in the WAT and more specifically in the BM as this is when it has been previously been reported that BMAT expands (Devlin *et al.*, 2010). Six-weeks of CR would therefore be described as long-term CR, rather than short-term fasting. Thus, the aim with the fasting prior to termination was to investigate long-term CR, rather than short-term fasting, hence it was required that both groups were fasted. This way, any dissimilarities observed would not be subjective by their variation in the short-term feeding prior to termination. A similar approach has been advocated in other recent large-scale CR studies in mice (Mitchell *et al.*, 2015). Based on the fasting of the AL mice, and refeeding of the CR mice, it is possible that the fasting might have affected the corticosterone synthesis in the AL mice, intensifying their stress levels above their natural concentration as they are not used to short-term fasting. Another option to consider would be the re-feeding of the CR mice at the same time that the AL mice had their food removed. Once the AL mice had their food removed, they received half a portion of AL food of what they would normally eat each day (1.5 g), and the CR mice received half a portion (1.05 g) of their daily CR diet ration (2.1 g). By refeeding the CR mice, their GC levels compared to previously in AT and BM could have decreased. Their circulatory corticosterone concentration at week six were decreased in comparison to previous week, suggesting that their tissue-specific levels could equally be affected. Based on the uncertainty of these results, I considered it was imperative to assess my fasting hypothesis. The six-week study showed that corticosterone concentration was increased by one-week of CR, therefore a one-week cohort was used to assess the fasting hypothesis as this would be sufficient for CR to increase plasma corticosterone. Based on the lack of diet differences, it was concluded that pursuing the short-term one-week CR cohort was imperative to address my hypothesis regarding effects of CR on GC action within BM and WAT.

Pursuing the short-term one-week CR cohort, and comparing these data to the six-week cohort, provided further insight into the relationship between CR duration,

circulating corticosterone, and tissue-specific GC effects. The GC target genes of the 15-week-old mice were significantly decreased (possibly due to re-feeding) in comparison to the 10-week-old mice. These results indicate that the long-term effects of CR are masked by the refeeding of the mice, rather than the overnight fasting. However, the age of the mice could have also impacted these results. Therefore, to overcome this, an aged-match cohort for six-week CR would have to be conducted, without fasting prior to termination, to compare to my current six-week CR cohort.

3.3.3. Causes and consequences of GC excess during CR

3.3.3.1. CR increases circulating and tissue-specific GCs

Previous study have shown that plasma corticosterone is increased after six weeks of CR (Cawthorn *et al.*, 2016). My results extend this previous study by showing that the increase begins after only one week of CR; persist throughout CR; and are greater in males than in females. Moreover, in the 10-week-old cohort, mass spectrometry confirmed that the CR effects are more significant in males than females, for circulatory corticosterone (Figure 3.6). Previously, decreased leptin was shown to contribute to hypercorticosteronaemia during fasting (Ahima *et al.*, 1996; Perry *et al.*, 2014). Based on my results, it could be that females have blunted increases in circulating corticosterone because they did not have decreased leptin (or fat mass) as much as males. In addition to circulatory levels, tissue-specific GC concentrations were also analysed. GCs were increased with CR in the BM, although, the CR effects did not vary between males and females for corticosterone concentration (Figure 3.7). Since GC regeneration in tissue is regulated by 11β-HSD1, it suggests that circulatory concentrations do not affect tissue-specific GCs, but instead, they are indeed regulated by 11β-HSD1.

The conversion of corticosterone to 11-DHC is catalysed by the enzyme 11β-HSD2. My results showed a decrease in the plasma ratio of 11-DHC to corticosterone in the 10-week-old males only on CR (Figure 3.6.F). Although, in the BM, Anova showed an overall decrease in both sexes (Figure 3.7.F). The 15-week-old mice lacked diet differences in both the plasma and BM, probably due to the fasting/re-feeding blunting the end results. These results could potentially suggest that 11β-HSD1 activity is decreased with CR in the BM in both males and females, and in the circulation in males only. However, these results could also be due to plentiful conversion of

corticosterone to 11-DHC by 11β-HSD2 with CR, hence 11-DHC regeneration is magnified. Furthermore, these results are different from a 11β-HSD1 activity measurement, as LC-MS/MS and mRNA results are not functional and whilst these might give an idea of activity, they are not informative of activity in a controlled way. Therefore, it cannot be concluded that 11β-HSD1 activity is necessarily lower, nor not important with CR. However, in the circulation, female mice lacked diet differences, suggesting that 11β-HSD1 activity was unaltered by the diet. Multiple comparison by ANOVA lacked diet differences in 11-DHC, suggesting that there was less 11-DHC to be converted by 11β-HSD1 into corticosterone, and the increased corticosterone was due to increased activity in the HPA-axis. So far, this ratio has not been investigated in the BM, neither in the circulation during CR or AN. However, the effect of circulatory GC excess has been investigated in CS patients. It was shown that the cortisone to cortisol ratio in plasma was significantly higher in patients compared to healthy adults. Circulatory cortisol concentrations were similar increased in CS patients. The hypercortisolism in the patients suggest a possible underperforming 11β-HSD2, or an overperforming 11β-HSD1 (Dötsch *et al.*, 2001). Although my own study induces an increase in circulatory corticosterone, the end effects of the ratio are not comparable to the results from the study using CS patients, as the conditions are massively different, and are also in different organisms.

With CR, *Hsd11b1* expression was up-regulated in both adipose depots and BM of the 15-week-old mice. These results suggest an increase in GC action in AT and BM. No previous research has yet identified a target gene that is increased with CR in the BM specifically, but these results are suggesting that *Hsd11b1* could be one. In the BM of 10-week-old mice, *Hsd11b1* expression was not upregulated. A possible reason behind this could be due to the lack of BMAT expansion during one-week CR (R. Sulston, unpublished data). Time course CR studies in the Cawthorn group have revealed that BMAT significantly expands past four-weeks of CR, with stronger differences at six-weeks of CR, similarly with *Hsd11b1* expression in whole bone (data not shown). This suggests that *Hsd11b1* could be a marker of increased adiposity in the BM. A previous publication showed that *in vitro* adipocyte differentiation increases with time during adipogenesis (Cheung *et al.*, 2007), further supporting the notion that *Hsd11b1* expression would increase during CR as BMAT equally increases. Thus, the lack of BMAT expansion with one-week CR could therefore explain the lack of diet differences in *Hsd11b1* expression. Further investigating the role of this gene in the

BM, especially during CR when BMAT is expanded, may offer an opportunity to better understand the relationship between GCs and BMAT during CR.

3.3.3.2. Consequences of GC excess during CR

Other GC target genes, such as, *Gilz, Fkbp5* and *Per1*, were also examined in adipose depots and BM. *Fkbp5* is a co-chaperone of heat shock protein 90 (hsp90) regulating GR sensitivity (Binder, 2009). Beyond the GR, *Fkbp5* can also bind to the AR, PR and MR. Furthermore, this gene has also been shown to interact with immunoregulatory pathways that are important for oncogenesis (further reviewed Zannas *et al.*, 2016). Since *Fkbp5* expression has previously been observed to increase due to GCs in AT (Pereira *et al.*, 2014), it was hypothesised that this target gene would also be increased in WAT with CR. My results showed varied results between the depots, the two cohorts and sexes (Figure 3.9.A-B, 3.10.G-H), suggesting that the CR effects can be diet, age-and/or sex-dependent. Similar results were found for *Gilz* (Figure 3.9/3.10 C-D), a GC target gene that is upregulated with GC treatment (D'Adamio *et al.*, 1997; Cheng *et al.*, 2013; Bruscoli *et al.*, 2015), has anti-inflammatory properties (Mittelstadt and Ashwell, 2001; Berrebi *et al.*, 2003) and is highly expressed in human adipocytes treated with dexamethasone (Lee *et al.*, 2011). *Gilz* is also downregulated in dendritic cells in respiratory allergic patients, but quickly upregulated post GC treatment. This further confirms its function as an anti-inflammatory gene (Ronchetti, Migliorati and Riccardi, 2015). A third GC target gene was also investigated; *Per1*, and similar findings were found as above (Figure 3.9/3.10 E/F). PER1 is an important circadian regulatory of cells (So *et al.*, 2009; Reddy *et al.*, 2012) and it also plays a role in cancers as the knockout of *Per1* in cells enhances tumour formation (Zhao *et al.*, 2016). Overall, the fasting effects seems to have affected the results in the 15-week-old mice, blunting the end-results. A conclusion of the target gene analysis is that CR generally is increasing the expression of the genes, but this seems to be influenced by the short-term fasting/re-feeding as not all genes show increases with CR. This underscores the importance of analysing multiple genes, and not just one, in both cohorts, to draw reliable conclusions about GC action in these tissues. Another factor influencing the GC target genes during CR could be androgens. It has recently been discovered that androgen receptor signalling can influence GC turnover in WAT (Spaanderman *et al.*, 2019). Based on these results, it would be possible that the results of the GC target gene in

my study could be influenced by androgens/AR. This could also alter the GC turnover of circulatory and tissue-specific levels during CR.

Increased GCs can alter adipocyte differentiation and lipolysis, causing an increase in circulating FAs (Karatsoreos *et al.*, 2010; Cassano *et al.*, 2012; Geer, Islam and Buettner, 2014). GCs can also act differently on specific adipose depots. For example, in the presence of insulin, GCs can cause a depot-specific increase in activation of cortisone in omental AT, contributing to visceral adiposity (Lee *et al.*, 2008). Moreover, although chronic GC excess in CS is associated with increased adiposity, it is also associated with increased lipolysis. In male mice (Karatsoreos *et al.*, 2010; Cassano *et al.*, 2012) and rats (Wu *et al.*, 2018), corticosterone administration causes weight gain and increased adiposity, but females were not included in these studies. In Cushing's disease, no differences between men and females have been observed with regard to cortisol concentration, although independently of sex, the patients do have increased cortisol. However, it is difficult to compare the effects of GC excess resulting from CR with that which results from exogenously administered corticosterone. Indeed, I found that plasma corticosterone concentrations in CR reach around 100-300 ng/mL, whereas concentrations of ~600 ng/mL occur when corticosterone is orally administered (Morgan *et al.*, 2014). Such high levels is likely to increase visceral adiposity and elevate corticosterone, but suppress the HPA axis (as observed with decreased adrenal gland masses) (Anagnostis *et al.*, 2009; Arnaldi *et al.*, 2012). Meanwhile, with CR, a mild elevation of corticosterone is observed, alongside decreased adiposity and improved insulin sensitivity (Fontana *et al.*, 2004).

In my study, we observed male mice losing fat mass (mostly gWAT) and having increased corticosterone concentration. In contrast, female mice did not lose fat mass, and they had less corticosterone concentration raise. These results suggest that GC are promoting lipolysis in male, but not in female gWAT. However, the females had increased effects of CR on *Gilz* and *Fkbp5* expression with CR in gWAT (Figure 3.10), suggesting that they might not resist the effects of GCs in gWAT after all (although they often have lower expression than males). To further confirm these results, lipolysis target genes could be investigated such as HSL, ATGL, LXR-α and LXR-β, or direct measurement of released lipolytic products from adipocytes in cultured media, or measurement of FA and glycerol in plasma with a lipolysis detection kit.

As 11β-HSD1 regulates the intracellular regeneration of corticosterone, it has been deemed important in the initiation of metabolic disorders. However, during CR, an increase in the expression of this enzyme suggests an increase in GC action, which is associated with anti-inflammatory properties. Although, selective overexpression of this enzyme is associated with visceral obesity, insulin-resistant diabetes and dyslipidemia (Masuzaki, 2001) and hepatic overexpression induces steatosis and insulin resistance without obesity (Paterson *et al.*, 2004). Conversely, the hypomorphic 11β-HSD1 KO mice have been reported to be resistant to these effects (Masuzaki, 2001; Morton *et al.*, 2004; Park *et al.*, 2014).

One study comparing WT vs 11β-HSD1 exon 5 KO mice revealed that the KOs are protected from certain effects of circulatory GC excess resulting from administration of corticosterone in the drinking water (Morgan *et al.*, 2014). Although the GC concentration was much higher than during CR, potentially seen as non-beneficial as with CR, the results suggests that 11β-HSD1 is a determinant of the consequences of GC excess and that knocking it out will improve metabolic abnormalities (Morgan *et al.*, 2014). Since the 11β-HSD1 KO mice can resist these effects, would they also be able to resist CR-associated decreases in body mass and fat mass? What about BMAT expansion that comes with CR? Formerly, Justesen *et al*., showed that the hypomorphic 11β-HSD1 KO mice completely lack BMAT in the tibia. Meanwhile, Couthino *et al.,* revealed the opposite, as did we in our lab (Chapter 4). Admittedly, no research on BMAT has been performed on null 11β-HSD1 KO mice during CR. As CR is known to increase BMAT, it is undefined whether 11β-HSD1 KO mice would resist this expansion, or not.

3.3.4. Future directions

This Chapter revealed that male mice lose fat mass with CR, whereas female mice do not. So far, the reason and the mechanism behind this is still unknown, but it is currently under further investigation in the lab. Future work regarding the sex differences could include ovariectomy studies to test the hypothesis that female sex hormones contribute to these sex differences, and that the ovariectomised mice would lose fat mass. Orchidectomy would also be an option, to further investigate the relationship between androgens and BMAT during CR. Alternatively, removal of fat pads around the ovaries and testis could be performed, and then subjecting the mice

to CR. A recent publication investigated the removal of fat pads around the ovaries and demonstrated that the fat pads are important for mouse reproduction (Wang *et al.*, 2017). In male mice, the fat pad surrounding the testis support spermatogenesis (Chu *et al.*, 2010). Although, a more direct and robust approach would still be the removal of the reproductive organs. It would be intriguing to have examined the bones from these mice, especially to quantify BMAT. The removal of the fat pads around the ovaries or ovariectomy results in reduced oestrogen secretion, therefore, it would be hypothesised that they would have increased BMAT. In contrast, increased testosterone has been shown to be associated with decreased BMAT in both men and women (Tamura *et al.*, 2005; Mistry *et al.*, 2018). Anorexic men were shown to have decreased testosterone over time (Wabitsch *et al.*, 2001). It would therefore be intriguing to further investigate the role of androgens in BMAT expansion during CR.

To overcome the fasting/re-feeding issue that we came across, an aged-matched cohort would have to be conducted for six-week CR. That way, the 15-week-old mice that were fasted/re-fed could be directly compared to the same aged mice that did not undergo fasting/re-feeding.

Further work regarding the endocrine effects of CR would include adrenalectomy, of both male and female mice to further investigate the effects of GCs during CR. By removing the adrenal glands, the synthesis of corticosterone would stop and circulatory concentration would drop. This would allow one to examine circulatory vs tissue-specific GC concentrations in both sexes during CR. Subsequently, measuring 11β-HSD1 activity during CR would be advantageous. Although we know that *Hsd11b1* expression is increased with CR, we do not know how its activity compares to that in AL-fed controls, and especially in the BM. To determine 11β-HSD1 reductase and dehydrogenase activity, BM cells from mice subject to CR could be cultured, with the addition of ^{3}H-substrate to the medium, to calculate conversation of substrate (11-DHC) to product (corticosterone). Dehydrogenase activity would also be measured to detect if the reverse conversation would occur in the BM. Although, since 11β-HSD2 is predominantly present in the kidneys, placenta and salivary glands, the dehydrogenase activity would not be expected to show. Alternatively, 11β-HSD1 activity can be measured from freshly isolated whole bone/bone only/BM only by incubating the tissue with a specific amount of 11-DHC for 3h. Thereafter, the steroids in the media can be extracted and corticosterone concentration can be

measured by ELISA (Hardy *et al.*, 2016). In addition, 90% of corticosterone is bound to binding globulins and 10% is free only, whereas, 11-DHC has greater free levels. Therefore, measuring binding globulins would be useful to determine the amount of corticosterone bound, and this can be done by ELISA. Another option, which I implemented in the following Chapters, is to stop the intracellular regeneration of corticosterone by knocking out the enzyme 11β-HSD1 globally. As previously mentioned, an unexpected response to CR is BMAT expansion. By knocking out 11β-HSD1, I further investigated circulatory and tissue-specific endocrine effects as well as the expansion of BMAT during CR.

Chapter 4. 11β-HSD1 KO male mice resist bone marrow adiposity expansion during caloric restriction, but female mice do not

4.1. Introduction

Unlike WAT, BMAT increases in diverse clinical conditions, including following CR in animals, and AN in humans, osteoporosis and excess GC treatment. The causes and consequences of this expansion remain unknown. CR-induced BMAT expansion may contribute to other adaptations to CR, including metabolic adaptations, bone loss and immunological changes. As previously mentioned (Chapter 3.1), during CR, BMAT contributes to increased circulating concentrations of adiponectin (Cawthorn *et al.*, 2014; Straub and Scherer, 2019), which might contribute to the health benefits of CR. Therefore, it is important to elucidate the mechanisms responsible for CR-induced BMAT expansion.

Previous data showed that during CR, when BMAT is significantly increased in comparison to control-fed mice, circulatory corticosterone concentration is also increased (Cawthorn *et al.*, 2016). Nonetheless, neither moderate (30%) nor excessive (40-50%) CR in rabbits is associated with increases in BMAT nor are circulating GCs altered during CR in rabbits. These data support the possibility that GC excess is required for CR-associated BMAT expansion (Cawthorn *et al.*, 2016). In addition to CR, GC administration also increases BMAT in animals and humans (Vande Berg *et al.*, 1999; Devlin *et al.*, 2010; Georgiou, Hui and Xian, 2012; Li *et al.*, 2013). GCs are not only elevated during CR in animals, but also in AN patients (Boyar *et al.*, 1977; Walsh *et al.*, 1978; Misra *et al.*, 2004; Lawson *et al.*, 2009), when BMAT also increases (Bredella *et al.*, 2009, 2014; Ecklund *et al.*, 2010).

The elevated BMAT in AN is inversely correlated to BMD (Bredella *et al.*, 2009, 2014). Young girls with AN have a greater risk of developing osteoporosis by exhibiting premature transformation of haematopoietic to adipose cells in the marrow (Ecklund *et al.*, 2010). Similarly, CR in animal models is associated with decreases in whole-body BMD (Berrigan *et al.*, 2005) and loss of cortical bone (Hamrick *et al.*, 2008).

Therefore, one possibility is that the expansion of BMAT during CR might be mediated by GC excess. Many effects of endogenous GC excess are mediated by 11β-HSD1, which catalyses intracellular regeneration of active GCs. The importance of 11β-HSD1 in regulating metabolic phenotypes has been highlighted in various tissues. For example, transgenic animal models overexpressing 11β-HSD1 in AT develop obesity, insulin resistance, dyslipidaemia and hypertension (Masuzaki, 2001; Masuzaki *et al.*, 2003). Conversely, hypomorphic 11β-HSD1 KO mice have the opposite phenotype, with lower plasma TG levels, improved insulin sensitivity and reduced visceral adiposity upon HFD (Morton *et al.*, 2001, 2004). Furthermore, the bone morphology of the hypomorphic 11β-HSD1 KO mice did not differ compared to the WTs (Justesen *et al.*, 2004). It has previously been demonstrated that the conversion of 11-DHC into corticosterone in mice, by 11β-HSD1, is a significant determinant of the effects of exogenous GC excess in mice (Morgan *et al.*, 2014). When 11β-HSD1 was deleted, the global and fat-specific KO had much greater resistance to the GC effects than the liver-specific KO (Paterson *et al.*, 2004; Lavery *et al.*, 2012; Harno *et al.*, 2013; Morgan *et al.*, 2014). However, it is worth noting that the global 11β-HSD1 exon 5 KO model used by Morgan *et al.,* (2014) and the null 11β-HSD1 KO which were created at Edinburgh University are full KOs compared to the model used by Justesen *et al*. Overall, based on this research, is it possible that my null 11β-HSD1 KO mice will also resist BMAT expansion during CR?

Chapter 3 reported that *Hsd11b1* expression is up-regulated in the BM after six-weeks of CR, but not after one-week. This coincides with the expansion of BMAT at six-weeks of CR, but not after only one-week of CR. Formerly, Justesen *et al.,* (2004) examined bones of hypomorphic 11β-HSD1 KO mice under normal conditions, and revealed that the mice were lacking BMAT in their tibia. However, a more-recent study showed that the same line of hypomorphic 11β-HSD1 KO mice do have BMAT present in their tibiae, at least when examined 3 weeks after initiation of joint inflammation (Coutinho *et al.*, 2012). Preliminary studies from our lab, completed prior to the start of my PhD studies, also indicate that BMAT is present in our full 11β-HSD1 KO mice (K. Suchacki, unpublished data).

Based on the evidence presented in Chapter 3, along with previous findings (Morgan *et al.*, 2014), my hypothesis is that 11β-HSD1 contributes to GC action within the BM

and thereby mediates BMAT expansion during CR. To determine if inhibiting intracellular regeneration of corticosterone globally is sufficient to prevent or attenuate BMAT expansion during CR, C57BL/6JOlaHsd control (WT) and 11β-HSD1 KO male and female mice were subject to CR for six weeks. Data for WT males and females, which were littermates of 11β-HSD1 KO mice, are shown in Chapter 3. To minimise animal use, the same WT data and cohorts are included in this Chapter, in which they are compared to data from their 11β-HSD1 KO littermates. Note that the WT and 11β-HSD1 KO mice underwent the experiments simultaneously, so comparisons are valid.

4.2 Results

4.2.1. CR causes weight loss in WT and 11β-HSD1 KO mice

Genotypes of mice were confirmed post-weaning by analysis of genomic DNA isolated from ear clips, as described in the Methods (2.1). To determine if CR affected body mass similarly in WT and KO, I measured body masses of the WT and KO mice over the course of the experiment. It was expected that mice on the CR diet would have a decrease in body mass compared to mice on the AL diet. Figure 1 shows the body mass progression of both WT (black lines) and KO (red lines) in male (Figure 4.1.A) and female (Figure 4.1.B) mice, measured weekly for six weeks. Males and females of both genotypes were randomly assigned to AL or CR diet, so both diet groups started at approximately the same body mass; an exception was for the AL-fed KO males, which had a higher body mass than AL-fed WT males even at week 0 of the experiment. However, KO males have been noticed to often be heavier than WTs (K. Chapman, personal communication). Although, it could also be a random sampling effect because similar KO effects were not observed in subsequent cohorts of mice (Chapter 6). Nevertheless, together these data show that, as expected, CR decreased body mass in males and females of each genotype.

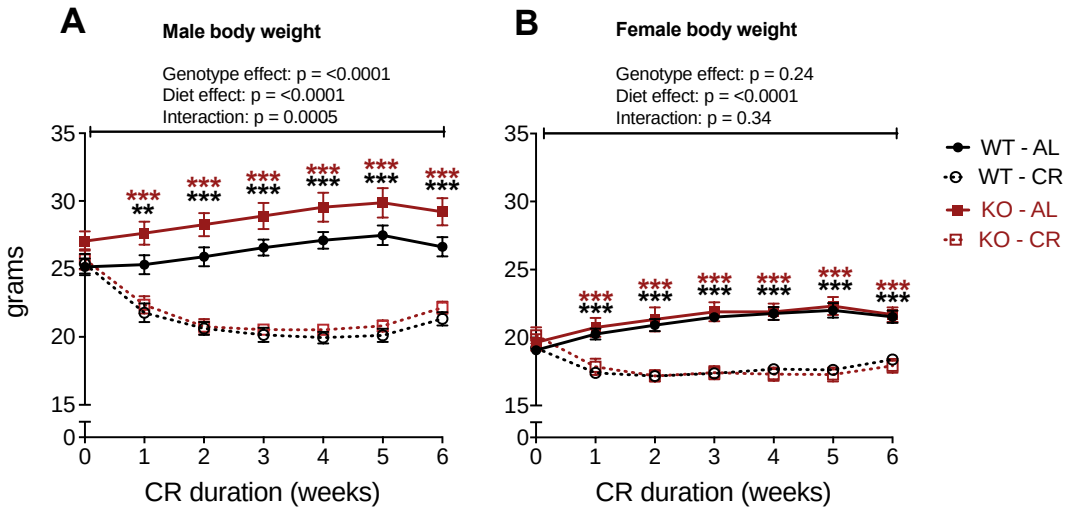

Figure 4.1. WT and 11β-HSD1 KO male and female mice lose body weight with 30% CR diet over six weeks. C57BL/6JOlaHsd (WT, black) and 11β-HSD1 KO (KO, red) male **(A)** and female **(B)** mice were fed *ad libitum* (AL, closed symbols, solid line) or 70% of *ad libitum* food intake (CR, open symbols, dotted line) for six weeks, from 9 weeks until 15 weeks of age. The evening prior to dissections, all mice were fasted/re-fed. The AL fed mice had their food removed and were given half a portion of the 70% of food that they were daily consuming (1.5g). The CR fed mice were also given half a portion (1.05g) of their 30% CR diet. The mice were weekly weighed. Data are mean +/- SEM and were analysed by 3-Way ANOVA with Sidak's multiple comparison test. n (WT AL male) = 7. n (WT CR male) = 11. n (KO AL male) = 8. n (KO CR male) = 8. n (WT AL female) = 8. n (WT CR female) = 13. n (KO AL female) = 5. n (KO CR female) = 8. ***: p<0.001.

4.2.2. 11β-HSD1 deficiency does not protect male mice against fat loss during CR

To further characterise the tissue losses and understand the association between the diet, genotype and body weight, body composition was measured weekly by TD-NMR throughout the six-week study.

Figure 4.2 presents fat and lean mass of WT and KO male and female mice, expressed as absolute mass (g) and as a % of total body mass (%). Male mice subject to CR showed significant fat mass loss as absolute mass (Figure 4.2.A) and as % of body mass (Figure 4.2.C). ANOVA confirmed a significant genotype and diet effect, as well as an interaction between the two for both absolute and % fat mass. A genotype difference in absolute fat mass (Figure 4.2.A) between the WT and KO male mice was also observed from week three to the final week, and only at week four as % of total body mass. This shows that the KO males had more fat, which this differs to previous data reporting that the hypomorphic KOs resist obesity on HFD (Morton *et al.*, 2004). The male mice on CR continued to show a decrease in fat mass until week two post-dietary intervention, where they reached maximum loss. Thereafter, from weeks four to six, fat mass began to increase in the CR males of each genotype. ANOVA for the female fat mass as absolute mass (Figure 4.2.B) and as % of body mass (Figure 4.2.D) revealed significant diet effects. Compared to WT AL-fed females, WT CR-fed females showed significantly decreased absolute fat mass at weeks four and five post-dietary intervention only (Figure 4.2.B).

A significant diet effect was revealed by ANOVA for the lean mass of both males (Figure 4.2.E, G) and females (Figure 4.2.F, H). In addition, a significant genotype effect for lean mass was present in males only. The absolute lean mass was significantly decreased in male (Figure 4.2.E) and female (Figure 4.2.F) mice subject to CR, regardless of genotype. In contrast, relative lean mass was increased in CR-fed vs AL-fed males (Figure 4.2.G) and only differed between WT AL-fed and CR-fed females at week five (Figure 4.2.H). This suggests that the female body mass losses observed in figure 4.1.B are due predominantly do decreases in lean mass, rather than fat mass. Whereas, in males, the decreased body mass is disproportionately due to loss of fat mass whilst lean mass is relatively protected.

The genotype differences observed in body composition in response to CR suggest that 11β-HSD1 deficiency does not protect male mice from losing fat mass, and instead may enhance the loss of fat mass during CR, as the difference between AL and CR is greater than for the WT males. Moreover, 11β-HSD1 does not protect females from maintaining their fat mass, as there are no significant genotype effects in females.

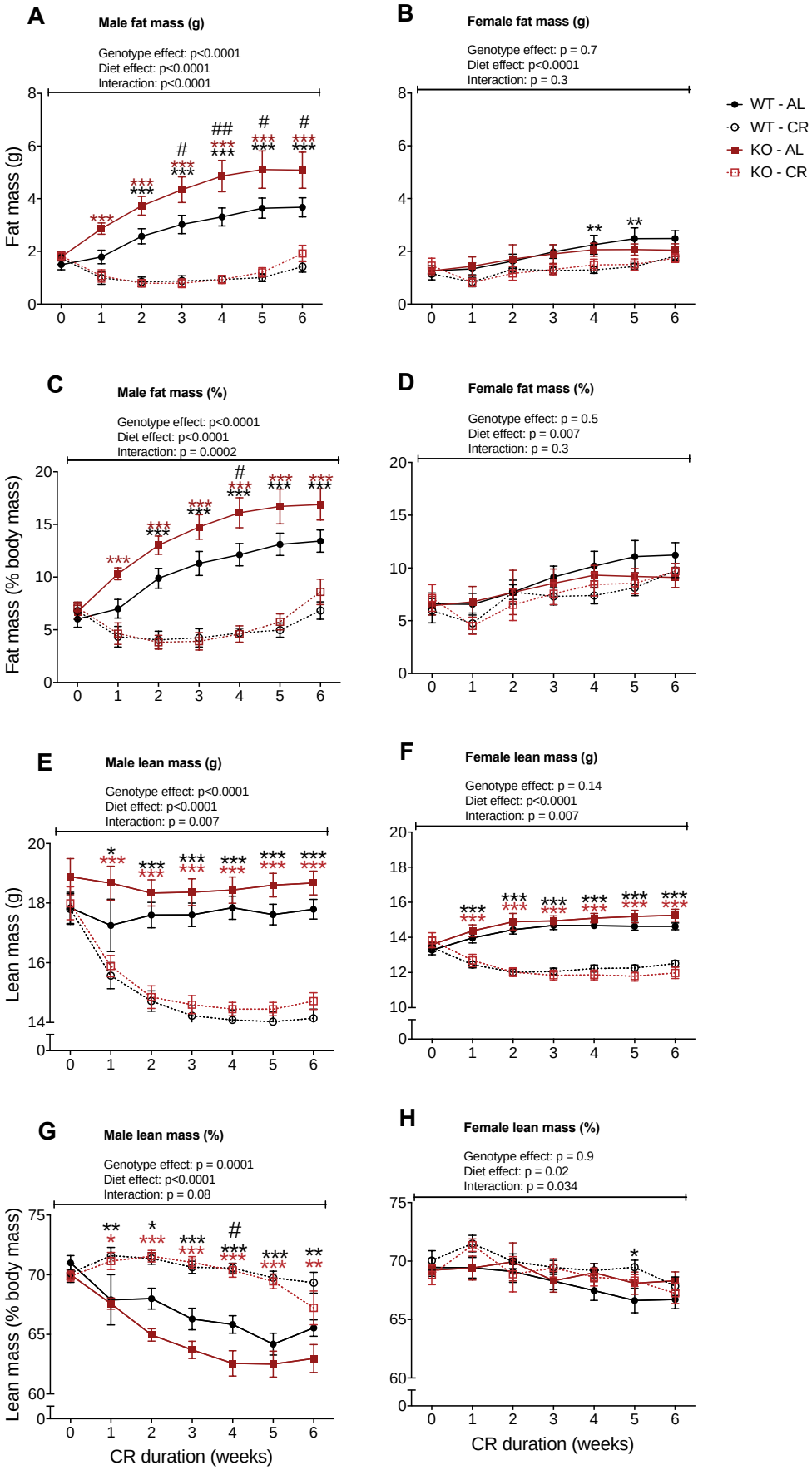
A
Male fat mass (g)
Genotype effect: p<0.0001
Diet effect: p<0.0001
Interaction: p<0.0001
Fat mass (g)
B
Female fat mass (g)
Genotype effect: p = 0.7
Diet effect: p<0.0001
Interaction: p = 0.3
WT - AL
WT - CR
KO - AL
KO - CR
C
Male fat mass (%)
Genotype effect: p<0.0001
Diet effect: p<0.0001
Interaction: p = 0.0002
Fat mass (% body mass)
D
Female fat mass (%)
Genotype effect: p = 0.5
Diet effect: p = 0.007
Interaction: p = 0.3
E
Male lean mass (g)
Genotype effect: p<0.0001
Diet effect: p<0.0001
Interaction: p = 0.007
Lean mass (g)
F
Female lean mass (g)
Genotype effect: p = 0.14
Diet effect: p<0.0001
Interaction: p = 0.007
G
Male lean mass (%)
Genotype effect: p = 0.0001
Diet effect: p<0.0001
Interaction: p = 0.08
Lean mass (% body mass)
CR duration (weeks)
H
Female lean mass (%)
Genotype effect: p = 0.9
Diet effect: p = 0.02
Interaction: p = 0.034
CR duration (weeks)

Figure 4.2. Body composition determined by TD-NMR revealed significant fat mass differences between WT and 11β-HSD1 KO male mice, whereas, female mice resisted fat mass loss. WT and 11β-HSD1 KO male and female mice were fed AL or CR diets and fasted/re-fed as described for Figure 4.2 and in Methods (2.1.2). All mice were weekly scanned by TD-NMR. Fat mass in male **(A)** and female **(B)** mice shown in grams. Fat mass in male **(C)** and female **(D)** mice shown as % of body mass. Lean mass in male **(E)** and female **(F)** mice shown in grams. Lean mass in male **(G)** and female **(H)** mice shown as % of body mass. Data is mean +/- SEM and were analysed by 3-Way ANOVA with Sidak's multiple comparison test. n (WT AL male) = 7. n (WT CR male) = 11. n (KO AL male) = 8. n (KO CR male) = 8. n (WT AL female) = 8. n (WT CR female) = 13. n (KO AL female) = 5. n (KO CR female) = 8. * (black): diet effect in WT mice. * (red): diet effect in KO mice. # (black): genotype effect in AL diet. *: $p<0.05$. **: $p<0.01$ ***: $p<0.001$#: $p<0.05$. ##: $p<0.01$.

4.2.3. Male mice on CR are susceptible to WAT loss, whereas females are not

In Chapter 3, I showed that the sex differences in fat loss during CR predominantly reflect changes in gonadal WAT and that WAT *Hsd11b1* expression is greater in males than in females (Figure 3.10 A-B). Thus, given the ability of 11β-HSD1 to influence visceral adiposity (Masuzaki, 2001; Desbriere *et al.*, 2006; Michailidou, Jensen, *et al.*, 2007; Veilleux *et al.*, 2010; Mlinar *et al.*, 2011; Wamil *et al.*, 2011) and the differences observed in total fat mass (Figure 4.2), I next investigated if 11β-HSD1 KO influences the effects of CR on specific adipose depots. To do so, at necropsy the adipose depots were sampled and weighed to determine diet and genotype differences. Figure 4.3 shows the absolute mass and % of body mass of iWAT, gWAT and mWAT in CR-and AL-fed WT and KO mice.

The subcutaneous iWAT decreased with CR as absolute mass (Figure 4.3.A) and as % of body mass (Figure 4.3.D) in male mice only. Similar sex-specific decreases were also observed for the visceral depots, gWAT (Figure 4.3.B, E) and mWAT (Figure 4.3.C, F), although for the latter ANOVA detected an overall diet effect only for absolute mWAT mass (Figure 4.3.C). No WAT loss was observed during CR in the female mice, and no diet or genotype differences were detected in BAT for either sex (Figure 4.4). This indicates that the loss detected in fat mass with TD-NMR is primarily from the WAT depots.

Overall, these data confirm the TD-NMR results that only male mice lose fat mass with CR and further show that decreased gWAT and iWAT are the main contributors to this effect. Moreover, they show that deficiency of 11β-HSD1 does not protect against CR-associated fat loss in males and does not influence the sex differences in this response.

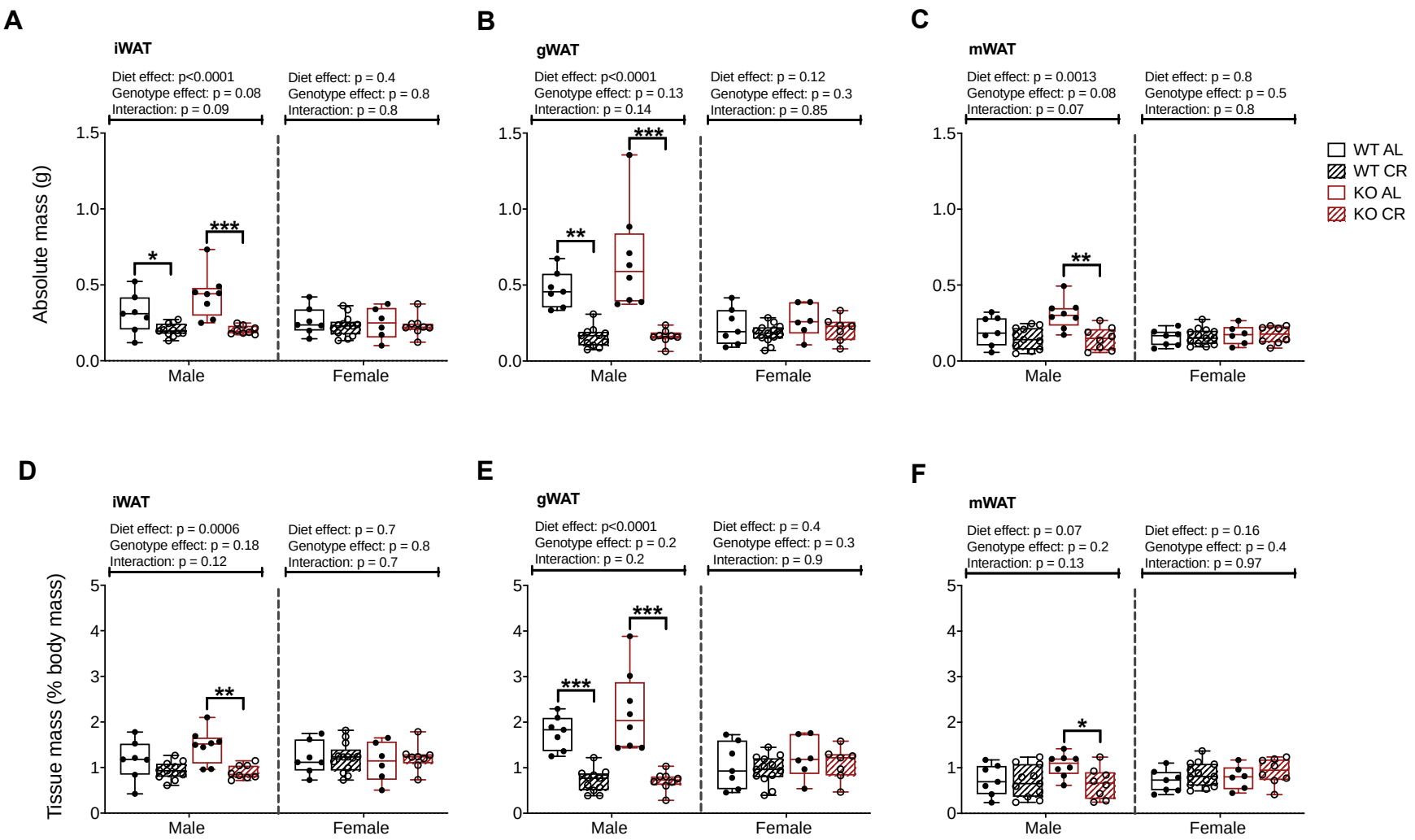
A
iWAT
Diet effect: p<0.0001
Genotype effect: p = 0.08
Interaction: p = 0.09
Diet effect: p = 0.4
Genotype effect: p = 0.8
Interaction: p = 0.8
Absolute mass (g)
Male
Female
B
gWAT
Diet effect: p<0.0001
Genotype effect: p = 0.13
Interaction: p = 0.14
Diet effect: p = 0.12
Genotype effect: p = 0.3
Interaction: p = 0.85
C
mWAT
Diet effect: p = 0.0013
Genotype effect: p = 0.08
Interaction: p = 0.07
Diet effect: p = 0.8
Genotype effect: p = 0.5
Interaction: p = 0.8
WT AL
WT CR
KO AL
KO CR
D
iWAT
Diet effect: p = 0.0006
Genotype effect: p = 0.18
Interaction: p = 0.12
Diet effect: p = 0.7
Genotype effect: p = 0.8
Interaction: p = 0.7
Tissue mass (% body mass)
E
gWAT
Diet effect: p<0.0001
Genotype effect: p = 0.2
Interaction: p = 0.2
Diet effect: p = 0.4
Genotype effect: p = 0.3
Interaction: p = 0.9
F
mWAT
Diet effect: p = 0.07
Genotype effect: p = 0.2
Interaction: p = 0.13
Diet effect: p = 0.16
Genotype effect: p = 0.4
Interaction: p = 0.97

Figure 4.3. 11β-HSD1 deficiency does not affect WAT mass in female mice and does not protect male mice from adipose loss with CR. WT and 11β-HSD1 KO male and female mice were fed AL or CR diets and fasted/re-fed as described for Figure 4.2 and in Methods (2.1.2). At necropsy, WAT (iWAT, gWAT and mWAT) depots were harvested and weighed. iWAT **(A)**, gWAT **(B)** and mWAT **(C)** in male and female mice in grams. iWAT **(D)**, gWAT **(E)** and mWAT **(F)** in male and female mice as % of body mass. Data points are presented with median, interquartile range and range shown by box and whisker plot, and were analysed by 2-Way ANOVA with Sidak's multiple comparison test. n (WT AL male) = 7. n (WT CR male) = 11. n (KO AL male) = 8. n (KO CR male) = 8. n (WT AL female) = 7. n (WT CR female) = 13. n (KO AL female) = 6. n (KO CR female) = 8/7. *: $p<0.05$. **: $p<0.01$ ***: $p<0.001$

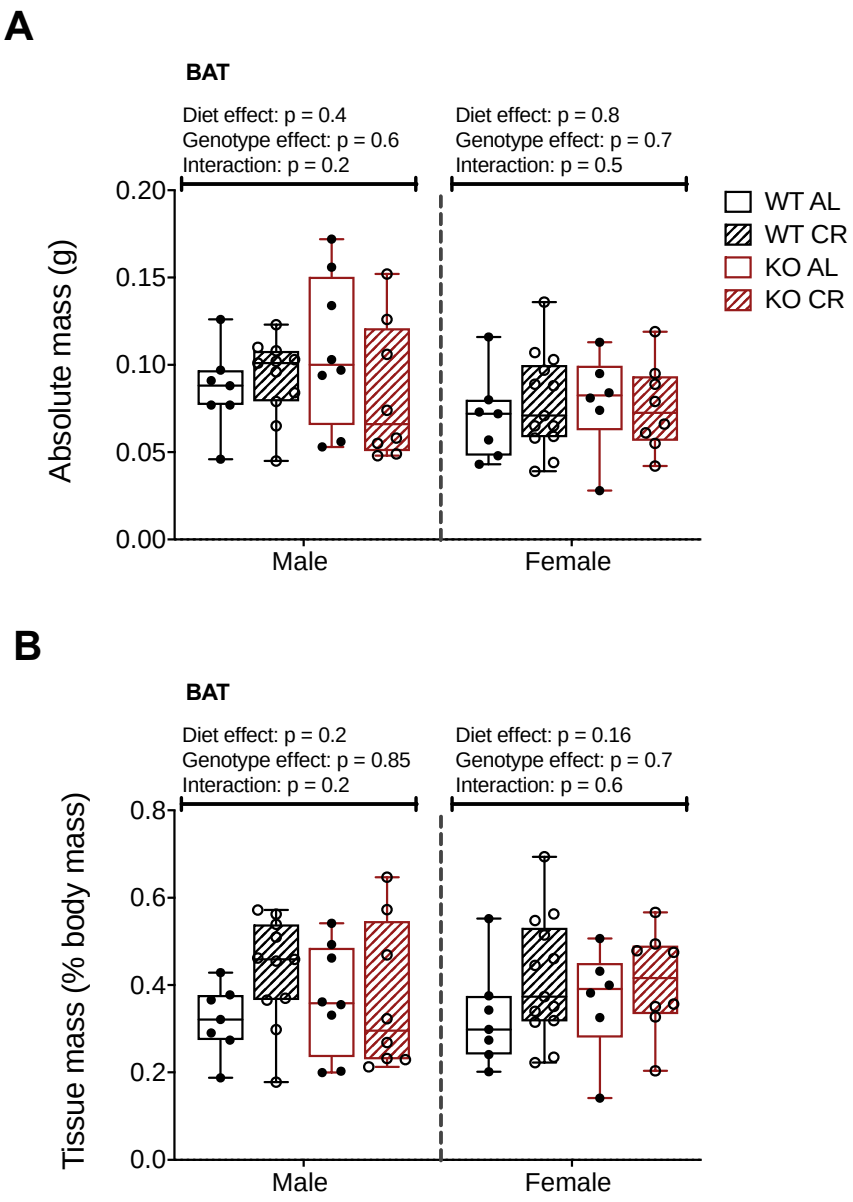

Figure 4.4. Neither CR nor 11β-HSD1 deficiency affects BAT mass. WT and 11β-HSD1 KO male and female mice were fed AL or CR diets and fasted/re-fed as described for Figure 4.2 and in Methods (2.12). At necropsy, BAT was harvested and weighed. BAT in male and female mice in grams **(A)** and as % of body mass **(B)**. Data points are presented with median, interquartile range and range shown by box and whisker plot, and were analysed by 3-Way ANOVA with Sidak's multiple comparison test. n (WT AL male) = 7. n (WT CR male) = 11. n (KO AL male) = 8. n (KO CR male) = 8. n (WT AL female) = 7. n (WT CR female) = 13. n (KO AL female) = 6. n (KO CR female) = 8.

4.2.4. 11β-HSD1 KO does not affect CR-induced hypercorticosteronaemia but increases adrenal mass in males

As shown in Chapter 3 and in previous studies, CR increases circulating GC concentrations and adrenal gland mass. However, 11β-HSD1 KO mice have been shown to resist the effects of exogenous corticosterone administration even though circulating plasma corticosterone concentrations and adrenal mass did not differ to those in WT mice (Morgan *et al.*, 2014). Thus, to determine if 11β-HSD1 KO alters the effects of CR on circulatory corticosterone concentration or adrenal mass, I next measured circulating corticosterone and adrenal gland masses in my cohorts of AL- and CR-fed WT and KO mice. Tail and core blood were collected for plasma. Adrenal glands were dissected and weighed as indicators of increased capacity for corticosterone synthesis.

Figure 4.5 shows corticosterone quantification by ELISA in male (Figure 4.5.A) and female (Figure 4.5.B) mice in plasma collected throughout the six weeks of CR. Significant diet effects were detected by 3-Way ANOVA for both sexes, with the mice subject to CR having increased circulatory corticosterone concentrations in comparison to mice on AL diet. No significant genotype differences were detected.

AL-fed females and AL-fed KO males showed increased circulating corticosterone concentration at week six, whereas CR-fed mice also showed a decrease at week six compared to previous weeks. One possibility is that these changes at week six reflect a technical issue relating to the sampling method: for previous weeks (0-5), blood was sampled approximately at 9am, prior to feeding the CR mice, whereas the measurement at week six was made prior to termination, following overnight fasting of the mice. As discussed in Chapter 3, the AL and CR mice were fed a set ration of food at approximately 18:00 on the evening prior to termination, to ensure that both groups were fasted for similar durations prior to cull. The rationale for this is that I was interested in assessing the effects of long-term CR, rather than short-term fasting effects. However, one concern is that this endpoint feeding/fasting regimen might alter GC action in a way that is not representative of the remainder of the CR protocol, thereby confounding downstream tissue-specific analyses of GC action. Therefore, to overcome this, I performed a short-term one-week CR experiment in which mice were

not fasted prior to necropsy. Thus, my subsequent analyses compared not only effects of sex, diet and genotype, but also compared the long-term six-week (15-weeks of age at necropsy, labelled as 'Chronic CR' in figures) and short-term one-week CR (10-weeks of age at necropsy, labelled as 'Acute CR' in figures) mice. One-week CR was used because, as shown in Figure 4.5, this is sufficient to induce hypercorticosteronaemia.

Figure 4.6 displays the adrenal gland masses. Six-weeks of CR significantly increased absolute and % adrenal gland mass in males but not in females (Figure 4.6.A, C), whereas no diet effects were detected in the 10-week-old mice (Figure 4.6.B, D). Consistent with previous findings (Bielohuby *et al.*, 2007), sex differences in adrenal mass were also apparent, with females having greater absolute and % mass than males at 15 weeks, and greater % adrenal mass in the 10-week cohort (Figure 4.6.A-D).

I further investigated the effects on corticosterone and 11-DHC by LC-MS/MS, because some journals will not accept ELISAs for steroid hormones because they are not specific enough. Furthermore, LC-MS/MS provides more precise readouts and can quantify several steroids at once. Figure 4.7. shows plasma corticosterone and 11-DHC as quantified by LC-MS/MS for both cohorts. In the 15-week-old mice, no diet or genotype effects were detected for corticosterone concentration (Figure 4.7.A). In contrast, in the 10-week-old mice corticosterone concentration (Figure 4.7.B) was significantly increased with CR in all groups except the KO males, in which there was only a trend for an increase. In the 15-week mice, ANOVA revealed significant genotype effects for 11-DHC in both sexes (Figure 4.7.C). Diet effects occurred in males only, with a significant increase detected in the CR-fed KO males compared to the AL-fed males (Figure 4.7.C). Moreover, in the 10-week-old cohort, ANOVA revealed that CR significantly increased 11-DHC in females and tended to increase 11-DHC in males (P = 0.08). Multiple comparisons for the 10-week cohort showed that 11-DHC was significantly increased in KO females on CR (Figure 4.7.D), perhaps resulting from increased regeneration via 11β-HSD2 or impaired conversion to corticosterone. To gauge the conversion of 11-DHC to corticosterone, the ratio of CORT to 11-DHC was calculated. As expected, ANOVA showed significant genotype effects in both cohorts, with the KO ratio being markedly reduced compared to that in WT mice (Figure 4.7. E, F), which would be consistent with lower 11β-HSD1 activity.

These results show a significant increase in circulatory corticosterone concentration throughout CR, but with the 10-week-old CR-fed KO males resisting the increase. This suggests that the fasting/re-feeding prior to termination might have affected the end-results of the 15-week-old mice, and that the KO males may have some resistance to CR-induced hypercorticosteronaemia. Based on previous research, revealing that 11β-HSD1 is a regulator of tissue-specific effects of circulating GC excess (Morgan *et al.*, 2014), the next step was to investigate *Hsd11b1* expression in peripheral tissues.

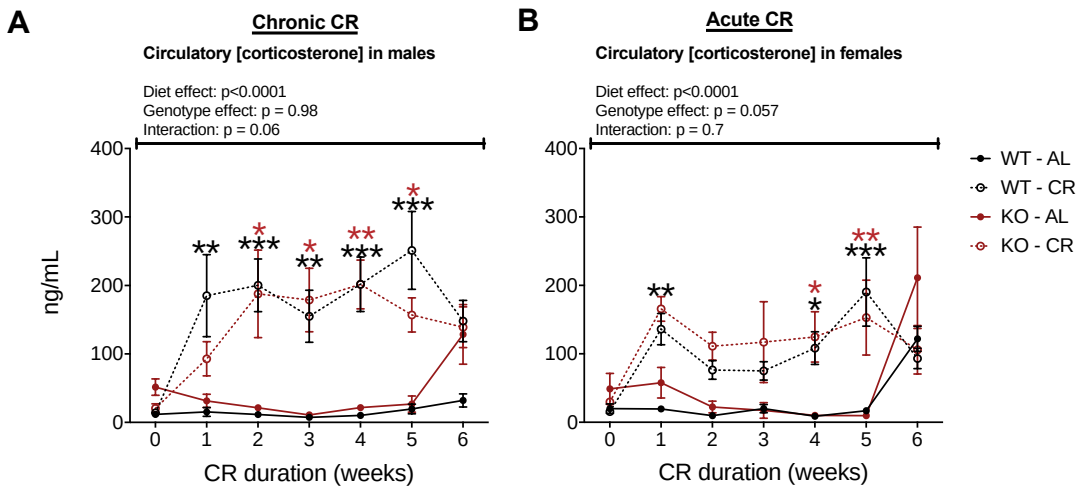

Figure 4.5. Circulating corticosterone concentration was increased in WT and 11β-HSD1 KO mice throughout the six weeks of CR. WT and 11β-HSD1 KO male and female mice were fed AL or CR diets and fasted/re-fed as described for Figure 4.2 and in Methods. Throughout the six weeks, blood was sampled from the tail vein and quantified by ELISA as described in Methods (2.4). Circulatory corticosterone concentration in male **(A)** and female **(B)** mice from weekly collected plasma, by ELISA. Data is mean +/- SEM and analysed by 3-Way ANOVA with Tukey's multiple comparisons test. n (WT AL male) = 7. n (WT CR male) = 10. n (KO AL male) = 5. n (KO CR male) = 6. n (WT AL female) = 7. n (WT CR female) = 7. n (KO AL female) = 4. n (KO CR female) = 5. *: p<0.05. **: p<0.01. ***: p<0.001.

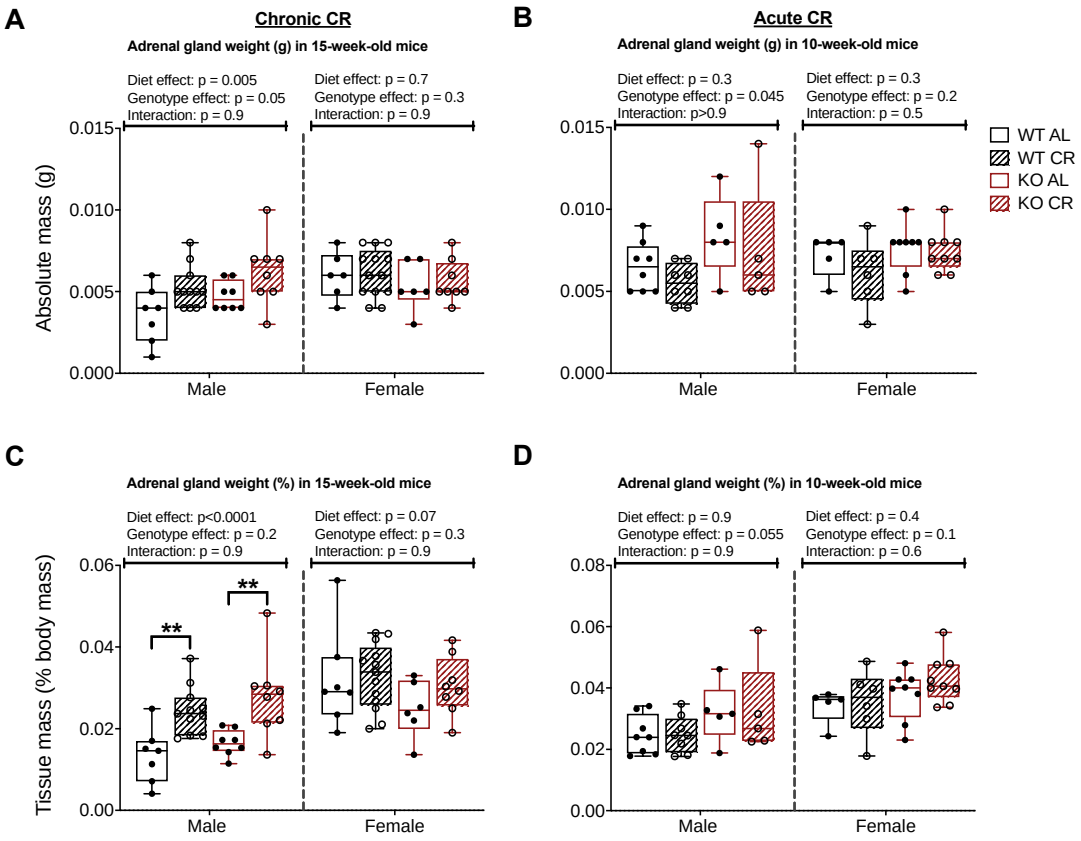

Figure 4.6. CR and 11β-HSD1 KO influence adrenal gland mass in a sex- and duration-dependent manner. WT and 11β-HSD1 KO male and female mice were fed AL or CR diets as described for Figure 4.2 and Methods (2.1.2), and fasted/re-fed as described in Methods (2.3.1). At necropsy, adrenal glands were dissected and weighed. Male and female adrenal glands shown in grams **(A)**. Male and female adrenal glands shown as % of body mass **(B)**. Data points are presented with median, interquartile range and range shown by box and whisker plot, and were analysed by 2-Way ANOVA with Sidak's multiple comparisons test. 15-week-old mice: n (WT AL male) = 7. n (WT CR male) = 11. n (KO AL male) = 8. n (KO CR male) = 8. n (WT AL female) = 7. n (WT CR female) = 13. n (KO AL female) = 6. n (KO CR female) = 8. 10-week-old mice: n (AL male) = 8. n (CR male) = 8. n (KO AL male) = 5. n (KO CR male) = 5. n (AL female) = 5. n (CR female) = 6. n (KO AL female) = 8. n (KO CR female) = 9. **: p<0.01.

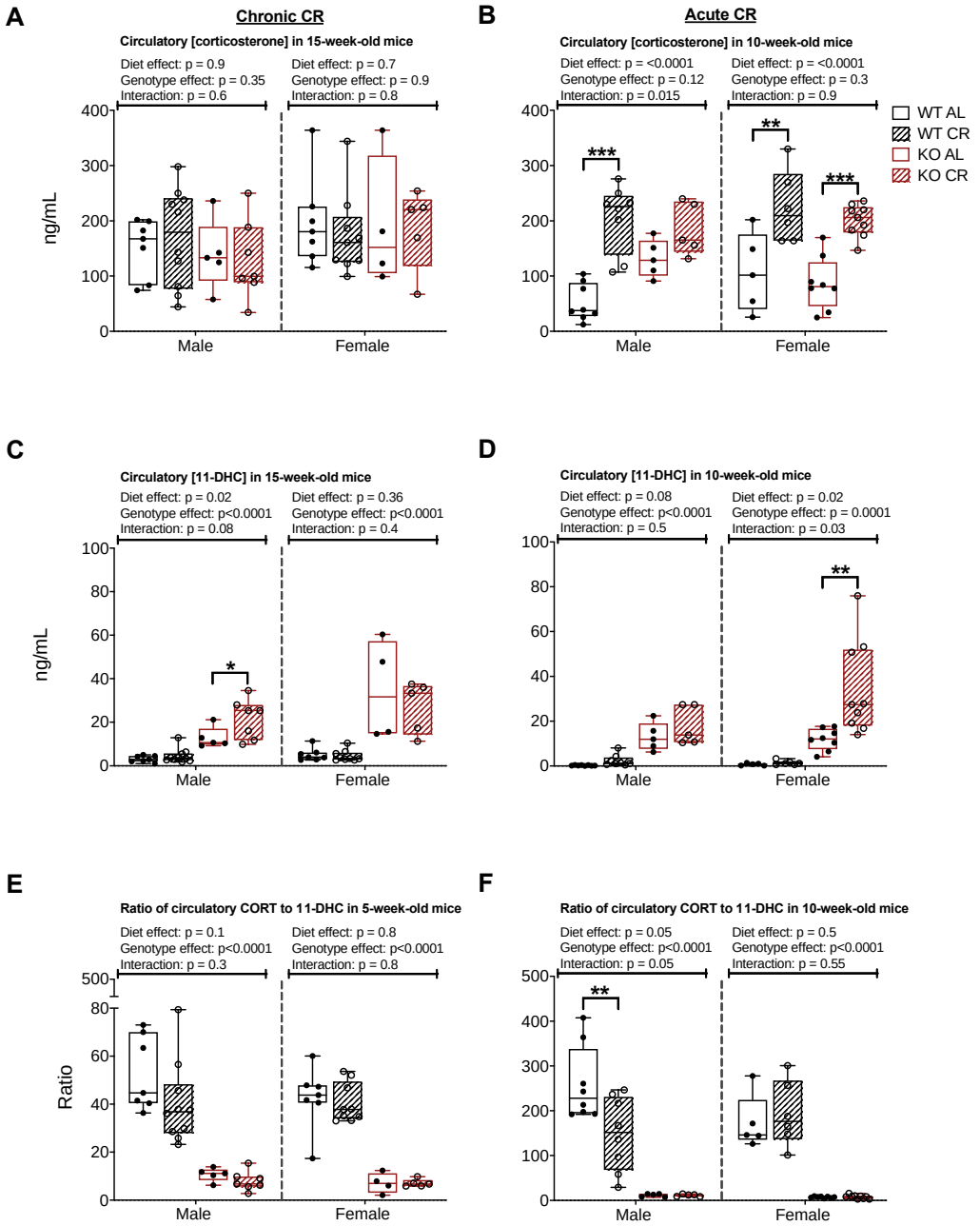

Figure 4.7. Circulatory GC regeneration is altered in 10-week-old mice subject to CR. WT and 11β-HSD1 KO male and female mice were fed AL or CR diets as described for Figure 4.2 and Methods (2.12), and fasted/re-fed as described in Methods (2.3.1). Prior to termination, end-point blood was sampled and quantified by LC-MS/MS as described in Methods (2.5.1). Circulating corticosterone concentration in 15-and **(A)** 10-week-old mice **(B)**. Circulating 11-DHC concentration in 15-and **(C)** 10-week-old mice **(D)**. Circulating ratio of corticosterone to 11-DHC ratio in 15-and **(E)** 10-week-old mice **(F)**. Data points are presented with median, interquartile range and range shown by box and whisker plot, and were analysed by 2-Way ANOVA with Sidak's multiple comparison test. 15-week-old mice: n (WT AL male) = 7. n (WT CR male) = 10. n (KO AL male) = 8. n (KO CR male) = 8. n (WT AL female) = 7. n (WT CR female) = 13. n (KO AL female) = 6. n (KO CR female) = 8. 10-week-old mice: n (WT AL male) = 8. n (WT CR male) = 8. n (KO AL male) = 5. n (KO CR male) = 5. n (WT AL female) = 5. n (WT CR female) = 6. n (KO AL female) = 8. n (KO CR female) = 9. *: p<0.05. **: p<0.01. ***: p<0.001.

4.2.5. CR is associated with increased *Hsd11b1* expression in WAT

The above findings confirm that CR increases plasma corticosterone regardless of genotype. However, 10-week-old CR-fed KO males resisted this increase, suggesting that other depots might also resist it. Previous data show that, compared to WT controls, 11β-HSD1 KO mice resist the effects of administrated corticosterone on WAT (Morgan *et al.*, 2014). Therefore, to determine if the KOs also resist these effects during CR, I next analysed the expression of GC target genes in iWAT and gWAT. I began by analysing expression of *Hsd11b1.*

As shown for iWAT (Figure 4.8.A) and gWAT (Figure 4.8.B), in the 15-week-old mice *Hsd11b1* expression was significantly increased with CR, whereas in the 10-week-old mice, *Hsd11b1* expression was upregulated with CR in the iWAT of WT females only (Figure 4.8.A). *Hsd11b1* mRNA was undetectable in the KOs, confirming the genotype of these mice.

These results suggest an increase in GC action in adipose depots with CR, particularly for longer-term CR. Therefore, additional GC target genes were next examined to investigate if this effect in WT mice extends to other transcriptional targets and is attenuated in WAT of the KO mice.

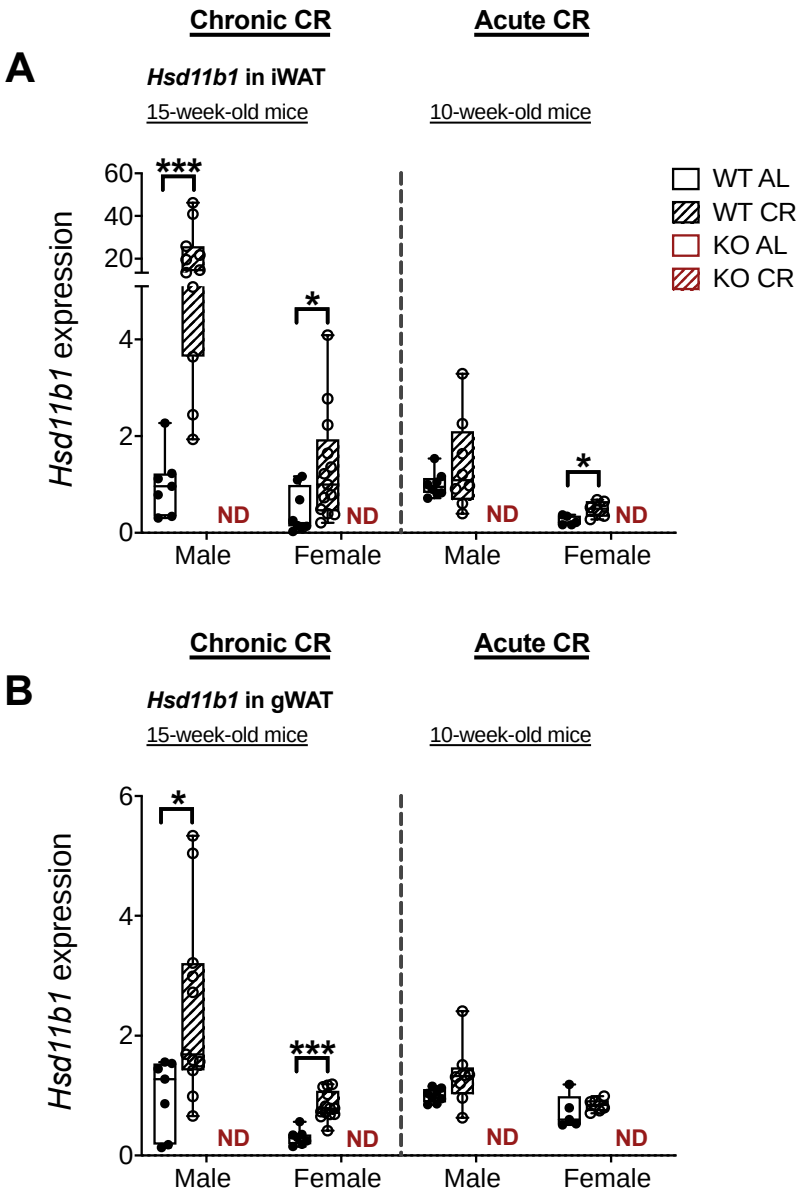

Figure 4.8. Long-term CR increases *Hsd11b1* expression in WAT. WT and 11β-HSD1 KO male and female mice were fed AL or CR diets as described for Figure 4.2 and Methods (2.1.2), and fasted/re-fed as described in Methods (2.3.1). At necropsy, iWAT and gWAT depots were removed and snap-frozen on dry ice, followed by cryopulverisation in liquid nitrogen. RNA extraction and reverse transcription to cDNA was then performed on all tissues. qPCR was performed to quantify expression of *Hsd11b1. Hsd11b1* was normalised to the geometric mean of the following housekeeping genes: *Ppia*, *Tbp* and *Hprt*, and presented as relative to the WT AL average of male and female mice together. *Hsd11b1* expression in iWAT of 15-and 10-week-old mice, respectively **(A)**. *Hsd11b1* expression in gWAT of 15-and 10-week-old mice, respectively **(B)**. Data points are presented with median, interquartile range and range shown by box and whisker plot, and were analysed by Mann-Whitney and/or Welch's test as appropriate. Fasted mice: n (WT AL male) = 7. n (WT CR male) = 10. n (KO AL male) = 5. n (KO CR male) = 7. n (WT AL female) = 7. n (WT CR female) = 9. n (KO AL female) = 4. n (KO CR female) = 5. Non-fasted mice: n (AL male) = 8. n (CR male) = 8. n (KO AL male) = 5. n (KO CR male) = 5. n (AL female) = 5. n (CR female) = 6. n (KO AL female) = 8. n (KO CR female) = 9. *: $p<0.05$. ***: $p<0.001$.

4.2.6. GC target gene expression in WAT of mice subject to CR

Figure 4.9 shows the expression of the GC target genes *Fkbp5, Gilz* and *Per1* in iWAT of 15-and 10-week-old mice. In the 15-week-old mice, ANOVA revealed a diet effect across both genotypes for *Fkbp5* expression in females, with the KO females on CR having decreased *Fkbp5* expression compared to the AL-fed females (Figure 4.9.A). Whereas, in the 10-week-old mice an overall diet effect was detected by ANOVA for males and females, with the CR mice having increased expression (Figure 4.9.B). Furthermore, a near-significant genotype effect was detected in females (p=0.0507), with the WT females on CR diet showing a higher expression of *Fkbp5* than the KO females on CR. *Gilz* expression was significantly increased in 15-week-old male mice subject to CR, and ANOVA revealed a similar diet effect in the females (Figure 4.9.C); this was unaffected by 11β-HSD1 KO. In the 10-week-old mice, ANOVA revealed that CR significantly increased *Gilz* mRNA across both genotypes of females, with a trend for this in male mice (Figure 4.9.D). CR significantly increased *Gilz* mRNA in WT females only (Figure 4.9.D). *Per1* mRNA was unaltered by diet or genotype in the 15-week-old mice (Figure 4.9.E). ANOVA showed a near-significant diet effect (p=0.056) for 10-week-old males, but a significant increase in *Per1* expression for WT males on CR (Figure 4.9.F). For the females, ANOVA revealed a diet and genotype effect, with an increased expression of *Per1* in the CR-fed WT females and a trend for this in KO females; however, *Per1* expression tended to be lower in iWAT of KO females compared to their WT counterparts (Figure 4.9.F).

Figure 4.10. shows the gene expression levels of *Fkbp5, Gilz* and *Per1* mRNA in gWAT of 15- and 10-week-old mice. ANOVA showed a significant diet effect for the 15-week-old females, with a decreased expression of *Fkbp5* in the CR-fed KO females compared to the AL-fed females (Figure 4.10.A). In the 10-week-old females, an overall diet effect *on Fkbp5 was* detected by ANOVA, with multiple comparison showing a significant increase in *Fkbp5* in the CR-fed WT females (Figure 4.10.B). ANOVA revealed significant diet effects for *Gilz mRNA* in 15-and 10-week-old females, but in opposite directions: decreased expression in 15-week-old KO females on CR, but increased in the 10-week old WT females on CR with a similar trend for the KO females (Figure 4.10.C-D). Figure 4.10.E shows *Per1* expression in 15-week-old mice, with an overall diet effect in the males only, pointing towards a decrease in expression with CR. Whereas, the ANOVA for the female mice shows an interaction between diet and genotype effect, with the CR-fed WTs increasing, and the CR-fed KOs decreasing *Per1* mRNA. In the 10-week-old mice, ANOVA showed a significant

diet effect for the *Per1* expression in males, with the CR-fed males having higher expression of *Per1*. Whereas, the CR-fed females show a similar but non-significant trend to increase *Per1* mRNA. (Figure 4.10.F).

These data reveal that both CR and 11β-HSD1 KO can influence GC target gene expression in WAT; however, these effects are complex, differing depending on the target gene analysed, the WAT depot assessed, the sex of the mice, and the CR regimen used. Importantly, in most cases there was no interaction between diet and genotype, indicating that 11β-HSD1 KO did not influence the effect of CR on these target genes. Thus, unlike in response to orally administered corticosterone, 11β-HSD1 KO does not robustly prevent the effects of CR-induced GCs on WAT gene expression.

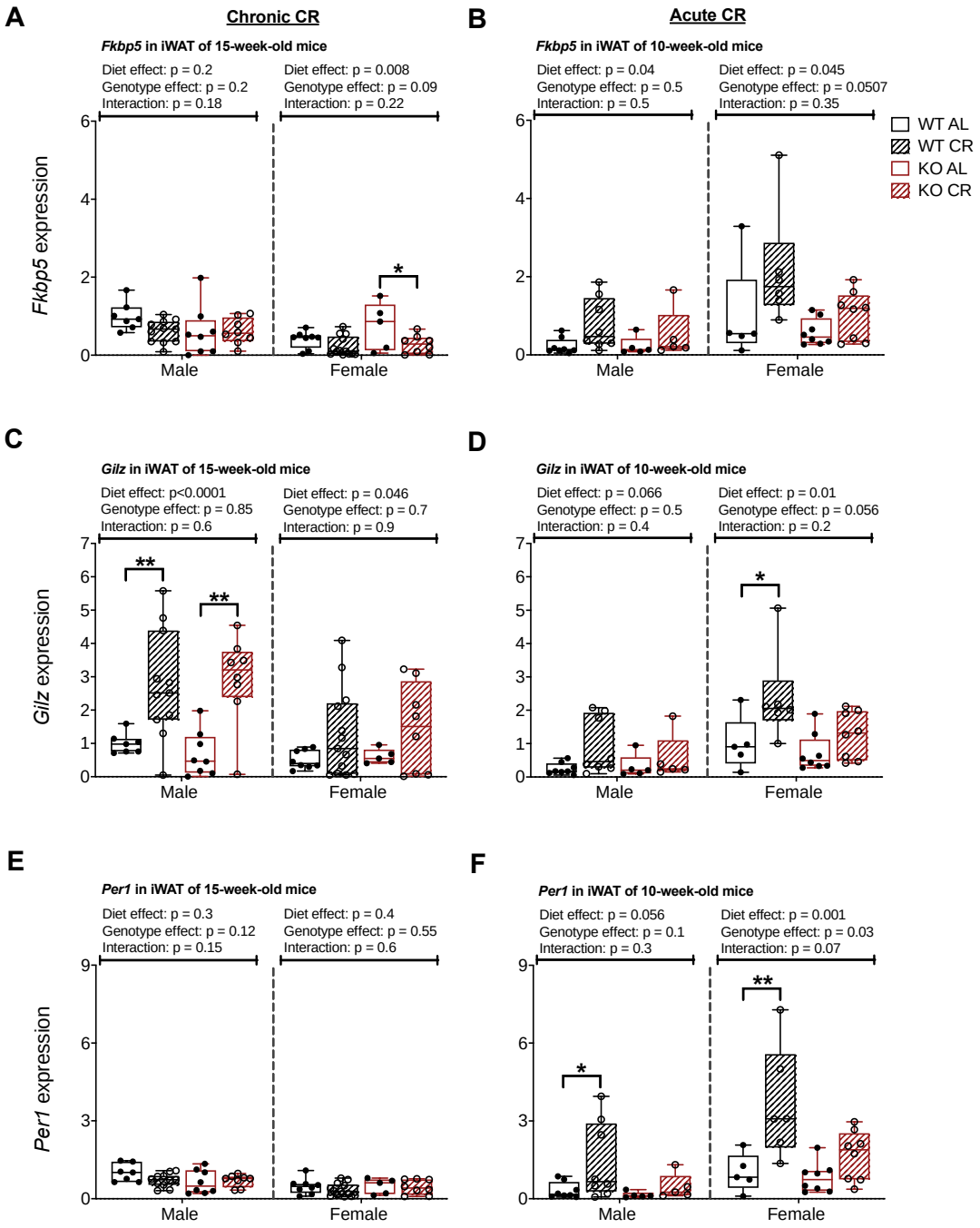

Figure 4.9. GC target gene expression in iWAT of 15-and 10-week-old mice on CR. WT and 11β-HSD1 KO male and female mice were fed AL or CR diets as described for Figure 4.2 and Methods (2.1.2), and fasted/re-fed as described in Methods (2.3.1). qPCR was performed to quantify expression of *Fkbp5, Gilz* and *Per1* in iWAT. Genes were normalised to the geometric mean of the following housekeeping genes: *Ppia*, *Tbp* and *Hprt*, and presented as relative to the WT AL average of male and female mice together. *Fkbp5* expression in 15-and **(A)** 10-week-old **(B)** mice. *Gilz* expression in 15-and **(C)** 10-week-old **(D)** mice. *Per1* expression in 15-and **(E)** 10-week-old **(F)** mice. Data points are presented with median, interquartile range and range shown by box and whisker plot and were analysed by 2-Way ANOVA with Sidak's multiple comparison test. Numbers of mice per group, and presentation of statistically significant differences between groups, are as described for figure 4.9. **: p<0.01.

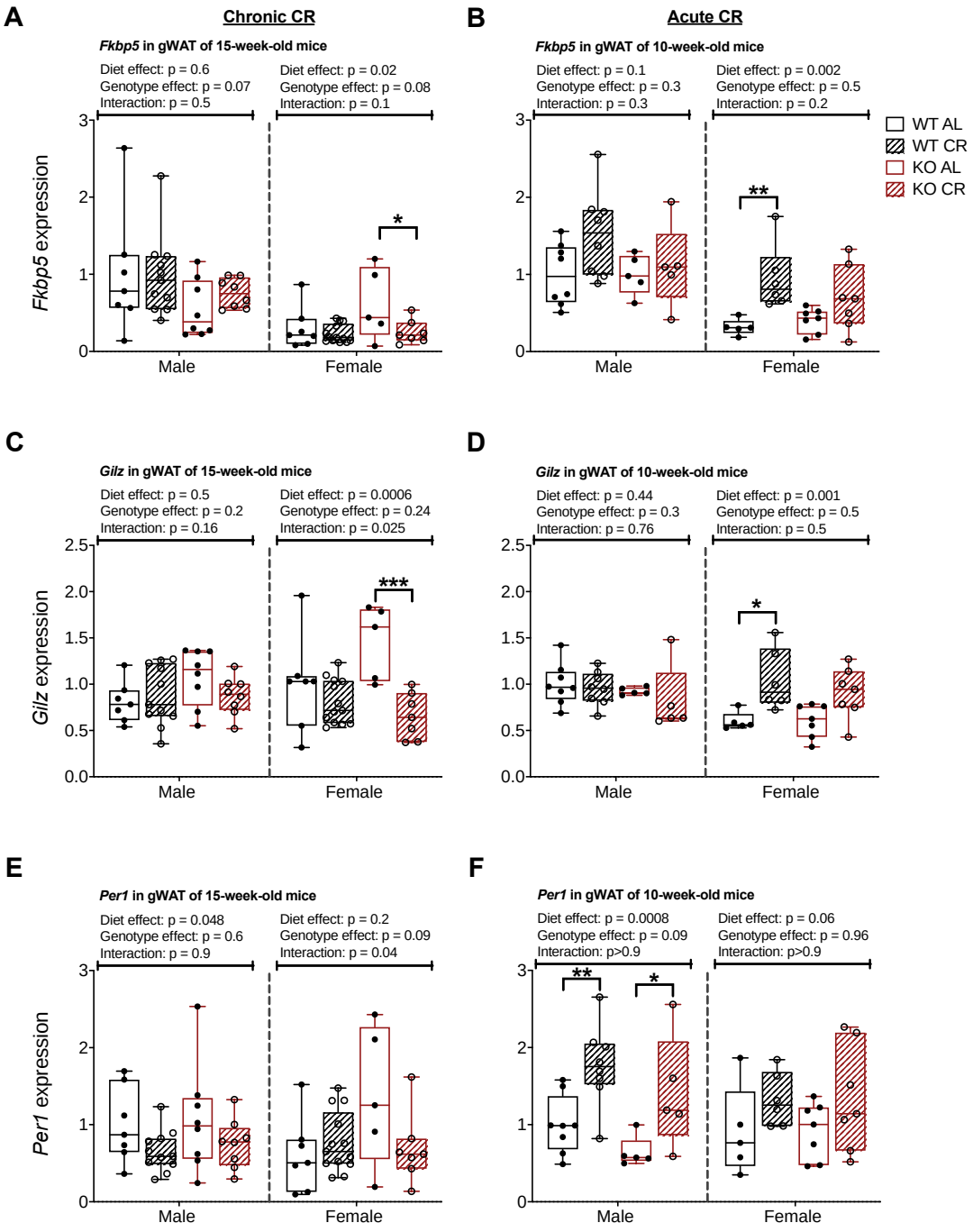

Figure 4.10. GC target gene expression in gWAT of 15-and 1-week-old mice on CR. WT and 11β-HSD1 KO male and female mice were fed AL or CR diets as described for Figure 4.2 and Methods (2.1.2), and fasted/re-fed as described in Methods (2.3.1). Expression of *Fkbp5, Gilz* and *Per1* was determined in gWAT of WT and KO mice, as described for Figure 4.10. *Fkbp5* expression in 15-and **(A)** 10-week-old **(B)** mice. *Gilz* expression in 15-and **(C)** 10-week-old **(D)** mice. *Per1* expression in 15-and **(E)** 10-week-old **(F)** mice. Data points are presented with median, interquartile range and range shown by box and whisker plot and were analysed by 2-Way ANOVA with Sidak's multiple comparison test. Numbers of mice per group, and presentation of statistically significant differences between groups, are as described for figure 4.9. **: p<0.01.

4.2.7. CR modulates BM GC regeneration

A key goal of the experiments in this chapter was to determine if 11β-HSD1 KO mice resist BMAT expansion during CR. Thus, despite the lack of genotype difference in circulating corticosterone concentration throughout CR and the complex results in WAT with the GC target genes, the 10-week-old CR-fed KO males did resist the increases in circulating corticosterone (Figure 4.7.B). Therefore, I next assessed the effects of CR and 11β-HSD1 KO on tissue GC concentrations and target gene expression within the BM. I began by using LC-MS/MS to measure corticosterone and 11-DHC concentrations.

Figure 4.11. shows concentrations of corticosterone, 11-DHC, and the CORT-to-11-DHC ratio in the BM of 15-and 10-week-old mice. An overall genotype effect was detected by ANOVA for 15- and 10-week-old females, with KOs having lower corticosterone concentration than WTs (Figure 4.11.A-B). The 15-week-old mice lacked diet differences, but ANOVA revealed significant diet differences for the 10-week-old mice. 10-week-old females and WT males on CR had significantly increased BM corticosterone concentration compared to AL-fed mice (Figure 4.11.B). This pattern is similar to that for circulating corticosterone concentrations (Figure 4.7.A-B). The 15-and 10-week old males showed genotype effects detected by ANOVA for 11-DHC concentration in the BM, whereas the females did not show this (Figure 4.11.C-D). The 15-week-old mice also failed to show diet effects (Figure 4.11.C), but the 10-week-old mice displayed significant diet effects, with the females and WT males on CR showing increased 11-DHC concentration compared to the KO males (Figure 4.11.D). For each cohort, further genotype differences were revealed by ANOVA for the ratio of CORT-to-11-DHC (Figure 4.11.E-F), with a lower ratio in the KOs indicating the expected decreases in corticosterone regeneration. In addition, this ratio was decreased with CR in 10-week-old WT males and females (Figure 4.11.F). Of importance for my hypothesis, male 11β-HSD1 KO mice resisted increased BM corticosterone concentrations during CR (Figure 4.11.B), raising the possibility that these male mice also resist other GC-mediated effects of CR within the BM.

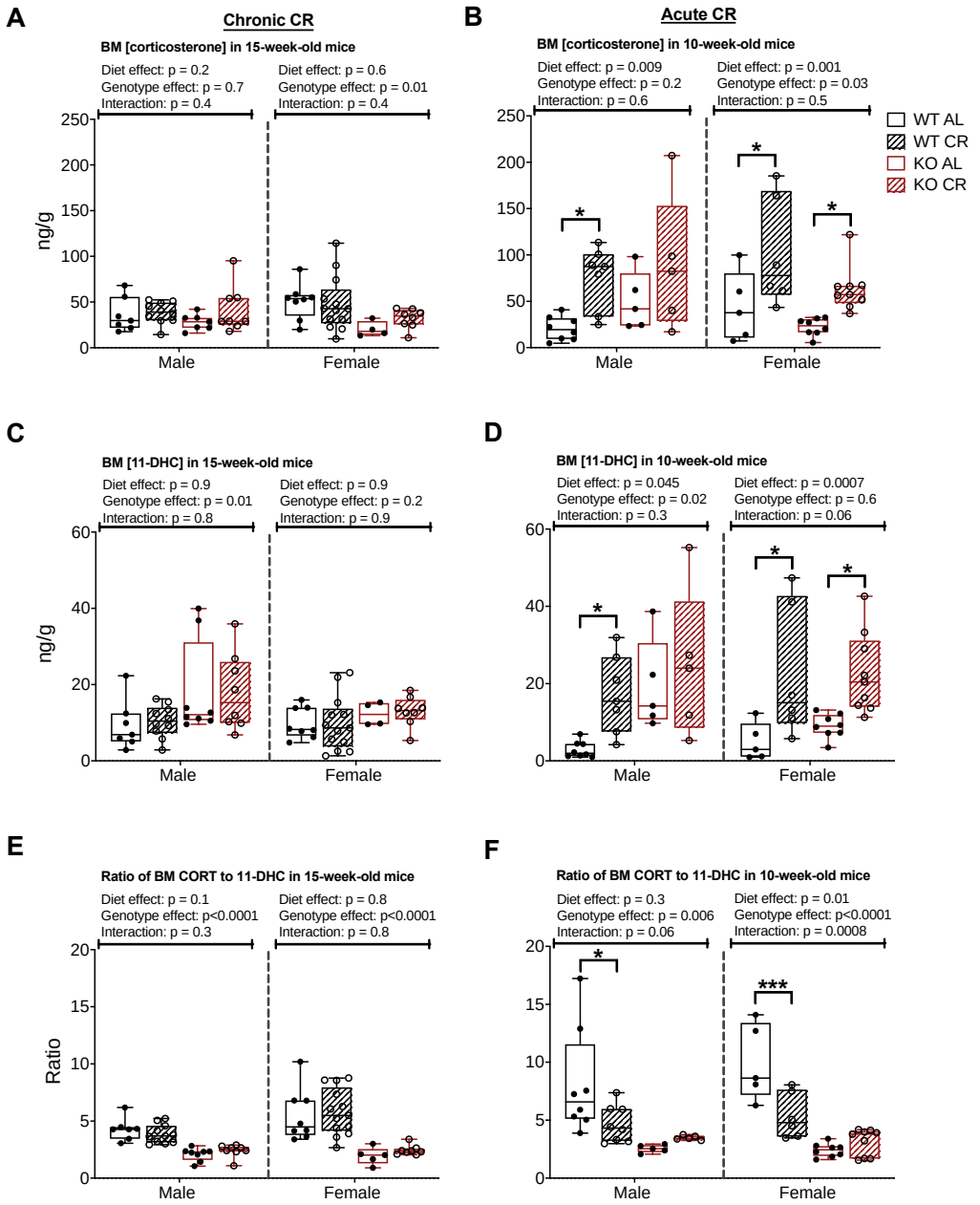

Figure 4.11. BM GC concentration is upregulated with CR. WT and 11β-HSD1 KO male and female mice were fed AL or CR diets as described for Figure 4.2 and Methods (2.1.2), and fasted/re-fed as described in Methods (2.3.1). Post termination, femurs were collected and the femoral BM was quantified for 11-DHC and corticosterone by LC-MS/MS, as described in Methods (2.5.2). BM corticosterone concentration in 15-and **(A)** 10-week-old **(B)** mice. BM 11-DHC concentration in 15- and **(C)** 10-week-old **(D)** mice. BM corticosterone to 11-DHC ratio in 15-and **(E)** 10-week-old **(F)** mice. Data points are presented with median, interquartile range and range shown by box and whisker plot, and were analysed by 2-Way ANOVA with Sidak's multiple comparison test. 15-week-old mice: n (WT AL male) = 7. n (WT CR male) = 11. n (KO AL male) = 7/8. n (KO CR male) = 8. n (WT AL female) = 7. n (WT CR female) = 13. n (KO AL female) = 6. n (KO CR female) = 8. 10-week-old mice: n (AL male) = 8. n (CR male) = 8. n (KO AL male) = 5. n (KO CR male) = 5. n (AL female) = 5. n (CR female) = 6. n (KO AL female) = 8. n (KO CR female) = 9. *: $p<0.05$. ***: $p<0.001$.

4.2.8. CR is associated with increased expression of GC target genes in the BM

I next investigated if the KO mice also resisted an increase in GC action within the BM by examining the expression of GC target genes.

Figure 4.12 shows expression of the GC target genes *Hsd11b1*, *Fkbp5, Gilz* and *Per1* in BM of 15-and 10-week-old mice. *Hsd11b1* was significantly increased with CR in 15-week-old WT mice (Figure 4.12.A) but not in 10-week-old WT mice (Figure 4.12.B) and, as expected, was undetectable in KO mice. ANOVA detected no diet or genotype effects for *Fkbp5* in males but revealed a diet effect for *Fkbp5* in 15-week-old females, with a decrease in CR-fed KO females (Figure 4.12.C). Overall diet effects were also detected in the 10-week-old mice (Figure 4.12.D), with increased *Fkbp5* for males and WT females on CR. *Gilz* expression was downregulated with CR in the 15-week-old KO females (Figure 4.12.E). However, in the 10-week-old mice, *Gilz* expression was increased with CR both across and within each genotype (Figure 4.12.F). *Per1* expression was unaltered by diet or genotype in the 15-week-old mice (Figure 4.12.G), but in the 10-week-old mice ANOVA showed significant diet effects (Figure 4.12.H). Multiple comparisons showed a significant increase in the 10-week-old females and WT males. Moreover, a significant genotype effect was present for *Per1* in the 10-week males, with KO mice having significantly lower expression than their WT counterparts (Figure 4.12.H). The 10-week data suggest that CR increases GC action within the BM and that 11β-HSD1 KO mice generally do not resist this. The 15-week data does not show these diet differences, suggesting the fasting prior to necropsy has altered GC target gene expression so that this does not reflect the effects of GC excess experienced throughout most of the duration of CR. Accordingly, the gene expression patterns observed in the 10-week cohorts might more accurately reflect the effects of CR on GC action within the BM, and the ability of 11β-HDS1 KO mice to resist these effects. However, it is also possible that expression of these transcripts does not fully reflect the consequences of long-term hypercorticosteronaemia during CR. Therefore, I next analysed BMAT to determine the effects of 11β-HSD1 KO on CR-induced BMAT expansion.

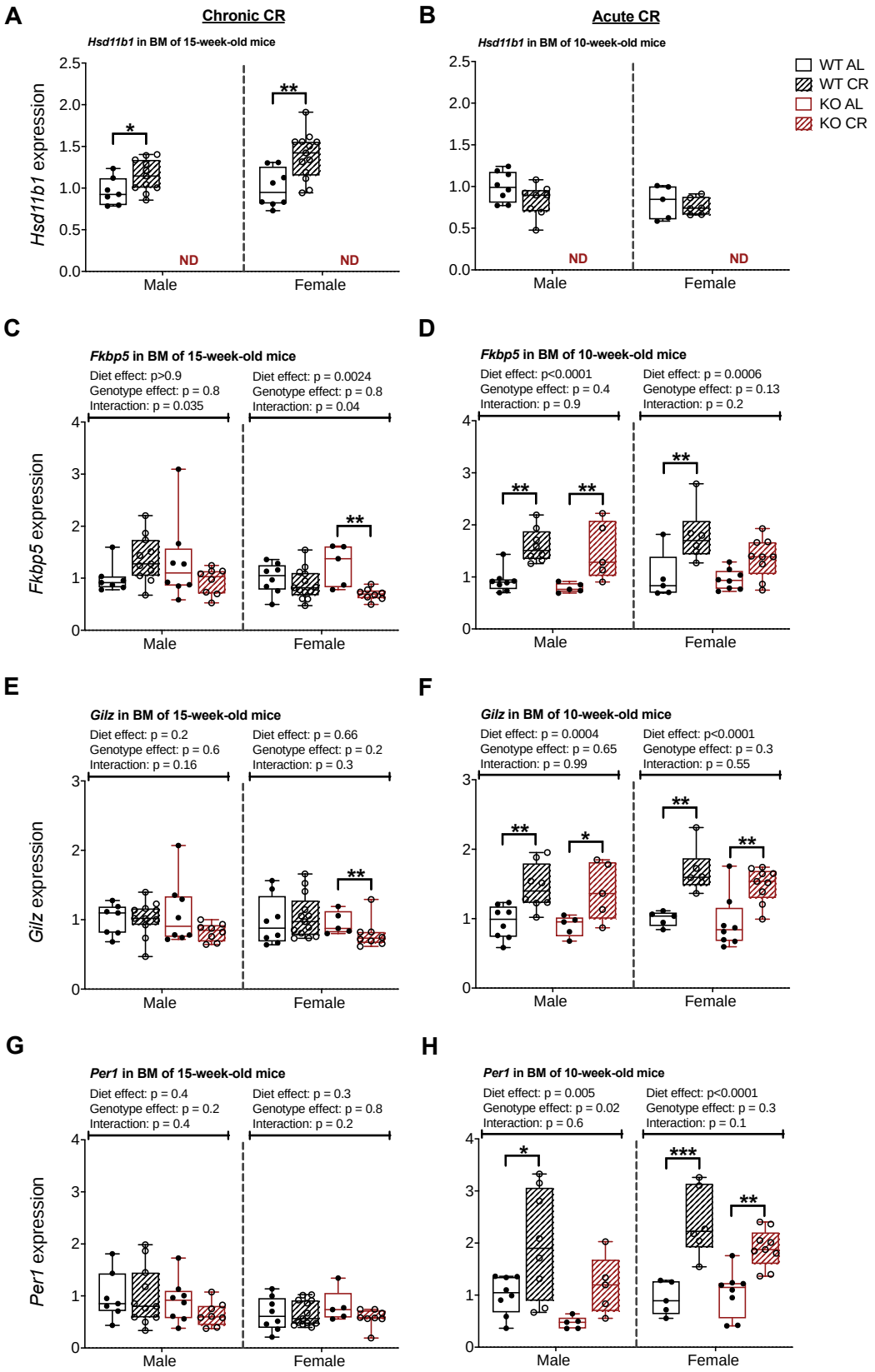

Figure 4.12. CR increases GC target gene expression in the BM. WT and 11β-HSD1 KO male and female mice were fed AL or CR diets as described for Figure 4.2 and Methods (2.1.2), and fasted/re-fed as described in Methods (2.3.1). Post

termination, the tibiae of the mice were collected and proceeded with as described in Methods. qPCR was performed to quantify expression of *Hsd11b1, Fkbp5, Gilz* and *Per1* in BM. Genes were normalised to the geometric mean of the following housekeeping genes: *Ppia*, *Tbp* and *Actb*, and presented as relative to the WT AL average of male and female mice together. *Hsd11b1* expression in 15-and **(A)** 10-week-old **(B)** mice. *Fkbp5* expression in 15-and **(C)** 10-week-old **(D)** mice. *Gilz* expression in 15-and **(E)** 10-week-old **(F)** mice. *Per1* expression in 15-and **(G)** 10-week-old **(H)** mice. Data points are presented with median, interquartile range and range shown by box and whisker plot, and were analysed by 2-Way ANOVA with Sidak's multiple comparison test (C-H), or by Mann-Whitney and/or Welch's test as appropriate (A-B). Numbers of mice per group, and presentation of statistically significant differences between groups, are as described for figure 4.12. **: $p<0.01$.

4.2.9. Male 11β-HSD1 KO mice, but not female, resist CR-induced BMAT expansion

CR has previously been shown to induce BMAT expansion in animals (Devlin *et al.*, 2010, 2016; Cawthorn *et al.*, 2016). As previously shown, circulatory (Figure 4.7.B) and BM (Figure 4.11.B) corticosterone concentration was increased with CR in all groups but the KO males. However, the results from the GC target genes (Figure 4.12) suggest that CR increases GC action within the BM and that 11β-HSD1 KO mice generally do not resist this; hence, it is unclear if the KO mice would resist other effects of CR within the BM. Therefore, I next analysed BMAT to investigate if the KOs resisted CR-induced BMAT expansion.

Figure 4.13 shows a respective osmium-stained tibia from each group, highlighting the proximal and distal parts of the bone that were analysed. Figure 4.14 shows the analysed BMAT in the tibiae of male and female mice, both in the proximal and distal regions of the bone, as well as total BMAT. Figure 4.14.A and B represent the proximal BMAT of male and female mice. For both sexes, ANOVA detected a significant diet effect (Figure 4.14.A-B), whereas a genotype effect was detected in males only (Figure 4.14.A). Multiple comparison showed significant increases in BMAT in the females (Figure 4.14.B) and WT males with CR but, notably, the KO males on CR resisted this expansion (Figure 4.14.A). For the distal BMAT, ANOVA detected similar diet effects for both sexes (Figure 4.14.C-D) but indicated no genotype effects. Multiple comparison showed identical increases with CR in distal as for proximal BMAT. Total BMAT also showed similar results (Figure 4.14.E-F), with ANOVA detecting a genotype effect in males only (Figure 4.14.E).

These results show that the KO male mice resist CR-induced BMAT expansion, whereas the KO females do not. These results are reminiscent of the BM corticosterone concentration (Figure 4.11.B), suggesting that the lack of CR-induced BMAT expansion in KO males might be due to the lack of increased BM corticosterone with CR.

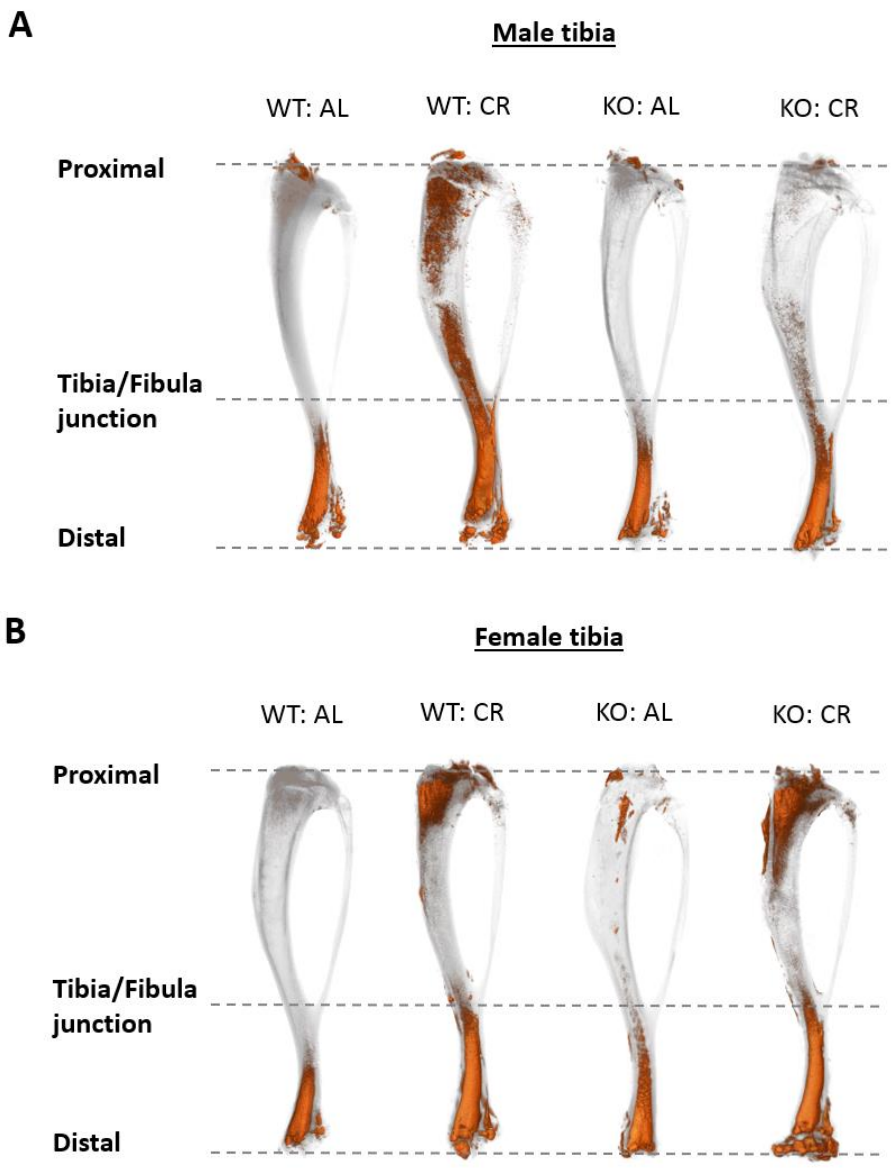

Figure 4.13. 11β-HSD1 KO males, but not females, are protected from BMAT expansion during CR. Young C57BL/6JOlaHsd (WT) and 11β-HSD1 KO (KO) male and female mice were fed *ad libitum* (AL) or 70% of *ad libitum* food intake (CR) for six weeks, from 9 weeks until 15 weeks of age. Post termination, bones were decalcified and stained with osmium tetroxide staining for 48 hours, and thereafter washed for 24 hours in Sorensen's buffer. Tibiae were scanned by uCT, and the images were visualised using CTvox (Bruker) software. **(A)** Male tibia bones representing one bone from each group. **(B)** Female tibia bones representing one bone from each group.

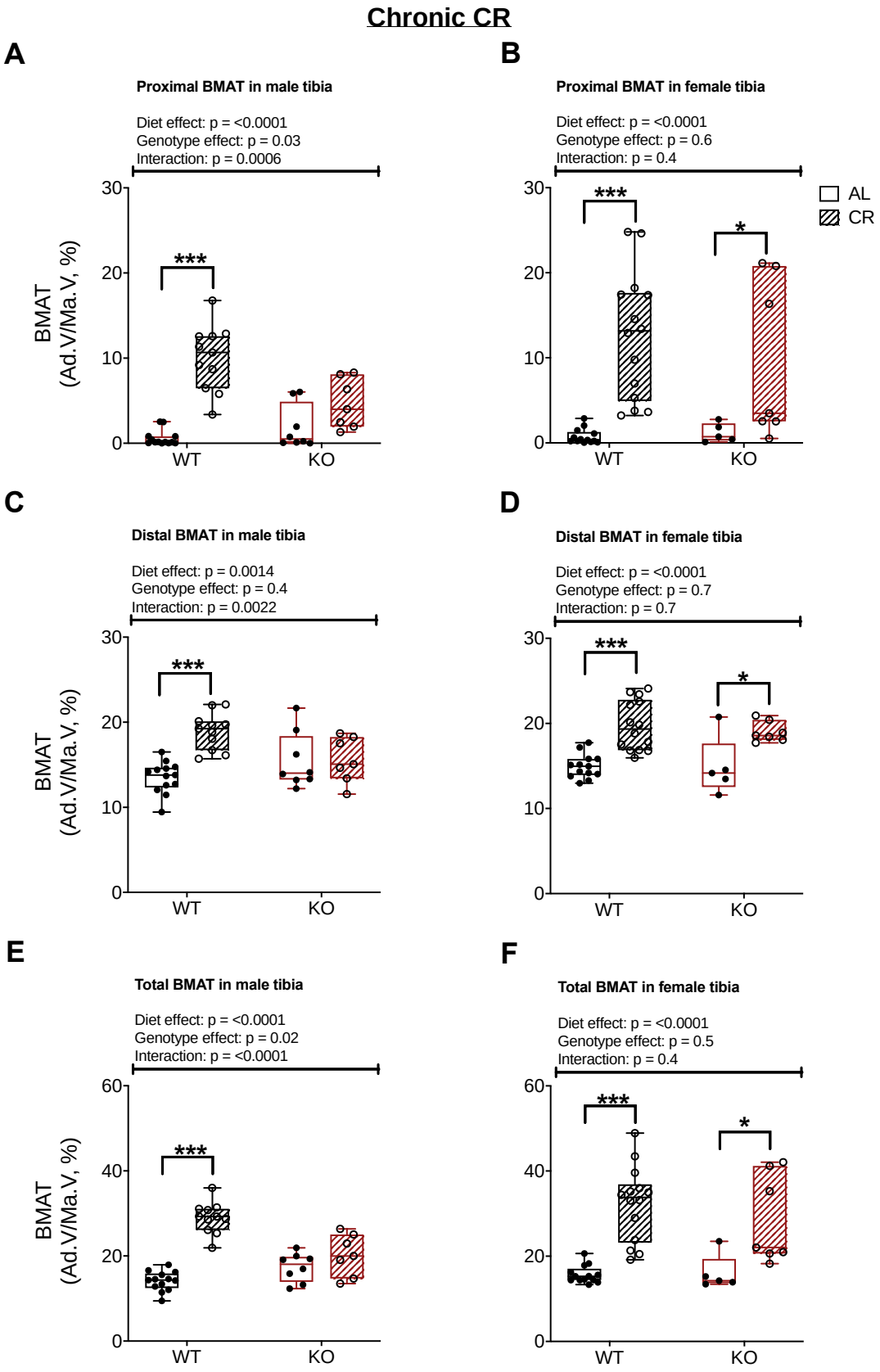

Figure 4.14. 11β-HSD1 KO males, but not females, are protected from BMAT expansion during CR. WT and 11β-HSD1 KO male and female mice were fed AL or CR diets as described for Figure 4.2 and Methods (2.1.2), and fasted/re-fed as

described in Methods (2.3.1). Post termination, bones were decalcified and stained with osmium tetroxide staining for 48 hours, and thereafter washed for 24 hours in Sorensen's buffer. Tibiae were then scanned at 12μm by μCT and analysed by CTan for BMAT as % of total medullary cavity. Proximal BMAT in male **(A)** and female **(B)** tibiae. Distal BMAT in male **(C)** and female **(D)** tibiae. Total BMAT in male **(E)** and female **(F)** tibiae. Data points are presented with median, interquartile range and range shown by box and whisker plot, and were analysed by 2-Way ANOVA with Sidak's multiple comparison test. n (WT AL male) = 13. n (WT CR male) = 11. n (KO AL male) = 8. n (KO CR male) = 7. n (WT AL female) = 13. n (WT CR female) = 14. n (KO AL female) = 5. n (KO CR female) = 7. *: $p<0.05$. **: $p<0.01$ ***: $p<0.001$.

4.2.10. CR is associated with decreased testosterone concentration in males, but increased in females

The BMAT (Figure 4.14) and BM corticosterone concentration (Figure 4.11.B) results suggest that there is an association between BMAT and corticosterone in males only. However, RNA data (Figure 4.12) are not consistent with this, with evidence of higher GC action within the BM during CR than AL in both males and females regardless of genotype. Therefore, I next investigated additional mechanisms that might explain the resistance of KO males to CR-induced BMAT expansion. Androgens have been shown to modulate BMAT formation (Tamura *et al.*, 2005), with age-induced BMAT expansion in old men being associated with decreased testosterone concentration (Mistry *et al.*, 2018). Furthermore, healthy lean men on CR have reduced testosterone concentrations (Cangemi *et al.*, 2010). Therefore, I measured testosterone concentrations in the circulation and BM to test if this is associated with the differences in BMAT expansion across the groups.

Figure 4.15. shows circulatory and BM testosterone concentration in the 15- and 10-week-old mice. 15-week-old males showed neither diet nor genotype differences, although a trend for decreased testosterone with CR was apparent (Figure 4.15.A). In addition, only two females on CR had detectable testosterone concentration. Conversely, the 10-week-old males showed an overall diet effect by ANOVA, with lower testosterone concentration in the CR-fed KOs (Figure 4.15.B). Similar results were found for the BM testosterone, with the 15-week-old mice lacking diet differences (Figure 4.15.C), and the 10-week-old mice showing lower testosterone concentrations with CR, particularly in the KO mice. Testosterone was present at measurable levels in the BM of some of the CR-fed females from the 15- and 10-week groups, suggesting that CR might increase testosterone in female mice. The ability to detect these low levels was facilitated by use of a more-sensitive calibration curve optimised for the BM. Based on these results, a clear difference between the long-term six-week CR vs short-term one-week CR cohorts was apparent, as previously mentioned regarding the fasting regimen. The KO males showed decreased testosterone concentration post-CR and, if anything, this effect was greater than in the WT males. Therefore, the resistance of male KO mice to CR-induced BMAT expansion is not explained by a failure to decrease testosterone during CR.

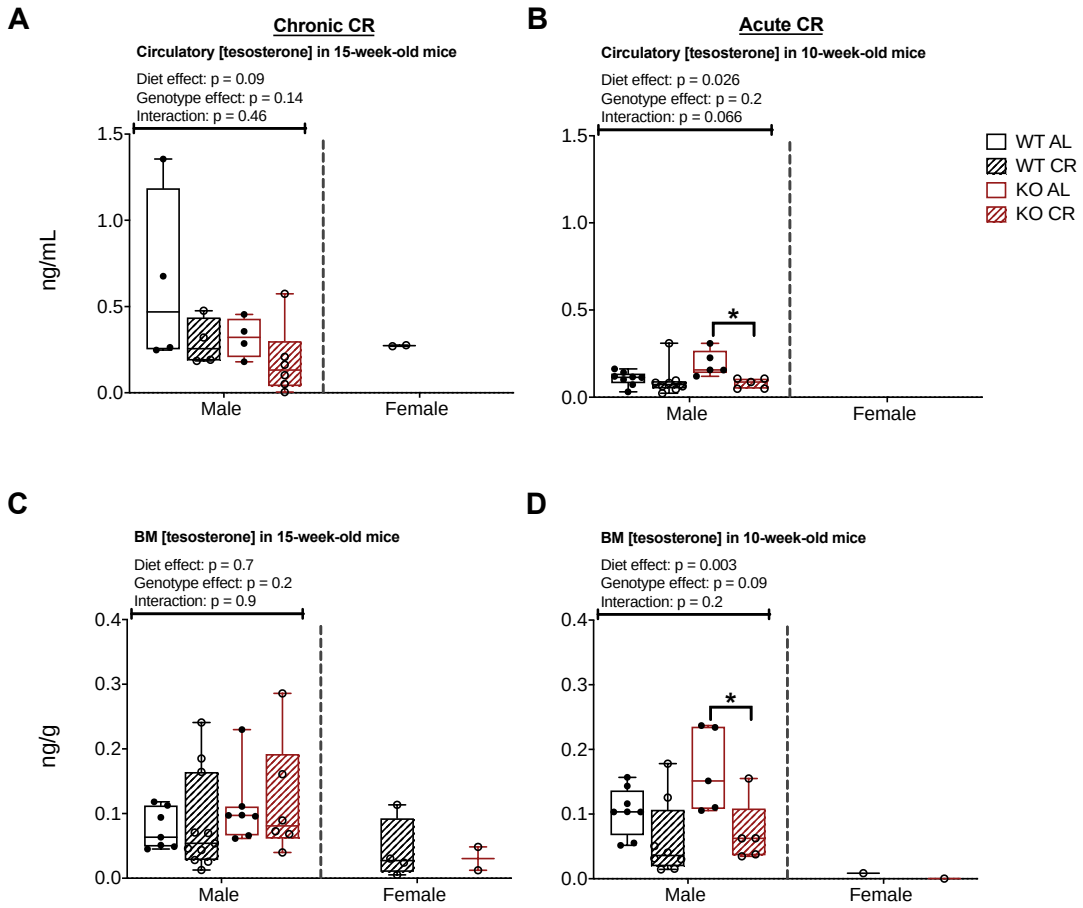

Figure 4.15. Testosterone is decreased in males; but increased in females on CR. WT and 11β-HSD1 KO male and female mice were fed AL or CR diets as described for Figure 4.2 and Methods (2.1.2), and fasted/re-fed as described in Methods (2.3.1). Post termination, femurs were collected and the femoral BM was quantified for testosterone by LC-MS/MS, as described in methods (2.5.2). Circulatory testosterone in 15-and **(A)** 10-week-old **(B)** mice. BM testosterone in 15-and **(C)** 10-week-old **(D)** mice. Data points are presented with median, interquartile range and range shown by box and whisker plot, and were analysed by 2-Way ANOVA with Sidak's multiple comparison test. Numbers of mice per group, and presentation of statistically significant differences between groups, are as described for figure 4.12. **: p<0.01.

4.2.11. 11β-HSD1 KO male mice have increased progesterone concentration within BM and plasma

As previously mentioned, it is unclear whether 11β-HSD1 KO mice resist GC action within the BM during CR as, although the 10-week-old CR-fed KO males resisted CR-induced BMAT expansion and increases in BM corticosterone concentration, my qPCR data (Figure 4.12.D, F, H) suggest increased GC action in all genotypes. The testosterone results suggest that the resistance to BMAT expansion in the KO males is not a result of a failure to decrease circulating or BM testosterone during CR. Therefore, I next explored if other steroid hormones might be influencing BMAT expansion. One well-established inhibitor of BMAT accumulation is oestradiol; hence, I hypothesised that the KO males might resist CR-induced BMAT accumulation owing to increases in oestradiol, and that BMAT expansion in females might be driven primarily by decreased oestradiol during CR. However, due to difficulties of analysing oestradiol in small amounts of plasma and BM, it was unfortunately not quantified. However, during the LC-MS/MS analysis, I was able to also analyse other steroid hormones, one of which was progesterone. Since the progesterone receptor has similar targets to the oestrogen receptor, one possibility is that progesterone may also modulate BMAT formation. Figure 4.16 shows the progesterone concentration in the BM of 15-and 10-week-old mice, and in the circulation of 10-week-old mice only. ANOVA revealed a significant genotype effect in each cohort for the males only (Figure 4.16.A-B), with the KOs having increased progesterone concentration compared to the WTs, regardless of diet. No differences were observed in the BM for the females. Circulatory progesterone was examined in 10-week-old mice only (Figure 4.16.C). ANOVA showed significant genotype as well as diet effects in the males only. CR-fed WT males also had increased progesterone concentration compared to AL-fed WT males. These results show that 11β-HSD1 KO increases progesterone in male, but not female mice. Moreover, given the ability of sex steroids to modulate BM adiposity, this difference might contribute to the resistance of the KO males to CR-induced BMAT expansion.

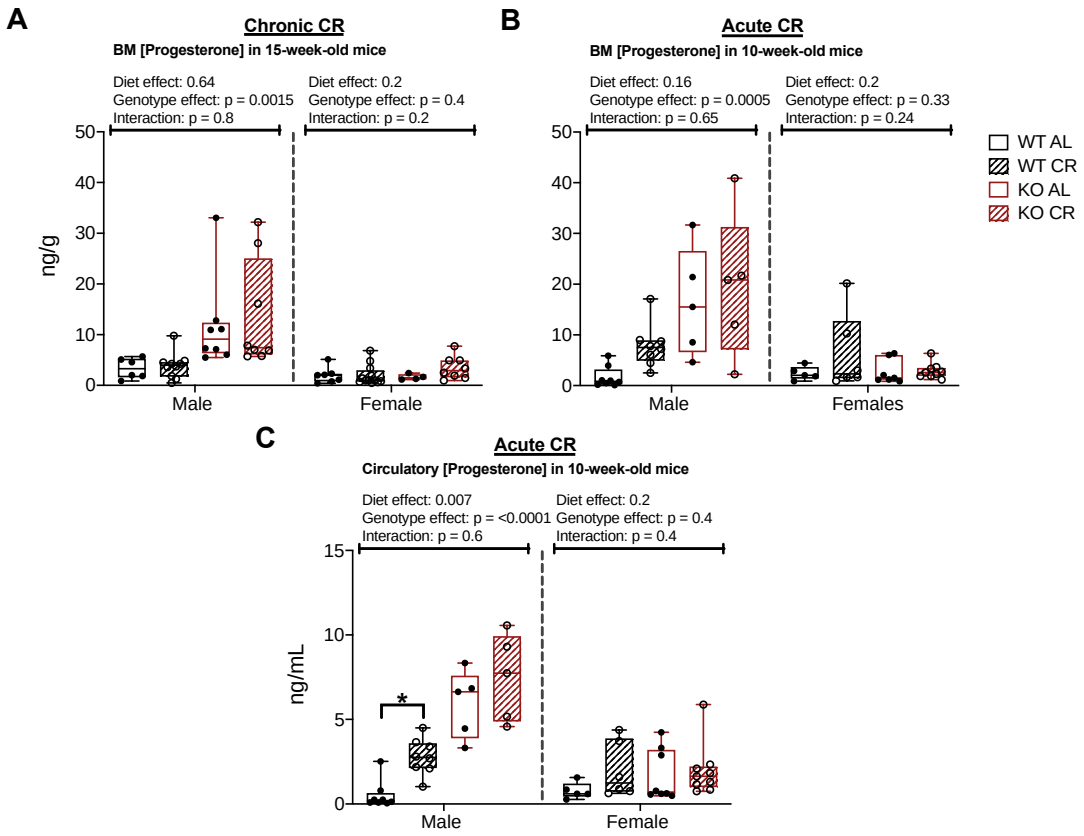

Figure 4.16. Circulatory and BM progesterone was increased in 11β-HSD1 KO male mice. WT and 11β-HSD1 KO male and female mice were fed AL or CR diets as described for Figure 4.2 and Methods (2.1.2), and fasted/re-fed as described in Methods (2.3.1). Post termination, femurs were collected and the femoral BM was quantified for progesterone by LC-MS/MS, as described in methods (2.5.2). **(A)** BM progesterone concentration in 15-week-old mice. **(B)** BM progesterone concentration in 10-week-old mice. **(C)** Circulatory progesterone concentration in 15-week-old mice. Data points are presented with median, interquartile range and range shown by box and whisker plot, and were analysed by 2-Way ANOVA with Sidak's multiple comparison test. 15-week-old mice: n (WT AL male) = 7. n (WT CR male) = 10. n (KO AL male) = 5. n (KO CR male) = 7. n (WT AL female) = 7. n (WT CR female) = 9. n (KO AL female) = 4. n (KO CR female) = 5. 10-week-old mice: n (AL male) = 8. n (CR male) = 8. n (KO AL male) = 5. n (KO CR male) = 5. n (AL female) = 5. n (CR female) = 6. n (KO AL female) = 8. n (KO CR female) = 9. *: $p<0.05$.

4.3. Discussion

4.3.1. AT effects in response to CR in 11β-HSD1 KO mice

In this chapter, I found that the KO males lose fat mass to a similar degree as their litter-matched controls. Previous research has shown that the hypomorphic 11β-HSD1 KO mice resist diet-induced obesity (Morton *et al.*, 2004) and further side effects of GC excess (Morgan *et al.*, 2014), suggesting that the lack of this enzyme can prevent obesity and associated metabolic dysregulation. However, my results show that these 11β-HSD1 KOs do not resist the effects of CR such as decreased adiposity, increased GC concentration and BMAT expansion (besides the KO males). This could be due to the genotype differences between the hypomorphic and null KOs. The hypomorphic KO model might also exert other effects on peripheral tissues that the null KO model does not, allowing the tissues to resist diet-induced obesity. Furthermore, on CR, the 11β-HSD1 male KOs drop to a similar level as the WTs, suggesting that the lack of 11β-HSD1 might enhance CR-associated fat loss in males only. This could be a result of 11β-HSD1 deficiency, or it could be a technical artefact as future cohorts did not show the same tendency regarding the body and fat mass of the AL-fed males. Interestingly, two cohorts of older 11β-HSD1 KO mice show opposite results regarding the fat mass, but this is further discussed in Chapter 6. Another reason why the KOs might be fatter could be due to the role of GCs in lipolysis. Dexamethasone increases lipolysis, FFA and glycerol in primary rat adipocytes in a dose-and time-dependent manner (Xu *et al.*, 2009). This would suggest that the AL-fed 11β-HSD1 KO males might have less corticosterone concentration allowing to resist lipolysis, but we know based on the circulatory corticosterone ELISA results (Figure 4.5.A) that there were no genotype differences. No genotype differences were found in BM of the 15-nor 10-week-old AL-fed KOs either, although, this might differ in WAT. Therefore, to further understand the genotype difference regarding fat mass in the males, one could quantify GC concentration in WAT. If WAT corticosterone concentration would be less than circulatory, or less than the WTs, it could explain the genotype difference.

In Chapter 3, I found that WT female mice on 30% CR maintained their fat mass, compared to male mice, who lost theirs. In this chapter, I revealed similar results with regards to the fat mass of 11β-HSD1 KO females subject to CR, as shown in Chapter

3. A possible reason for this could be to maintain a healthy reproductive system, as discussed in more depth in section 3.3.1. Compared to studies including male mice, fewer studies include female mice, especially in experiments where 11β-HSD1 KO mice are used; this is the case both for the hypomorphic and null 11β-HSD1 KO models from Edinburgh University, and the 11β-HSD1 exon 5 KO from Birmingham University (Kotelevtsev *et al.*, 1997; Morgan *et al.*, 2014; Larner *et al.*, 2016; Johnson *et al.*, 2017; Verma *et al.*, 2018). This is most likely due to the common perception, often erroneous, that the oestrous cycle of female mice confounds the end results. In addition, due to most studies from Edinburgh involving the hypomorphic 11β-HSD1 KO model, very few are done on the more recent null KO model, and only one (Vandermosten *et al.*, 2017) out of four (Johnson *et al.*, 2017; Zhang *et al.*, 2017; Verma *et al.*, 2018) involves female mice. Therefore, the lack of previous studies in female null 11β-HSD1 KO mice makes it challenging to compare to other research and potential mechanisms. Similarly, additional KO models with regards to GC excess, such as global and/or adipose-specific GR KO mouse, have not yet been investigated during CR. This identifies a gap in the literature, and investigating it further would help to elucidate the function of GCs during CR.

4.3.2. Effects of metabolic hormones on CR-induced BMAT expansion

The main finding of this chapter was that 11β-HSD1 KO males resisted CR-induced BMAT expansion, whereas the KO females did not. Furthermore, the KO males had significantly increased circulatory and BM progesterone concentration regardless of diet compared to the females and WT males. The results indicate that intracellular regeneration of corticosterone by 11β-HSD1 is not necessary for BMAT expansion with CR in females, but it is in males. Instead, progesterone could be associated with the resistance of BMAT expansion during CR in the KO males. However, although there is this association between increased progesterone and unaltered BMAT volume, it does not mean that GCs are not involved in mediating BMAT expansion with CR in males. Although progesterone might play a role in BMAT expansion, it cannot be determined without further *in vitro* experiments (as I have mentioned in the next section, 4.3.3). Progesterone may be a marker of change in CR, but it might not necessarily indicate that it causes any changes.

The KO model that I used intervened with the intracellular regeneration of GCs by 11β-HSD1 only, but the adrenal glands were still releasing circulatory GCs that could have impacted the end-results; hence, the 11β-HSD1 KOs are not GC insufficient. Because of this, it is possible that the KO males are more resistant to circulatory GCs within the BM, even though they generally did not resist up-regulation of the GC target genes (Figure 4.12), compared to KO females. However, the GC target genes alone is not enough to infer GC function. Therefore, directly quantifying 11β-HSD1 activity in BM and potentially AT would be beneficial to my current results. In addition, the resistance of GCs within the BM was further confirmed by LC-MS/MS results, which showed increased corticosterone in females and WT males, but not KO males (Figure 4.11.B). Another reason for the CR-induced BMAT expansion could be due to decreased GR affinity in the bone/BM, protecting the tissue from GC excess. This has been reported in AN and CS patients with high GC concentrations (Invitti *et al.*, 1999). Since the 11β-HSD1 KO females did not resist the effects of CR, GC excess might not be the main driver of CR-induced BMAT expansion in females; something else could be influencing this, with or without GCs, suggesting novel sex differences with regards to GC excess and BMAT expansion. This suggests that a different KO model could be used to better test if GCs can contribute to BMAT expansion in females. Considering that progesterone is the precursor to testosterone and oestradiol, it could be hypothesised that the KO males resisted BMAT expansion due to their high progesterone concentration. Given that the oestrogen receptor and progesterone receptor have overlapping transcriptional targets (Tamm *et al.*, 2009), it is possible that progesterone could inhibit BMAT, just like oestradiol (Griffith *et al.*, 2012; Limonard *et al.*, 2015). Alternatively, the increased progesterone in the KO males may result in increased oestradiol concentrations, thereby suppressing BMAT expansion. This suggests that progesterone and/or oestradiol could play a role alongside GCs in CR-induced BMAT expansion. One way to test this would be by directly measuring oestradiol in the circulation and BM, alongside aromatase, the enzyme that converts androgens into oestrogens. Further evidence demonstrates relationships between GCs and progesterone. For example, a previous publication revealed that progestin (a synthetic form of progesterone) can bind to the GR and induce anti-GC effects in adipocyte precursor cells in rats (Xu, Hoebeke and Björntorp, 1990). Similarly, progesterone has been shown to supress gene expression in myometrial cells via the GR rather than the PR, but it acts on both nuclear receptors to increase expression

(Lei *et al.*, 2012). These results suggest that CR-induced BMAT expansion and GC target genes could be driven not only by GCs, but also by progesterone/PR.

Besides CR, another model of GC excess is CS. CS patients have increased circulating GCs as well as increased BMAT (Maurice *et al.*, 2018). However, patients in remission that lack GC excess have decreased BMAT (Geer *et al.*, 2012). This further supports my hypothesis that GC excess does impact BMAT formation, dependently or independently of other mechanisms/hormones. One way to test this would be to examine a different KO model that prohibits complete GC action and subject these KOs to CR. A robust model would be a GR KO in osteoblasts, as it has previously been proven that GCs cannot induce bone loss in the absence of GR expression in osteoblasts (Rauch *et al.*, 2010). This suggests that the GR KO in osteoblasts resists the action of GCs in bone. Whether these GR KOs in osteoblasts would resist CR-induced BMAT expansion has not been tested. However, since the GR KOs resist bone loss upon GC treatment, and that BMAds derive from the same precursor as osteoblasts (Liu *et al.*, 2013; Chen *et al.*, 2014), it is possible that they would also resist BMAT expansion. Other models of GC excess have shown that GCs can act in sexually dimorphic manner (Duma *et al.*, 2010; Quinn and Cidlowski, 2016; Spaanderman *et al.*, 2019). For example, GC administration in rats showed opposite gene expression in males vs females, and 84 additional GC-responsive genes were detected in males, suggesting that the anti-inflammatory effects of GC are more effective in males compared to females (Duma *et al.*, 2010). A recent finding revealed different patterns of GC-androgen crosstalk in various metabolic tissues, for example, the androgen receptor (AR) inducing GR signalling in WAT and BAT (Spaanderman *et al.*, 2019). Previous research has highlighted the importance and sensitivity of sex hormones between visceral and subcutaneous adipose depots (Rodriguez-Cuenca *et al.*, 2005). Investigating this further and including BMAT as another depot, and subjecting mice to CR or GC treatment, could give us more information about the endocrine functions of CR on BMAT expansion. Since these studies are not focused on CR/fasting, it is possible that the results could be influenced by the interplay of several receptors and/or hormones in the bone and/or BM. Due to the lack of research in CR-induced BMAT expansion and steroid hormones, these claims are still to be confirmed.

It is also worth noticing that effects of increased GCs resulting from CR with that which results from exogenously administered corticosterone differ as previously discussed (Section 3.3.3.2). Moreover, unlike in response to orally administered corticosterone (Morgan *et al.*, 2014), the null 11β-HSD1 KO mice do not robustly resist tissue-specific effects of GC excess during CR. The reason behind this could be that the two ways of increasing GCs are different (CR vs excessive GC administration) with distinctive end-results for each model; exogenous corticosterone promoting visceral adiposity, and CR decreasing it. Other differences between my results and Morgans (Morgan *et al.*, 2014) includes hypercorticosteroneaemia. Morgan et al., showed much higher concentrations compared to my results. Furthermore, I showed enlarged adrenal glands, whereas, the Morgan study showed HPA axis suppression and atrophied adrenal glands (Morgan *et al.*, 2014). This further proves that the end-results between the two models differ. A limitation to my study is that I did not measure corticosterone concentration throughout the day, only prior to feeding. Therefore, although the CR-fed mice have increased GCs, these concentrations might be altered following feeding. In addition, the conversion of corticosterone to 11-DHC is catalysed by the enzyme 11β-HSD2, and back into corticosterone intracellularly by 11β-HSD1. My results showed an overall genotype decrease in corticosterone-to-11-DHC ratio in the 15- and 10-week-old KO mice, in the BM and circulation. These results are evidently due to the lack of 11β-HSD1. It further suggests either less corticosterone synthesised by the adrenals, or plentiful conversion of corticosterone to 11-DHC by 11β-HSD2. Since the 11β-HSD1 KO mice cannot convert 11-DHC back into corticosterone, it is possible that the adrenals compensate by over-producing corticosterone, which further activates 11β-HSD2 into converting corticosterone to 11-DHC. One way to test this would be to measure the expression and/or activity of 11β-HSD2 within the kidneys.

4.3.3. Future directions

To summarise, this Chapter revealed that 11β-HSD1 KO male mice resist CR-induced BMAT expansion, whereas the KO females did not. Unexpectedly, the KO males also had increased progesterone concentration compared to females and WT males. To investigate the progesterone hypothesis, different experiments could be conducted to reveal whether progesterone impacts BMAT expansion during CR. Firstly, oral progesterone in the drinking water can be administered to KO male mice on CR to

determine if it stops BMAT expansion. In addition, although the CR-fed WT males had increased progesterone concentration, it would be intriguing to further administer them progesterone to test if this would influence BMAT formation with CR.

Secondly, PR antagonists (e.g. Mifepristone (Chabbert-Buffet *et al.*, 2005)) could be administered to KO male mice on CR to determine if this allows BMAT to expand. These experiments would investigate whether progesterone has an impact on CR-induced BMAT expansion. Alternatively, WT and KO female mice can be administered progesterone in the drinking water to see if it would influence BMAT expansion, even when on a normal AL diet. In addition, the expression of the receptors for progesterone and GCs could be quantified, as well as circulating and BM oestradiol concentrations. To further understand the role of GCs on BMAT expansion during CR, it is also possible to investigate the function of progesterone, testosterone, leptin, adiponectin and other hormones *in vitro*. By investigating these hormones in addition to GCs, it might give us more insight into the mechanism that regulates BMAT expansion during basal conditions but also CR. This would be done by challenging WT and KO mice with CR, and after 6 weeks of CR, flush out the tibial BM and examine the proliferation and differentiation of cells into adipocytes and osteoblasts. One can also challenge the differentiated cells with the various hormones like progesterone and examine any genotype and/or diet differences. It would also be possible to do an identical experiment with the remaining flushed out bone, and compare between the BM and bone cells. The BM cells can further be divided into MSCs and haematopoietic cells by magnetic cell sorting using negative selection of CD45, CD31 and Ter119 cells to obtain BM-MSCs. The positive haematopoietic cells can also be examined for comparison and to determine the effects of these hormones on the haematopoietic environment (Tencerova *et al.*, 2018).

In Section 3.3.4 I mentioned several future experiments to further address the role of GCs, and 11β-HSD1, in the effects of CR. For example, during CR it would be informative to measure 11β-HSD1 activity in the BM and in other tissues of interest, to determine if this contributes to increased GC action. Another experiment to further investigate the role of GCs in CR, including the sex differences, would be to perform adrenalectomy. This would completely stop the synthesis of GCs and also of other steroid hormones that are synthesised by the adrenals, such as mineralocorticoids (e.g. aldosterone) and androgens (e.g. testosterone). Furthermore, ovariectomy can

also be performed on female mice, to determine how big of an impact sex hormones have on BMAT expansion during CR. To further apprehend any associations between the sex hormones (progesterone, testosterone), one can also look at the correlations between the hormones (circulatory and BM) and lean/fat mass as well as BMAT.

The long-term six-week vs short-term one-week CR, further discussed in Section 3.3.2, exhibited different results. Therefore, to draw firmer conclusions regarding the effects of CR on GC target genes, an aged-matched cohort of six-week CR, without the fasting/re-feeding prior to termination, would have to performed. However, since we know that GCs are increased within a week of CR, and that BMAT does not increase until four weeks of CR (Cawthorn lab, *unpublished data*), a short-term one-week CR cohort could be done with fasting/re-feeding prior to termination to compared to my current one-week CR mice that were not fasted.

Beyond BMAT expansion, another effect of CR and GC excess is bone loss. Several studies have demonstrated that BMAT expansion leads to bone loss (Shen *et al.*, 2007, 2012; Rharass and Lucas, 2018). Therefore, in the next chapter I present my investigation into the effects of CR and lack of intracellular regeneration of GCs on bone morphology in WT and 11β-HSD1 KO mice.

Chapter 5. 11β-HSD1 KO protects against caloric restriction-induced bone loss in male but not in female mice

5.1. Introduction

The studies in chapter 4 revealed that 11β-HSD1 KO males resist the effects of CR-induced BMAT expansion, whereas females do not. The effects of CR on bone mass have been well examined in rodents (Berrigan *et al.*, 2005; Speakman and Mitchell, 2011), in which CR induces the loss of cortical bone, but maintenance or increased trabecular bone (Hamrick *et al.*, 2008). In contrast, a different publication showed no tibial bone loss after 4 weeks of graded CR (Mitchell *et al.*, 2015). This suggests that the CR protocol can have different end-results on bone morphology.

Increased BMAT often coincides with bone loss, for example in CR, AN, ageing, osteoporosis, GC therapy and oestrogen deficiency. This supports the hypothesis that BMAT expansion might contribute to bone loss during CR and in other conditions. Furthermore, BMAT expansion has also been associated with weakened bone (Schellinger *et al.*, 2001). Patients with AN, have also been diagnosed with bone loss, and consequently higher osteoporosis risk (Schellinger *et al.*, 2004; Legroux-Gérot *et al.*, 2007; Di Iorgi *et al.*, 2008; Bredella *et al.*, 2009; Ecklund *et al.*, 2010; Veldhuis-Vlug and Rosen, 2017, 2018; Muruganandan, Govindarajan and Sinal, 2018). Impaired bone strength at the distal tibia was also discovered in young adults with AN and increased BMAT, once again pointing towards the negative association between bone strength and BMAT (Singhal *et al.*, 2018). Furthermore, GCs can also promote bone loss, as well as increased BMAT (Vande Berg *et al.*, 1999). In addition, circulatory cortisol concentration in patients with AN is associated decreased bone formation (Misra *et al.*, 2004; Lawson *et al.*, 2009). These findings confirm that CR/AN, GC excess and BMAT expansion are typically each associated with bone loss. However, whether GCs promote bone loss in CR, and the involvement of BMAT expansion in this response, remains to be addressed. Nevertheless, one study of male mice shows that a lack of BMAT does not necessarily protect against bone loss

(Keune *et al.*, 2017), while a study in rabbits found that CR-associated bone loss occurred without increasing BMAT (Cawthorn *et al.*, 2016).

Based on my findings in chapter 4, one approach to address this possibility would be through analysing if 11β-HSD1 KO influences CR-induced bone loss. 11β-HSD1 activity in bone was shown to predict the impact of GCs on bone by predicting reduced bone formation markers (Cooper *et al.*, 2003). Furthermore, treatment of primary human osteoblastic cells with cortisol or dexamethasone significantly increased 11β-HSD1 activity (Cooper *et al.*, 2002). This suggests that 11β-HSD1 activity could be an important mediator for predicting GIO, and that it can influence GC action in bone. Past publication investigated the bone phenotype in hypomorphic 11β-HSD1 KO mice during normal conditions and showed that there were no differences between WT and KOs (Justesen *et al.*, 2004). However, these mice were not examined under other conditions similar to CR and/or fasting, and also are not a full 11β-HSD1 KO; thus, whether complete lack of 11β-HSD1 prevents bone loss in CR remains unknown. Moreover, total 11β-HSD1 KO can prevent BMAT expansion in males (Chapter 4), confirming that 11β-HSD1 can impact at least some skeletal effects of CR. More recently, 11β-HSD1 exon 5 KO male mice treated with corticosterone showed almost a complete protection against bone loss compared to WT mice, who had decreased bone volume. However, this study did not include female mice (Fenton *et al.*, 2019). Therefore, based on my results from previous Chapter, and this current finding (Fenton *et al.*, 2019), my hypothesis is that male 11β-HSD1 KO mice, but not females, will resist the effects of CR-induced bone loss. To address this, I studied the effects of CR on bone microarchitecture in AL-and CR-fed WT and 11β-HSD1 KO male and female mice. Trabecular and cortical bone parameters were analysed to determine the effects of CR on bone morphology.

5.2. Results

5.2.1. Trabecular bone is maintained with CR in males but increased in females

To test if deficiency of 11β-HSD1 prevents CR-induced bone loss, I first used μCT to measure trabecular and cortical microarchitecture in the tibiae of WT and KO mice after six weeks of AL or CR diet.

Figure 5.1 shows representative cross sections of the proximal tibial metaphysis (Figure 5.1.A) and graphs of key trabecular parameters (Figure 5.1.B-E), as recommended in previous guidelines (Bouxsein *et al.*, 2010). ANOVA showed a significant effect of CR in trabecular bone volume (BV/TV) in females, but not males, and this was unaffected by genotype (Figure 5.1.B). A similar diet effect was observed for trabecular number by ANOVA, with significant increases in CR-fed WT and KO females (Figure 5.1.D). However, no significant differences were detected for the other parameters in females, nor for any of these parameters in males.

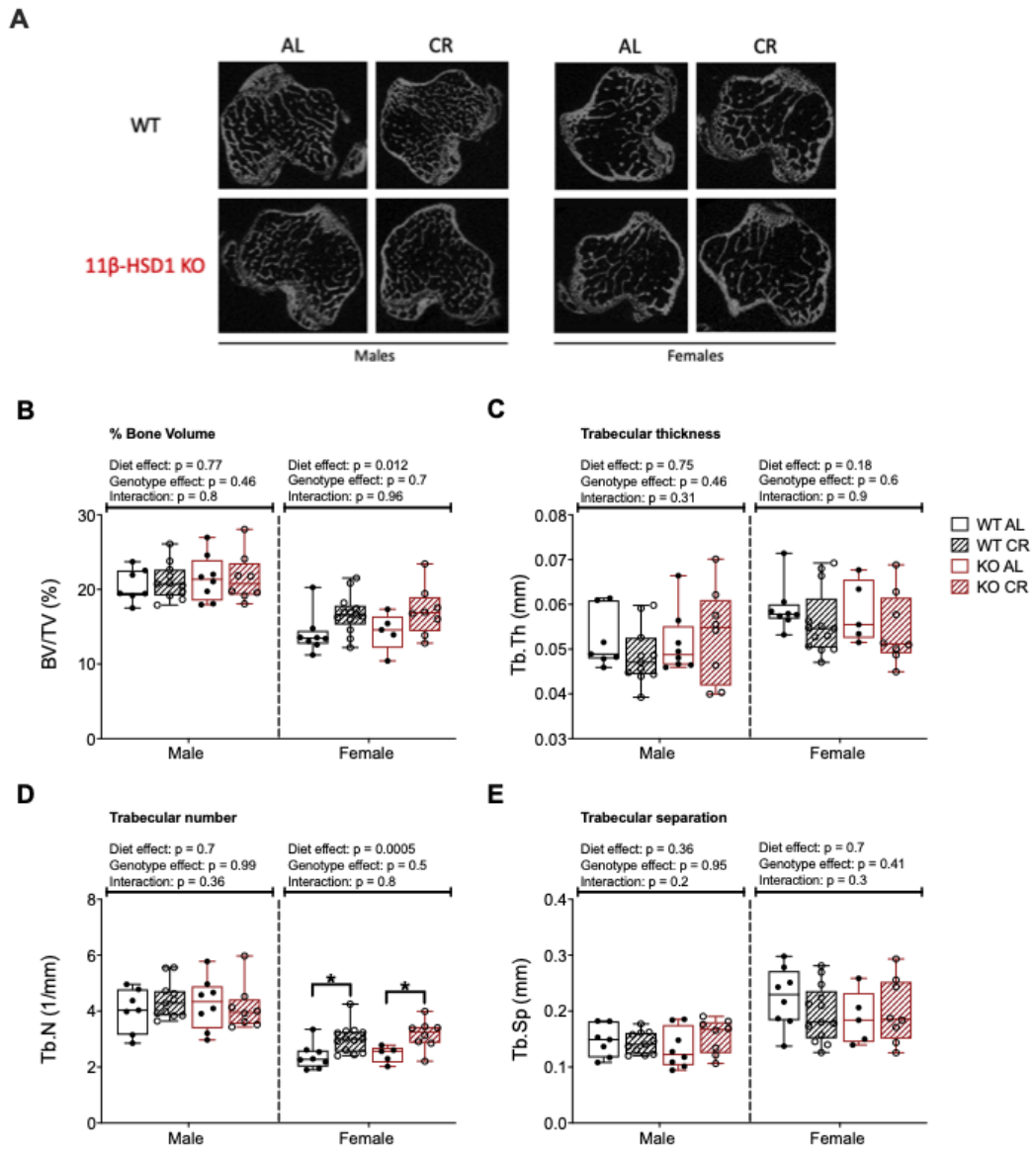

Figure 5.1. Female mice on CR have increased trabecular mass. C57BL/6JOlaHsd (WT, black) and 11β-HSD1 KO (KO, red) male and female mice were fed *ad libitum* (AL, closed symbols, solid line) or 70% of *ad libitum* food intake (CR, open symbols, dotted line) for six weeks, from 9 weeks until 15 weeks of age. The evening prior to dissections, all mice were fasted/re-fed as described in Methods (2.3.1). The AL fed mice had their food removed, and were given half a portion of the 70% of food that they were daily consuming (1.5g). The CR fed mice were also given half a portion (1.05g) of their 30% CR diet. Post termination, bones were fixated in 10% formaldehyde for seven days. Tibiae were then embedded in layers in 1% agarose in a universal tube, followed by being scanned at 6μm by uCT and analysed by CTan. **(A)** Representative 2D images of μCT horizontal trabecular bone section, with the white being the trabecular bone. **(B)** Bone volume fraction (%) (BV/TV). **(C)** Trabecular thickness (mm) (Tb.Th). **(D)** Trabecular number (1/mm) (Tb.N). **(E)** Trabecular separation (mm) (Tr.S). Data points are presented with median, interquartile range and range shown by box and whisker plot, and were analysed by 2-Way ANOVA with Sidak's multiple comparison test. n (WT AL male) = 7. n (WT CR male) = 11. n (KO AL male) = 8. n (KO CR male) = 8. n (WT AL female) = 8. n (WT CR female) = 13. n (KO AL female) = 5. n (KO CR female) = 8. *: $p<0.05$.

5.2.2. CR-fed female mice have decreased cortical bone compared to males

Previous studies have shown that, in mice, CR causes loss of cortical bone but not trabecular bone (Hamrick *et al.*, 2008). Therefore, I next analysed tibial cortical bone parameters. Representative images of the cortical bone from each group are shown in figure 5.2.A, while the key variables to report when describing cortical bone morphology, as recommended in previous guidelines (Bouxsein *et al.*, 2010), are shown in Figure 5.2.B-E.

ANOVA showed an overall genotype effect for cortical bone area (Ct.Ar) in males (Figure 5.2.B), with the KOs having increased bone area compared to the WTs. Furthermore, ANOVA also showed a genotype effect between the CR-fed males, with the KO males having an increase in cortical bone area compared to the WTs, although insignificantly ($p=0.0629$). This suggests a potential resistance to bone loss. In contrast, the females genotype did not influence Ct.Ar but an overall diet effect was detected, with the CR-fed females having significantly lower Ct.Ar than the AL-fed females. In addition, ANOVA detected that CR significantly decreased cortical area fraction in females (5.2.D), with multiple comparisons further showing a significant difference between the AL- and CR-fed WT females. However, no significant effects of diet or genotype were detected for cortical area fraction in males (Figure 5.2.D), or for the remaining cortical parameters in either sex of mice (Figure 5.2.C, E).

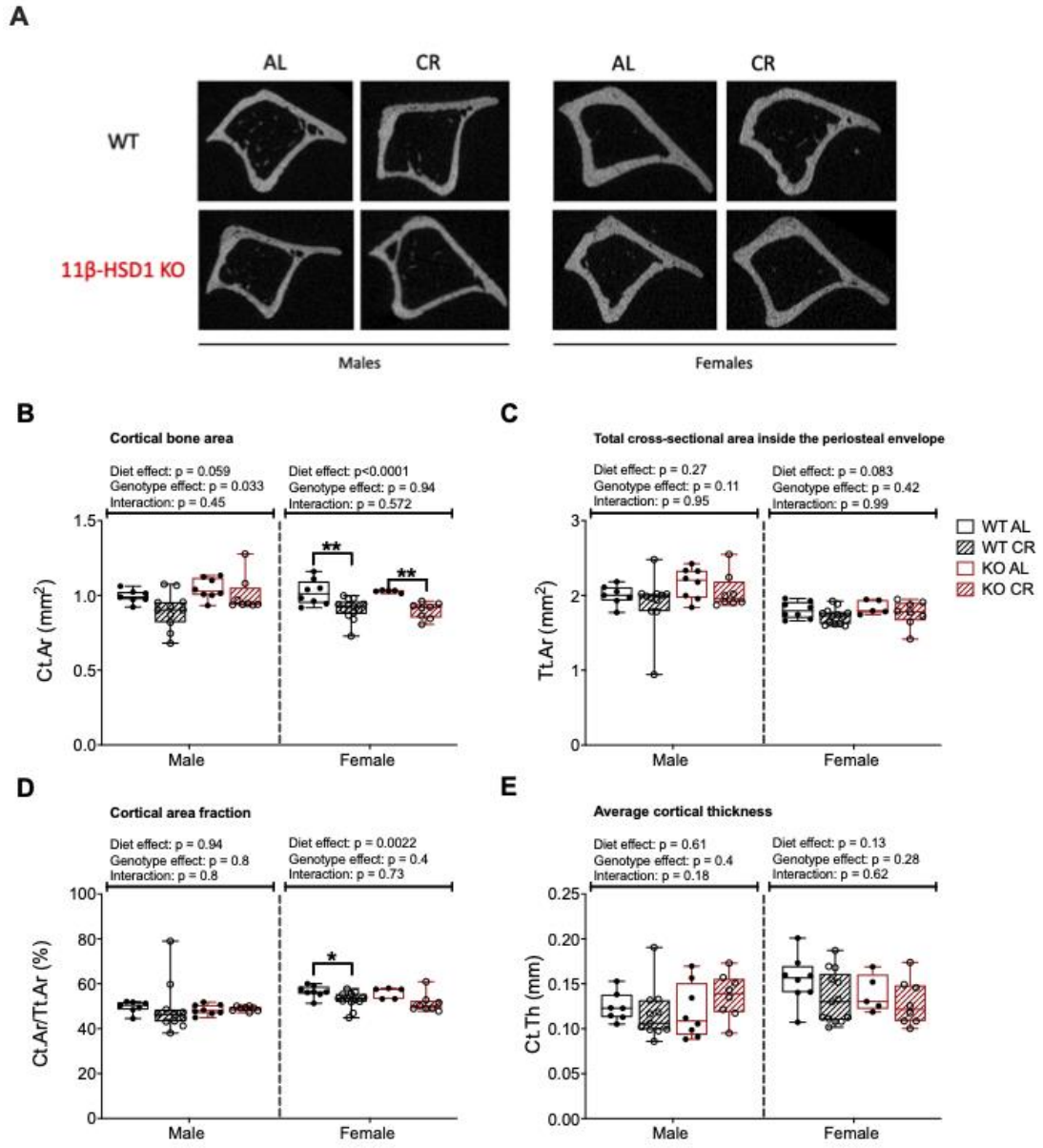

Figure 5.2. Cortical bone area is maintained with CR in 11β-HSD1 KO males. WT and 11β-HSD1 KO male and female mice were fed AL or CR diets and fasted/re-fed as described for Figure 5.1 and in Methods (2.3.1). Tibiae were scanned by μCT as described in Figure 5.1 and in Methods (2.7)**. (A)** Representative 2D images of μCT horizontal cortical bone section, with the white being the cortical bone. **(B)** Cortical bone area (mm_2) (Ct.Ar). **(C)** Total cross-sectional area inside the periosteal envelope (mm_2) (Tt.Ar). **(D)** Cortical area fraction (%) (Ct.Ar/Tt.Ar) **(E)** Average cortical thickness (mm) (Ct.Th). Data points are presented with median, interquartile range and range shown by box and whisker plot, and were analysed by 2-Way ANOVA with Sidak's multiple comparison test. Numbers of mice per group, and presentation of statistically significant differences between groups, are as described for figure 5.1. *: p<0.05. **: p<0.01.

5.2.3. CR is associated with decreased tibial *Bglap* expression

The bone morphology results revealed that, during CR, trabecular bone was maintained or increased. However, while cortical bone was lost in CR-fed females and WT males, 11β-HSD1 KO males resist it (Figure 5.2.B). Since the p value between CR-fed WT and KO males was just below significant (p=0.0629), I next wanted to further examine bone remodelling at a molecular level. To do so I used qPCR to examine the transcript level of *Bglap* (osteocalcin), which is used as a molecular marker of bone formation (Ducy *et al.*, 1996; Zoch, Clemens and Riddle, 2016) in tibial bone.

As shown in Figure 5.5, an overall diet effect was detected by ANOVA for both males and females, with decreased *Bglap* expression for the CR-fed mice. Multiple comparison was further used to assess diet effects within each genotype (and vice versa), confirming that CR significantly decreased *Bglap* expression in WT males and KO females. In addition, a diet x genotype interaction was detected for the females, revealing that the effect of CR was greater in the KO than in WT females. However, no genotype difference was detected by ANOVA for the males, suggesting that the KO males are similarly susceptible to bone loss as the WTs.

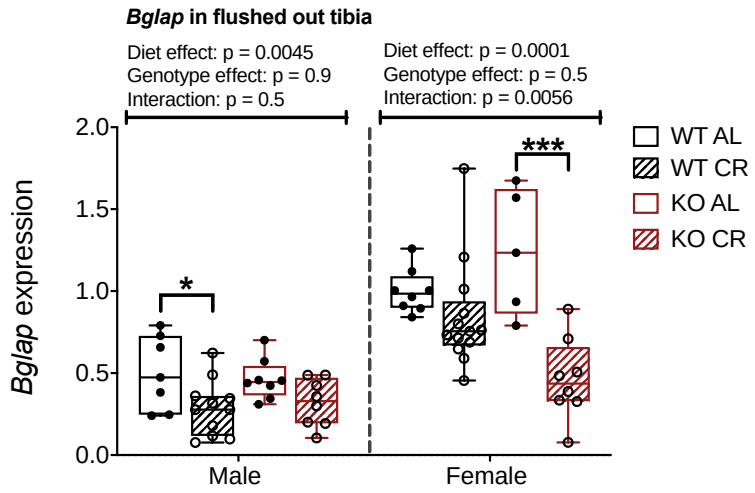

Figure 5.3. Bone formation marker, *Bglap*, is decreased with CR. WT and 11β-HSD1 KO male and female mice were fed AL or CR diets and fasted/re-fed as described for Figure 5.1 and in Methods (2.3.1). Post termination, the tibiae were snap-frozen on dry ice, followed by BM isolation, RNA extraction and reverse transcription to cDNA. qPCR was performed to quantify expression of *Bglap*. *Bglap* was normalised to geomean of the following housekeeping genes: *Ppia*, *Tbp* and *Actb*, and presented as relative to the WT AL average of male and female mice together. Data points are presented with median, interquartile range and range shown by box and whisker plot, and were analysed by 2-Way ANOVA with Sidak's multiple comparison test. Data points are presented with median, interquartile range and range shown by box and whisker plot, and were analysed by 2-Way ANOVA with Sidak's multiple comparison test. n (WT AL male) = 7. n (WT CR male) = 11. n (KO AL male) = 8. n (KO CR male) = 8. n (WT AL female) = 8. n (WT CR female) = 13. n (KO AL female) = 5. n (KO CR female) = 8. *: $p<0.05$. ***: $p<0.001$.

5.2.4. CR and 11β-HSD1 deficiency are not associated with changes in tibial GC action

In chapters 3 and 4 I found that both circulatory and BM corticosterone concentrations are increased during CR. Therefore, I next addressed if CR alters GC action within the bone tissue, after removal of the BM. Due to time constraints I could not measure GC concentrations within these bone samples. Instead, GC target genes were examined to determine the effects of CR and 11β-HSD1 KO on GC action within bone. I first analysed *Hsd11b1* expression as this was found to be a possible marker of increased GC action in WAT and BM. Nonetheless, no diet differences were detected between the WT mice, while expression in the KOs was non-detectable, as predicted (Figure 5.4).

To further investigate if GC action in bone is altered with CR, additional GC targets were examined. Figure 5.5 shows the expression of *Fkbp5* (Figure 5.5.A), *Gilz* (Figure 5.5.B) and *Per* (Figure 5.5.C). ANVOA detected an overall tendency for CR to decrease *Fkbp5* in females ($p=0.053$) and to increase *Per1* in males ($p=0.055$). However, no significant diet or genotype differences were detected by ANOVA for any of the genes, indicating that neither CR nor 11β-HSD1 KO exerts robust effects on GC target gene expression within tibial bone.

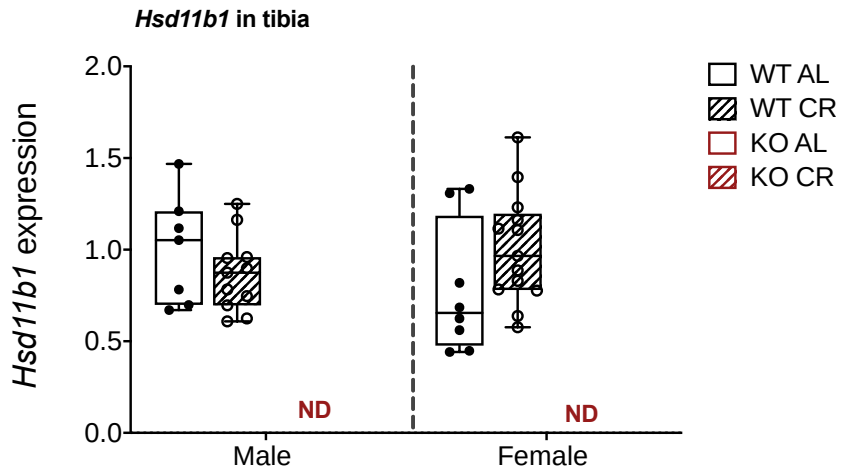

Figure 5.4. Tibial *Hsd11b1* expression is not increased with CR. WT and 11β-HSD1 KO male and female mice were fed AL or CR diets and fasted/re-fed as described for Figure 5.1 and in Methods. Post termination, the tibiae were snap-frozen on dry ice, followed by BM isolation, RNA extraction and reverse transcription to cDNA. qPCR was performed to quantify expression of *Hsd11b1*. *Hsd11b1* was normalised to geomean of the following housekeeping genes: *Ppia*, *Tbp* and *Actb*, and presented as relative to the WT AL average of male and female mice together. Data points are presented with median, interquartile range and range shown by box and whisker plot, and were analysed by Mann-Whitney (males) and Welch's (females) test. Numbers of mice per group, and presentation of statistically significant differences between groups, are as described for figure 5.3.

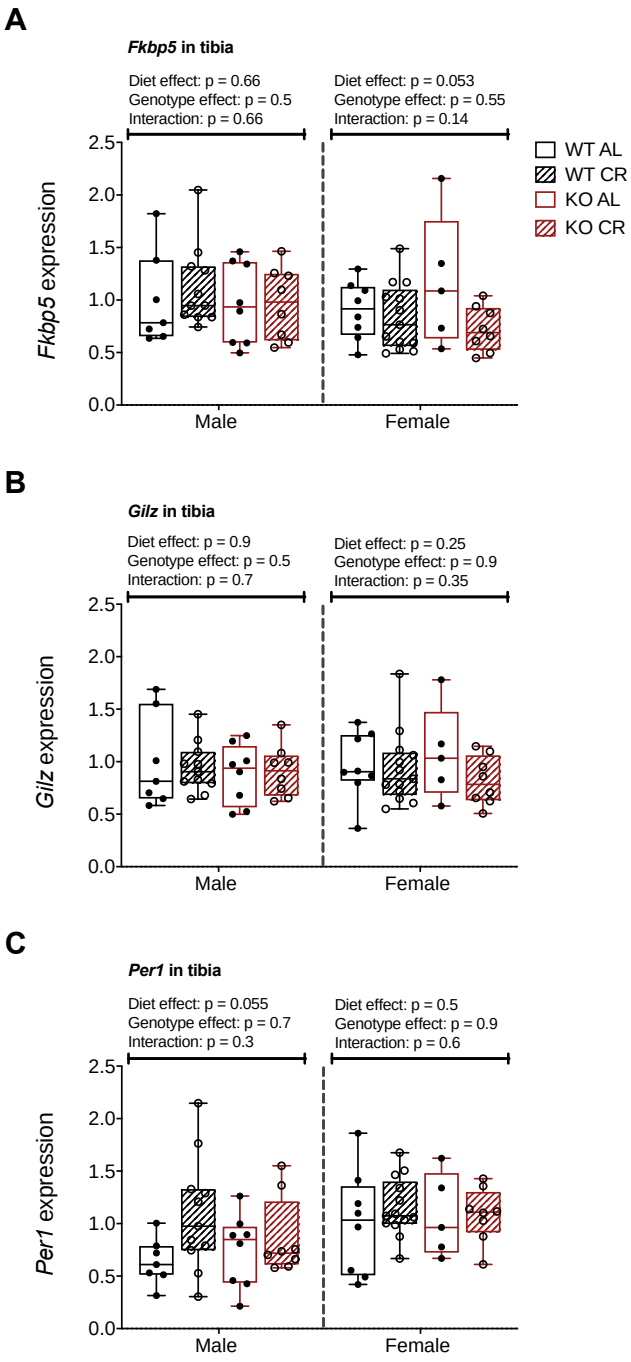

Figure 5.5. Tibial GC target genes are not modified with CR. WT and 11β-HSD1 KO male and female mice were fed AL or CR diets and fasted/re-fed as described for Figure 5.1 and in Methods. Post termination, the tibiae were snap-frozen on dry ice, followed by BM isolation, RNA extraction and reverse transcription to cDNA. qPCR was performed to quantify expression of *Fkbp5, Gilz* and *Per1*. The genes were normalised to geomean of the following housekeeping genes: *Ppia*, *Tbp* and *Actb*, and presented as relative to the WT AL average of male and female mice together. *Fkbp5* **(A)**, *Gilz* **(B)** and *Per1* **(C)** expression. Data points are presented with median, interquartile range and range shown by box and whisker plot, and were analysed by 2-Way ANOVA with Sidak's multiple comparison test. Numbers of mice per group, and presentation of statistically significant differences between groups, are as described for figure 5.3.

5.3. Discussion

5.3.1. Effects of CR and 11β-HSD1 on bone

The effects of CR on decrease bone mass have previously been demonstrated in animals (Baek *et al.*, 2008; Hamrick *et al.*, 2008; Devlin *et al.*, 2010; Speakman and Mitchell, 2011; Behrendt *et al.*, 2016; Cawthorn *et al.*, 2016). In addition, one of the publications showed maintenance of trabecular, but loss of cortical bone mass with CR (Hamrick *et al.*, 2008), similarly to my results in this chapter. However, a different publication showed no bone loss with CR in mice (Mitchell *et al.*, 2015). Moreover, decreased bone mass without BMAT expansion was found in rabbits on CR (Cawthorn *et al.*, 2016). The variety in the end-results from these studies could be due to duration and percentage of CR, as well as the species. Overall, it suggests that CR can have diverse effects on bone morphology, where BMAT expansion is not always increased. However, my findings in this chapter, where the CR-fed KO males resisted BMAT expansion and minor cortical bone loss, it suggests that bone loss might be necessary for BMAT expansion, or vice versa. Nevertheless, that is not always the case as bone loss and BMAT expansion do not always coincide, as previously published; bone loss without changes in BMAT volume (Gokalp *et al.*, 2011; Devlin and Rosen, 2015; Cawthorn *et al.*, 2016; Keune *et al.*, 2017) and/or altered BMAT without bone loss or with increased bone mass (Schellinger *et al.*, 2004; Doucette *et al.*, 2015; Iwaniec *et al.*, 2016; Sheu *et al.*, 2017; Yu *et al.*, 2017). However, for my findings, GC excess might be necessary for the CR-induced BMAT expansion and bone loss. As presented in previous chapter, BM corticosterone concentration in the CR-fed KO males was not increased as in the WTs (Figure 4.11.B). The females and WT males all had increased corticosterone concentration in the BM and circulation, as well as increased BMAT and bone loss. This suggests that an increase in BM corticosterone concentration is necessary for BMAT expansion and more bone loss with CR. It also suggests that the KO males are resistant to circulatory GCs, whereas, the KO females are not. Instead, other hormones could be involved in the regulation of BMAT expansion and bone loss with CR in females, as previously discussed in Chapter 4, section 4.3. One of those hormones could be oestrogen (already discussed in Chapter 3 and 4) and/or leptin. Leptin decreases with CR (Devlin *et al.*, 2010; Cawthorn *et al.*, 2016), suggesting that hypoleptinemia could be involved in the formation of BMAT and bone loss. However, treating CR-fed mice

with leptin did not improve bone formation, but it did blunt BMAT expansion (Devlin *et al.*, 2016). Leptin concentration was not measured in my study; however, it would be informative to measure it and test if the circulatory concentration varies between the genotypes on CR. I would expect all CR-fed mice to have decreased concentrations, however, the concentration of leptin in the KO males might not be decreased. Since leptin treatment blunts BMAT expansion (Devlin *et al.*, 2016), perhaps it also protects against bone loss, or at least reduces the effect of CR in the KO males. However, the effect of leptin on bone have been contradicting. Some publications found that leptin deficient mice had increased bone mass (Amling, Takeda and Karsenty, 2000; Ducy *et al.*, 2000; Karsenty, 2001), whilst others found decreased bone mass (Lorentzon, Alehagen and Boquist, 1986; Steppan *et al.*, 2000) compared to controls. A different publication found that the effect of leptin differs throughout the skeleton, with decreased cortical thickness and trabecular volume in the femur, but increased density and trabecular bone volume in the lumbar spine (Hamrick *et al.*, 2004). Overall, this is a complex topic that needs further researching. Furthermore, when quantifying for bone morphology, it would be informative to also measure BMAT volume, as bone loss/formation does not always coincide with BMAT expansion as previously mentioned.

In addition, *Bglap* expression was decreased with CR in WT males and KO females, whereas no diet differences were detected for KO males and WT females. Osteocalcin is restricted to the osteoblast lineage (Lian *et al.*, 1998), therefore, the *Bglap* expression in Figure 5.3 might just hint towards a decrease in osteoblast differentiation rather than absolute bone loss. Furthermore, GCs can also inhibit osteocalcin in osteoblasts, which might enhance GIO (Leclerc *et al.*, 2005; Rauch *et al.*, 2010). However, other genes associated with bone formation would be informative to include, such as collagen type 1 (*Col1a1*) and Runt-related transcription factor 2 (*Runx2)* and additional *in vitro* experiments. Interestingly, trabecular bone was not only maintained, but trabecular bone volume (Figure 5.1.B) and number (Figure 5.1.D) were significantly increased in females only. Trabecular bone volume and number were increased in the females, but no changes were detected for trabecular spacing. This might be offset by trends towards a decrease in trabecular thickness. However, more numbers might be needed to actually determine if there is a significance or not. In addition, the time frame for measuring bone morphology at 6 weeks of CR might not be enough to induce more significant bone loss as the levels

of GCs are not as excessive as when orally administrating it (Morgan *et al.*, 2014; Fenton *et al.*, 2019). In comparison to my results, Hamrick et al., found increased vertebral trabecular bone volume, albeit in male mice (Hamrick *et al.*, 2008). The CR experimental method did however differ between the studies. I performed 30% CR for six weeks, whereas Hamrick performed CR for a total of ten weeks, with increased restriction starting on 10% and ending on 40%. Overall, my results show a similarity to previous findings by Hamrick et al., and since 11β-HSD1 KO mice have not been put on CR until now, it indicates that the KO males might resist CR effects. This possibility is also consistent with the key finding from Chapter 4, that the KO males resist CR-induced BMAT expansion. However, to be more certain regarding the resistance effects of 11β-HSD1 KO males during CR, it would be informative to add more numbers to the groups, and potentially testing a more extreme CR, for example longer duration and/or greater percentage decrease in food intake. Altogether, these findings suggest that 11β-HSD1 activity does regulate BMAT and possibly bone formation with CR.

In contrast to the bone analysis and *Bglap* expression, my results show that CR does not significantly affect expression of GC target genes in bone. Here, it is once again worth highlighting that these 15-week-old mice were fasted/re-fed prior to termination, which might have blunted the end-term results of CR on gene expression. Indeed, this effect was evident for transcript expression within the BM (Figure 4.12). To overcome this, it would be interesting to analyse the bones from the short-term CR and AL mice, which did not undergo the fasting/re-feeding regimen prior to the endpoint. In addition, to further understand how GCs in bone are affected by CR in WT and KO mice, measuring GC concentrations by LC-MS/MS would be beneficial. This would give us a broader idea on how bone-specific GC concentration correlates with BM and plasma GC concentration.

The skeletal effects of CR in humans are also becoming better understood. Although CR can promote healthy ageing, it was revealed that it comes at a cost of bone loss in sites of where osteoporotic fractures are commonly found (Villareal *et al.*, 2016). This was investigated in a two-year clinical trial, where the effects of CR on bone in non-obese young adults were examined. On the other hand, to prevent bone loss at sites of osteoporotic fractures, it was shown that exercise-induced weight loss is a better option than CR as it preserves BMD (Villareal *et al.*, 2006). This suggests that

eating a healthy diet, in addition to exercise, might be a better option to evade the side-effects of CR on bone. My CR mice, regardless of genotype, were more active than the AL-fed mice. However, it is yet to be researched if 11β-HSD1 KO mice maintain bone mass if put on daily exercise instead of CR. Although the bone loss was not major, based on the previous mentioned publication showing that exercise is better to maintain bone, it would be expected for these KOs to maintain bone mass. Moreover, examining how adipocyte and osteocyte differentiation in bone/BM varies in CR, and especially in 11β-HSD1 KO mice, would be favourable to further understand the role of 11β-HSD1 and BMAT expansion/bone loss. A previous publication examined the BM in the distal femur and proximal tibia in adolescent girls with AN (Ecklund *et al.*, 2010). The MRI scans showed that girls with AN have decreased red marrow compared to controls, suggesting premature conversion of red marrow to adipocytes. The adipocyte expansion could have hindered osteoblast differentiation, resulting in increased BMAT and bone loss. It is possible that these findings could equally mirror what is happening during CR.

Further work on CR also needs to be conducted on a molecular level to understand the pathway(s) that leads to BMAT expansion and bone loss. Although, primary osteoblast can respond to corticosterone (Bellows, Ciaccia and Heersche, 1998), confirming that bone can directly respond to GCs. It has also been published that 11β-HSD1 activity in osteoblastis increased by GCs (Cooper *et al.*, 2001). This further confirms the role of 11β-HSD1 in bone. While no research has been conducted on 11β-HSD1 KO mice during CR, bone morphology was analysed on the hypomorphic KOs during normal conditions. It was found that no differences were detected between the WT and hypomorphic KOs with regards to bone morphology (Justesen *et al.*, 2004). Compared to my AL-fed WT and KO mice, my results further confirm Justesen *et al.,* findings, although the KO models differ. However, my study is more consistent between the groups of mice as I quantified bone morphology on 15-week-old mice in all groups, whereas, Justesen *et al.,* studied bone in male mice at ~4 months and at ~20 months of age, and in females at 7.5-11 months and ~20 months of age (Justesen *et al.*, 2004). The difference in age could affect the end-results of the hypomorphic KOs. Moreover, they also reported the lack of BMAT in these KOs, which I have proved otherwise. Thus, more research has to be conducted to determine the effects of 11β-HSD1 on bone, especially with CR.

5.3.4. Future directions

Due to time constraints, GC target genes were not examined in the bones from the 10-week-CR cohorts. Similarly, the femurs from the 15-week-old CR were not optimised for LC-MS/MS quantification. For future analysis, these two experiments could be performed to compare results between the bone, BM and plasma.

Static and dynamic histomorphometry could be performed to assess rates of bone formation and possibly resorption. Together, it would allow the quantification of bone cells (osteoblast and osteoclasts) as well as bone formation rates. Furthermore, a new three-dimensional approach to measure bone remodelling has been published (Slyfield *et al.*, 2012). Compared to the traditional histomorphometry, this new approach can also measure the number and size of individual resorption cavities and bone forming sites. However, it is important to notice that there are limitations to this new approach, hence it cannot be assumed it is flawless. For example, osteoclasts are not visualised, hence resorption cavities are identified based on surface irregularities. The serum markers for bone formation and resorption, Propeptides of type 1 collagen (P1NP) and C-terminal telopeptide (CTX-1) respectively, have been proposed to be used as reference markers (Vasikaran *et al.*, 2011). In addition to P1NP, other common bone formation markers are alkaline phosphatase (ALP) and osteocalcin. ALP is an enzyme in osteoblast membranes and it is important for bone mineralisation, hence it can be measured as a marker of mineralisation (Shetty *et al.*, 2016). Osteocalcin is synthesised by osteoblast, and it can be quantified by an ELISA in mouse serum and also from cell culture supernatants (Ferron, Wei, Yoshizawa, Ducy, *et al.*, 2010). Besides CTX-1, different bone resorption markers include TRAP and Cathepsin K. They are both expressed by osteoclasts. TRAP is increased during for example osteoporosis, and Cathepsin K is secreted during active bone resorption (Shetty *et al.*, 2016).

Although there might be an association between the effect of CR and GCs on bone, there is no experimental data in this study that can confirm it. Therefore, correlations between bone, BMAT and GCs and further *in vitro* experiments would be of interest and necessary to establish these associations. *In vitro* work would answer further questions regarding the cortical bone loss and trabecular maintenance/increase, for example to isolate and differentiate BMSCs. Osteogenic cells can be compared to adipose-derived cells, especially from mice on CR. Moreover, colony-forming unit

(CFU) assays to measure how many progenitors are present and viable to proliferate in a given population of cells. Hence, primary cells would be preferred instead of cell lines, to have the option to study bone cells from genetically altered mice. Additionally, cells from AL mice can be treated with dexamethasone and compared between genotypes. The increase in corticosterone in females and WT males, but not KO males, might also indicate that the loss in cortical bone might be affected due to GCs enhancing osteoclast differentiation and regulation of RANK and osteoprotegerin (Swanson *et al.*, 2006; He *et al.*, 2016). This is something that could be further investigated if the aim is to determine if CR-induced bone loss is induced by an increase in osteoclasts or a decrease in osteoblasts. RANKL and osteoprotegerin can be measured by ELISA in whole bone (Swanson *et al.*, 2006).

To summarise this chapter, trabecular bone mass was maintained, whereas, cortical bone mass was lost with CR in all mice, but less so in the CR-fed KO males. Since the cortical results are not as robust as with the BMAT volume, more numbers could be added to the groups to see if it gives more robust effects. There is no evidence that CR increases GC action in bones, or that the KOs resist this. However, the end-results could be affected by the fasting/re-feeding protocol. Overall, this suggest the following; that the KOs do not resist the effects of CR on bone, although it seems like the KO males could resist cortical bone loss but not robustly, or that GCs might not be involved in bones loss during CR. The findings between BMAT and cortical bone mass in the CR-fed KO males suggest that BMAT expansion is not necessary for cortical bone loss, even if it is minor. However, if more mice were added to the groups, and it would show a clear resistance in bone loss in the KO males, it would be informative to measure GC concentrations in the bone to investigate if they are involved in the resistance, meaning decreased concentration in the KOs, and increased in the WTs. On the other hand, if the CR-fed KO males showed a clearer decrease in cortical bone, it would suggest that they do not resist the effects of CR on bone mass, but instead they resist CR-induced BMAT expansion. Previous research has showed that BMAT expansion and bone loss are not always associated, and this KO model would further add to it. Once again, measuring bone GC concentration would be informative to determine how/if big of a role GCs play a role here and to compare with BM GC concentration. Another option could be that these 11β-HSD1 KOs are not a suitable model to address this hypothesis. Like previously mentioned, I think that the osteoblast specific GR KO model would be a more suitable model (Rauch *et al.*, 2010) since the KOs resisted the effects of GC excess.

Beyond CR, ageing also increases circulating GC concentrations. Furthermore, several studies have demonstrated that BMAT and bone loss also increase with ageing. To determine if 11β-HSD1 KO mice have blunted BMAT expansion and bone loss with ageing, in my next chapter I investigated the effects of ageing on bone in WT and 11β-HSD1 KO mice.

Chapter 6. Ageing-related corticosterone and bone marrow adiposity expansion are associated with bone loss in WT and 11β-HSD1 deficient mice

6.1. Introduction

My results from the previous chapters revealed that CR-fed 11β-HSD1 KO females do not resist CR-induced BMAT expansion, whereas KO males do. Moreover, for WT males and for females of each genotype, CR increased circulatory and BM corticosterone concentration. Cortical bone loss was evident in females (both genotypes) but CR-fed KO males resisted the cortical bone loss compared to WT males. These results suggest that, in KO males only, resistance to increased circulatory and BM corticosterone may then limit BMAT expansion and bone loss during CR. This raises the possibility that deficiency of 11β-HSD1 might also influence bone loss and BMAT expansion in other conditions of GC excess. One such condition, of great relevance to public health, is ageing. It is well established that ageing is associated with GC excess (Purnell *et al.*, 2004), BMAT expansion and bone loss (Ambrosi *et al.*, 2017), which can result in osteoporosis. Ageing-related osteoporosis is a major public health burden and therefore understanding the mechanism behind it could reveal new therapeutic strategies of benefit to human health.

Age-related osteoporosis is often associated with increased BMAT, including increased number and size of BMAds. This increase in BMAT is inversely correlated with trabecular bone volume (Justesen *et al.*, 2001). Furthermore, vertebral cortical bone loss also occurs with ageing, but this is predominantly observed in women rather than men (Chen *et al.*, 2010; Christiansen *et al.*, 2011). In addition to bone morphology, BMAT accumulation is also sex-dependent with ageing. Thus, in males BMAT increases with age at a gradual and consistent rate, whereas in females BMAT more rapidly accumulates between 55 and 65 years of age. Consequently, above 60 years of age females have increased BMAT volume compared to age-matched males (Griffith *et al.*, 2012; Roldan-Valadez *et al.*, 2013). Perhaps unsurprisingly, this age-associated BMAT expansion in females is associated with menopause and decreased

oestrogen. Oestrogen directly decreases BMAT (Limonard *et al.*, 2015); hence, as oestrogen concentration decreases during menopause, BMAT expands.

Based on these findings, one hypothesis that has attracted a relatively large amount of interest is that BMAT contributes to age-related bone loss (Devlin and Rosen, 2015; Veldhuis-Vlug and Rosen, 2018). Given that ageing is also associated with GC excess (Purnell *et al.*, 2004), in the present chapter I investigated the hypothesis that that age-related increases in GC action drive age-associated BMAT expansion and bone loss. Justesen *et al.,* analysed bone morphology in male and female WT and hypomorphic 11β-HSD1 KO mice (Justesen *et al.*, 2004). Here, bone morphology was studied in male mice at ~4 months and at ~20 months of age, and in females at 7.5-11 months and ~20 months of age (Justesen *et al.*, 2004). Age-induced bone loss was evident in both genotypes, with similar bone formation and resorption parameters, but no differences were observed between the genotypes. They also showed that young 11β-HSD1 KO males lacked BMAds, which were present in age-matched WTs. However, there are several limitations to their study: BMAT was not analysed in the older mice; the 'young' mice (~4-months for males, and 7.5-11 months for females) were not particularly young; the ages of the 'young' and 'old' mice differ between the sexes; and the KO model used is hypomorphic, rather than a complete KO. These limitations are likely to confound the BMAT and bone phenotype results. Indeed, Justesen *et al.,* concluded that the young KO male mice lack BMAT, whereas my results have shown that BMAT development is normal in young, AL-fed KO mice. Furthermore, another independent study confirms that BMAds are present in the hypomorphic 11β-HSD1 KO mice (Coutinho *et al.*, 2012). However, the effect of 11β-HSD1 KO on age-related BMAT expansion or bone loss has not been tested using the null 11β-HSD1 KO mice. Thus, to determine whether age-related increases of GCs drive age-associated BMAT expansion and bone loss, I examined bone morphology and BMAT in 42-and 70-week-old WT and 11β-HSD1 KO mice. The reason for using 42-and 70-week-old mice, rather than much older mice, is due to tumour formation and additional health issues that arise beyond 18 months of age. This has been observed in WT and 11β-HSD1 KO mice, and also in other transgenic models in our group; hence, it is independent of genotype. Therefore, the concern with using much older mice is that it would introduce confounding pathological effects, which I wanted to avoid. The practical work in this chapter was completed with assistance from two undergraduate students. The first student, Iris Pruñonosa, contributed to this chapter by examining 42-week-old and 70-week-old female mice

(first cohorts, designated as 42.1 and 70.1, respectively). The second student, Rachel Bell, continued the work by further examining 42-week-old male and female mice. I co-supervised both students and continued the research by adding to the numbers of the 42-week-old mice (second cohort, referred to as 42.2) and also including a new cohort of 70-week-old mice (referred to as 70.2). Mice in cohort 1 (42.1 and 70.1) were analysed separately to mice in cohort 2 (42.2 and 70.2) because, in the first cohort, all of the WTs were in one cage and all of the KOs were in a separate cage, and therefore any genotype effect may simply have resulted from cage effects. In contrast, in the second cohort the genotypes were mixed together among the various cages (Summarised in Table 6.1). Therefore, to determine if their housing had an impact on age-related body weight gain, fat mass, BMAT expansion and bone loss, the cohorts were examined separately but they are presented alongside each other to aid in the comparison and interpretation of these results.

	Control cohort	**Cohort 1**		**Cohort 2**	
	15	**42.1**	**70.1**	**42.2**	**70.2**
Number of mice	15 WT and 13 KO	4 WT and 3 KO	3 WT and 4 KO	13 WT and 13 KO	12 WT and 17 KO
Sex of aged mice	Mixed.	All females.		Mixed.	
Cage set up	Single housed.	Genotypes were separated: WT and KO in separated cages.		Genotypes were mixed in cages.	
Body mass	Yes	Yes	Yes	Yes	Yes
TD-NMR measurements	Yes	Yes	No	Yes	Yes
Adipose depots mass	Yes	Yes	Yes	Yes	Yes
Adrenal glands mass	Yes	Yes	No	Yes	Yes
Corticosterone ELISA	Yes	Yes	Yes	Yes	Yes
BMAT analysis	Yes	Yes	Yes	Yes	No
Bone analysis	Yes	Yes	Yes	Yes	No

Table 6.1. Experimental set up for Chapter 6 of the older Cohort 1 and 2, including control.

6.2. Results

6.2.1. 11β-HSD1 KO influences ageing-associated increases in body mass

Before characterising the effects of the 11β-HSD1 KO on age-related GC excess, bone loss and BMAT expansion, I first addressed if lack of 11β-HSD1 influences the increases in body mass and changes in body composition that occur with ageing. The rationale for this was two-fold. Firstly, it is unclear if ageing-related increases in body mass or development of obesity are influenced by GC excess or are altered in the null 11β-HSD1 KO mice. Secondly, weight gain and obesity, as well as GCs, can influence BMAT and bone architecture; hence, if the former are influenced by 11β-HSD1 KO then this might contribute to any skeletal phenotypes observed.

Cohort one comprised females only, whereas cohort two included both males and females. At necropsy the KO mice differed in size to their WT counterparts, but this effect was strikingly different between the two cohorts. Thus, for cohort one the KOs were much smaller than WTs, whereas in cohort two the opposite phenotype was apparent. This was confirmed by the body masses of the mice (Figure 6.1). A significant age effect was detected by 2-way ANOVA, with the 70-week-old mice having a consistent increase in body weight compared to the 15-week-old (control) mice. The KO females also showed a decrease in body weight gain at 70-weeks of age compared to the WTs in the first cohort only (Figure 6.1.A). Figure 6.1.B shows the body weight of the second cohort of 42 and 70-week-old mice, male and female, compared to control mice. A significant age effect was detected by 3-Way ANOVA, with both male and female mice having increased body weight with ageing. A clear sex effect was similarly detected, with the male mice being heavier. The 70-week-old KO female mice from the second cohort (70.2) showed a minor trend for being heavier compared to the WT, although this was not statistically significant ((p=0.27) Figure 6.1.B). The first cohort (70.1), showed the opposite result. This striking difference between the cohorts suggests that cage effects may have contributed to the phenotype, because for cohort 1 the WT and KO mice were housed in separate cages throughout. Therefore, the remainder of the results in this chapter will be presented as two separate cohorts.

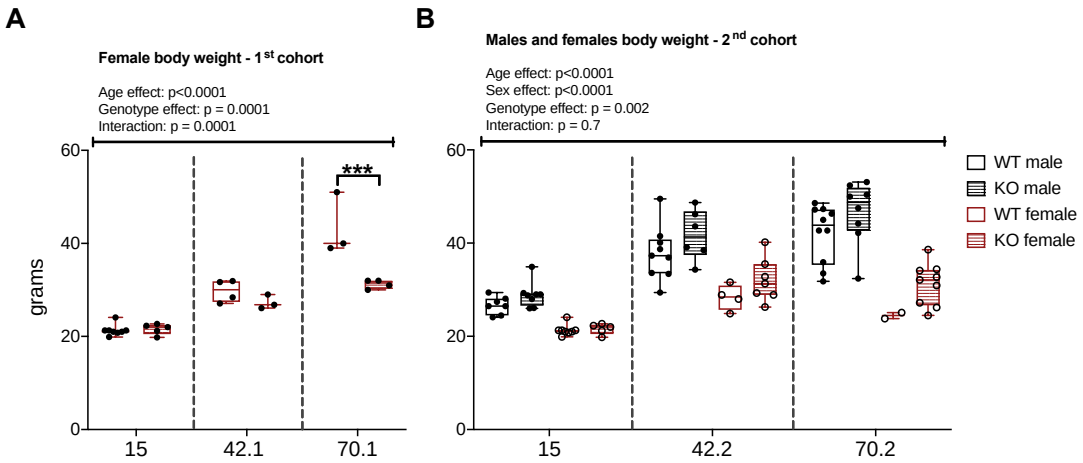

Figure 6.1. Ageing increases body weight in male and female mice. 15- (control), 42-and 70-week-old C57BL/6JOlaHsd (WT, transparent box) and 11β-HSD1 KO (KO, patterned box) male (black) and female (red) mice were fed AL chow diet (15-week-old mice) and/or standard chow diet (42-and 70-week-old mice) until appropriate age. The morning prior to termination, the 42-and 70-week-old mice were fasted for one hour and weighed thereafter. The control mice were fasted overnight and weighed in the morning. First cohort (stated as 42.1 and 70.1) were all females, with the genotypes separated in each cage. The second cohort (stated as 42.2 and 70.2) consisted of male and female mice with mixed genotypes in each cage. The 15-week-old control mice were single-housed. Body weight of the first **(A)** and second **(B)** cohort. Data points are presented with median, interquartile range and range shown by box and whisker plot and were analysed by 2-Way (A) or 3-Way (B) ANOVA with Sidak's multiple comparison test. The interaction from 3-Way ANOVA is between all three variables. First cohort: n (15 WT female) = 8. n (15 KO female) = 5. n (42.1 WT female) = 4. n (42.1 KO female) = 3. n (70.1 WT female) = 3. n (70.1 KO female) = 4. Second cohort: n (15 WT male) = 7. n (15 KO male) = 8. n (15 WT female) = 8. n (15 KO female) = 5. n (42.2 WT male) = 9. n (42.2 KO male) = 6. n (42.2 WT female) = 4. n (42.2 KO female) = 7. n (70.2 WT male) = 10. n (70.2 KO male) = 8. n (70.2 WT female) = 2. n (70.2 KO female) = 9. ***: p<0.001.

6.2.2. 11β-HSD1 KO influences ageing-associated changes in body composition

To determine the basis for these genotypic differences in total body mass, TD-NMR was used to assess body composition. Ageing is associated with increased fat mass (He *et al.*, 2018) and can further influence BMAT and bone morphology and therefore I postulated that 11β-HSD1 KO influences body mass primarily through effects on fat mass.

Figure 6.2 shows the fat mass data obtained by TD-NMR in both cohorts, presented both as absolute mass (Figure 6.2.A-B) and as % of body mass (Figure 6.2.C-D). For the first cohort of females, TD-NMR was not done in the 70-week-old mice and therefore only data from the 15.1 and 42.1 females is presented. Here, 2-Way ANOVA confirmed significant age, genotype and interaction effects (Figure 6.2.A, C), with multiple comparisons showing a decrease in the 42.1 KO females compared to the WTs. For the second cohort there were significant effects of age, sex and genotype, both for absolute fat mass (Figure 6.2.B) and % body fat (Figure 6.2.D). Thus, the older mice had increased fat mass compared to young mice; males had increased fat mass compared to the females; and an overall genotype effect was also detected, with KO mice generally having greater fat mass than WT at 42 and 70 weeks of age. These observations support the possibility that the KO mice have altered body mass because of differences in fat mass. However, as shown in Figure 6.3, changes in lean mass were also detected. In the first female cohort, both for absolute lean mass (Figure 6.3.A) and % lean mass (Figure 6.3.C) there were overall age, genotype and interaction effects detected by ANOVA. Absolute lean mass increased with age, whereas % lean mass decreased. Lean mass was also significantly higher in KO vs WT females at 42 weeks of age (Figure 6.3.A, C). Similar age effects were also observed in the second cohort of mice, in which sex effects were also apparent (Figure 6.3.B, D). However, unlike in the first cohort, in the second cohort no genotype effects were detected for absolute lean mass (Figure 6.3.B) while % lean mass was significantly lower in KO vs WT mice at 42 or 70 weeks of age (Figure 6.3.D). These differences in lean mass are generally the opposite to the differences in fat mass and further demonstrate that 11β-HSD1 KO can influence ageing-associated changes in body composition.

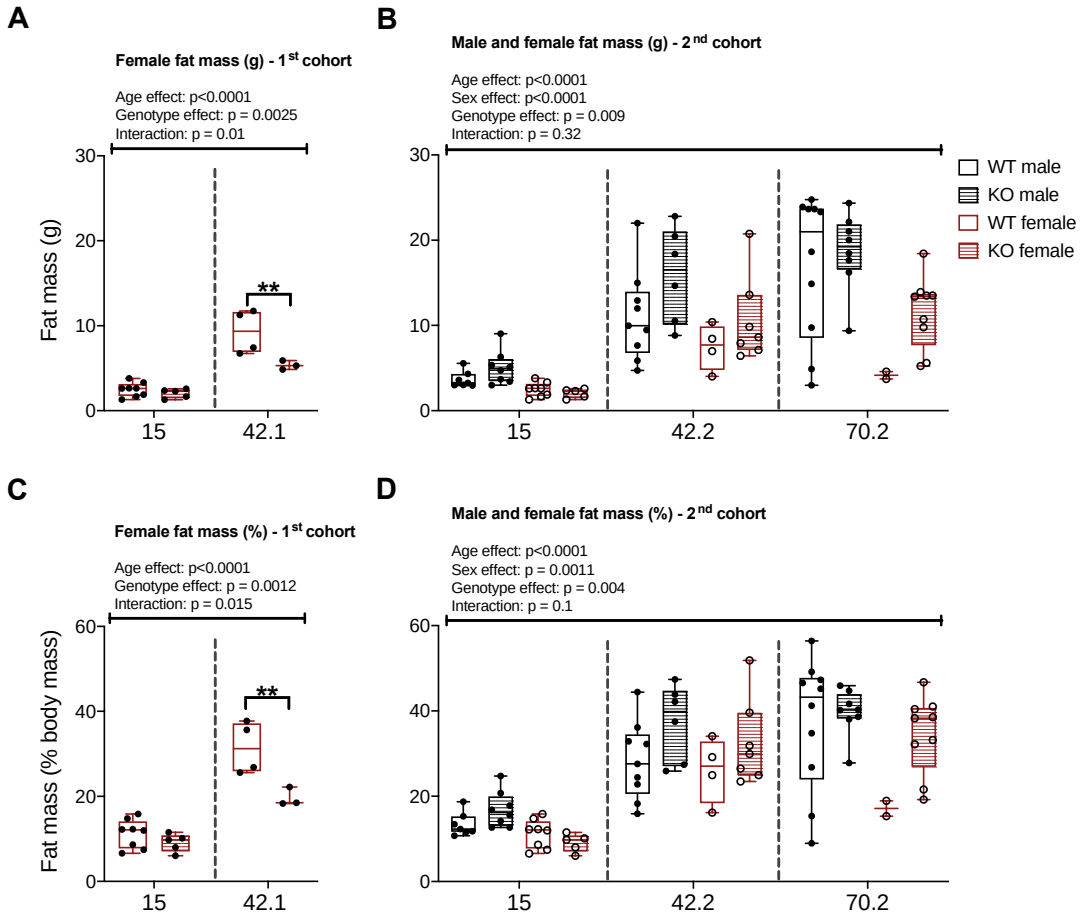

Figure 6.2. Older 11β-HSD1 KO mice do not resist age-induced adiposity compared to control mice. 15- (control), 42-and 70-week-old C57BL/6JOlaHsd (WT, transparent box) and 11β-HSD1 KO (KO, patterned box) male (black) and female (red) mice were fed and fasted as described in Figure 6.2. The day prior to termination, the mice were scanned for fat mass by TD-NMR. The 70-week-old female mice from the first cohort were not scanned due to the uncertainty of how stressful it would have been for aged mice to be scanned in a tight tube. However, after additional ageing studies in the lab, it was decided that it was safe to scan the aged mice. Fat mass of the first **(A)** and second **(B)** cohort shown in grams. Fat mass of the first **(C)** and second **(D)** cohort shown as % of body mass. Data points are presented with median, interquartile range and range shown by box and whisker plot and were analysed by 2-Way (A and C) or 3-Way (B and D) ANOVA with Sidak's multiple comparison test. Numbers of mice per group, and presentation of statistically significant differences between groups, are as described for figure 6.1. **: p<0.05.

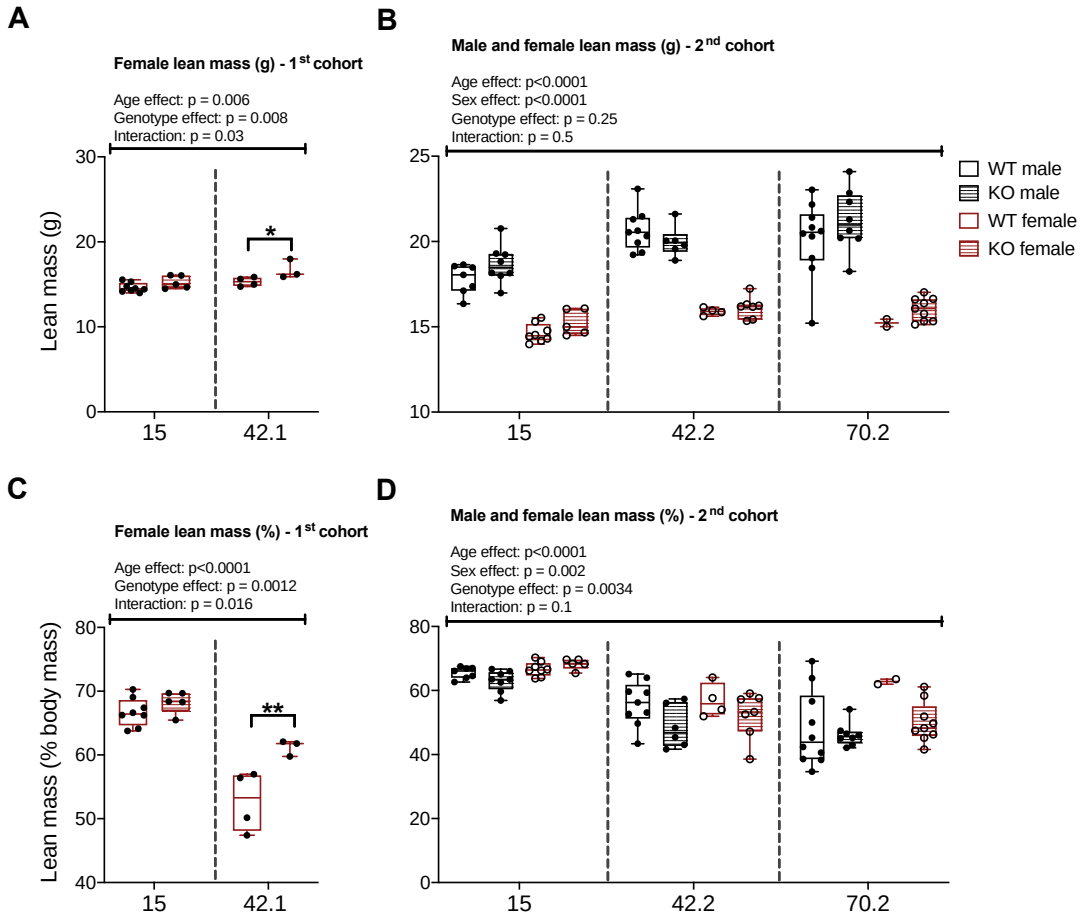

Figure 6.3. Older 11β-HSD1 KO mice do not resist lean mass loss compared to control mice. 15- (control), 42-and 70-week-old C57BL/6JOlaHsd (WT, transparent box) and 11β-HSD1 KO (KO, patterned box) male (black) and female (red) mice were fed and fasted as described in Figure 6.2. The day prior to termination, the mice were scanned for lean mass by TD-NMR. Lean mass of the first **(A)** and second **(B)** cohort shown in grams. Lean mass of the first **(C)** and second **(D)** cohort shown as % of body mass. Data points are presented with median, interquartile range and range shown by box and whisker plot, and were analysed by 2-Way (A and C) or 3-Way (B and D) ANOVA with Sidak's multiple comparison test. Numbers of mice per group, and presentation of statistically significant differences between groups, are as described for figure 6.1. **: $p<0.05$.

6.2.3. Age-associated sex differences in WAT

My previous results (Chapter 4) show that certain WAT depots contribute disproportionately to changes in total-body fat mass. Therefore, I next analysed the masses of different WAT depots in the two cohorts of 15-, 42-and 70-week-old mice. Figure 6.4 shows the absolute mass of iWAT (Figure 6.4.A-B) and as % of body mass (Figure 6.4.C-D). ANOVA detected age, genotype and interaction effects for the female iWAT in the first cohort, with the KOs having significantly less iWAT than WTs at 42 and 70 weeks of age (Figure 6.4.A, C). On the other hand, in the second cohort, ANOVA detected age, sex and genotype effect, without an interaction between the factors. No significant differences were detected between the genotypes either (Figure 6.4.B). iWAT as % of body mass showed overall age and genotype effect, with the mass increasing with age and the KOs generally having increased % iWAT mass compared to WTs (Figure 6.4.D).

Figure 6.5 shows the absolute mass of gWAT (Figure 6.5. A-B), and as % of body mass (Figure 6.5.C-D). Overall age and genotype effects were detected by ANOVA in both cohorts, with the depot increasing with age. In the first cohort, gWAT was decreased in the older KO female mice (Figure 6.5.A, C). Whereas, in the second cohort, an overall genotype effect by ANOVA confirmed higher gWAT mass in the KOs than in the WTs. Figure 6.6 shows the mass of mWAT as absolute mass (Figure 6.6.A-B), and as % of body mass (Figure 6.6.C-D). Both cohorts showed an age effect detected by ANOVA, with the older mice having increased mWAT mass. The results of mWAT were similar to iWAT and gWAT, with less mWAT in the first cohort of the older KO female mice (Figure 6.6.A, C), and increased mWAT in KO vs WT for each sex in the second cohort (Figure 6.6.B, D). KO males of the second cohort showed an increase in mWAT at 15 weeks of age (Figure 6.6.B).

Overall, these results confirm the changes in fat mass observed with TD-NMR and further reveal that the genotype effects are greatest for the visceral depots of gWAT and mWAT, with smaller effects on iWAT.

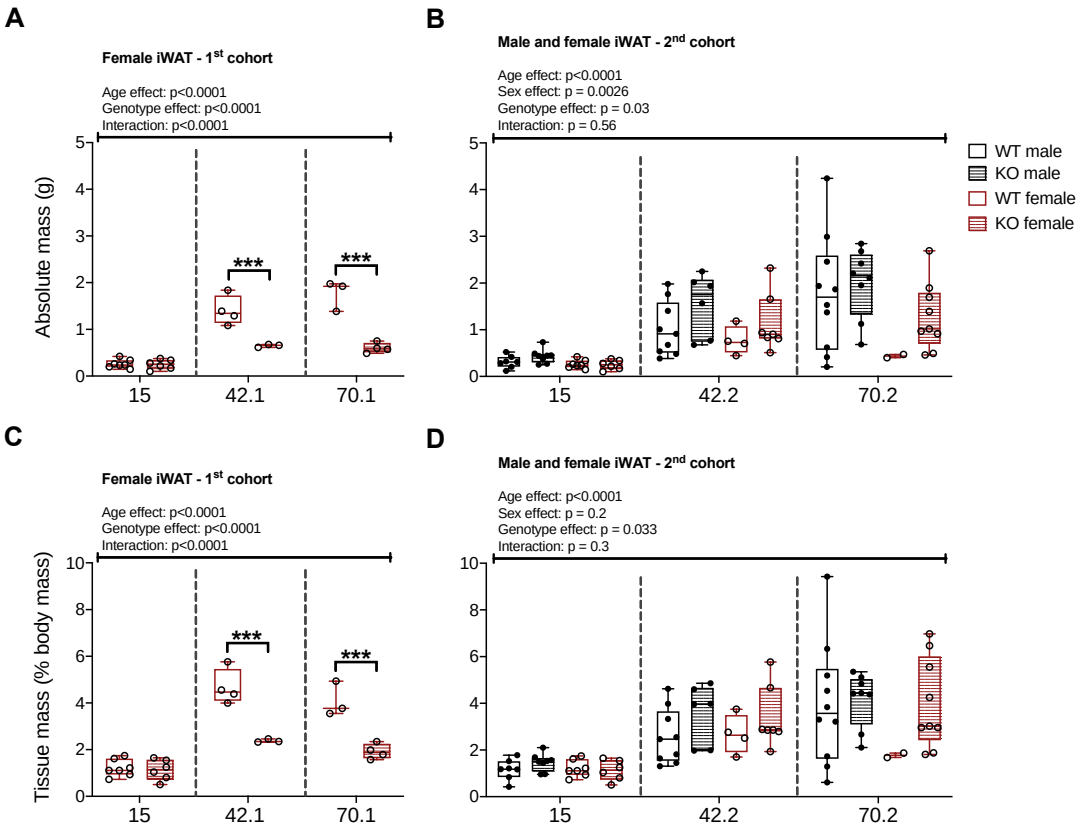

Figure 6.4. iWAT increases with age in male and female mice. 15- (control), 42- and 70-week-old C57BL/6JOlaHsd (WT, transparent box) and 11β-HSD1 KO (KO, patterned box) male (black) and female (red) mice were fed and fasted as described in Figure 6.2. Post termination, iWAT was collected and weighed. iWAT of first **(A)** and second **(B)** cohort shown in grams. iWAT of first **(C)** and second **(D)** cohort shown as % of body mass. Data points are presented with median, interquartile range and range shown by box and whisker plot, and were analysed by 2-Way (A and C) or 3-Way (B and D) ANOVA with Sidak's multiple comparison test. Numbers of mice per group, and presentation of statistically significant differences between groups, are as described for figure 6.1.

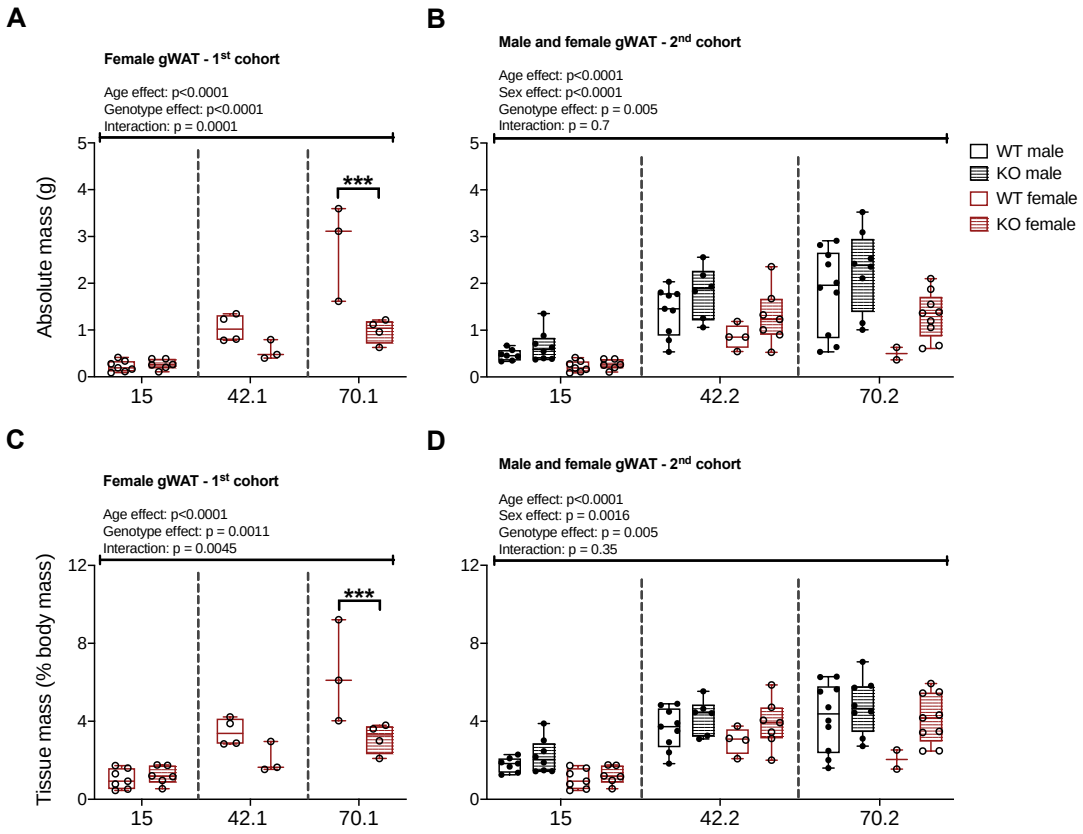

Figure 6.5. gWAT increases with ageing in male and female mice. 15- (control), 42-and 70-week-old C57BL/6JOlaHsd (WT, transparent box) and 11β-HSD1 KO (KO, patterned box) male (black) and female (red) mice were fed and fasted as described in Figure 6.2. Post termination, gWAT was collected and weighed. gWAT of first **(A)** and second **(B)** cohort shown in grams. gWAT of first **(C)** and second **(D)** cohort shown as % of body mass. Data points are presented with median, interquartile range and range shown by box and whisker plot, and were analysed by 2-way (A and C) or 3-way (B and D) ANOVA with Sidak's multiple comparison test. Numbers of mice per group, and presentation of statistically significant differences between groups, are as described for figure 6.1.

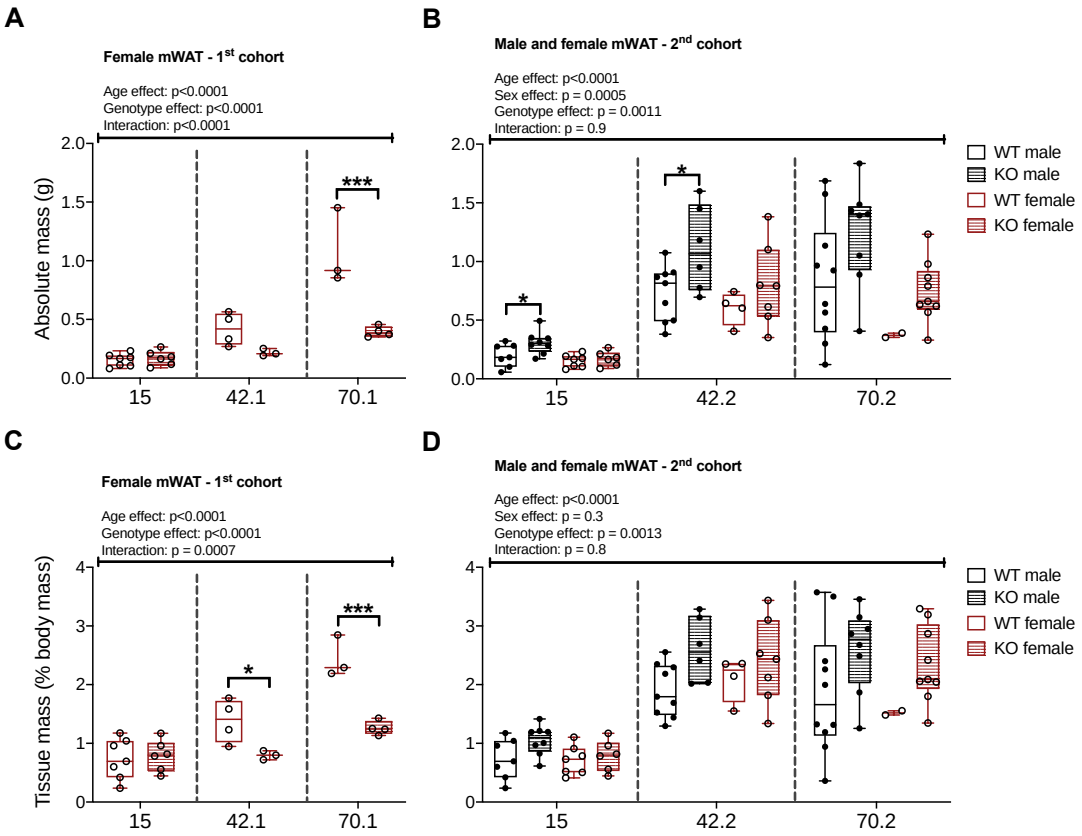

Figure 6.6. mWAT increases with ageing in male and female mice. 15- (control), 42-and 70-week-old C57BL/6JOlaHsd (WT, transparent box) and 11β-HSD1 KO (KO, patterned box) male (black) and female (red) mice were fed and fasted as described in Figure 6.2. Post termination, gWAT was collected and weighed. gWAT of first **(A)** and second **(B)** cohort shown in grams. gWAT of first **(C)** and second **(D)** cohort shown as % of body mass. Data points are presented with median, interquartile range and range shown by box and whisker plot, and were analysed by 2-way (A and C) or 3-way (B and D) ANOVA with Sidak's multiple comparison test. Numbers of mice per group, and presentation of statistically significant differences between groups, are as described for figure 6.1. *: p<0.05.

6.2.4. 11β-HSD1 KO exerts subtle effects on age-related changes in adrenal mass and circulating corticosterone

To next determine if the increased adiposity was associated with age-related changes in GC action, at necropsy adrenal glands were collected and weighed (Figure 6.7) and end-point plasma was collected for quantifying plasma corticosterone concentration by ELISA (Figure 6.8). In the first cohort of mice the adrenal glands were analysed from 15-week and 42-week-old groups only, because the adrenals from the 70-week-old mice were not collected at the time. ANOVA confirmed that adrenals were heavier in the 42-week-old compared to 15-week-old mice, regardless of genotype (Figure 6.7.A). Significant age effects were also detected in the second cohort, except that here, compared to the 15-week-old mice, adrenal masses were lower in the 42.2 mice but similar in the 70.2 mice (Figure 6.7.B). For the adrenal masses as % of body mass in the second cohort, there were strongly significant differences between the sexes, with female mice having heaver adrenals compared to the males in proportion to their body mass (Figure 6.7.D); this is consistent with the literature (Bielohuby *et al.*, 2007). Whether expressed as absolute mass or % body mass, ANOVA confirmed a significant interaction between age, sex and genotype for the second cohort of mice (Figure 6.7.B, D). However, no interaction was present between genotype x age, nor genotype x sex ($p=0.5$ and $p=0.8$, respectively). This indicates that the genotype does not influence the complex effects of age and sex on adrenal mass.

Figure 6.8 shows the circulating corticosterone concentration in both cohorts. ANOVA detected an age effect in the first cohort, with the older females having increased plasma corticosterone (Figure 6.8.A). In the second cohort a similar age effect was detected while a genotype effect was also apparent, with KOs having greater corticosterone concentration than WTs at 42 and 70 weeks of age (Figure 6.8.B). Overall, these results show that circulating corticosterone concentrations are increased with age in both genotypes.

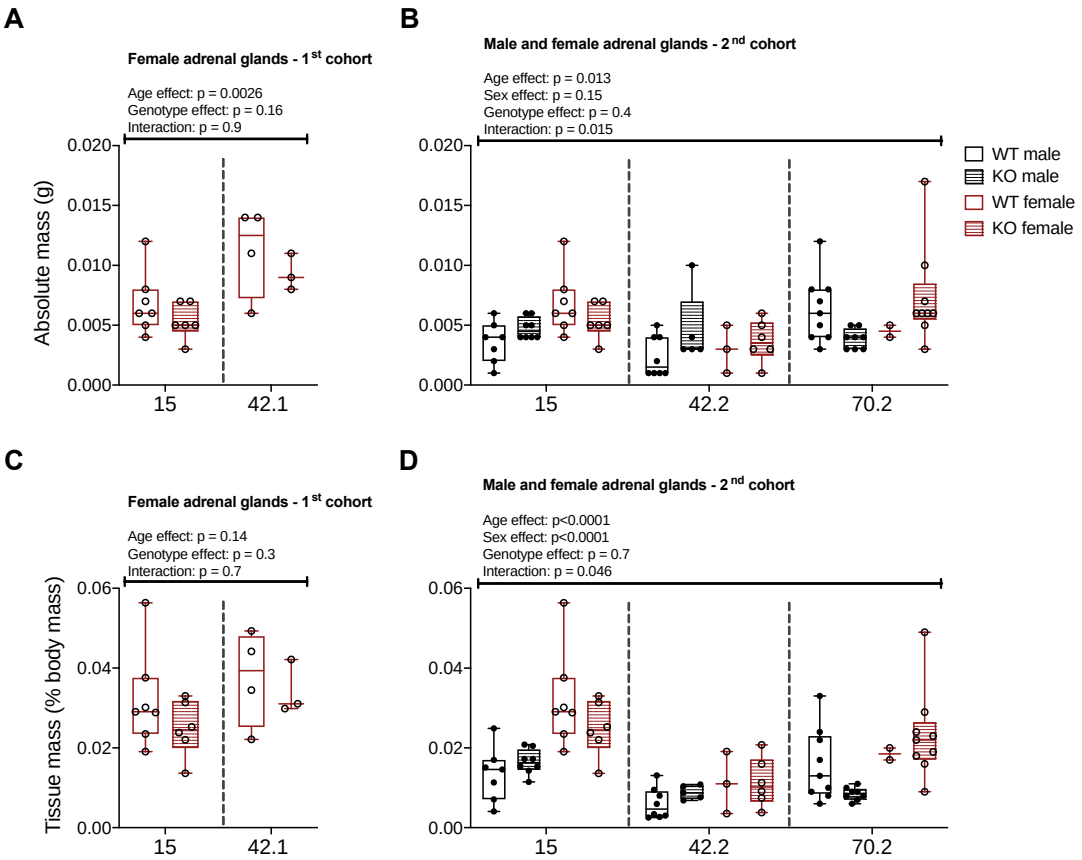

Figure 6.7. Adrenal glands in older WT and 11β-HSD1 KO male and female mice. 15- (control), 42-and 70-week-old C57BL/6JOlaHsd (WT, transparent box) and 11β-HSD1 KO (KO, patterned box) male (black) and female (red) mice were fed and fasted as described in Figure 6.2. Post termination, adrenal glands was harvested and weighed. Adrenal glands of first **(A)** and second **(B)** cohort shown in grams. Adrenal glands of first **(C)** and second **(D)** cohort shown as % of body mass. Data points are presented with median, interquartile range and range shown by box and whisker plot, and were analysed by 2-way (A and C) or 3-way (B and D) ANOVA with Sidak's multiple comparison test. First cohort: n (15 WT female) = 8. n (15 KO female) = 5. n (42.1 WT female) = 4. n (42.1 KO female) = 3. Second cohort: n (15 WT male) = 7. n (15 KO male) = 8. n (15 WT female) = 8. n (15 KO female) = 5. n (42.2 WT male) = 9. n (42.2 KO male) = 6. n (42.2 WT female) = 4. n (42.2 KO female) = 7. n (70.2 WT male) = 10. n (70.2 KO male) = 8. n (70.2 WT female) = 2. n (70.2 KO female) = 9.

A

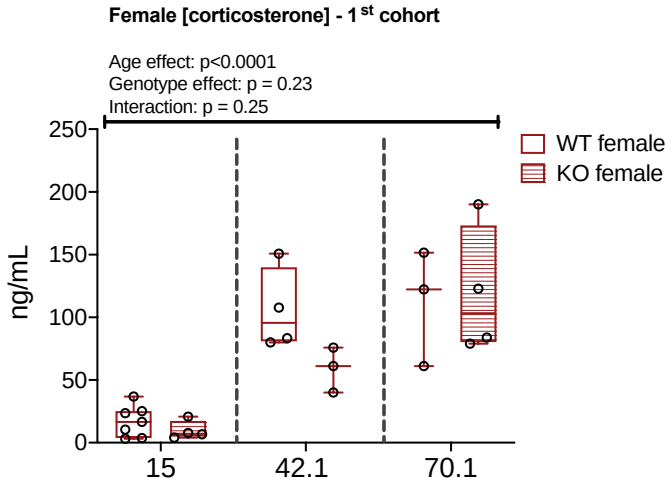

B

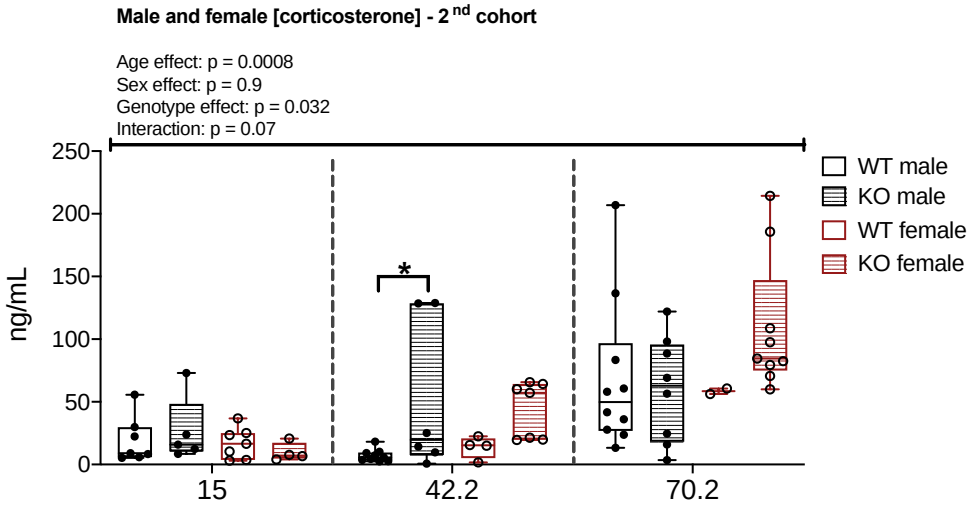

Figure 6.8. Circulating corticosterone concentration was increased in older mice. 15- (control), 42-and 70-week-old C57BL/6JOlaHsd (WT, transparent box) and 11β-HSD1 KO (KO, patterned box) male (black) and female (red) mice were fed and fasted as described in Figure 6.2. Post termination, blood was sampled and quantified by corticosterone ELISA as described in methods (2.4). **(A)** Circulatory corticosterone concentration in first **(A)** and second **(B)** cohort of mice. Data points are presented with median, interquartile range and range shown by box and whisker plot, and were analysed by 2-way (A) or 3-way (B) ANOVA with Sidak's multiple comparison test. Numbers of mice per group, and presentation of statistically significant differences between groups, are as described for figure 6.1. *: p<0.05.

6.2.5. 11β-HSD1 deficiency does not prevent ageing-associated BMAT expansion

I next investigated if these age-associated increases in circulating corticosterone are related to increased BMAT and whether this relationship is altered in the 11β-HSD1 KO mice. To do so, I quantified BMAT volume by osmium tetroxide staining; owing to time constraints, BMAT in the second cohort of 70-week-old mice could not be measured.

Figure 6.9 shows the analysed BMAT in the proximal and distal regions of the tibiae of male and female mice, as well as total BMAT in the tibiae. In the proximal BMAT of the first cohort, ANOVA detected age and genotype effects. The older mice had increased proximal BMAT compared to young mice, and the 42.1 KO females had decreased BMAT compared to WT females (Figure 6.9.A). In contrast, in the second cohort no genotype effects were detected although significant age and sex effects were apparent, as well as a significant interaction between age, sex and genotype. Thus, the older mice had increased BMAT, and the 42.2 females had greater proximal BMAT volume than the males (Figure 6.9.B). Furthermore, ANOVA detected age effects for both cohorts in the distal BMAT (Figure 6.9.C-D). The second cohort also had a sex effect present, with less distal BMAT in the females than the males (Figure 6.9.D). Finally, for total BMAT, ANOVA detected significant age effects, with the older mice having increased BMAT in both cohorts (Figure 6.9.E-F). However, unlike for proximal BMAT, genotype had no significant effect on distal BMAT or total BMAT.
Based on my previous results showing that corticosterone is increased in older mice, and the BMAT results showing expansion with ageing, these observations suggest that age-associated hypercorticosteronaemia might contribute to the expansion of BMAT. Although genotype significantly influences the effect of age and sex on proximal BMAT in the second cohort of mice (Figure 6.9.B), these effects are complex, and it is clear that lack of 11β-HSD1 is not sufficient to block age-associated BMAT expansion.

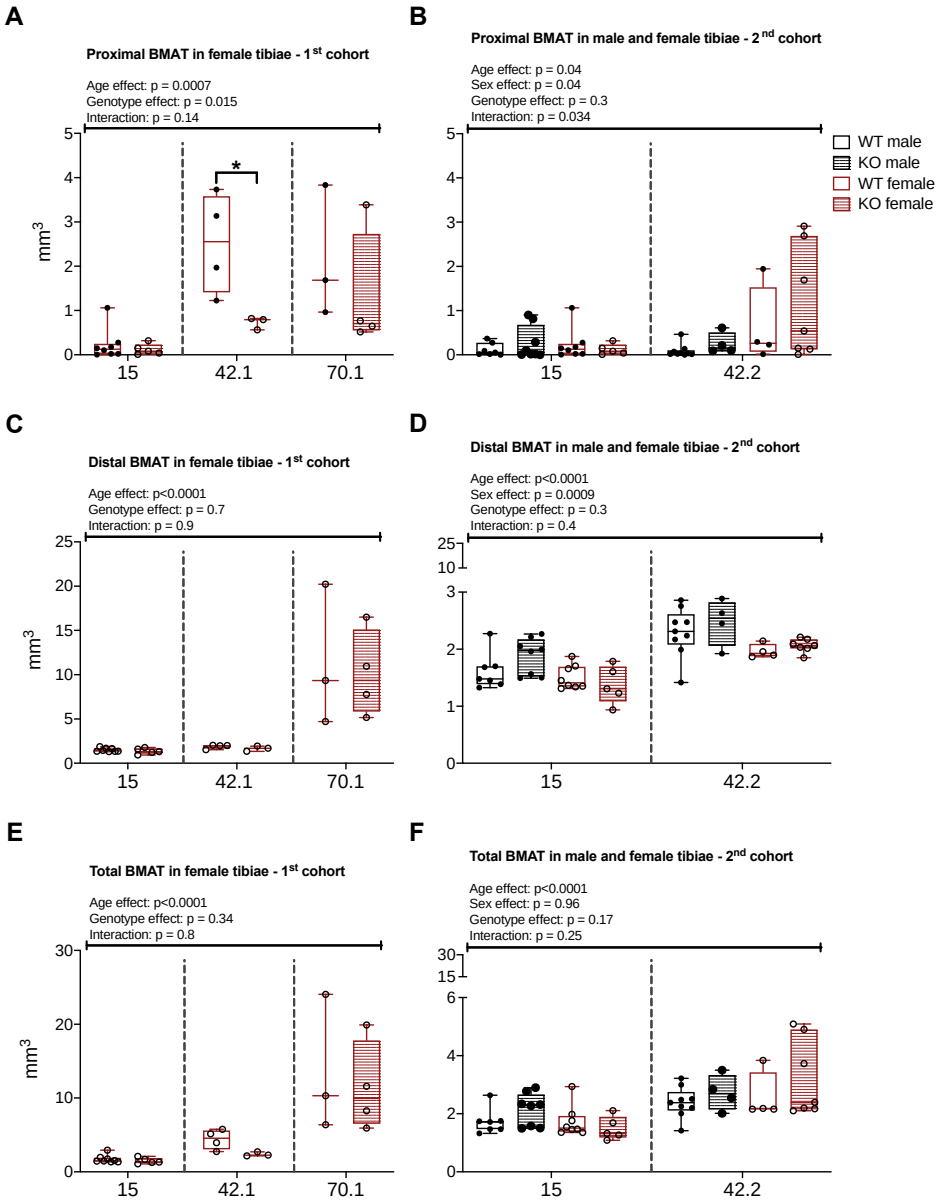

Figure 6.9. Older mice have increased BMAT expansion compared to young controls. 15- (control), 42-and 70-week-old C57BL/6JOlaHsd (WT, transparent box) and 11β-HSD1 KO (KO, patterned box) male (black) and female (red) mice were fed and fasted as described in Figure 6.2. Post termination, bones were decalcified and stained with osmium tetroxide staining for 48 hours, and thereafter washed for 24 hours in Sorensen's buffer. Tibiae were then embedded in layers in 1% agarose in a universal tube, followed by being scanned at 12μm by uCT and analysed by CTan for BMAT (mm_3). Proximal BMAT in first **(A)** and second **(B)** cohort. Distal BMAT in first **(C)** and second **(D)** cohort. Total BMAT in first **(E)** and second **(F)** cohort. Data points are presented with median, interquartile range and range shown by box and whisker plot, and were analysed by 2-way (A, C and E) or 3-way (B, D and F) ANOVA with Sidak's multiple comparison test. First cohort: n (15 WT female) = 8. n (15 KO female) = 5. n (42.1 WT female) = 4. n (42.1 KO female) = 3. n (70.1 WT female) = 3. n (70.1 KO female) = 4. Second cohort: n (15 WT male) = 7. n (15 KO male) = 8. n (15 WT female) = 8. n (15 KO female) = 5. n (42.2 WT male) = 9. n (42.2 KO male) = 6. n (42.2 WT female) = 4. n (42.2 KO female) = 7. *: $p<0.05$.

6.2.6. 11β-HSD1 KO does not protect against age-associated bone loss

All 42-and 70-week old mice showed increased circulating corticosterone concentrations, as well as BMAT expansion. However, based on qPCR for GC target genes, only KO females showed an increase in GC action in whole bone (data not shown). To determine whether increased GCs and/or BMAT expansion are associated with bone loss in the older mice, and whether the KOs resist these ageing-related effects, tibiae were analysed for trabecular and cortical morphology; owing to time constraints, these parameters in the second cohort of 70-week-old mice could not be measured.

Figure 6.10 shows the trabecular bone morphology of 15-, 42-and 70-week old mice. ANOVA detected a strong age effect for the first (Figure 6.10.A) and second (Figure 6.10.B) cohorts, with the older mice having decreased trabecular bone volume. Furthermore, the second cohort also showed a sex effect, with the females having less trabecular bone volume than males. Trabecular thickness was increased at 70-weeks of age in the first cohort (Figure 6.10.C), but no age effects were present between 15-week-old and 42-week-old mice in the first or second cohorts (Figure 6.10.C, D). ANOVA detected an age effect for trabecular number in the first (Figure 6.10.E) and second (Figure 6.10.F) cohorts, with the older mice having decreased trabecular number. Furthermore, the second cohort also showed sex effects, with the females having less trabecular number than the males (Figure 6.10.F). Finally, trabecular separation was increased with age in the first cohort (Figure 6.10.G), but unaltered in the second cohort (Figure 6.10.H). However, an overall sex effect was detected by ANOVA for the second cohort, with females having increased trabecular separation compared to the males (Figure 6.10.H). Overall, these data show that ageing is associated with trabecular bone loss but that this is not influenced by 11β-HSD1 KO. Figure 6.11 shows the cortical bone morphology of 15-, 42-and 70-week old mice. In the first cohort of mice there were no significant age or genotype effects on cortical thickness, whereas in the second cohort ANOVA confirmed an age and sex effect, with cortical thickness decreasing with ageing but being greater in females than in males (Figure 6.11.B). In both cohorts, ANOVA confirmed that mean total cross-sectional bone area decreased with ageing, regardless of sex (Figure 6.11.C-D). Similar to the trabecular parameters, no genotype effects were found, indicating that 11β-HSD1 KO does not influence age-associated cortical bone loss.

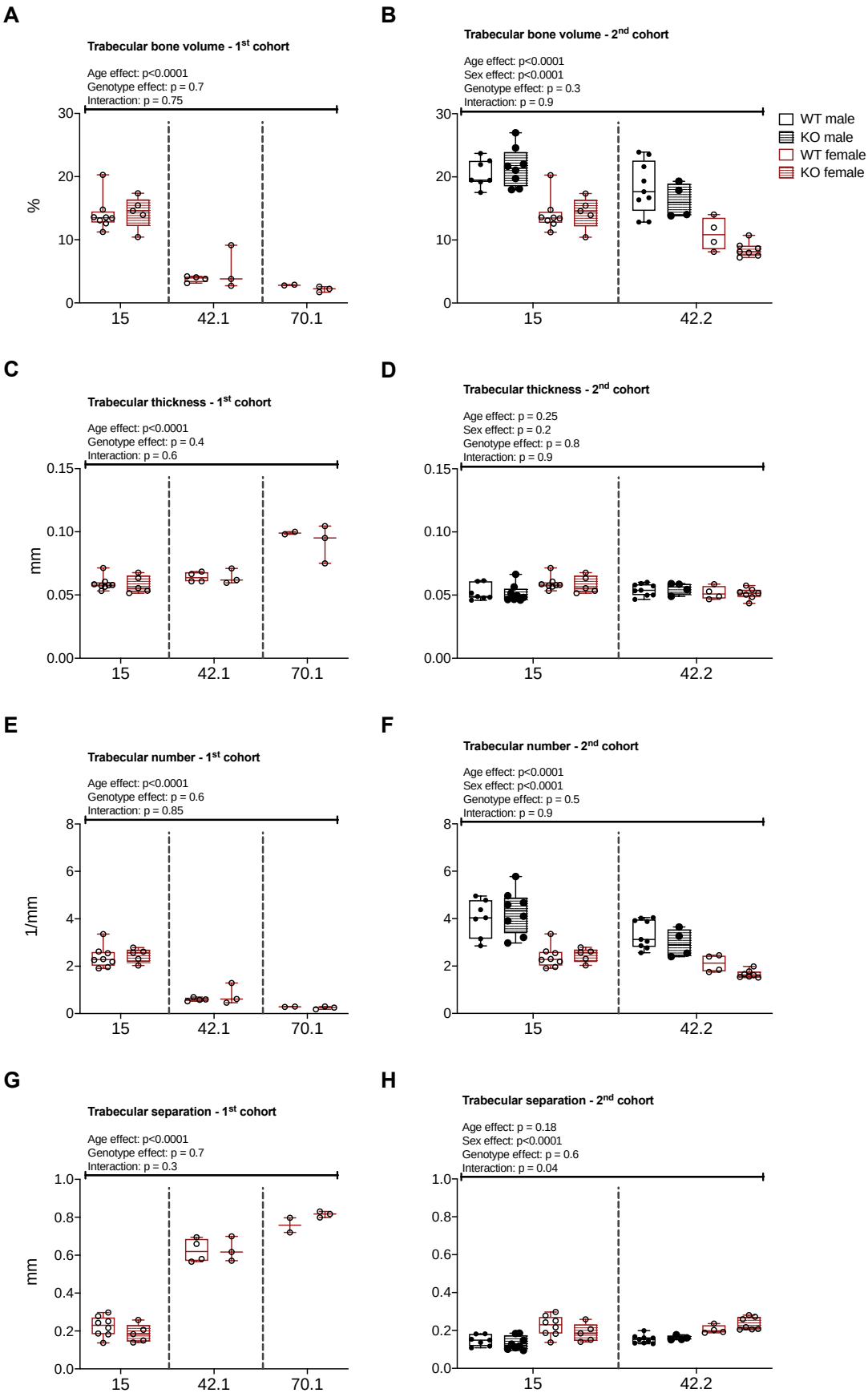
A
Trabecular bone volume - 1st cohort
Age effect: p<0.0001
Genotype effect: p = 0.7
Interaction: p = 0.75
%
30
20
10
0
15
42.1
70.1
B
Trabecular bone volume - 2nd cohort
Age effect: p<0.0001
Sex effect: p<0.0001
Genotype effect: p = 0.3
Interaction: p = 0.9
WT male
KO male
WT female
KO female
30
20
10
0
15
42.2
C
Trabecular thickness - 1st cohort
Age effect: p<0.0001
Genotype effect: p = 0.4
Interaction: p = 0.6
mm
0.15
0.10
0.05
0.00
15
42.1
70.1
D
Trabecular thickness - 2nd cohort
Age effect: p = 0.25
Sex effect: p = 0.2
Genotype effect: p = 0.8
Interaction: p = 0.9
0.15
0.10
0.05
0.00
15
42.2
E
Trabecular number - 1st cohort
Age effect: p<0.0001
Genotype effect: p = 0.6
Interaction: p = 0.85
1/mm
8
6
4
2
0
15
42.1
70.1
F
Trabecular number - 2nd cohort
Age effect: p<0.0001
Sex effect: p<0.0001
Genotype effect: p = 0.5
Interaction: p = 0.9
8
6
4
2
0
15
42.2
G
Trabecular separation - 1st cohort
Age effect: p<0.0001
Genotype effect: p = 0.7
Interaction: p = 0.3
mm
1.0
0.8
0.6
0.4
0.2
0.0
15
42.1
70.1
H
Trabecular separation - 2nd cohort
Age effect: p = 0.18
Sex effect: p<0.0001
Genotype effect: p = 0.6
Interaction: p = 0.04
1.0
0.8
0.6
0.4
0.2
0.0
15
42.2

Figure 6.10. Trabecular bone is lost with ageing in WT and 11β-HSD1 KO mice. 15- (control), 42-and 70-week-old C57BL/6JOlaHsd (WT, transparent box) and 11β-HSD1 KO (KO, patterned box) male (black) and female (red) mice were fed and fasted as described in Figure 6.2. Post termination, bones were fixated in 10% formaldehyde for seven days. Tibiae were then embedded in layers in 1% agarose in a universal tube, followed by being scanned at 6μm by uCT and analysed by CTan. Trabecular bone volume (%) in first **(A)** and second **(B)** cohort. Trabecular thickness (mm) in first **(C)** and second **(D)** cohort. Trabecular number (1/mm) in first **(E)** and second **(F)** cohort. Trabecular separation (mm) in first **(G)** and second **(H)** cohort. Data points are presented with median, interquartile range and range shown by box and whisker plot, and were analysed by 2-way (A, C, E and G) or 3-way (B, D, F and H) ANOVA with Sidak's multiple comparison test. Numbers of mice per group, and presentation of statistically significant differences between groups, are as described for figure 6.9.

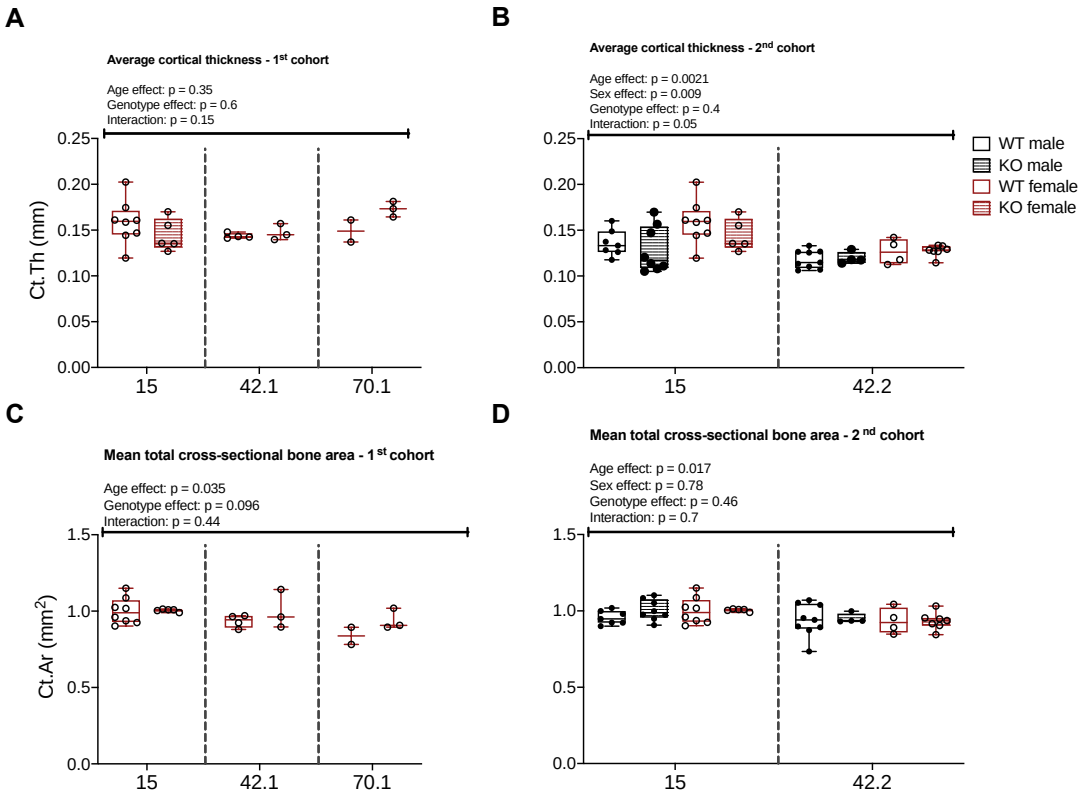

Figure 6.11. Age-related cortical bone loss is not influenced by 11β-HSD1. 15- (control), 42-and 70-week-old C57BL/6JOlaHsd (WT, transparent box) and 11β-HSD1 KO (KO, patterned box) male (black) and female (red) mice were fed and fasted as described in Figure 6.2. Post termination, bones were fixated in 10% formaldehyde for seven days. Tibiae were then embedded in layers in 1% agarose in a universal tube, followed by being scanned at 6μm by uCT and analysed by CTan. Average cortical thickness (mm) in first **(A)** and second **(B)** cohort. Mean total cross-section bone area (mm_2) in first **(C)** and second cohort **(D)**. Data points are presented with median, interquartile range and range shown by box and whisker plot, and were analysed by 2-way (A, C) or 3-way (B, C) ANOVA with Sidak's multiple comparison test. Numbers of mice per group, and presentation of statistically significant differences between groups, are as described for figure 6.9.

6.2.8. Ageing-associated corticosterone and BMAT expansion are associated with bone loss

The above results show that 11β-HSD1 deficiency does not prevent BMAT expansion or protect against bone loss with ageing. To further understand the relationship between BMAT expansion and bone loss in this context, and if circulating corticosterone might influence these parameters, linear regression analysis was performed for the 15-, 42.2-and 70.1-week-old mice. The remaining 70-week-old mice (70.2) were not included because there was not enough time to complete the µCT bone analysis for this group.

Table 6.2 shows the linear regression analysis of male mice. Circulating corticosterone was not significantly associated with BMAT volume or with any other trabecular or cortical parameters in WT or KO males. Unlike circulating corticosterone, BMAT volume was significantly and inversely associated with trabecular bone volume fraction (BV/TV) and number (Tb.N) in both genotypes and showed a significant positive association with trabecular spacing (Tb.Sp) in KO mice only. Indeed, the strength of these associations between BMAT and trabecular bone was greater in the KO than in the WT mice, suggesting that lack of 11β-HSD1 may influence the relationship between BMAT and trabecular bone remodelling. In contrast, BMAT was not significantly associated with cortical bone parameters in either genotype. Table 6.3 shows the linear regression analysis of female mice. Unlike in males, a significant positive association was found between corticosterone and total BMAT, regardless of genotype. Similarly, in each genotype trabecular bone volume fraction (BV/TV) and trabecular number (Tb.N) were negatively associated with corticosterone as well as BMAT. Cortical bone area (Ct.Ar) was also negatively associated with BMAT in WT females. In addition, corticosterone and BMAT were positively associated with trabecular spacing (Tb.S) and thickness (Tb.Th), although, for corticosterone, the latter was significant only for WT mice. Unlike in males, the strengths of these associations were generally greater in WT than in KO mice, suggesting that 11β-HSD1 may contribute to the ability of corticosterone and/or BMAT expansion to modulate skeletal remodelling with ageing. Overall these results suggest that age-associated BMAT expansion in males might not be associated with corticosterone, whereas in females it is. Furthermore, bone loss, particularly for trabecular bone, is associated with increased corticosterone concentration and BMAT expansion.

	Linear regression analysis for male mice with ageing								
	Circulating corticosterone				Total BMAT				
	WT		KO		WT		KO		
	R_2	*P* value	R_2	*P* value	R_2	*P* value	R_2	*P* value	
T.BMAT	0.136	0.159	0.002	0.909					
BV/TV	0.016	0.645	0.001	0.923	0.392	**0.010**	0.619	**0.012**	
Tb.Th	0.028	0.533	0.159	0.288	0.006	0.768	0.309	0.120	
Tb.N	0.002	0.860	0.050	0.564	0.321	**0.022**	0.815	**0.001**	
Tb.S	0.019	0.609	0.190	0.241	0.201	0.081	0.453	**0.047**	
Ct.Th	0.153	0.134	0.175	0.263	0.155	0.132	0.0001	0.979	
Ct.Ar	0.042	0.446	1.312e-005	0.993	0.001	0.899	0.13	0.341	

Table 6.2. Linear regression analysis of WT and KO male mice, with circulating corticosterone (ng/mL) and total BMAT volume (mm_3) in tibiae as constant variables. Data from 15-and 42-week old male mice was pooled together to observe changes with ageing. BV/TV = % Bone volume fraction (Segmented bone volume to the entire volume of the region of interest). Tb.Th = Trabecular thickness (Average thickness of trabeculae). Tb.N = Trabecular number (Average number of trabeculae per unit length). Tr.S = Trabecular separation (Average distance between trabeculae). Ct.Th = Average cortical thickness (mm). Ct.Ar = Mean total cross-section bone area (mm_2). P values in bold represent statistical significance. Direction of association is indicated by cell colour: Green = positive and Red = negative, with darker shades used for statistically significant values. n (15 WT male) = 6. n (15 KO male) = 5. n (42.2 WT male) = 9. n (42.2 KO male) = 4.

	Linear regression analysis for female mice with ageing									
	Circulating corticosterone					Total BMAT				
	WT			KO		WT			KO	
	R_2	*P* value		R_2	*P* value	R_2	*P* value		R_2	*P* value
T.BMAT	0.725	**0.0001**		0.622	**0.001**					
BV/TV	0.567	**0.003**		0.534	**0.003**	0.651	**0.001**		0.540	**0.003**
Tb.Th	0.624	**0.001**		0.182	0.128	0.658	**0.001**		0.404	**0.015**
Tb.N	0.624	**0.001**		0.581	**0.002**	0.718	**0.0003**		0.670	**0.0003**
Tb.S	0.782	**<0.0001**		0.558	**0.002**	0.726	**0.0002**		0.749	**<0.0001**
Ct.Th	2.605e-005	0.987		0.139	0.190	0.066	0.396		0.239	0.076
Ct.Ar	0.230	0.097		0.067	0.371	0.424	**0.0159**		0.074	0.346

Table 6.3. Linear regression analysis of WT and KO female mice, with circulating corticosterone (ng/mL) and total BMAT volume (mm_3) in tibiae as constant variables. Data from 15,42-and 70-week old female mice was pooled together to observe changes with ageing. BV/TV = % Bone volume fraction (Segmented bone volume to the entire volume of the region of interest). Tb.Th = Trabecular thickness (Average thickness of trabeculae). Tb.N = Trabecular number (Average number of trabeculae per unit length). Tr.S = Trabecular separation (Average distance between trabeculae). Ct.Th = Average cortical thickness (mm). Ct.Ar = Mean total cross-section bone area (mm_2). Statistical significance and the direction of the associations are indicated as for table 6.1. n (15 WT female) = 7. n (15 KO female) = 4. n (42.2 WT female) = 4. n (42.2 KO female) = 7. n (70.1 WT female) = 3. n (70.1 KO female) = 4. Please note, for 70-week-old total BMAT vs. bone parameters n (WT female) = 2, and n (KO female) = 3.

6.3. Discussion

6.3.1 Cohort-dependent variability in the phenotypes of 11β-HSD1 KO mice.

The aim with this chapter was to investigate if ageing-associated GC excess mediates BMAT expansion and bone loss in null 11β-HSD1 KO mice, with the hypothesis that the increased GCs with ageing contribute to BMAT expansion and bone loss. Furthermore, as mentioned in the introduction, the analysis of two cohorts were presented side-by-side in this chapter for comparison due to possible cage and/or cohort effects. The WT and KO mice in the first cohort were caged separately, whereas the second cohort had mixed genotypes in each cage. My results showed clear differences between the two cohorts, and due to the first cohort having the WT and KO mice in separate cages, it is impossible to distinguish between cage and genotype effects within this cohort. Several studies have investigated how different cage parameters, for example temperature, nesting material, space, shelter and provision of gnawing sticks, affect mice (Latham and Mason, 2004; Bailoo *et al.*, 2018). Furthermore, besides housing, different facilities can also impact the mice, for example their gut microbiota (Spychala *et al.*, 2018), which can also further change with ageing (Spychala *et al.*, 2018). In addition, null 11β-HSD1 KO mice have an altered gut microbiome compared to WT counterparts, and this differs between normal chow and Western diet (Johnson *et al.*, 2017). Therefore, it is possible that the cohorts were exposed to a somewhat different environmental factors throughout their lifetime which influenced them in such ways that our end-results differed between the cohorts. In addition, the cages containing the separate genotypes could have been in different parts of the room, which could have further influenced the cage effects. Therefore, the second cohort allows more trustworthy and robust conclusions to be drawn, because (1) mice in the first cohort had WT and KO mice in separate cages, and (2) the numbers for the second cohort are larger.

6.3.2. Effect of 11β-HSD1 KO on age-related changes in body mass and composition

Mice at 42 and 70 weeks of age, in both cohorts, had increased body weight compared to the 15-week-old controls. The older mice also had increased fat mass,

including the female mice. Although female mice resist fat loss during CR (Chapter 3), they did not resist fat mass gain with ageing. It has previously been reported in humans that ageing is associated with obesity (Hajek *et al.*, 2015), and especially that obesity predominantly increases among women between 30-65-years of age (von Ruesten *et al.*, 2011).

A different study also demonstrated that with ageing, total fat tissue increases in women only, whereas percentage body fat increases in both men and women (He *et al.*, 2018). Based on these results, it is clear that increased body weight with ageing is due to increased fat mass. In my study, the older mice also had decreased lean mass as percentage of body mass, which is common with ageing unless regular exercise is performed (Abizanda *et al.*, 2016). Overall, these findings suggest that 11β-HSD1 deficiency does not protect against increases in age-associated adiposity; in contrast, the data from the second, more-robust cohort, indicate that lack of 11β-HSD1 may exacerbate increased adiposity with ageing. Compared to previous studies investigating 11β-HSD1 KO mice and adiposity, my results are the opposite, at least for the second cohort. One previous study showed that overexpression of 11β-HSD1 in AT results in increased adiposity (Masuzaki, 2001), whereas the hypomorphic 11β-HSD1 KO mice on HFD exhibit reduced fat mass compared to age-matched controls (Morton *et al.*, 2004; Wamil *et al.*, 2011). However, it is worth remembering that the 11β-HSD1 KO model used in these latter studies is the hypomorphic KO. Therefore, the difference in adiposity resistance in these two KO models could differ.

6.3.3. Effect of 11β-HSD1 KO on BMAT expansion and bone loss with ageing

As discussed in the introduction to this chapter, Justesen *et al.,* previously reported that the hypomorphic 11β-HSD1 KO mice lack BMAds (Justesen *et al.*, 2004). Herein, I show that 42-and 70-week old null 11β-HSD1 KO male and female mice do not lack BMAT. Instead, the KOs had age-related increases in BMAT. However, in the proximal BMAT in the KO females from the second cohort, BMAT was significantly decreased compared to the WT females, although it was still present. Based on the knowledge that the first cohort had the genotypes separated in different cages, and

that the body composition, adipose depots and BMAT volume vary significantly between the genotypes, it suggests that these results could reflect cage effects, as discussed above. Interestingly, the BMAT phenotype tracks with the overall adiposity/obesity phenotype. This confirms previous studies suggesting that obesity is associated with increased BMAT, including with ageing (Patel *et al.*, 2018). It also highlights the need to measure body composition if robust conclusions are to be drawn about any BMAT phenotype. Therefore, based on the differences in the first cohort, the results from the second cohort are more robust and informative regarding possible influences of 11β-HSD1 with ageing. There are several possible explanations for these different results, and also several reasons why my present findings allow firmer conclusions to be drawn. For example, as described in the introduction, the Justesen *et al.,* (2004) study used a hypomorphic KO, whereas I studied a null KO model (Vandermosten *et al.*, 2017; Zhang *et al.*, 2017; Verma *et al.*, 2018). Furthermore, Justesen *et al.,* (2004) analysed BMAT by static histomorphometry, with six sections of bone per animal, and in the proximal tibiae only. Conversely, I used osmium tetroxide-staining with μCT to quantify BMAT in the entire tibia. This method, which was not available in 2004, allows far more comprehensive and robust BMAT quantification. Thus, my findings show that null 11β-HSD1 KO mice do not lack BMAT and that they still undergo age-related BMAT expansion.

6.3.4. Influence of 11β-HSD1 KO on the relationships between circulating corticosterone, BMAT expansion and bone loss with ageing

Despite these differences in the BMAT phenotype, both my findings and those of Justesen *et al.,* (2004) show that hypomorphic and null 11β-HSD1 KO does not affect trabecular or cortical parameters. However, I found that the age-associated changes in trabecular and cortical bone are associated with increased corticosterone concentration and BMAT expansion in both sexes. Several previous studies also found increased circulating corticosterone concentration in the hypomorphic 11β-HSD1 KO mice compared to age-matched controls (Kotelevtsev *et al.*, 1997; Harris *et al.*, 2001; Yau *et al.*, 2001), but on a different background compared to my null KOs. However, other publications did not find this difference in circulating corticosterone concentrations in 11β-HSD1 exon 5 and the null KO mice (Abrahams *et al.*, 2012;

Morgan *et al.*, 2014; Verma *et al.*, 2018), nor did one study that used hypomorphic 11β-HSD1 KO mice (Joyce L. W. Yau *et al.*, 2015). This means that the end results between the KOs with the different background strains do vary, as previously published (Carter *et al.*, 2009). The correlations between BMAT volume and bone parameters were predominantly negative, suggesting that age-related BMAT expansion is associated with increased bone loss, supporting previous findings (Devlin and Rosen, 2015; Veldhuis-Vlug and Rosen, 2018). Indeed, the strength of these associations between BMAT and trabecular bone was greater in the KO than in the WT mice, suggesting that lack of 11β-HSD1 may influence the relationship between BMAT and trabecular bone remodelling. The association between BMAT and cortical bone was insignificantly positive for KOs and negative for WTs. This suggests that the lack of 11β-HSD1 might protect against cortical bone loss with subsequent BMAT expansion.

Previous work on the hypomorphic 11β-HSD1 KO mice following 21 days of induced arthritis showed similar trabecular bone loss, and less cortical bone loss, compared to WT mice (Coutinho, 2009). No changes were observed two days following the induced arthritis, suggesting that the results observed at the later time point were not due to initial differences between the genotypes. This is similar to the lack of skeletal differences reported by Justesen *et al.,* (2004) and between the AL-fed WT and KO mice in Chapter 5. However, these arthritis studies used young WT and KO mice between 8 and 12-weeks of age, and therefore they do not inform about the potential impact of the KO on bone with ageing. In addition, in my studies in 15-, 42-and 70-week old mice, further parameters could be included to determine in greater depth the effect of BMAT expansion on cortical bone.

In contrast to the males, the associations between corticosterone/BMAT and bone parameters were generally greater in the females. This suggests that 11β-HSD1 may contribute to the ability of corticosterone and/or BMAT expansion to modulate skeletal remodelling with ageing in females. In addition, a previous publication showed that trabecular bone loss in females can occur independently of oestradiol, suggesting it is potentially more susceptible to GCs (Syed *et al.*, 2010). To address this, mass spectrometry would need to be performed on plasma to determine GCs and sex hormone concentrations, while markers of oestrogen action within bone and BM could be assessed.

Surprisingly, corticosterone and total BMAT were not associated in males but were positively associated in females. From these results, one interpretation is that, in both sexes, bone loss during ageing could be influenced by increased corticosterone concentrations and BMAT expansion, and that increased circulating corticosterone may contribute to BMAT expansion in females, but not in males. However, other factors could also influence this shift, such as sex hormones (i.e. progesterone, testosterone). Besides bone loss and BMAT expansion, the older mice, regardless of genotype, also had increased circulating corticosterone concentration compared to the 15-week-old mice. Further work would need to be conducted to add to the numbers, and additional experiments to determine if other hormones could be involved in these effects. For example, mass spectrometry could be performed to determine the concentration of the hormones in the circulation and BM between the genotypes.

A factor that could explain the bone mass loss in the null KOs could be the age. It is possible that the mice do lose some bone mass throughout their life, but after a certain age they maintain it compared to the WTs. The mice used in this chapter were 42- and 70-weeks old (~10 and 16 months old, respectively). Compared to previous studies on the hypomorphic 11β-HSD1 KO mice with regards to ageing, mice around 18-26-months of age have been used to investigate the role of 11β-HSD1 in other age-related conditions (Yau *et al.*, 2001; Sooy *et al.*, 2010; Joyce L.W. Yau *et al.*, 2015). However, none of these analysed the bone phenotype, and therefore future studies should use older mice to further test the role of null 11β-HSD1 in age-related bone loss and BMAT expansion.

Since most of the studies involving 11β-HSD1 KO mice involve the hypomorphic model, many gaps in knowledge remain that could be addressed using null 11β-HSD1 KO model. Based on previous publications, the inhibition of 11β-HSD1 protects against the deleterious effects of excess GCs (Morgan *et al.*, 2014). Moreover, increased expression and activity of 11β-HSD1 in bone has been shown to cause age-induced bone loss and increase the risk of GIO (Cooper *et al.*, 2002). Since the hypomorphic model often showed improved results, one would expect the null KO model to potentially exhibit even greater improvements due to having a complete lack of *Hsd11b1* expression. However, a different publication showed that 11β-HSD1 plays a protective role in the suppression of joint destruction and bone loss in inflammatory

diseases (Hardy *et al.*, 2018). Based on this, and if aged null 11β-HSD1 KO mice have increased inflammation, they might exhibit bone loss, either to a similar or greater extent compared to age-matched WT controls. Therefore, more research is necessary to understand the mechanism behind age-induced BMAT expansion and bone loss, and if other factors such as sex hormones and/or inflammation further aggravate the effects.

6.3.3. Limitations and future directions

To further understand how ageing affects null 11β-HSD1 KO mice in regards to BMAT expansion and bone loss, the addition of more mice would be necessary. Although, since the KOs did not resist circulatory effects of GCs with regards to BMAT expansion and bone loss, it potentially undermines the reasoning for adding more mice to the groups. To further understand how GCs affect BMAT and bone with ageing, the BM should be flushed out to examine GC target genes, as well as in the bone. In addition, performing mass spectrometry on plasma and BM would be important to determine if there are any differences between systemic and tissue-specific GC concentration. Due to time constraints, the bones from the 70-week-old mice from the second cohort were not analysed. Therefore, bone analysis and BMAT quantification needs to be done on the 70-week-old mice from the second cohort to determine if BMAT does increase with ageing in the second cohort, as found in the first cohort, and if bone loss is consistent with ageing. In humans, femoral neck fracture is common with ageing (Woolf, 2003), and associations between BMAT and fracture risk have also been reported (Wehrli *et al.*, 2000; Justesen *et al.*, 2001; Schwartz *et al.*, 2013). This suggests that the older mice might have decreased femoral bone mass. Based on my hypothesis, the KO mice should resist the age-induced bone loss. However, the older mice did not resist tibial bone loss, and might therefore not resist femoral bone loss either. Past publications have either shown an inverse association between BMAT and bone loss, or no changes, as previously discussed in the introduction. However, a more recent publication showed that greater BMAT is not associated with bone density/strength in men, but is associated with trabecular bone loss in older women (mean age of 80.9) (Woods *et al.*, 2019). It would therefore be scientifically and clinically beneficial to scan and analyse the proximal femurs of the mice to determine if deficiency of 11β-HSD1 protects against femoral bone loss as well as to determine the association between BMAT and bone loss with

ageing. The findings of Woods *et al.,* (2019) could be explained by the decrease in sex hormones, which might cause BMAT expansion and bone loss. However, they adjusted for circulatory oestradiol and testosterone concentration, but did not come across any associations between BMAT and bone loss (Woods *et al.*, 2019). Instead, a different publication found that trabecular bone loss in female mice is not associated with oestradiol, but potentially with GCs (Syed *et al.*, 2010). Therefore, the work of Woods *et al.,* (2019) would benefit from measuring circulatory GCs, as they could be significantly increased in the women and therefore influence the associations with bone loss.

As mentioned above, the lack of resistance in BMAT expansion and bone loss with ageing undermines the reasoning for adding more mice to the groups. The reason for the KOs not resisting BMAT expansion is still to be explored. Since the KO model still has circulating active corticosterone, a more efficient model that lacks complete GC action might be more efficient to test my hypothesis (further discussed below). In the CR study, only the male KOs resisted BMAT expansion with CR, which could potentially be due to altered progesterone. However, since mass spectrometry was not performed on the ageing mice in this chapter, it cannot be concluded if progesterone is involved in the effects on BMAT and bone. A decrease in progesterone has shown to inversely correlate with bone mass (Seifert-Klauss *et al.*, 2012), suggesting that the female mice might have decreased concentrations regardless of genotype. In addition, ageing has also been shown to be associated with inflammation, termed inflammaging (Franceschi and Campisi, 2014; Franceschi *et al.*, 2018). This causes an increase in circulatory GC concentrations (Sergio, 2008; Baylis *et al.*, 2013), potentially contributing to the pathological effects observed such as bone loss, increased BMAT and body adiposity. To determine if the observed results are due to age-induced GCs and/or inflammaging, inflammatory markers could be measured in the plasma such as IL-1β, IL-6/12/18, TNF-α, IFN-γ (pro-inflammatory) and TGF-β and IL-10 (anti-inflammatory). Corticosteroid binding globulin (CBG) could also be measured in the plasma to determine the amount of corticosterone that is bound by this protein. However, the corticosterone ELISA used in this thesis is provided with a steroid displacement reagent to release bound corticosterone to CBGs. Although, to compare between free and bound corticosterone, one could use a different ELISA to measure the free corticosterone and also do the assay for CBG measurement, if there would be enough plasma for

both assays. This would further address the hypothesis in this chapter by being able to draw more-accurate conclusions regarding GC availability and action. One could also assay 11β-HSD1 enzymatic activity in the BM from the control and older WT and KO mice, for example using assays that have previously been reported (Hardy *et al.*, 2007; Patel *et al.*, 2012; Morgan *et al.*, 2014; Loerz *et al.*, 2017).

Instead of adding more numbers to the 11β-HSD1 KOs, it would be interesting and potentially more productive to work on a different mouse model that robustly resists the effects of GCs, especially within the skeleton. For example, compared to WT mice, mice with conditional KO of the GR in osteoblasts resist the effects of GCs on bone formation (Rauch *et al.*, 2010); however, BMAT was not analysed in these mice. Furthermore, mice with a mutation that disrupts GR dimerization did not resist bone loss, and neither did mice lacking the GR in osteoclasts (Rauch *et al.*, 2010). Bone resorption was not changed in the osteoblast-specific GR KO mice, suggesting that GC-induced bone loss occurs by suppression of GC action in osteoblasts, reducing bone formation, rather than increasing bone resorption. Based on these results, I would not expect increased BM adiposity in the osteoblast-specific GR KO mice compared to the WT mice, although this remains to be determined. In addition, if BMAT would not differ between the genotypes in normal conditions, it would be interesting put these KOs on CR and quantify BMAT. Additional models that can resist the effect of excess GC could also be used to further address the hypothesis, for example 11β-HSD2 overexpression in mice on CR, or adrenalectomy to block circulating GCs. These options would further help to understand the function of BMAT with ageing, and potential inhibitors of 11β-HSD1 and/or GR, or overexpression of 11β-HSD2 for age-related bone loss. In addition, the correlation data in this Chapter are associations and do not imply cause and effect, but they do indicate that these are all related (GCs, bone and BMAT). Whether the same correlations would be expected for the CR cohort is still to be defined at a later point. It is also possible that these correlations have less to do with ageing, but more with the overall results and the link between GCs, BMAT and bone, either direct or indirect through factors such as progesterone, testosterone and other hormones.

Chapter 7. Discussion

7.1. Summary

The mechanism regulating BMAT expansion and bone loss during CR and with ageing remains incompletely understood. Therefore, the focus of this thesis was to investigate if GCs are mediators of CR- and/or ageing-induced BMAT expansion and bone loss.

In **Chapter 3**, I show that CR increases circulating and BM GC concentration. Furthermore, GC target genes are upregulated with CR in AT and BM. This suggests that GC action is increased with CR in AT and BM. In addition, *Hsd11b1* was significantly increased in the BM of 15-week-old, but not 10-week-old CR-fed WT mice. Moreover, *Hsd11b1* was not altered in the BM-free bones of the 15-week-old mice, suggesting that *Hsd11b1* could be a potential marker of increased BM adiposity, as BMAT was not increased in the 10-week-old mice (R. Sulston, unpublished data). Furthermore, *Hsd11b1* expression is highly expressed in subcutaneous WAT compared to stromal vascular fraction in obese patients. However, after weight loss, the expression is non-detectable in WAT, but unaltered in stromal vascular fraction (Methlie *et al.*, 2013). Moreover, other publications similarly showed increased *Hsd11b1* expression in subcutaneous and intraabdominal WAT compared to stromal vascular fraction (Gesta *et al.*, 2006), as well as increased *Hsd11b1* expression with adipogenesis (Cheung *et al.*, 2007). This supports my finding that *Hsd11b1* expression might be a marker of increased BM adiposity.

In **Chapter 4**, the main finding was that 11β-HSD1 activity is required for CR-induced BMAT expansion in males but not in females. In **Chapter 5** I found that CR causes cortical bone loss in males and females, with ANOVA showing a genotype effect, pointing towards greater cortical mass in KO males compared to WTs. However, an insignificant p value (p=0.0629) was detected between the CR-fed males. Based on the results, it is difficult to say whether the CR-fed KO males resist CR-induced bone loss or not, as the effects are not that robust. Therefore, further work is necessary to determine the effect of CR and 11β-HSD1 on cortical mass in KO males. If more mice are added to the groups, and the KO males do resist bone loss with CR, then it suggests that BMAT expansion might be required for CR-induced bone loss, at least in mice. If not, then it would suggest that BMAT expansion is not necessary for bone

loss. As previously mentioned, BMAT volume and bone loss are not always associated, for example rabbits on CR had bone loss without increased BMAT (Cawthorn *et al.*, 2016). The 15-week-old mice did not show increased GC action nor increased GC concentration, presumably due to fasting/re-feeding. The 10-week-old KOs did not resist increased GC target genes either. Overall, these findings suggest that the 11β-HSD1 KO model does not resist excess GCs. Therefore, based on my findings, progesterone was considered as an additional potential regulator of BMAT and bone during CR, which will be further discussed below in section 7.2.

Finally, in **Chapter 6** I found that BMAT volume increases with ageing, regardless of genotype. Furthermore, BMAT was positively associated with plasma corticosterone in females, but not males. Age-associated changes in trabecular and cortical bone were however associated with increased corticosterone concentration and BMAT expansion in both sexes. This suggests that GCs might be necessary for BMAT expansion in older females, but not in males.

Based on my overall findings, in the following sections I will discuss whether GCs are potential regulatory of BMAT expansion and bone loss during CR and ageing, as well as if the 11β-HSD1 KO model is the best model to test my hypothesis.

7.2. GCs as potential mediators of CR-and age-induced BMAT expansion and bone loss

Based on the findings in this thesis, further research is necessary to determine if GCs do or do not mediate CR-induced BMAT expansion and bone loss. Although an association was found between corticosterone and BMAT in KO males, this was not observed in females. Interestingly, the CR-fed KO males on one-week CR resisted increased corticosterone in the BM, suggesting a potential resistance to GC action and that tissue-specific corticosterone production might be necessary for BMAT expansion. Subsequently, for the older mice, I found an association between BMAT and corticosterone in female mice only. An explanation for the resistance in the increased corticosterone in the CR-fed KO males is that the AL-fed KOs already have CR-like concentrations of corticosterone. Therefore, if GCs drive BMAT expansion, the AL KO males should have greater BMAT volume than the AL-fed WT males. Based on the BMAT quantification, there is a near-significant p value (p=0.0881)

between the AL-fed males, with the KO males having a slightly greater BMAT volume than the WTs. Furthermore, the KOs did not resist the up-regulation of the GC target genes. For the older mice, LC-MS/MS was not performed. This would however be informative to do in the future to determine if the older mice have increased GCs in the plasma compared to the BM, and if the KO males maintain the increased progesterone with ageing. Although, since the KO males were heavier and fatter than the WTs, and obesity is associated with increased BMAT volume (Patel *et al.*, 2018), the increased body adiposity could explain the greater BMAT in the AL KO males. Overall, both the CR and ageing study revealed novel sex differences with regards to BMAT expansion and bone loss.

Based on the presented results, there is contradicting evidence for the KOs resisting CR-induced GCs and for GCs increasing BMAT with CR. Therefore, I thought the progesterone findings might explain some of the results since the GR and PR share a number of target genes (Wan and Nordeen, 2002) and also GCs and mineralocorticoids cross-talk with the PR to induce effects of progesterone *in vitro* (Leo *et al.*, 2004). Interestingly, progesterone was significantly increased in the 15- and 10-week-old KO males compared to females and WT males. This suggests that that progesterone might play a role in regulating CR-induced BMAT expansion and bone loss, dependently or independently of GCs, as previously discussed in Chapter 4. On the contrary, progesterone was also increased in CR-fed WT males in 10-week-old mice, and 15-week-old males showing a similar trend. Compared to the findings in the KOs, this supports the conclusion that progesterone might stimulate BMAT expansion, rather than suppressing it. However, no formal correlations were drawn between progesterone and other factors in Chapter 4, and no *in vitro* work was performed. Therefore, it cannot be concluded that progesterone does regulate BMAT expansion. Instead, it can be hypothesis that it plays a role, but further work is necessary to determine this. Although, for progesterone to stimulate BMAT expansion, it would suggest bone mass might decrease, or it might not be affected. This is in contrast to previous publications that have shown that progesterone promotes bone formation (Verhaar *et al.*, 1994; Seifert-Klauss and Prior, 2010) and is used to treat osteoporosis in menopausal women (Seifert-Klauss *et al.*, 2012; Prior, 2018). Thus, the idea that it would also stimulate BMAT formation would be intriguing, as to my knowledge no model or regulator has been proposed to subsequently expand BMAT and induce bone formation. Progesterone is the precursor to oestrogen

(Hanukoglu, 1992), and since oestrogen blocks BMAT expansion (Limonard *et al.*, 2015) and both hormones decrease in menopausal women, it would be postulated that progesterone would have similar effect on BMAT. However, that might be with ageing when the hormones decrease, but the effect of progesterone on BMAT in 15-week-old mice might differ with CR. Furthermore, progesterone predominantly stimulates osteoblast formation (Verhaar *et al.*, 1994; Seifert-Klauss and Prior, 2010) instead of adipocyte differentiation, which might explain the resistance in BMAT expansion in the KO males, and the minor bone loss resistance. Since the KO males had increased progesterone concentration, even compared to the females, it would explain why the females did not resist CR-induced bone loss. Progesterone also increases the number of alkaline phosphatase-expressing cells (marker of bone formation) in the lumbar vertebrae of both male and female rats (Ishida and Heersche, 1997). Although, progesterone did exert greater adipocyte differentiation in the female rats compared to the males (Ishida and Heersche, 1997). Overall, these findings suggest that progesterone is important for bone formation and this might explain the minor bone loss in the KO males. However, it does not explain the increased BMAT volume in the CR-fed WT mice with increased progesterone concentration compared to the AL-fed WT mice. Furthermore, osteoblasts express PR (Eriksen *et al.*, 1988; Wei *et al.*, 1993) and oestrogen can stimulate the PR (Ekka *et al.*, 1987; Quadros and Wagner, 2008). This suggests that certain effects on bone that are thought to be regulated by oestrogen, might be regulated by progesterone. Whether it is the same for BMAT expansion with CR and ageing in humans, or for ovariectomised animals, remains to be determined. Moreover, to understand the possible relationship between GCs, progesterone and oestrogen, it would be informative to quantify the expression of GR, MR, PR and ER by qPCR as well as *in vitro* experiments to determine the differentiation between the genotypes, diets and ageing and the addition of these hormones to the differentiated adipocyte and osteoblast cells. Based on this, it is possible that the decreased progesterone in the CR-fed females and WT males might have targeted the BMAds instead of the bone cells, and/or perhaps the progesterone was not significantly increased to target either in the AL-fed mice. On the other hand, the KO males had increased progesterone, unaltered BMAT and relatively unaltered bone mass.

Recent findings revealed different patterns of GC-androgen crosstalk in various metabolic tissues, for example in WAT and BAT, where the AR can stimulate

expression of GC target genes (Spaanderman *et al.*, 2019). These findings suggest that the expression of GC target genes, which were increased with CR, and the BMAT outcome could have been influenced by androgens. Herein, such GC-androgen crosstalk was not investigated in bone or BM, hence it can only be assumed that if it had an impact on WAT and BAT, it might also affect BMAT and its microenvironment since BMAT has been reported to have endocrine functions. Although several studies have confirmed the presence of both AR and ER in BM (Gruber *et al.*, 1999; Oreffo *et al.*, 1999; Mantalaris *et al.*, 2001; Bonnelye and Aubin, 2002), and AR KO mice have decreased bone formation and increased BMAT (Russell *et al.*, 2018). AR was not quantified in our study, hence, no conclusions can be drawn in regards to CR and 11β-HSD1 ablation in the BM. Although, testosterone concentration in plasma and BM was increased in CR-fed females, but decreased in CR-fed males. The 10-week-old KO males showed a greater decrease in testosterone concentration with CR compared to WTs, suggesting that testosterone might be necessary for BMAT expansion with CR. However, the results of Russell *et al.,* suggest that the lack of androgens allows for BMAT expansion. It is worth noting that the lack of AR might affect other hormones besides testosterone, hence the contradicting results. In addition, previous research has revealed that osteocalcin release stimulates testosterone proliferation which further stimulate bone growth and maintenance in male mice, but not females (Oury *et al.*, 2011). Therefore, the maintenance of trabecular bone mass, and very minor cortical bone loss with CR could have been maintained by increased circulatory osteocalcin. However, to determine whether this is the case, circulatory osteocalcin needs to be measured in CR mice. The same experiment could be implemented in the older mice, to determine if osteocalcin decreased with ageing and whether that is or is not associated with bone loss and increased BMAT. A key question arising from these findings regarding steroid hormones is whether GCs are indeed mediating CR-and age-induced BMAT expansion and, if so, are they doing it dependently or independently of other hormones such as progesterone?

7.3. Implications of BMAT expansion in disease

As previously reviewed in the introduction, increased BMAT and bone loss often coincide in different physiological and disease contexts (Section 1.2.2). Based on my findings, blocking 11β-HSD1 in men with AN and/or osteoporosis might be an option

to prevent BMAT expansion and potentially bone loss, since the KO males showed a potential resistance to bone loss. Pharmacological agents could be used for this (further discussed in section 7.4). Although, since the KO female mice did not resist BMAT expansion nor bone loss, this approach might not benefit women. However, it is important to note that the effects on mice with CR and ageing, are not always corresponding to humans. For example, the effects of GCs on BAT differ between human and mouse (Ramage *et al.*, 2016). An additional factor to consider is the progression of the disease, as the inhibition of 11β-HSD1 might be more beneficial prior to the disease becoming more adverse. The more adverse the disease is, the inhibition of 11β-HSD1 could worsen the side-effects. For example, the lack of 11β-HSD1 during rheumatoid arthritis enhances inflammation (Hardy *et al.*, 2018).

Furthermore, the role of BMAT during CR is still not fully known. Besides the associations with bone, where BMAT expansion and bone loss often coincide (but not always as previously mentioned), it remains to be explored if BMAT contributes to other effects of CR. Based on a recent study, it is possible that the effects of CR on immunity could be mediated by BMAT. Under basal conditions, WAT is the predominant hub for memory T cells, but during CR it declines. BMAT however expands during the same condition, promoting memory T cell accumulation within the BM (Collins *et al.*, 2019). While circulatory GCs were elevated, BM GC concentration was much lower at baseline and CR, similar to our findings. The high concentration of circulating GCs and the interaction between GCs and the GR on T cells could have affected the downfall of memory T cells in the circulation. Therefore, the lower concentration of GCs in the BM, could have promoted the T cell accumulation in the BM to protect the cells from the detrimental effects of GCs. An increase in red blood cells was also observed in the BM during CR, suggesting that this increase could have influenced the accumulation of memory T cells (Collins *et al.*, 2019). These findings highlight potential roles of BMAT expansion during CR and immunological memory preservation and function. BMAT has previously been reported to act as an endocrine organ due to the release of adiponectin (Cawthorn *et al.*, 2014). Now, these recent findings of Collins *et al.,* further confirm the BM as an endocrine organ responding to stress aimed at immunological memory. However, further work is necessary to understand the mediators involved in this process and how BM adiposity affects it during CR.

7.4. Future directions

There are several further lines of investigation that could be pursued to overcome some of the technical limitations and/or further address the conclusions of my thesis. In terms of experiments, quantifying circulating and BM oestradiol concentration would have aided interpretation of the progesterone data. Since progesterone was increased, I would expect similar results for oestradiol as progesterone ultimately converts into oestrogen, as well as other hormones (Hanukoglu, 1992). If so, this might also explain the minor lack in cortical bone loss in the CR-fed KO males, as BMAT volume and bone mass are often inversely correlated (Justesen *et al.*, 2001; Devlin *et al.*, 2010; Di Iorgi *et al.*, 2010; Fazeli *et al.*, 2013; Fazeli and Klibanski, 2019), and oestrogen inhibits BMAT expansion (Limonard *et al.*, 2015). Furthermore, Syed *et al.,* demonstrated that trabecular bone loss in female mice occurs independently of oestradiol, suggesting it is potentially more susceptible to GCs (Syed *et al.*, 2010). Compared to my results, based on the findings of Syed *et al.*, it suggests that the oestradiol concentration in the CR females might be low. Therefore, measuring plasma and BM oestradiol concentration in male and female mice would allow us to make a firmer conclusion regarding what is allowing the CR-fed KO males to resist BMAT expansion and possibly cortical bone loss. If BM oestradiol is not increased during CR, it could instead point towards progesterone as an independent regulator of BMAT expansion and bone loss. Although, it has been published that the combination of oestrogen and progesterone is more effective to prevent bone loss than oestrogen alone (Issar *et al.*, 2006; Seifert-Klauss *et al.*, 2012; Prior, 2018), but BMAT was not investigated. In addition, the relationship between circulatory progesterone and GC concentration has been reported during stress (Kalil *et al.*, 2013), with an increase in both hormones compared to non-stressed rats. This suggests that oestradiol might also be increased in conditions of stress, such as CR, mirroring the increased progesterone concentrations. To further test the progesterone finding, one could administer progesterone antagonists to the KO males. If such antagonists restore bone loss and BMAT expansion, this would support the identification of progesterone as a regulator of BMAT and bone loss. One caveat is that such antagonists might also indirectly influence the concentration and/or functions of GCs and/or oestradiol; hence, mass spectrometry would also need to be performed on plasma and BM to determine the concentrations of such hormones, to determine if they were influencing the BMAT and bone phenotype post-antagonism

of progesterone. In the older mice, corticosterone and BMAT were each correlated with age-induced bone loss. However, the lack of LC-MS/MS analysis in plasma and BM limits our ability to determine if progesterone also plays a part in this. Overall, in the CR study the increased BM and plasma progesterone concentrations in the KO males raises the possibility that, in this context, progesterone might have a protective effect to limit bone loss and BMAT expansion with CR. However, no correlations were drawn between bone parameters and the progesterone, and neither between progesterone/corticosterone and fat/lean mass. That could further give us more insight into the relationship between these hormones and adiposity and bone.

A disadvantage to using 11β-HSD1 KO mice is that they still have GCs. The intracellular regeneration of corticosterone is absent, but adrenal production of circulatory corticosterone is not. To overcome this, either a different KO model could be used, for example osteoblast GR KO model that has previously shown to resist effects of excess GCs on bone (Rauch *et al.*, 2010), as previously discussed in Chapter 4 and 6 (4.3.2 and 6.3.4, respectively). Adrenalectomy could also be performed. By removing the adrenal glands, the synthesis of corticosterone would stop and circulatory concentration would drop. This would allow us to investigate if BMAT expands during CR in the absence of circulatory and intracellular GCs and, perhaps even more importantly, if the adrenalectomised KO mice would survive on calorie deficit.

In the past our lab's protocol for qPCR from bone involved grinding up the whole bone and then assessing expression of adipocyte markers as a readout of BM adiposity (Cawthorn *et al.*, 2014; Sulston *et al.*, 2016). However, this does not distinguish gene expression between BM and bone. Therefore, in my PhD I optimised the protocol to flush out the BM and do qPCR on the BM alone, followed by the bone itself. This way, the results are more accurate for the gene expression in each tissue. However, there is one more possible optimisation that could be performed which includes isolating the BMAds and stromal cells from the BM. This would allow for even more precise quantification of target gene expression. A limitation with this is that a mouse bone is very small and several mouse bones might have to be pooled together for each group, which means more experimental mice and higher costs. Although, it is not impossible as it has been previously performed (Fan *et al.*, 2017). An additional experiment that would be intriguing to do would to sort and analyse the nuclei from BMAds (Wu *et al.*,

2019). Such single-cell approaches to characterise BMAds from AL- vs CR-fed mice would be interesting, as it would give us more information about BMAd function, potentially identify further BMAd subtypes, and reveal how CR impacts not just the amount of BMAT, but also the properties of BMAds on a single-cell level.

Pharmacological approaches could also be used to further address my hypothesis and strengthen my conclusions. For example, metyrapone, a steroidogenesis inhibitor that has previously been used to block adrenal GC production (Lorivel, Gras and Hilber, 2010; Murphy *et al.*, 2017). This drug could be used to inhibit GC synthesis in WT animals, and simultaneously have them on CR to investigate BMAT volume and bone morphology. A second option would be the GR antagonist RU486, which has previously been used to deteriorate adrenal steroidogenesis in patients with CS (Leo *et al.*, 2004; Johanssen and Allolio, 2007). Based on these agents, I would expect BMAT expansion to be blocked with CR and ageing, if indeed GCs are strong regulators of BMAT expansion. However, RU486 also targets the PR and AR, hence the results can once again be reflecting more than the effect of one hormone (Zhang, 2006; Raaijmakers, Versteegh and Uitdehaag, 2009). Moreover, progesterone antagonists could also be used to test the role of progesterone on CR-and ageing-induced BMAT expansion and bone loss as previously discussed in Chapter 4, section 4.3.3.

Regarding using a more robust KO model that lacks complete GC action would include the GR KO in osteoblasts, as previously discussed in Section 4.3.2 and 6.3.4. Briefly, this KO model resists the effects of GCs on bone loss (Rauch *et al.*, 2010). Using this KO model would benefit our current understanding and findings regarding the relationship between GCs, BMAT expansion and bone loss. A different model to consider would be the global knockout of Osx, which has previously been reported to suppresses adipogenesis via PPARγ *in vitro* (Han *et al.*, 2016). Furthermore, BM adipocytes have been reported to derive from progenitor cells expressing Osx (Chen *et al.*, 2014). Therefore, Osterix-Cre x *Pparg-floxed* KO mice may be one way to specifically ablate BMAT, but not other AT depots. If successful, this could be an ideal model to investigate the formation of BMAds and if Osx expressing cells are part of the BMAds formation. Furthermore, based on my findings that BMAT expansion might be necessary in CR-fed KO males to lose bone mass, I would also want to address if the lack of BMAT in Osterix-Cre x *Pparg-floxed* KO mice would prevent bone loss.

A recent publication used an Osx-Cre mouse model to investigate the role of GCs on BMAT during CR (Pierce *et al.*, 2019). However, there are some limitations to this study, which raises questions to how interpretable their results are. The mice had the GR deleted in the BM osteoprogenitors (Osx-Cre), and the control groups they used did not include a non-floxed Cre+. Since the Osx-Cre model already has a skeletal phenotype of delayed bone formation (Huang and Olsen, 2015; Wang, Mishina and Liu, 2015; Dallas *et al.*, 2018) the results of this study are difficult to interpret without including the non-floxed Cre+ controls. The authors argued this by saying that the skeletal phenotype is not present past 12 weeks (Davey *et al.*, 2012), and the mice they used were 6 months old. They reported that the AL-and CR-fed GR KO mice had reduced bone mass, but significantly increased BMAT compared to the controls. These results are contradicting every publication regarding GCs and BMAT volume, and regarding GC therapy in patients that show increased BMAT (Vande Berg *et al.*, 1999). Due to their results being the opposite of all previous publications, and their lack of use of an appropriate non-floxed Cre+ control group, it is difficult from this study to draw reliable conclusions about the role of GCs in CR-induced bone loss and BMAT expansion.

7.4. Conclusions

The most notable finding of my PhD research is that 11β-HSD1 KO confers resistance to CR-induced BMAT expansion in male mice, but not in females. However, it remains unclear if this is through blockade of GC action, or if other mechanisms are involved. Based on the CR and ageing study, the overall results suggest that there is an association in between GCs and BMAT expansions. However, considering some of my findings, such as the lack of increased GC action in WAT and BM with CR and ageing, as well as bone loss in all mice, less so in the CR-fed KO males and the increased progesterone concentration in the KO males, it is possible that GCs might not induce these effects alone and that other factors such as progesterone, oestradiol and/or testosterone are involved that might further influence the physiological and pathological implications of BMAT. From a clinical research perspective, it is important to investigate and disclose these mediators and pathways as they can be used to improve bone health in patients with AN, CS, osteoporosis and other bone diseases. Furthermore, targeting BMAT instead of the bone itself could be an alternative that might include less side effects, as bone loss.

Chapter 8. Bibliography

Abdallah, B. M. *et al.* (2004) 'Regulation of Human Skeletal Stem Cells Differentiation by Dlk1/Pref-1', *Journal of Bone and Mineral Research*, 19(5), pp. 841–852. doi: 10.1359/jbmr.040118.

Abella, E. *et al.* (2002) 'Bone Marrow Changes in Anorexia Nervosa Are Correlated With the Amount of Weight Loss and Not With Other Clinical Findings', *American Journal of Clinical Pathology*, 118(4), pp. 582–588. doi: 10.1309/2Y7X-YDXK-006B-XLT2.

Abizanda, P. *et al.* (2016) 'Energetics of Aging and Frailty: The FRADEA Study', *The Journals of Gerontology Series A: Biological Sciences and Medical Sciences*, 71(6), pp. 787–796. doi: 10.1093/gerona/glv182.

Abrahams, L. *et al.* (2012) 'Biomarkers of hypothalamic–pituitary–adrenal axis activity in mice lacking 11β-HSD1 and H6PDH', *Journal of Endocrinology*, 214(3), pp. 367–372. doi: 10.1530/JOE-12-0178.

Adler, B. J., Kaushansky, K. and Rubin, C. T. (2014) 'Obesity-driven disruption of haematopoiesis and the bone marrow niche', *Nature Reviews Endocrinology*, 10(12), pp. 737–748. doi: 10.1038/nrendo.2014.169.

Ahima, R. S. *et al.* (1996) 'Role of leptin in the neuroendocrine response to fasting', *Nature*, 382(6588), pp. 250–252. doi: 10.1038/382250a0.

Ahima, R. S. *et al.* (1997) 'Leptin accelerates the onset of puberty in normal female mice.', *Journal of Clinical Investigation*, 99(3), pp. 391–395. doi: 10.1172/JCI119172.

Ahima, R. S. (2008) 'Revisiting leptin's role in obesity and weight loss', *Journal of Clinical Investigation*, 118(7), pp. 2380–2383. doi: 10.1172/JCI36284.

Ahima, R. S. and Flier, J. S. (2000) 'Adipose Tissue as an Endocrine Organ', *Trends in Endocrinology & Metabolism*, 11(8), pp. 327–332. doi: 10.1016/S1043-2760(00)00301-5.

Allen, B. D. *et al.* (2019) 'Hyperadrenocorticism of calorie restriction contributes to its anti-inflammatory action in mice', *Aging Cell*, 18(3), p. e12944. doi: 10.1111/acel.12944.

Allen, J. E. *et al.* (1995) 'Fat Cells in Red Bone Marrow of Human Rib: Their Size and Spatial Distribution with Respect to the Radon-derived Dose to the Haemopoietic Tissue', *International Journal of Radiation Biology*, 68(6), pp. 669–678. doi: 10.1080/09553009514551681.

Ambrosi, T. H. *et al.* (2017) 'Adipocyte Accumulation in the Bone Marrow during Obesity and Aging Impairs Stem Cell-Based Hematopoietic and Bone Regeneration', *Cell Stem Cell*, 20(6), pp. 771-784.e6. doi: 10.1016/j.stem.2017.02.009.

Ambrosi, T. H. and Schulz, T. J. (2017) 'The emerging role of bone marrow adipose tissue in bone health and dysfunction', *Journal of Molecular Medicine*. Journal of Molecular Medicine, 95(12), pp. 1291–1301. doi: 10.1007/s00109-017-1604-7.

Amiche, M. A. *et al.* (2018) 'Impact of cumulative exposure to high-dose oral glucocorticoids on fracture risk in Denmark: a population-based case-control study', *Archives of Osteoporosis*, 13(1), p. 30. doi: 10.1007/s11657-018-0424-x.

Amling, M., Takeda, S. and Karsenty, G. (2000) 'A neuro (endo)crine regulation of bone remodeling', *BioEssays*, 22(11), pp. 970–975. doi: 10.1002/1521-1878(200011)22:11<970::AID-BIES3>3.0.CO;2-L.

Anagnostis, P. *et al.* (2009) 'The pathogenetic role of cortisol in the metabolic syndrome: A hypothesis', *Journal of Clinical Endocrinology and Metabolism*, 94(8), pp. 2692–2701. doi: 10.1210/jc.2009-0370.

Aquila, H., Link, T. A. and Klingenberg, M. (1985) 'The uncoupling protein from brown fat mitochondria is related to the mitochondrial ADP/ATP carrier. Analysis of sequence homologies and of folding of the protein in the membrane.', *The EMBO Journal*, 4(9), pp. 2369–2376. doi: 10.1002/j.1460-2075.1985.tb03941.x.

Arai, H. *et al.* (2008) 'A case of cortisol producing adrenal adenoma without phenotype of Cushing's syndrome due to impaired 11beta-hydroxysteroid dehydrogenase 1 activity.', *Endocrine journal*, 55(4), pp. 709–15. doi: 10.1507/endocrj.k08e-008.

de Araújo, I. M. *et al.* (2017) 'Marrow adipose tissue spectrum in obesity and type 2 diabetes mellitus', *European Journal of Endocrinology*, 176(1), pp. 21–30. doi: 10.1530/EJE-16-0448.

Arita, Y. *et al.* (1999) 'Paradoxical Decrease of an Adipose-Specific Protein, Adiponectin, in Obesity', *Biochemical and Biophysical Research Communications*, 257(1), pp. 79–83. doi: 10.1006/bbrc.1999.0255.

Arnaldi, G. *et al.* (2012) 'Advances in the epidemiology, pathogenesis, and management of Cushing's syndrome complications.', *Journal of endocrinological investigation*, 35(4), pp. 434–48. doi: 10.1007/BF03345431.

Baek, K. *et al.* (2008) 'Food restriction and simulated microgravity: effects on bone and serum leptin', *Journal of Applied Physiology*, 104(4), pp. 1086–1093. doi: 10.1152/japplphysiol.01209.2007.

Bailoo, J. D. *et al.* (2018) 'Effects of Cage Enrichment on Behavior, Welfare and

Outcome Variability in Female Mice', *Frontiers in Behavioral Neuroscience*, 12(October), pp. 1–20. doi: 10.3389/fnbeh.2018.00232.

Baum, T. *et al.* (2012) 'Does vertebral bone marrow fat content correlate with abdominal adipose tissue, lumbar spine bone mineral density, and blood biomarkers in women with type 2 diabetes mellitus?', *Journal of Magnetic Resonance Imaging*, 35(1), pp. 117–124. doi: 10.1002/jmri.22757.

Baylis, D. *et al.* (2013) 'Understanding how we age: insights into inflammaging', *Longevity & Healthspan*, 2(1), p. 8. doi: 10.1186/2046-2395-2-8.

Behrendt, A.-K. *et al.* (2016) 'Dietary Restriction-Induced Alterations in Bone Phenotype: Effects of Lifelong Versus Short-Term Caloric Restriction on Femoral and Vertebral Bone in C57BL/6 Mice', *Journal of Bone and Mineral Research*, 31(4), pp. 852–863. doi: 10.1002/jbmr.2745.

Bellows, C., Ciaccia, A. and Heersche, J. (1998) 'Osteoprogenitor cells in cell populations derived from mouse and rat calvaria differ in their response to corticosterone, cortisol, and cortisone1', *Bone*, 23(2), pp. 119–125. doi: 10.1016/S8756-3282(98)00084-2.

Berendsen, A. D. and Olsen, B. R. (2015) 'Bone development', *Bone*, 80(3), pp. 14–18. doi: 10.1016/j.bone.2015.04.035.

Berner, H. S. *et al.* (2004) 'Adiponectin and its receptors are expressed in bone-forming cells', *Bone*, 35(4), pp. 842–849. doi: 10.1016/j.bone.2004.06.008.

Berrebi, D. *et al.* (2003) 'Synthesis of glucocorticoid-induced leucine zipper (GILZ) by macrophages: An anti-inflammatory and immunosuppressive mechanism shared by glucocorticoids and IL-10', *Blood*, 101(2), pp. 729–738. doi: 10.1182/blood-2002-02-0538.

Berrigan, D. *et al.* (2005) 'Phenotypic effects of calorie restriction and insulin-like growth factor-1 treatment on body composition and bone mineral density of C57BL/6 mice: implications for cancer prevention.', *In vivo (Athens, Greece)*, 19(4), pp. 667–74.

Berry, D. C. *et al.* (2013) 'The developmental origins of adipose tissue', *Development*, 140(19), pp. 3939–3949. doi: 10.1242/dev.080549.

Bielohuby, M. *et al.* (2007) 'Growth analysis of the mouse adrenal gland from weaning to adulthood: time- and gender-dependent alterations of cell size and number in the cortical compartment', *American Journal of Physiology-Endocrinology and Metabolism*, 293(1), pp. E139–E146. doi: 10.1152/ajpendo.00705.2006.

Bigelow, C. L. and Tavassoli, M. (1984) 'Fatty Involution of Bone Marrow in Rabbits',

Cells Tissues Organs, 118(1), pp. 60–64. doi: 10.1159/000145823.

Binder, E. B. (2009) 'The role of FKBP5, a co-chaperone of the glucocorticoid receptor in the pathogenesis and therapy of affective and anxiety disorders', *Psychoneuroendocrinology*, 34(1), pp. S186–S195. doi: 10.1016/j.psyneuen.2009.05.021.

Bodkin, N. L. *et al.* (2003) 'Mortality and Morbidity in Laboratory-maintained Rhesus Monkeys and Effects of Long-term Dietary Restriction', *The Journals of Gerontology Series A: Biological Sciences and Medical Sciences*, 58(3), pp. B212–B219. doi: 10.1093/gerona/58.3.B212.

Bonnelye, E. and Aubin, J. E. (2002) 'Differential Expression of Estrogen Receptor-Related Receptor α and Estrogen Receptors α and β in Osteoblasts In Vivo and In Vitro', *Journal of Bone and Mineral Research*, 17(8), pp. 1392–1400. doi: 10.1359/jbmr.2002.17.8.1392.

Bosy-Westphal, A. *et al.* (2005) 'Determinants of plasma adiponectin levels in patients with anorexia nervosa examined before and after weight gain', *European Journal of Nutrition*, 44(6), pp. 355–359. doi: 10.1007/s00394-005-0533-3.

Botolin, S. *et al.* (2005) 'Increased bone adiposity and PPARγ2 expression in type I diabetic mice', *Endocrinology*, 146(8), pp. 3622–3631. doi: 10.1210/en.2004-1677.

Botolin, S. and McCabe, L. R. (2007) 'Bone loss and increased bone adiposity in spontaneous and pharmacologically induced diabetic mice', *Endocrinology*, 148(1), pp. 198–205. doi: 10.1210/en.2006-1006.

Bouxsein, M. L. *et al.* (2010) 'Guidelines for assessment of bone microstructure in rodents using micro-computed tomography', *Journal of Bone and Mineral Research*, 25(7), pp. 1468–1486. doi: 10.1002/jbmr.141.

Boyar, R. M. *et al.* (1977) 'Cortisol Secretion and Metabolism in Anorexia Nervosa', *New England Journal of Medicine*, 296(4), pp. 190–193. doi: 10.1056/NEJM197701272960403.

Brady, L. S. *et al.* (1990) 'Altered expression of hypothalamic neuropeptide mRNAs in food-restricted and food-deprived rats.', *Neuroendocrinology*, 52(5), pp. 441–7. doi: 10.1159/000125626.

Bravenboer, N. *et al.* (2019) 'Standardised Nomenclature, Abbreviations, and Units for the study of Bone Marrow Adiposity: Report of the Nomenclature Working Group of the International Bone Marrow Adiposity Society', *Frontiers in Endocrinology*.

Bredella, M. A. *et al.* (2009) 'Increased bone marrow fat in anorexia nervosa', *Journal of Clinical Endocrinology and Metabolism*, 94(6), pp. 2129–2136. doi:

10.1210/jc.2008-2532.

Bredella, M. A. *et al.* (2011) 'Vertebral Bone Marrow Fat Is Positively Associated With Visceral Fat and Inversely Associated With IGF-1 in Obese Women', *Obesity*, 19(1), pp. 49–53. doi: 10.1038/oby.2010.106.

Bredella, M. A. *et al.* (2014) 'Marrow fat composition in anorexia nervosa', *Bone*, 66, pp. 199–204. doi: 10.1016/j.bone.2014.06.014.

Bruley, C. *et al.* (2006) 'A novel promoter for the 11β-hydroxysteroid dehydrogenase type 1 gene is active in lung and is C/EBPα independent', *Endocrinology*, 147(6), pp. 2879–2885. doi: 10.1210/en.2005-1621.

Bruscoli, S. *et al.* (2015) 'Lack of glucocorticoid-induced leucine zipper (GILZ) deregulates B-cell survival and results in B-cell lymphocytosis in mice', *Blood*, 126(15), pp. 1790–1801. doi: 10.1182/blood-2015-03-631580.

Camhi, S. M. *et al.* (2011) 'The Relationship of Waist Circumference and BMI to Visceral, Subcutaneous, and Total Body Fat: Sex and Race Differences', *Obesity*, 19(2), pp. 402–408. doi: 10.1038/oby.2010.248.

Cangemi, R. *et al.* (2010) 'Long-term effects of calorie restriction on serum sex-hormone concentrations in men', *Aging Cell*, 9(2), pp. 236–242. doi: 10.1111/j.1474-9726.2010.00553.x.

Cannon, B. and Nederfaard, J. (2004) 'Brown Adipose Tissue: Function and Physiological Significance', *Physiological Reviews*, 84(1), pp. 277–359. doi: 10.1152/physrev.00015.2003.

Caratti, G. *et al.* (2015) 'Glucocorticoid receptor function in health and disease', *Clinical Endocrinology*, 83(4), pp. 441–448. doi: 10.1111/cen.12728.

Carter, R. N. *et al.* (2009) 'Hypothalamic-Pituitary-Adrenal Axis Abnormalities in Response to Deletion of 11β-HSD1 is Strain-Dependent', *Journal of Neuroendocrinology*, 21(11), pp. 879–887. doi: 10.1111/j.1365-2826.2009.01899.x.

Cassano, A. E. *et al.* (2012) 'Anatomic, hematologic, and biochemical features of C57BL/6NCrl mice maintained on chronic oral corticosterone', *Comparative Medicine*, 62(5), pp. 348–360.

Cawthorn, W. P. *et al.* (2014) 'Bone marrow adipose tissue is an endocrine organ that contributes to increased circulating adiponectin during caloric restriction', *Cell Metabolism*, 20(2), pp. 368–375. doi: 10.1016/j.cmet.2014.06.003.

Cawthorn, W. P. *et al.* (2016) 'Expansion of bone marrow adipose tissue during caloric restriction is associated with increased circulating glucocorticoids and not with hypoleptinemia', *Endocrinology*, 157(2), pp. 508–521. doi: 10.1210/en.2015-1477.

Chabbert-Buffet, N. *et al.* (2005) 'Selective progesterone receptor modulators and progesterone antagonists: mechanisms of action and clinical applications', *Human Reproduction Update*, 11(3), pp. 293–307. doi: 10.1093/humupd/dmi002.

Chacón, F. *et al.* (2005) '24-Hour Changes in ACTH, Corticosterone, Growth Hormone, and Leptin Levels in Young Male Rats Subjected to Calorie Restriction', *Chronobiology International*, 22(2), pp. 253–265. doi: 10.1081/CBI-200053522.

Chapman, K., Holmes, M. and Seckl, J. (2013) '11B-Hydroxysteroid Dehydrogenases: Intracellular Gate-Keepers of Tissue Glucocorticoid Action.', *Physiological reviews*, 93(3), pp. 1139–206. doi: 10.1152/physrev.00020.2012.

Chehab, F. F. (1997) 'Early Onset of Reproductive Function in Normal Female Mice Treated with Leptin', *Science*, 275(5296), pp. 88–90. doi: 10.1126/science.275.5296.88.

Chen, H. *et al.* (2010) 'Age- and gender-dependent changes in three-dimensional microstructure of cortical and trabecular bone at the human femoral neck', *Osteoporosis International*, 21(4), pp. 627–636. doi: 10.1007/s00198-009-0993-z.

Chen, J. *et al.* (2014) 'Osx-Cre targets multiple cell types besides osteoblast lineage in postnatal mice', *PLoS ONE*, 9(1), pp. 1–6. doi: 10.1371/journal.pone.0085161.

Cheng, Q. *et al.* (2013) 'GILZ Overexpression Inhibits Endothelial Cell Adhesive Function through Regulation of NF- B and MAPK Activity', *The Journal of Immunology*, 191(1), pp. 424–433. doi: 10.4049/jimmunol.1202662.

Cheung, K. J. *et al.* (2007) 'Xanthine Oxidoreductase Is a Regulator of Adipogenesis and PPARγ Activity', *Cell Metabolism*, 5(2), pp. 115–128. doi: 10.1016/j.cmet.2007.01.005.

Christiansen, B. A. *et al.* (2011) 'Mechanical contributions of the cortical and trabecular compartments contribute to differences in age-related changes in vertebral body strength in men and women assessed by QCT-based finite element analysis', *Journal of Bone and Mineral Research*, 26(5), pp. 974–983. doi: 10.1002/jbmr.287.

Chu, Y. *et al.* (2010) 'Epididymal Fat Is Necessary for Spermatogenesis, but not Testosterone Production or Copulatory Behavior', *Endocrinology*, 151(12), pp. 5669–5679. doi: 10.1210/en.2010-0772.

Cianflone, K., Xia, Z. and Chen, L. Y. (2003) 'Critical review of acylation-stimulating protein physiology in humans and rodents.', *Biochimica et biophysica acta*, 1609(2), pp. 127–43. doi: 10.1016/s0005-2736(02)00686-7.

Clark, B. J. *et al.* (1994) 'The purification, cloning, and expression of a novel luteinizing hormone-induced mitochondrial protein in MA-10 mouse Leydig tumor cells.

Characterization of the steroidogenic acute regulatory protein (StAR).', *The Journal of Biological Chemistry*, 269(45), pp. 28314–28322. doi: 7961770.

Coelho, M., Oliveira, T. and Fernandes, R. (2013) 'Biochemistry of adipose tissue: An endocrine organ', *Archives of Medical Science*, 9(2), pp. 191–200. doi: 10.5114/aoms.2013.33181.

Collins, N. *et al.* (2019) 'The Bone Marrow Protects and Optimizes Immunological Memory during Dietary Restriction', *Cell*. Elsevier Inc., 178(5), pp. 1088-1101.e15. doi: 10.1016/j.cell.2019.07.049.

Condon, J. *et al.* (1997) 'Ontogeny and sexual dimorphic expression of mouse type 2 11β-hydroxysteroid dehydrogenase', *Molecular and Cellular Endocrinology*, 127(2), pp. 121–128. doi: 10.1016/S0303-7207(97)04000-8.

Cooper, M. . *et al.* (2000) 'Expression and functional consequences of 11β-hydroxysteroid dehydrogenase activity in human bone', *Bone*, 27(3), pp. 375–381. doi: 10.1016/S8756-3282(00)00344-6.

Cooper, M. S. *et al.* (2001) 'Modulation of 11β-hydroxysteroid dehydrogenase isozymes by proinflammatory cytokines in osteoblasts: An autocrine switch from glucocorticoid inactivation to activation', *Journal of Bone and Mineral Research*, 16(6), pp. 1037–1044. doi: 10.1359/jbmr.2001.16.6.1037.

Cooper, M. S. *et al.* (2002) 'Osteoblastic 11β-Hydroxysteroid Dehydrogenase Type 1 Activity Increases With Age and Glucocorticoid Exposure', *Journal of Bone and Mineral Research*, 17(6), pp. 979–986. doi: 10.1359/jbmr.2002.17.6.979.

Cooper, M. S. *et al.* (2003) '11β-Hydroxysteroid Dehydrogenase Type 1 Activity Predicts the Effects of Glucocorticoids on Bone', *The Journal of Clinical Endocrinology & Metabolism*, 88(8), pp. 3874–3877. doi: 10.1210/jc.2003-022025.

Cooper, M. S. *et al.* (2005) 'Circulating cortisone levels are associated with biochemical markers of bone formation and lumbar spine BMD: the Hertfordshire Cohort Study', *Clinical Endocrinology*, 62(6), pp. 692–697. doi: 10.1111/j.1365-2265.2005.02281.x.

Cordes, C. *et al.* (2016) 'MR-Based Assessment of Bone Marrow Fat in Osteoporosis, Diabetes, and Obesity', *Frontiers in Endocrinology*, 7(June), pp. 1–7. doi: 10.3389/fendo.2016.00074.

Coutinho, A. E. (2009) *Consequences of 11b-hydroxysteroid dehydrogenase deficiency during inflammatory responses*. University of Edinburgh.

Coutinho, A. E. *et al.* (2012) '11B-Hydroxysteroid Dehydrogenase Type 1, But Not Type 2, Deficiency Worsens Acute Inflammation and Experimental Arthritis in Mice',

Endocrinology, 153(1), pp. 234–240. doi: 10.1210/en.2011-1398.

Coutinho, A. E. and Chapman, K. E. (2011) 'The anti-inflammatory and immunosuppressive effects of glucocorticoids, recent developments and mechanistic insights', *Molecular and Cellular Endocrinology*, 335(1), pp. 2–13. doi: 10.1016/j.mce.2010.04.005.

Craft, C. S. *et al.* (2018) 'Molecular differences between subtypes of bone marrow adipocytes.', *Current molecular biology reports*, 4(1), pp. 16–23. doi: 10.1007/s40610-018-0087-9.

Craft, C. S. and Scheller, E. L. (2017) 'Evolution of the Marrow Adipose Tissue Microenvironment', *Calcified Tissue International*, 100(5), pp. 461–475. doi: 10.1007/s00223-016-0168-9.

D'Adamio, F. *et al.* (1997) 'A new dexamethasone-induced gene of the leucine zipper family protects T lymphocytes from TCR/CD3-activated cell death', *Immunity*, 7(6), pp. 803–812. doi: 10.1016/S1074-7613(00)80398-2.

Dallas, S. L. *et al.* (2018) 'Mouse Cre Models for the Study of Bone Diseases', *Current Osteoporosis Reports*, 16(4), pp. 466–477. doi: 10.1007/s11914-018-0455-7.

Davey, R. A. *et al.* (2012) 'Decreased body weight in young Osterix-Cre transgenic mice results in delayed cortical bone expansion and accrual', *Transgenic Research*, 21(4), pp. 885–893. doi: 10.1007/s11248-011-9581-z.

Desbriere, R. *et al.* (2006) '11β-Hydroxysteroid Dehydrogenase Type 1 mRNA is Increased in Both Visceral and Subcutaneous Adipose Tissue of Obese Patients*', *Obesity*, 14(5), pp. 794–798. doi: 10.1038/oby.2006.92.

Devlin, M. J. *et al.* (2010) 'Caloric restriction leads to high marrow adiposity and low bone mass in growing mice', *Journal of Bone and Mineral Research*, 25(9), pp. 2078–2088. doi: 10.1002/jbmr.82.

Devlin, M. J. (2011) 'Why does starvation make bones fat?', *American Journal of Human Biology*, 23(5), pp. 577–585. doi: 10.1002/ajhb.21202.

Devlin, M. J. *et al.* (2016) 'Daily leptin blunts marrow fat but does not impact bone mass in calorie-restricted mice', *Journal of Endocrinology*, 229(3), pp. 295–306. doi: 10.1530/JOE-15-0473.

Devlin, M. J. and Rosen, C. J. (2015) 'The bone–fat interface: basic and clinical implications of marrow adiposity', *The Lancet Diabetes & Endocrinology*, 3(2), pp. 141–147. doi: 10.1016/S2213-8587(14)70007-5.

Diegel, C. R. *et al.* (2019) 'An Osteocalcin-deficient mouse strain without endocrine abnormalities', *bioRxiv*. doi: 10.1101/732800.

DiMascio, L. *et al.* (2007) 'Identification of Adiponectin as a Novel Hemopoietic Stem Cell Growth Factor', *The Journal of Immunology*, 178(6), pp. 3511–3520. doi: 10.4049/jimmunol.178.6.3511.

DiVasta, A. D. *et al.* (2011) 'Bioavailability of Vitamin D in Malnourished Adolescents with Anorexia Nervosa', *The Journal of Clinical Endocrinology & Metabolism*, 96(8), pp. 2575–2580. doi: 10.1210/jc.2011-0243.

Dolezalova, R. *et al.* (2007) 'Changes of endocrine function of adipose tissue in anorexia nervosa: comparison of circulating levels versus subcutaneous mRNA expression', *Clinical Endocrinology*, 67(5), pp. 674–678. doi: 10.1111/j.1365-2265.2007.02944.x.

Dong, M. *et al.* (2018) 'Role of brown adipose tissue in metabolic syndrome, aging, and cancer cachexia', *Frontiers of Medicine*, 12(2), pp. 130–138. doi: 10.1007/s11684-017-0555-2.

Dötsch, J. *et al.* (2001) 'Effect of glucocorticoid excess on the cortisol/cortisone ratio', *Steroids*, 66(11), pp. 817–820. doi: 10.1016/S0039-128X(01)00117-9.

Doucette, C. R. *et al.* (2015) 'A High Fat Diet Increases Bone Marrow Adipose Tissue (MAT) But Does Not Alter Trabecular or Cortical Bone Mass in C57BL/6J Mice', *Journal of Cellular Physiology*, 230(9), pp. 2032–2037. doi: 10.1002/jcp.24954.

Ducy, P. *et al.* (1996) 'Increased bone formation in osteocalcin-deficient mice.', *Nature*, 382(6590), pp. 448–52. doi: 10.1038/382448a0.

Ducy, P. *et al.* (2000) 'Leptin inhibits bone formation through a hypothalamic relay: a central control of bone mass.', *Cell*, 100(2), pp. 197–207. doi: 10.1016/s0092-8674(00)81558-5.

Duma, D. *et al.* (2010) 'Sexually Dimorphic Actions of Glucocorticoids Provide a Link to Inflammatory Diseases with Gender Differences in Prevalence', *Science Signaling*, 3(143), pp. ra74–ra74. doi: 10.1126/scisignal.2001077.

Ecklund, K. *et al.* (2010) 'Bone marrow changes in adolescent girls with anorexia nervosa', *Journal of Bone and Mineral Research*, 25(2), pp. 298–304. doi: 10.1359/jbmr.090805.

Ekka, E. *et al.* (1987) 'Estradiol-induced progesterone receptor synthesis in normal and diabetic ovariectomized rat uterus', *Journal of Steroid Biochemistry*, 28(1), pp. 61–64. doi: 10.1016/0022-4731(87)90125-7.

Elbaz, A., Rivas, D. and Duque, G. (2009) 'Effect of estrogens on bone marrow adipogenesis and Sirt1 in aging C57BL/6J mice', *Biogerontology*, 10(6), pp. 747–755. doi: 10.1007/s10522-009-9221-7.

Eriksen, E. *et al.* (1988) 'Evidence of estrogen receptors in normal human osteoblast-like cells', *Science*, 241(4861), pp. 84–86. doi: 10.1126/science.3388021.

Ersek, A. *et al.* (2016) 'Strain dependent differences in glucocorticoid-induced bone loss between C57BL/6J and CD-1 mice', *Scientific Reports*, 6(1), p. 36513. doi: 10.1038/srep36513.

Espelund, U. *et al.* (2005) 'Fasting Unmasks a Strong Inverse Association between Ghrelin and Cortisol in Serum: Studies in Obese and Normal-Weight Subjects', *The Journal of Clinical Endocrinology & Metabolism*, 90(2), pp. 741–746. doi: 10.1210/jc.2004-0604.

European Medicines Agency (2011) 'Guideline on bioanalytical method validation'.

Ewart-Toland, A. *et al.* (1999) 'Effect of the Genetic Background on the Reproduction of Leptin-Deficient Obese Mice*', *Endocrinology*, 140(2), pp. 732–738. doi: 10.1210/endo.140.2.6470.

Falank, C., Fairfield, H. H. and Reagan, M. R. (2016) 'Signaling interplay between Bone Marrow Adipose Tissue and Multiple Myeloma cells', *Frontiers in Endocrinology*, 7, pp. 1–15. doi: 10.3389/fendo.2016.00067.

Fan, C. *et al.* (2016) 'Combination chemotherapy with cyclophosphamide, epirubicin and 5-fluorouracil causes trabecular bone loss, bone marrow cell depletion and marrow adiposity in female rats', *Journal of Bone and Mineral Metabolism*, 34(3), pp. 277–290. doi: 10.1007/s00774-015-0679-x.

Fan, Y. *et al.* (2017) 'Parathyroid Hormone Directs Bone Marrow Mesenchymal Cell Fate', *Cell Metabolism*, 25(3), pp. 661–672. doi: 10.1016/j.cmet.2017.01.001.

Fazeli, P. K. *et al.* (2010) 'Preadipocyte Factor-1 Is Associated with Marrow Adiposity and Bone Mineral Density in Women with Anorexia Nervosa', *The Journal of Clinical Endocrinology & Metabolism*, 95(1), pp. 407–413. doi: 10.1210/jc.2009-1152.

Fazeli, P. K. *et al.* (2012) 'Marrow fat and preadipocyte factor-1 levels decrease with recovery in women with anorexia nervosa', *Journal of Bone and Mineral Research*, 27(9), pp. 1864–1871. doi: 10.1002/jbmr.1640.

Fazeli, P. K. *et al.* (2013) 'Marrow fat and bone-new perspectives', *Journal of Clinical Endocrinology and Metabolism*, 98(3), pp. 935–945. doi: 10.1210/jc.2012-3634.

Fazeli, P. K. and Klibanski, A. (2019) 'The paradox of marrow adipose tissue in anorexia nervosa', *Bone*. Elsevier Inc., 118, pp. 47–52. doi: 10.1016/j.bone.2018.02.013.

Feig, P. U. *et al.* (2011) 'Effects of an 11β-hydroxysteroid dehydrogenase type 1 inhibitor, MK-0916, in patients with type 2 diabetes mellitus and metabolic syndrome',

Diabetes, Obesity and Metabolism, 13(6), pp. 498–504. doi: 10.1111/j.1463-1326.2011.01375.x.

Feldman, K. *et al.* (2012) 'The rs4844880 polymorphism in the promoter region of the HSD11B1 gene associates with bone mineral density in healthy and postmenopausal osteoporotic women', *Steroids*, 77(13), pp. 1345–1351. doi: 10.1016/j.steroids.2012.08.014.

Fenton, C. G. *et al.* (2019) '11β-HSD1 plays a critical role in trabecular bone loss associated with systemic glucocorticoid therapy', *Arthritis Research & Therapy*. Arthritis Research & Therapy, 21(1), p. 188. doi: 10.1186/s13075-019-1972-1.

Ferraù, F. *et al.* (2019) 'High bone marrow fat in patients with Cushing's syndrome and vertebral fractures', *Endocrine*, pp. 1–8. doi: 10.1007/s12020-019-02034-4.

Ferron, M., Wei, J., Yoshizawa, T., Ducy, P., *et al.* (2010) 'An ELISA-based method to quantify osteocalcin carboxylation in mice', *Biochemical and Biophysical Research Communications*. United States, 397(4), pp. 691–696. doi: 10.1016/j.bbrc.2010.06.008.

Ferron, M., Wei, J., Yoshizawa, T., Del Fattore, A., *et al.* (2010) 'Insulin Signaling in Osteoblasts Integrates Bone Remodeling and Energy Metabolism', *Cell*, 142(2), pp. 296–308. doi: 10.1016/j.cell.2010.06.003.

Fontana, L. *et al.* (2004) 'Long-term calorie restriction is highly effective in reducing the risk for atherosclerosis in humans', *Proceedings of the National Academy of Sciences*, 101(17), pp. 6659–6663. doi: 10.1073/pnas.0308291101.

Fontana, L. *et al.* (2016) 'Effects of 2-year calorie restriction on circulating levels of IGF-1, IGF-binding proteins and cortisol in nonobese men and women: a randomized clinical trial', *Aging Cell*, 15(1), pp. 22–27. doi: 10.1111/acel.12400.

Franceschi, C. *et al.* (2018) 'Inflammaging: a new immune–metabolic viewpoint for age-related diseases', *Nature Reviews Endocrinology*, 14(10), pp. 576–590. doi: 10.1038/s41574-018-0059-4.

Franceschi, C. and Campisi, J. (2014) 'Chronic Inflammation (Inflammaging) and Its Potential Contribution to Age-Associated Diseases', *The Journals of Gerontology Series A: Biological Sciences and Medical Sciences*, 69(1), pp. S4–S9. doi: 10.1093/gerona/glu057.

Fulzele, K. *et al.* (2010) 'Insulin Receptor Signaling in Osteoblasts Regulates Postnatal Bone Acquisition and Body Composition', *Cell*, 142(2), pp. 309–319. doi: 10.1016/j.cell.2010.06.002.

Gao, Y. *et al.* (2015) 'Magnetic Resonance Imaging–Measured Bone Marrow Adipose

Tissue Area Is Inversely Related to Cortical Bone Area in Children and Adolescents Aged 5–18 Years', *Journal of Clinical Densitometry*, 18(2), pp. 203–208. doi: 10.1016/j.jocd.2015.03.002.

Gathercole, L. L. *et al.* (2013) '11β-Hydroxysteroid Dehydrogenase 1: Translational and Therapeutic Aspects', *Endocrine Reviews*, 34(4), pp. 525–555. doi: 10.1210/er.2012-1050.

Geer, E. B. *et al.* (2012) 'Body Composition and Cardiovascular Risk Markers after Remission of Cushing's Disease: A Prospective Study Using Whole-Body MRI', *The Journal of Clinical Endocrinology & Metabolism*, 97(5), pp. 1702–1711. doi: 10.1210/jc.2011-3123.

Geer, E. B., Islam, J. and Buettner, C. (2014) 'Mechanisms of Glucocorticoid-Induced Insulin Resistance', *Endocrinology and Metabolism Clinics of North America*, 43(1), pp. 75–102. doi: 10.1016/j.ecl.2013.10.005.

Geiser, F. *et al.* (2001) 'Magnetic Resonance Spectroscopic and Relaxometric Determination of Bone Marrow Changes in Anorexia Nervosa', *Psychosomatic Medicine*, 63(4), pp. 631–637. doi: 10.1097/00006842-200107000-00016.

Georgiou, K. R. *et al.* (2012) 'Methotrexate chemotherapy reduces osteogenesis but increases adipogenic potential in the bone marrow', *Journal of Cellular Physiology*, 227(3), pp. 909–918. doi: 10.1002/jcp.22807.

Georgiou, K. R., Hui, S. K. and Xian, C. J. (2012) 'Regulatory pathways associated with bone loss and bone marrow adiposity caused by aging, chemotherapy, glucocorticoid therapy and radiotherapy.', *American journal of stem cells*, 1(3), pp. 205–24.

Germain, N. *et al.* (2007) 'Constitutional thinness and lean anorexia nervosa display opposite concentrations of peptide YY, glucagon-like peptide 1, ghrelin, and leptin', *The American Journal of Clinical Nutrition*, 85(4), pp. 967–971. doi: 10.1093/ajcn/85.4.967.

Gesta, S. *et al.* (2006) 'Evidence for a role of developmental genes in the origin of obesity and body fat distribution', *Proceedings of the National Academy of Sciences*, 103(17), pp. 6676–6681. doi: 10.1073/pnas.0601752103.

Ghali, O. *et al.* (2016) 'Increased Bone Marrow Adiposity in a Context of Energy Deficit: The Tip of the Iceberg?', *Frontiers in endocrinology*, 7(September), p. 125. doi: 10.3389/fendo.2016.00125.

Gifford, R. M. *et al.* (2019) 'Positive adaptation of HPA axis function in women during 44 weeks of infantry-based military training', *Psychoneuroendocrinology*,

110(September), p. 104432. doi: 10.1016/j.psyneuen.2019.104432.

Giovannini, C. *et al.* (1990) 'Beta-Endorphin, Insulin, ACTH and Cortisol Plasma Levels during Oral Glucose Tolerance Test in Obesity after Weight Loss', *Hormone and Metabolic Research*, 22(02), pp. 96–100. doi: 10.1055/s-2007-1004859.

Goedecke, J. H. *et al.* (2006) 'Glucocorticoid metabolism within superficial subcutaneous rather than visceral adipose tissue is associated with features of the metabolic syndrome in South African women', *Clinical Endocrinology*, 65(1), pp. 81–87. doi: 10.1111/j.1365-2265.2006.02552.x.

Gokalp, G. *et al.* (2011) 'Evaluation of vertebral bone marrow fat content by chemical-shift MRI in osteoporosis', *Skeletal Radiology*, 40(5), pp. 577–585. doi: 10.1007/s00256-010-1048-4.

Grad, I. and Picard, D. (2007) 'The glucocorticoid responses are shaped by molecular chaperones', *Molecular and Cellular Endocrinology*, 275(1–2), pp. 2–12. doi: 10.1016/j.mce.2007.05.018.

Grauer, W. O. *et al.* (1984) 'Quantification of body fat distribution in the abdomen using computed tomography.', *The American Journal of Clinical Nutrition*, 39(4), pp. 631–7. doi: 10.1093/ajcn/39.4.631.

Grey, A. *et al.* (2012) 'Pioglitazone increases bone marrow fat in type 2 diabetes: results from a randomized controlled trial', *European Journal of Endocrinology*, 166(6), pp. 1087–1091. doi: 10.1530/EJE-11-1075.

Griffith, J. F. *et al.* (2005) 'Vertebral Bone Mineral Density, Marrow Perfusion, and Fat Content in Healthy Men and Men with Osteoporosis: Dynamic Contrast-enhanced MR Imaging and MR Spectroscopy', *Radiology*, 236(3), pp. 945–951. doi: 10.1148/radiol.2363041425.

Griffith, J. F. *et al.* (2006) 'Vertebral marrow fat content and diffusion and perfusion indexes in women with varying bone density: MR evaluation', *Radiology*, 241(3), pp. 831–838. doi: 10.1148/radiol.2413051858.

Griffith, J. F. *et al.* (2012) 'Bone marrow fat content in the elderly: A reversal of sex difference seen in younger subjects', *Journal of Magnetic Resonance Imaging*, 36(1), pp. 225–230. doi: 10.1002/jmri.23619.

Griffiths, W. J. and Wang, Y. (2019) 'Oxysterol research: a brief review', *Biochemical Society Transactions*, 47(2), pp. 517–526. doi: 10.1042/BST20180135.

Gruber, R. *et al.* (1999) 'Expression of the vitamin D receptor, of estrogen and thyroid hormone receptor α- and β-isoforms, and of the androgen receptor in cultures of native mouse bone marrow and of stromal/osteoblastic cells', *Bone*, 24(5), pp. 465–

473. doi: 10.1016/S8756-3282(99)00017-4.
de Guia, R. M., Rose, A. J. and Herzig, S. (2014) 'Glucocorticoid hormones and energy homeostasis', *Hormone Molecular Biology and Clinical Investigation*, 19(2), pp. 117–128. doi: 10.1515/hmbci-2014-0021.
Haagensen, A. L. *et al.* (2008) 'Low prevalence of vitamin D deficiency among adolescents with anorexia nervosa', *Osteoporosis International*, 19(3), pp. 289–294. doi: 10.1007/s00198-007-0476-z.
Hainer, V. *et al.* (1992) 'Effect of 4-wk treatment of obesity by very-low-calorie diet on anthropometric, metabolic, and hormonal indexes', *The American Journal of Clinical Nutrition*, 56(1), pp. 281S-282S. doi: 10.1093/ajcn/56.1.281S.
Hajek, A. *et al.* (2015) 'Prevalence and determinants of overweight and obesity in old age in Germany', *BMC Geriatrics*, 15(1), p. 83. doi: 10.1186/s12877-015-0081-5.
Hamrick, M. W. *et al.* (2004) 'Leptin deficiency produces contrasting phenotypes in bones of the limb and spine', *Bone*, 34(3), pp. 376–383. doi: 10.1016/j.bone.2003.11.020.
Hamrick, M. W. *et al.* (2005) 'Leptin Treatment Induces Loss of Bone Marrow Adipocytes and Increases Bone Formation in Leptin-Deficient ob/ob Mice', *Journal of Bone and Mineral Research*, 20(6), pp. 994–1001. doi: 10.1359/JBMR.050103.
Hamrick, M. W. *et al.* (2006) 'Injections of leptin into rat ventromedial hypothalamus increase adipocyte apoptosis in peripheral fat and in bone marrow', *Cell and Tissue Research*, 327(1), pp. 133–141. doi: 10.1007/s00441-006-0312-3.
Hamrick, M. W. *et al.* (2008) 'Caloric Restriction Decreases Cortical Bone Mass but Spares Trabecular Bone in the Mouse Skeleton: Implications for the Regulation of Bone Mass by Body Weight', *Journal of Bone and Mineral Research*, 23(6), pp. 870–878. doi: 10.1359/jbmr.080213.
Han, Y. *et al.* (2016) 'Osterix represses adipogenesis by negatively regulating PPARγ transcriptional activity', *Scientific Reports*. Nature Publishing Group, 6(October), pp. 1–11. doi: 10.1038/srep35655.
Handelsman, D. J. and Wartofsky, L. (2013) 'Requirement for Mass Spectrometry Sex Steroid Assays in the Journal of Clinical Endocrinology and Metabolism', *The Journal of Clinical Endocrinology & Metabolism*, 98(10), pp. 3971–3973. doi: 10.1210/jc.2013-3375.
Hanukoglu, I. (1992) 'Steroidogenic enzymes: Structure, function, and role in regulation of steroid hormone biosynthesis', *Journal of Steroid Biochemistry and Molecular Biology*, 43(8), pp. 779–804. doi: 10.1016/0960-0760(92)90307-5.

Hardie, L. *et al.* (1997) ‘Circulating leptin in women: A longitudinal study in the menstrual cycle and during pregnancy’, *Clinical Endocrinology*, 47(1), pp. 101–106. doi: 10.1046/j.1365-2265.1997.2441017.x.

Hardy, R. *et al.* (2007) ‘Local and systemic glucocorticoid metabolism in inflammatory arthritis’, *Annals of the Rheumatic Diseases*, 67(9), pp. 1204–1210. doi: 10.1136/ard.2008.090662.

Hardy, R. S. *et al.* (2016) ‘11β-Hydroxysteroid dehydrogenase type 1 within muscle protects against the adverse effects of local inflammation’, *The Journal of Pathology*, 240(4), pp. 472–483. doi: 10.1002/path.4806.

Hardy, R. S. *et al.* (2018) ‘11 Beta-hydroxysteroid dehydrogenase type 1 regulates synovitis, joint destruction, and systemic bone loss in chronic polyarthritis’, *Journal of Autoimmunity*, 92(May), pp. 104–113. doi: 10.1016/j.jaut.2018.05.010.

Harno, E. *et al.* (2013) ‘11-Dehydrocorticosterone Causes Metabolic Syndrome, Which Is Prevented when 11β-HSD1 Is Knocked Out in Livers of Male Mice’, *Endocrinology*, 154(10), pp. 3599–3609. doi: 10.1210/en.2013-1362.

Harris, H. J. *et al.* (2001) ‘Intracellular regeneration of glucocorticoids by 11beta-hydroxysteroid dehydrogenase (11beta-HSD)-1 plays a key role in regulation of the hypothalamic-pituitary-adrenal axis: analysis of 11beta-HSD-1-deficient mice.’, *Endocrinology*, 142(1), pp. 114–20. doi: 10.1210/endo.142.1.7887.

Harsløf, T. *et al.* (2011) ‘Rosiglitazone decreases bone mass and bone marrow fat’, *Journal of Clinical Endocrinology and Metabolism*, 96(5), pp. 1541–1548. doi: 10.1210/jc.2010-2077.

Hauner, H., Schmid, P. and Pfeiffer, E. F. (1987) ‘Glucocorticoids and insulin promote the differentiation of human adipocyte precursor cells into fat cells’, *Journal of Clinical Endocrinology and Metabolism*, 64(4), pp. 832–835. doi: 10.1210/jcem-64-4-832.

He, M. *et al.* (2016) ‘Effect of glucocorticoids on osteoclast function in a mouse model of bone necrosis’, *Molecular Medicine Reports*, 14(2), pp. 1054–1060. doi: 10.3892/mmr.2016.5368.

He, X. *et al.* (2018) ‘Age- and sex-related differences in body composition in healthy subjects aged 18 to 82 years’, *Medicine*, 97(25), p. e11152. doi: 10.1097/MD.0000000000011152.

Henneicke, H. *et al.* (2011) ‘Corticosterone selectively targets endo-cortical surfaces by an osteoblast-dependent mechanism’, *Bone*, 49(4), pp. 733–742. doi: 10.1016/j.bone.2011.06.013.

Hermanowski-Vosatka, A. *et al.* (2005) ‘11β-HSD1 inhibition ameliorates metabolic

syndrome and prevents progression of atherosclerosis in mice', *The Journal of Experimental Medicine*, 202(4), pp. 517–527. doi: 10.1084/jem.20050119.

Herroon, M. *et al.* (2013) 'Bone marrow adipocytes promote tumor growth in bone via FABP4-dependent mechanisms', *Oncotarget*, 4(11), pp. 2108–2123. doi: 10.18632/oncotarget.1482.

Heymsfield, S. B. *et al.* (1999) 'Recombinant leptin for weight loss in obese and lean adults: a randomized, controlled, dose-escalation trial.', *American Medical Association*, 282(16), pp. 1568–75. doi: 10.1001/jama.282.16.1568.

Himbert, C. *et al.* (2017) 'A systematic review of the interrelation between diet- and surgery-induced weight loss and vitamin D status', *Nutrition Research*, 38(801), pp. 13–26. doi: 10.1016/j.nutres.2016.12.004.

Ho, J. *et al.* (2007) 'Moderate Weight Loss Reduces Renin and Aldosterone but does not Influence Basal or Stimulated Pituitary-adrenal Axis Function', *Hormone and Metabolic Research*, 39(9), pp. 694–699. doi: 10.1055/s-2007-985354.

Holmes, M. C. *et al.* (2006) '11β-Hydroxysteroid dehydrogenase type 2 protects the neonatal cerebellum from deleterious effects of glucocorticoids', *Neuroscience*, 137(3), pp. 865–873. doi: 10.1016/j.neuroscience.2005.09.037.

Horowitz, M. C. *et al.* (2017) 'Bone marrow adipocytes', *Adipocyte*. Taylor & Francis, 6(3), pp. 193–204. doi: 10.1080/21623945.2017.1367881.

Houthoofd, K. *et al.* (2002) 'Axenic growth up-regulates mass-specific metabolic rate, stress resistance, and extends life span in Caenorhabditis elegans', *Experimental Gerontology*, 37(12), pp. 1369–1376. doi: 10.1016/S0531-5565(02)00173-0.

Hu, E., Liang, P. and Spiegelman, B. M. (1996) 'AdipoQ Is a Novel Adipose-specific Gene Dysregulated in Obesity', *Journal of Biological Chemistry*, 271(18), pp. 10697–10703. doi: 10.1074/jbc.271.18.10697.

Huang, W. and Olsen, B. R. (2015) 'Skeletal defects in Osterix-Cre transgenic mice', *Transgenic Research*, 24(1), pp. 167–172. doi: 10.1007/s11248-014-9828-6.

Hundertmark, S. *et al.* (1994) 'Gestational age dependence of 11β-hydroxysteroid dehydrogenase and its relationship to the enzymes of phosphatidylcholine synthesis in lung and liver of fetal rat', *Biochimica et Biophysica Acta (BBA) - Lipids and Lipid Metabolism*, 1210(3), pp. 348–354. doi: 10.1016/0005-2760(94)90239-9.

Hussain, Z. and Khan, J. A. (2017) 'Food intake regulation by leptin: Mechanisms mediating gluconeogenesis and energy expenditure', *Asian Pacific Journal of Tropical Medicine*, 10(10), pp. 940–944. doi: 10.1016/j.apjtm.2017.09.003.

Huttunen, P., Hirvonen, J. and Kinnula, V. (1981) 'The occurrence of brown adipose

tissue in outdoor workers', *European Journal of Applied Physiology and Occupational Physiology*, 46(4), pp. 339–345. doi: 10.1007/BF00422121.

Hwang, J.-Y. *et al.* (2009) 'HSD11B1 polymorphisms predicted bone mineral density and fracture risk in postmenopausal women without a clinically apparent hypercortisolemia', *Bone*, 45(6), pp. 1098–1103. doi: 10.1016/j.bone.2009.07.080.

Invitti, C. *et al.* (1999) 'Glucocorticoid receptors in anorexia nervosa and cushing's disease', *Biological Psychiatry*, 45(11), pp. 1467–1471. doi: 10.1016/S0006-3223(98)00189-9.

Di Iorgi, N. *et al.* (2008) 'Reciprocal relation between marrow adiposity and the amount of bone in the axial and appendicular skeleton of young adults', *Journal of Clinical Endocrinology and Metabolism*, 93(6), pp. 2281–2286. doi: 10.1210/jc.2007-2691.

Di Iorgi, N. *et al.* (2010) 'Bone acquisition in healthy young females is reciprocally related to marrow adiposity', *Journal of Clinical Endocrinology and Metabolism*, 95(6), pp. 2977–2982. doi: 10.1210/jc.2009-2336.

Ishida, Y. and Heersche, J. N. M. (1997) 'Progesterone stimulates proliferation and differentiation of osteoprogenitor cells in bone cell populations derived from adult female but not from adult male rats', *Bone*, 20(1), pp. 17–25. doi: 10.1016/S8756-3282(96)00315-8.

Issar, M. *et al.* (2006) 'Differences in the glucocorticoid to progesterone receptor selectivity of inhaled glucocorticoids.', *The European respiratory journal*, 27(3), pp. 511–6. doi: 10.1183/09031936.06.00060005.

Iwahashi, H. *et al.* (2003) 'Plasma Adiponectin Levels in Women with Anorexia Nervosa', *Hormone and Metabolic Research*, 35(9), pp. 537–540. doi: 10.1055/s-2003-42655.

Iwaniec, U. T. *et al.* (2016) 'Room temperature housing results in premature cancellous bone loss in growing female mice: implications for the mouse as a preclinical model for age-related bone loss', *Osteoporosis International*, 27(10), pp. 3091–3101. doi: 10.1007/s00198-016-3634-3.

James, S. L. *et al.* (2018) 'Global, regional, and national incidence, prevalence, and years lived with disability for 354 diseases and injuries for 195 countries and territories, 1990–2017: a systematic analysis for the Global Burden of Disease Study 2017', *The Lancet*, 392(10159), pp. 1789–1858. doi: 10.1016/S0140-6736(18)32279-7.

Jamieson, P. M. (1995) '11 Beta-Hydroxysteroid Dehydrogenase Is an Exclusive 11

Beta- Reductase in Primary Cultures of Rat Hepatocytes: Effect of Physicochemical and Hormonal Manipulations', *Endocrinology*, 136(11), pp. 4754–4761. doi: 10.1210/en.136.11.4754.

Jamieson, P. M., Chapman, K. E. and Seckl, J. R. (1999) 'Tissue- and temporal-specific regulation of 11β-hydroxysteroid dehydrogenase type 1 by glucocorticoids in vivo', *Journal of Steroid Biochemistry and Molecular Biology*, 68(5–6), pp. 245–250. doi: 10.1016/S0960-0760(99)00037-0.

Javed, A., Chen, H. and Ghori, F. Y. (2010) 'Genetic and Transcriptional Control of Bone Formation', *Oral and Maxillofacial Surgery Clinics of North America*, 22(3), pp. 283–293. doi: 10.1016/j.coms.2010.05.001.

Jia, D. *et al.* (2006) 'Glucocorticoids Act Directly on Osteoclasts to Increase Their Life Span and Reduce Bone Density', *Endocrinology*, 147(12), pp. 5592–5599. doi: 10.1210/en.2006-0459.

Johanssen, S. and Allolio, B. (2007) 'Mifepristone (RU 486) in Cushing's syndrome', *European Journal of Endocrinology*, 157(5), pp. 561–569. doi: 10.1530/EJE-07-0458.

Johnson, J. S. *et al.* (2017) '11β-hydroxysteroid dehydrogenase-1 deficiency alters the gut microbiome response to Western diet', *Journal of Endocrinology*, 232(2), pp. 273–283. doi: 10.1530/JOE-16-0578.

Johnstone, A. *et al.* (2004) 'Influence of short-term dietary weight loss on cortisol secretion and metabolism in obese men', *European Journal of Endocrinology*, 150(2), pp. 185–194. doi: 10.1530/eje.0.1500185.

Justesen, J. *et al.* (2001) 'Adipocyte tissue volume in bone marrow is increased with aging and in patients with osteoporosis.', *Biogerontology*, 2(3), pp. 165–71. doi: 10.1023/A.

Justesen, J. *et al.* (2004) 'Mice deficient in 11beta-hydroxysteroid dehydrogenase type 1 lack bone marrow adipocytes, but maintain normal bone formation', *Endocrinology*, 145(4), pp. 1916–1925. doi: 10.1210/en.2003-1427.

Kalil, B. *et al.* (2013) 'Role of sex steroids in progesterone and corticosterone response to acute restraint stress in rats: sex differences', *Stress*, 16(4), pp. 452–460. doi: 10.3109/10253890.2013.777832.

Karatsoreos, I. N. *et al.* (2010) 'Endocrine and physiological changes in response to chronic corticosterone: A potential model of the metabolic syndrome in mouse', *Endocrinology*, 151(5), pp. 2117–2127. doi: 10.1210/en.2009-1436.

Karsenty, G. (2001) 'Leptin controls bone formation through a hypothalamic relay.', *Recent progress in hormone research*. United States, 56, pp. 401–415. doi:

10.1210/rp.56.1.401.

Karsenty, G. (2006) ‘Convergence between bone and energy homeostases: Leptin regulation of bone mass’, *Cell Metabolism*, 4(5), pp. 341–348. doi: 10.1016/j.cmet.2006.10.008.

Karsenty, G. and Oury, F. (2014) ‘Regulation of male fertility by the bone-derived hormone osteocalcin’, *Molecular and Cellular Endocrinology*, 382(1), pp. 521–526. doi: 10.1016/j.mce.2013.10.008.

Katsimbri, P. (2017) ‘The biology of normal bone remodelling’, *European Journal of Cancer Care*, 26(6), p. e12740. doi: 10.1111/ecc.12740.

Kehler, D. S. (2019) ‘Age-related disease burden as a measure of population ageing’, *The Lancet Public Health*, 4(3), pp. e123–e124. doi: 10.1016/S2468-2667(19)30026-X.

Kenny, R. *et al.* (2014) ‘Effects of mild calorie restriction on anxiety and hypothalamic-pituitary-adrenal axis responses to stress in the male rat’, *Physiological Reports*, 2(3), p. e00265. doi: 10.1002/phy2.265.

Keune, J. A. *et al.* (2017) ‘Bone Marrow Adipose Tissue Deficiency Increases Disuse-Induced Bone Loss in Male Mice’, *Scientific Reports*, 7(1), p. 46325. doi: 10.1038/srep46325.

Khosla, S. *et al.* (2001) ‘Relationship of Serum Sex Steroid Levels to Longitudinal Changes in Bone Density in Young Versus Elderly Men’, *The Journal of Clinical Endocrinology & Metabolism*, 86(8), pp. 3555–3561. doi: 10.1210/jcem.86.8.7736.

Kim, H.-J. *et al.* (2006) ‘Glucocorticoids suppress bone formation via the osteoclast’, *The Journal of Clinical Investigation*, 116(8), pp. 2152–2160. doi: 10.1172/JCI28084DS1.

Kipari, T. *et al.* (2013) ‘11β-hydroxysteroid dehydrogenase type 1 deficiency in bone marrow-derived cells reduces atherosclerosis’, *The FASEB Journal*, 27(4), pp. 1519–1531. doi: 10.1096/fj.12-219105.

Kitajima, M. *et al.* (2007) ‘Effects of glucocorticoid on adipocyte size in human bone marrow’, *Medical Molecular Morphology*, 40(3), pp. 150–156. doi: 10.1007/s00795-007-0367-6.

Klar, R. M. (2018) ‘The Induction of Bone Formation: The Translation Enigma’, *Frontiers in Bioengineering and Biotechnology*, 6(JUN), pp. 1–13. doi: 10.3389/fbioe.2018.00074.

Klebanov, S. *et al.* (1995) ‘Hyperadrenocorticism, Attenuated Inflammation, and the Life-Prolonging Action of Food Restriction in Mice’, *The Journals of Gerontology*

Series A: Biological Sciences and Medical Sciences, 50A(2), pp. B78–B82. doi: 10.1093/gerona/50A.2.B78.

Kotelevtsev, Y. *et al.* (1997) '11 beta Hydroxysteroid dehydrogenase type 1 knockout mice show attenuated glucocorticoid-inducible responses and resist hyperglycemia on obesity or stress', *Proceedings of the National Academy of Sciences*, 94(26), pp. 14924–14929. doi: 10.1073/pnas.94.26.14924.

Kricun, M. E. (1985) 'Red-yellow marrow conversion: its effect on the location of some solitary bone lesions.', *Skeletal radiology*, 14, pp. 10–19. doi: 10.1007/BF00361188.

Laharrague, P. *et al.* (1998) 'High expression of leptin by human bone marrow adipocytes in primary culture', *The FASEB Journal*, 12(9), pp. 747–752. doi: 10.1096/fasebj.12.9.747.

Lakshmi, V. and Monder, C. (1988) 'Purification and characterization of the corticosteroid 11 beta-dehydrogenase component of the rat liver 11 beta-hydroxysteroid dehydrogenase complex.', *Endocrinology*, 123(5), pp. 2390–8. doi: 10.1210/endo-123-5-2390.

Larner, D. P. *et al.* (2016) 'Male 11β-HSD1 Knockout Mice Fed Trans-Fats and Fructose Are Not Protected From Metabolic Syndrome or Nonalcoholic Fatty Liver Disease', *Endocrinology*, 157(9), pp. 3493–3504. doi: 10.1210/en.2016-1357.

Latham, N. and Mason, G. (2004) 'From house mouse to mouse house: the behavioural biology of free-living Mus musculus and its implications in the laboratory', *Applied Animal Behaviour Science*, 86(3–4), pp. 261–289. doi: 10.1016/j.applanim.2004.02.006.

Lavery, G. G. *et al.* (2012) 'Lack of Significant Metabolic Abnormalities in Mice with Liver-Specific Disruption of 11β-Hydroxysteroid Dehydrogenase Type 1', *Endocrinology*, 153(7), pp. 3236–3248. doi: 10.1210/en.2012-1019.

Lawson, E. A. *et al.* (2009) 'Hypercortisolemia Is Associated with Severity of Bone Loss and Depression in Hypothalamic Amenorrhea and Anorexia Nervosa', *The Journal of Clinical Endocrinology & Metabolism*, 94(12), pp. 4710–4716. doi: 10.1210/jc.2009-1046.

Lecka-Czernik, B. *et al.* (2017) 'Marrow Adipose Tissue: Skeletal Location, Sexual Dimorphism, and Response to Sex Steroid Deficiency', *Frontiers in Endocrinology*, 8(AUG), pp. 1–12. doi: 10.3389/fendo.2017.00188.

Leclerc, N. *et al.* (2005) 'Glucocorticoids inhibit osteocalcin transcription in osteoblasts by suppressing Egr2/Krox20-binding enhancer', *Arthritis & Rheumatism*, 52(3), pp. 929–939. doi: 10.1002/art.20872.

Lee, A. M. C. *et al.* (2019) 'Individual or combination treatments with lapatinib and paclitaxel cause potential bone loss and bone marrow adiposity in rats', *Journal of Cellular Biochemistry*, 120(3), pp. 4180–4191. doi: 10.1002/jcb.27705.

Lee, M.-J. *et al.* (2011) 'Pathways regulated by glucocorticoids in omental and subcutaneous human adipose tissues: a microarray study', *American Journal of Physiology-Endocrinology and Metabolism*, 300(3), pp. E571–E580. doi: 10.1152/ajpendo.00231.2010.

Lee, M. J. *et al.* (2008) 'Depot-specific regulation of the conversion of cortisone to cortisol in human adipose tissue', *Obesity*, 16(6), pp. 1178–1185. doi: 10.1038/oby.2008.207.

Lee, N. K. *et al.* (2007) 'Endocrine Regulation of Energy Metabolism by the Skeleton', *Cell*, 130(3), pp. 456–469. doi: 10.1016/j.cell.2007.05.047.

Legroux-Gérot, I. *et al.* (2007) 'Evaluation of Bone Loss and Its Mechanisms in Anorexia Nervosa', *Calcified Tissue International*, 81(3), pp. 174–182. doi: 10.1007/s00223-007-9038-9.

Lei, K. *et al.* (2012) 'Progesterone acts via the nuclear glucocorticoid receptor to suppress IL-1β-induced COX-2 expression in human term myometrial cells.', *PloS one*, 7(11), p. e50167. doi: 10.1371/journal.pone.0050167.

Lenherr-Taube, N. *et al.* (2020) 'Low PTH Levels in Adolescents With Anorexia Nervosa', *Frontiers in Pediatrics*, 8(March), pp. 1–7. doi: 10.3389/fped.2020.00099.

Leo, J. C. L. *et al.* (2004) 'Glucocorticoid and Mineralocorticoid Cross-Talk with Progesterone Receptor to Induce Focal Adhesion and Growth Inhibition in Breast Cancer Cells', *Endocrinology*, 145(3), pp. 1314–1321. doi: 10.1210/en.2003-0732.

Lepper, C. and Fan, C. M. (2010) 'Inducible lineage tracing of Pax7-descendant cells reveals embryonic origin of adult satellite cells', *Genesis*, 48(7), pp. 424–436. doi: 10.1002/dvg.20630.

Levay, E. A. *et al.* (2010) 'Calorie restriction at increasing levels leads to augmented concentrations of corticosterone and decreasing concentrations of testosterone in rats', *Nutrition Research*, 30(5), pp. 366–373. doi: 10.1016/j.nutres.2010.05.001.

Li, G.-W. *et al.* (2013) 'The temporal characterization of marrow lipids and adipocytes in a rabbit model of glucocorticoid-induced osteoporosis', *Skeletal Radiology*, 42(9), pp. 1235–1244. doi: 10.1007/s00256-013-1659-7.

Li, X. *et al.* (2010) 'Mild Calorie Restriction Induces Fat Accumulation in Female C57BL/6J Mice', *Obesity*, 18(3), pp. 456–462. doi: 10.1038/oby.2009.312.

Lian, J. B. *et al.* (1998) 'Osteocalcin gene promoter: unlocking the secrets for

regulation of osteoblast growth and differentiation.', *Journal of Cellular Biochemistry*, 30–31, pp. 62–72. Available at: http://www.ncbi.nlm.nih.gov/pubmed/9893257.

Limonard, E. J. *et al.* (2015) 'Short-Term Effect of Estrogen on Human Bone Marrow Fat', *Journal of Bone and Mineral Research*, 30(11), pp. 2058–2066. doi: 10.1002/jbmr.2557.

Lin, G. L. and Hankenson, K. D. (2011) 'Integration of BMP, Wnt, and notch signaling pathways in osteoblast differentiation', *Journal of Cellular Biochemistry*, 112(12), pp. 3491–3501. doi: 10.1002/jcb.23287.

Lin, L., Dai, S.-D. and Fan, G.-Y. (2010) 'Glucocorticoid-induced differentiation of primary cultured bone marrow mesenchymal cells into adipocytes is antagonized by exogenous Runx2.', *APMIS*, 118(8), pp. 595–605. doi: 10.1111/j.1600-0463.2010.02634.x.

Lin, S. J., Defossez, P. A. and Guarente, L. (2000) 'Requirement of NAD and SIR2 for life-span extension by calorie restriction in Saccharomyces cerevisiae.', *Science*, 289(5487), pp. 2126–8. doi: 10.1126/science.289.5487.2126.

Lindblom, J. *et al.* (2005) 'Differential regulation of nuclear receptors, neuropeptides and peptide hormones in the hypothalamus and pituitary of food restricted rats', *Molecular Brain Research*, 133(1), pp. 37–46. doi: 10.1016/j.molbrainres.2004.09.025.

Liu, L.-F. *et al.* (2011) 'Characterization of age-related gene expression profiling in bone marrow and epididymal adipocytes', *BMC Genomics*, 12(1), p. 212. doi: 10.1186/1471-2164-12-212.

Liu, L. *et al.* (2013) 'Age-Related Modulation of the Effects of Obesity on Gene Expression Profiles of Mouse Bone Marrow and Epididymal Adipocytes', *PLoS ONE*, 8(8), p. e72367. doi: 10.1371/journal.pone.0072367.

Liu, Y. *et al.* (2003) 'Leptin Activation of Corticosterone Production in Hepatocytes May Contribute to the Reversal of Obesity and Hyperglycemia in Leptin-Deficient ob/ob Mice', *Diabetes*, 52(6), pp. 1409–1416. doi: 10.2337/diabetes.52.6.1409.

Liu, Y. *et al.* (2013) 'Osterix-Cre Labeled Progenitor Cells Contribute to the Formation and Maintenance of the Bone Marrow Stroma', *PLoS ONE*, 8(8). doi: 10.1371/journal.pone.0071318.

Livingstone, D. E. W. *et al.* (2000) 'Understanding the Role of Glucocorticoids in Obesity: Tissue-Specific Alterations of Corticosterone Metabolism in Obese Zucker Rats1', *Endocrinology*, 141(2), pp. 560–563. doi: 10.1210/endo.141.2.7297.

LoCascio, V. *et al.* (1990) 'Bone loss in response to long-term glucocorticoid therapy',

Bone and Mineral, 8(1), pp. 39–51. doi: 10.1016/0169-6009(91)90139-Q.

Loerz, C. *et al.* (2017) 'Regulation of 11β-hydroxysteroid dehydrogenase type 1 following caloric restriction and re-feeding is species dependent', *Chemico-Biological Interactions*, 276, pp. 95–104. doi: 10.1016/j.cbi.2017.02.018.

Lönn L, Kvist H, Ernest I, S. L. (1994) 'Changes in Body Composition and Adipose Tissue Distribution After Treatment of Women With Cushing's Syndrome', *Metabolism*, 43(12), pp. 1517–1522.

Lorentzon, R., Alehagen, U. and Boquist, L. (1986) 'Osteopenia in mice with genetic diabetes', *Diabetes Research and Clinical Practice*, 2(3), pp. 157–163. doi: 10.1016/S0168-8227(86)80017-1.

Lorivel, T., Gras, M. and Hilber, P. (2010) 'Effects of corticosterone synthesis inhibitor metyrapone on anxiety-related behaviors in Lurcher mutant mice', *Physiology and Behavior*, 101(2), pp. 309–314. doi: 10.1016/j.physbeh.2010.05.011.

Luz Neto, L. M. da *et al.* (2019) 'Differences in cortisol concentrations in adolescents with eating disorders: a systematic review', *Jornal de Pediatria*, 95(1), pp. 18–26. doi: 10.1016/j.jped.2018.02.007.

Machann, J. *et al.* (2005) 'Age and gender related effects on adipose tissue compartments of subjects with increased risk for type 2 diabetes: A whole body MRI/MRS study', *Magnetic Resonance Materials in Physics, Biology and Medicine*, 18(3), pp. 128–137. doi: 10.1007/s10334-005-0104-x.

Maeda, K. *et al.* (1996) 'cDNA Cloning and Expression of a Novel Adipose Specific Collagen-like Factor, apM1 (AdiposeMost Abundant Gene Transcript 1)', *Biochemical and Biophysical Research Communications*, 221(2), pp. 286–289. doi: 10.1006/bbrc.1996.0587.

Mantalaris, A. *et al.* (2001) 'Localization of androgen receptor expression in human bone marrow.', *The Journal of pathology*, 193(3), pp. 361–6. doi: 10.1002/1096-9896(0000)9999:9999<::AID-PATH803>3.0.CO;2-W.

Masoro, E. J., Yu, B. P. and Bertrand, H. A. (1982) 'Action of food restriction in delaying the aging process.', *Proceedings of the National Academy of Sciences of the United States of America*, 79(13), pp. 4239–41. doi: 10.1073/pnas.79.13.4239.

Masuzaki, H. (2001) 'A Transgenic Model of Visceral Obesity and the Metabolic Syndrome', *Science*, 294(5549), pp. 2166–2170. doi: 10.1126/science.1066285.

Masuzaki, H. *et al.* (2003) 'Transgenic amplification of glucocorticoid action in adipose tissue causes high blood pressure in mice', *Journal of Clinical Investigation*, 112(1), pp. 83–90. doi: 10.1172/JCI200317845.

Mattiucci, D. *et al.* (2018) 'Bone marrow adipocytes support hematopoietic stem cell survival', *Journal of Cellular Physiology*, 233(2), pp. 1500–1511. doi: 10.1002/jcp.26037.

Maurice, F. *et al.* (2018) 'Active Cushing syndrome patients have increased ectopic fat deposition and bone marrow fat content compared to cured patients and healthy subjects: A pilot 1H-MRS study', *European Journal of Endocrinology*, 179(5), pp. 1–31. doi: 10.1530/EJE-18-0318.

Mauriège, P. *et al.* (1999) 'Regional and gender variations in adipose tissue lipolysis in response to weight loss.', *Journal of lipid research*, 40(9), pp. 1559–71.

Mayo-Smith, W. *et al.* (1989) 'Intravertebral fat measurement with quantitative CT in patients with Cushing disease and anorexia nervosa.', *Radiology*, 170(3), pp. 835–838. doi: 10.1148/radiology.170.3.2916039.

Methlie, P. *et al.* (2013) 'Changes in adipose glucocorticoid metabolism before and after bariatric surgery assessed by direct hormone measurements', *Obesity*, 21(12), pp. 2495–2503. doi: 10.1002/oby.20449.

Meunier, P. *et al.* (1971) 'Osteoporosis and the replacement of cell populations of the marrow by adipose tissue. A quantitative study of 84 iliac bone biopsies.', *Clinical orthopaedics and related research*, 80, pp. 147–154. doi: 10.1097/00003086-197110000-00021.

Meyer, T. E. *et al.* (2006) 'Long-term caloric restriction ameliorates the decline in diastolic function in humans', *Journal of the American College of Cardiology*, 47(2), pp. 398–402. doi: 10.1016/j.jacc.2005.08.069.

Michailidou, Z., Jensen, M. D., *et al.* (2007) 'Omental 11β-hydroxysteroid dehydrogenase 1 correlates with fat cell size independently of obesity', *Obesity*, 15(5), pp. 1155–1163. doi: 10.1038/oby.2007.618.

Michailidou, Z., Coll, A. P., *et al.* (2007) 'Peripheral mechanisms contributing to the glucocorticoid hypersensitivity in proopiomelanocortin null mice treated with corticosterone.', *The Journal of Endocrinology*, 194(1), pp. 161–70. doi: 10.1677/JOE-07-0090.

Michalakis, K. *et al.* (2013) 'The complex interaction between obesity, metabolic syndrome and reproductive axis: A narrative review', *Metabolism*, 62(4), pp. 457–478. doi: 10.1016/j.metabol.2012.08.012.

Misra, M. *et al.* (2004) 'Alterations in Cortisol Secretory Dynamics in Adolescent Girls with Anorexia Nervosa and Effects on Bone Metabolism', *The Journal of Clinical Endocrinology & Metabolism*, 89(10), pp. 4972–4980. doi: 10.1210/jc.2004-0723.

Misra, M. *et al.* (2005) 'Ghrelin and Bone Metabolism in Adolescent Girls with Anorexia Nervosa and Healthy Adolescents', *The Journal of Clinical Endocrinology & Metabolism*, 90(9), pp. 5082–5087. doi: 10.1210/jc.2005-0512.

Misra, M. *et al.* (2006) 'Nutrient intake in community-dwelling adolescent girls with anorexia nervosa and in healthy adolescents', *The American Journal of Clinical Nutrition*, 84(4), pp. 698–706. doi: 10.1093/ajcn/84.4.698.

Mistry, S. D. *et al.* (2018) 'Sex hormones are negatively associated with vertebral bone marrow fat', *Bone*, 108(3), pp. 20–24. doi: 10.1016/j.bone.2017.12.009.

Mitchell, S. E. *et al.* (2015) 'The effects of graded levels of calorie restriction: I. impact of short term calorie and protein restriction on body composition in the C57BL/6 mouse', *Oncotarget*, 6(18), pp. 15902–30. doi: 10.18632/oncotarget.4142.

Mittelstadt, P. R. and Ashwell, J. D. (2001) 'Inhibition of AP-1 by the Glucocorticoid-inducible Protein GILZ', *Journal of Biological Chemistry*, 276(31), pp. 29603–29610. doi: 10.1074/jbc.M101522200.

Mlinar, B. *et al.* (2011) 'Expression of 11β-hydroxysteroid dehydrogenase type 1 in visceral and subcutaneous adipose tissues of patients with polycystic ovary syndrome is associated with adiposity', *The Journal of Steroid Biochemistry and Molecular Biology*, 123(3–5), pp. 127–132. doi: 10.1016/j.jsbmb.2010.12.002.

Modan-Moses, D. *et al.* (2007) 'Modulation of adiponectin and leptin during refeeding of female anorexia nervosa patients', *Journal of Clinical Endocrinology and Metabolism*, 92(5), pp. 1843–1847. doi: 10.1210/jc.2006-1683.

Mohamad, N. V., Soelaiman, I.-N. and Chin, K.-Y. (2016) 'A concise review of testosterone and bone health', *Clinical Interventions in Aging*, Volume 11, pp. 1317–1324. doi: 10.2147/CIA.S115472.

Moisan, M. P., Edwards, C. R. and Seckl, J. R. (1992) 'Differential promoter usage by the rat 11 beta-hydroxysteroid dehydrogenase gene.', *Molecular Endocrinology*, 6(7), pp. 1082–1087. doi: 10.1210/mend.6.7.1508221.

Monteleone, P. *et al.* (2008) 'Plasma Obestatin, Ghrelin, and Ghrelin/Obestatin Ratio Are Increased in Underweight Patients with Anorexia Nervosa But Not in Symptomatic Patients with Bulimia Nervosa', *The Journal of Clinical Endocrinology & Metabolism*, 93(11), pp. 4418–4421. doi: 10.1210/jc.2008-1138.

Moonen, M. P. B., Nascimento, E. B. M. and van Marken Lichtenbelt, W. D. (2019) 'Human brown adipose tissue: Underestimated target in metabolic disease?', *Biochimica et Biophysica Acta (BBA) - Molecular and Cell Biology of Lipids*, 1864(1), pp. 104–112. doi: 10.1016/j.bbalip.2018.05.012.

Morgan, S. A. *et al.* (2014) '11 -HSD1 is the major regulator of the tissue-specific effects of circulating glucocorticoid excess', *Proceedings of the National Academy of Sciences*, 111(24), pp. E2482–E2491. doi: 10.1073/pnas.1323681111.

Morgan, S. A., Hassan-Smith, Z. K. and Lavery, G. G. (2016) 'Mechanisms in endocrinology: Tissue-specific activation of cortisol in Cushing's syndrome', *European Journal of Endocrinology*, 175(2), pp. R81–R87. doi: 10.1530/EJE-15-1237.

Morton, N. M. *et al.* (2001) 'Improved Lipid and Lipoprotein Profile, Hepatic Insulin Sensitivity, and Glucose Tolerance in 11β-Hydroxysteroid Dehydrogenase Type 1 Null Mice', *Journal of Biological Chemistry*, 276(44), pp. 41293–41300. doi: 10.1074/jbc.M103676200.

Morton, N. M. *et al.* (2004) 'Novel adipose tissue-mediated resistance to diet-induced visceral obesity in 11 beta-hydroxysteroid dehydrogenase type 1-deficient mice.', *Diabetes*, 53(4), pp. 931–8. doi: 10.2337/diabetes.53.4.931.

Morton, N. M. *et al.* (2005) 'A Polygenic Model of the Metabolic Syndrome With Reduced Circulating and Intra-Adipose Glucocorticoid Action', *Diabetes*, 54(12), pp. 3371–3378. doi: 10.2337/diabetes.54.12.3371.

Mostoufi-Moab, S. *et al.* (2015) 'Adverse Fat Depots and Marrow Adiposity Are Associated With Skeletal Deficits and Insulin Resistance in Long-Term Survivors of Pediatric Hematopoietic Stem Cell Transplantation', *Journal of Bone and Mineral Research*, 30(9), pp. 1657–1666. doi: 10.1002/jbmr.2512.

Murphy, M. O. *et al.* (2017) 'Postnatal treatment with metyrapone attenuates the effects of diet-induced obesity in female rats exposed to early-life stress', *American Journal of Physiology - Endocrinology and Metabolism*, 312(2), pp. E98–E108. doi: 10.1152/ajpendo.00308.2016.

Muruganandan, S., Govindarajan, R. and Sinal, C. J. (2018) 'Bone Marrow Adipose Tissue and Skeletal Health', *Current Osteoporosis Reports*, 16(4), pp. 434–442. doi: 10.1007/s11914-018-0451-y.

Muzumdar, R. *et al.* (2008) 'Visceral adipose tissue modulates mammalian longevity', *Aging Cell*, 7(3), pp. 438–440. doi: 10.1111/j.1474-9726.2008.00391.x.

Nakamura, T. *et al.* (2007) 'Estrogen Prevents Bone Loss via Estrogen Receptor α and Induction of Fas Ligand in Osteoclasts', *Cell*, 130(5), pp. 811–823. doi: 10.1016/j.cell.2007.07.025.

Nakano, Y. *et al.* (1996) 'Isolation and Characterization of GBP28, a Novel Gelatin-Binding Protein Purified from Human Plasma', *Journal of Biochemistry*, 120(4), pp.

803–812. doi: 10.1093/oxfordjournals.jbchem.a021483.
Narita, T. *et al.* (2018) 'Differential response to caloric restriction of retroperitoneal, epididymal, and subcutaneous adipose tissue depots in rats', *Experimental Gerontology*, 104(July 2017), pp. 127–137. doi: 10.1016/j.exger.2018.01.016.
Naveiras, O. *et al.* (2009) 'Bone-marrow adipocytes as negative regulators of the haematopoietic microenvironment', *Nature*, 460(7252), pp. 259–263. doi: 10.1038/nature08099.
Newton, A. *et al.* (2013) 'The relationships among total body fat, bone mineral content and bone marrow adipose tissue in early-pubertal girls', *BoneKEy Reports*, 2(4), pp. 1–7. doi: 10.1038/bonekey.2013.49.
O'Brien, C. A. *et al.* (2004) 'Glucocorticoids Act Directly on Osteoblasts and Osteocytes to Induce Their Apoptosis and Reduce Bone Formation and Strength', *Endocrinology*, 145(4), pp. 1835–1841. doi: 10.1210/en.2003-0990.
Obri, A. *et al.* (2018) 'Osteocalcin in the brain: from embryonic development to age-related decline in cognition', *Nature Reviews Endocrinology*, 14(3), pp. 174–182. doi: 10.1038/nrendo.2017.181.
Oreffo, R. O. C. *et al.* (1999) 'Expression of estrogen receptor-alpha in cells of the osteoclastic lineage', *Histochemistry and Cell Biology*, 111(2), pp. 125–133. doi: 10.1007/s004180050342.
Oskis, A. *et al.* (2012) 'Diurnal patterns of salivary cortisol and DHEA in adolescent anorexia nervosa', *Stress*, 15(6), pp. 601–607. doi: 10.3109/10253890.2012.661493.
Oury, F. *et al.* (2011) 'Endocrine Regulation of Male Fertility by the Skeleton', *Cell*, 144(5), pp. 796–809. doi: 10.1016/j.cell.2011.02.004.
Pankevich, D. E. *et al.* (2010) 'Caloric Restriction Experience Reprograms Stress and Orexigenic Pathways and Promotes Binge Eating', *Journal of Neuroscience*, 30(48), pp. 16399–16407. doi: 10.1523/JNEUROSCI.1955-10.2010.
Pansini, V. *et al.* (2014) '3 Tesla 1 H MR spectroscopy of hip bone marrow in a healthy population, assessment of normal fat content values and influence of age and sex', *Journal of Magnetic Resonance Imaging*, 39(2), pp. 369–376. doi: 10.1002/jmri.24176.
Pantoja, C., Huff, J. T. and Yamamoto, K. R. (2008) 'Glucocorticoid Signaling Defines a Novel Commitment State during Adipogenesis In Vitro', *Molecular Biology of the Cell*, 19(10), pp. 4032–4041. doi: 10.1091/mbc.e08-04-0420.
Park, J. S. *et al.* (2014) 'A novel 11β-HSD1 inhibitor improves diabesity and osteoblast differentiation', *Journal of Molecular Endocrinology*, 52(2), pp. 191–202. doi:

10.1530/JME-13-0177.

Pasiakos, S. M. *et al.* (2011) 'Appetite and Endocrine Regulators of Energy Balance After 2 Days of Energy Restriction: Insulin, Leptin, Ghrelin, and DHEA-S', *Obesity*, 19(6), pp. 1124–1130. doi: 10.1038/oby.2010.316.

Paszynska, E. *et al.* (2016) 'Salivary alpha-amylase, secretory IgA and free cortisol as neurobiological components of the stress response in the acute phase of anorexia nervosa', *The World Journal of Biological Psychiatry*, 17(4), pp. 266–273. doi: 10.3109/15622975.2016.1163419.

Patel, N. V. and Finch, C. E. (2002) 'The glucocorticoid paradox of caloric restriction in slowing brain aging', *Neurobiology of Aging*, 23(5), pp. 707–717. doi: 10.1016/S0197-4580(02)00017-9.

Patel, P. *et al.* (2012) 'Expression of 11β-hydroxysteroid dehydrogenase enzymes in human osteosarcoma: potential role in pathogenesis and as targets for treatments', *Endocrine-Related Cancer*, 19(4), pp. 589–598. doi: 10.1530/ERC-12-0079.

Patel, V. S. *et al.* (2018) 'Marrow Adiposity and Hematopoiesis in Aging and Obesity: Exercise as an Intervention', *Current Osteoporosis Reports*, 16(2), pp. 105–115. doi: 10.1007/s11914-018-0424-1.

Paterson, J. M. *et al.* (2004) 'Metabolic syndrome without obesity: Hepatic overexpression of 11 -hydroxysteroid dehydrogenase type 1 in transgenic mice', *Proceedings of the National Academy of Sciences*, 101(18), pp. 7088–7093. doi: 10.1073/pnas.0305524101.

Patsch, J. M. *et al.* (2013) 'Bone marrow fat composition as a novel imaging biomarker in postmenopausal women with prevalent fragility fractures', *Journal of Bone and Mineral Research*, 28(8), pp. 1721–1728. doi: 10.1002/jbmr.1950.

Paulmyer-Lacroix, O. *et al.* (2002) 'Expression of the mRNA coding for 11β-hydroxysteroid dehydrogenase type 1 in adipose tissue from obese patients: An in situ hybridization study', *Journal of Clinical Endocrinology and Metabolism*, 87(6), pp. 2701–2705. doi: 10.1210/jc.87.6.2701.

Pereira, M. J. *et al.* (2014) 'FKBP5 expression in human adipose tissue increases following dexamethasone exposure and is associated with insulin resistance', *Metabolism: Clinical and Experimental*. Elsevier B.V., 63(9), pp. 1198–1208. doi: 10.1016/j.metabol.2014.05.015.

Perry, R. J. *et al.* (2014) 'Leptin reverses diabetes by suppression of the hypothalamic-pituitary- adrenal axis', *Nature Medicine*, 20(7), pp. 759–763. doi: 10.1038/nm.3579.

Petrovic, N. *et al.* (2010) 'Chronic Peroxisome Proliferator-activated Receptor γ (PPARγ) Activation of Epididymally Derived White Adipocyte Cultures Reveals a Population of Thermogenically Competent, UCP1-containing Adipocytes Molecularly Distinct from Classic Brown Adipocytes', *Journal of Biological Chemistry*, 285(10), pp. 7153–7164. doi: 10.1074/jbc.M109.053942.

Phillips, K. J. (2019) 'Beige Fat, Adaptive Thermogenesis, and Its Regulation by Exercise and Thyroid Hormone', *Biology*, 8(3), p. 57. doi: 10.3390/biology8030057.

Piccinin, M. A. and Khan, Z. A. (2014) 'Pathophysiological role of enhanced bone marrow adipogenesis in diabetic complications', *Adipocyte*, 3(4), pp. 263–272. doi: 10.4161/adip.32215.

Pierce, J. L. *et al.* (2019) 'The glucocorticoid receptor in osteoprogenitors regulates bone mass and marrow fat', *Journal of Endocrinology*, 243(1), pp. 27–42. doi: 10.1530/JOE-19-0230.

Pop, L. M. *et al.* (2017) 'Impact of pioglitazone on bone mineral density and bone marrow fat content', *Osteoporosis International*, 28(11), pp. 3261–3269. doi: 10.1007/s00198-017-4164-3.

Porter, M. H. *et al.* (2004) 'Sexual dimorphism in the response of adipose mass and cellularity to graded caloric restriction', *Obesity Research*, 12(1), pp. 131–140. doi: 10.1038/oby.2004.18.

Prior, J. C. (2018) 'Progesterone for the prevention and treatment of osteoporosis in women', *Climacteric*, 21(4), pp. 366–374. doi: 10.1080/13697137.2018.1467400.

Purnell, J. Q. *et al.* (2004) 'Association of 24-Hour Cortisol Production Rates, Cortisol-Binding Globulin, and Plasma-Free Cortisol Levels with Body Composition, Leptin Levels, and Aging in Adult Men and Women', *The Journal of Clinical Endocrinology & Metabolism*, 89(1), pp. 281–287. doi: 10.1210/jc.2003-030440.

Putignano, P. *et al.* (2001) 'Salivary cortisol measurement in normal-weight, obese and anorexic women: comparison with plasma cortisol', *European Journal of Endocrinology*, 145(2), pp. 165–171. doi: 10.1530/eje.0.1450165.

Quadros, P. S. and Wagner, C. K. (2008) 'Regulation of Progesterone Receptor Expression by Estradiol Is Dependent on Age, Sex and Region in the Rat Brain', *Endocrinology*, 149(6), pp. 3054–3061. doi: 10.1210/en.2007-1133.

Quinn, M. A. and Cidlowski, J. A. (2016) 'Endogenous hepatic glucocorticoid receptor signaling coordinates sex-biased inflammatory gene expression', *The FASEB Journal*, 30(2), pp. 971–982. doi: 10.1096/fj.15-278309.

Raaijmakers, H. C. A., Versteegh, J. E. and Uitdehaag, J. C. M. (2009) 'The X-ray

Structure of RU486 Bound to the Progesterone Receptor in a Destabilized Agonistic Conformation', *Journal of Biological Chemistry*, 284(29), pp. 19572–19579. doi: 10.1074/jbc.M109.007872.

Racette, S. B. *et al.* (2006) 'One year of caloric restriction in humans: feasibility and effects on body composition and abdominal adipose tissue.', *The journals of gerontology. Series A, Biological sciences and medical sciences*, 61(9), pp. 943–50. doi: 10.1093/gerona/61.9.943.

Ramage, L. E. *et al.* (2016) 'Glucocorticoids Acutely Increase Brown Adipose Tissue Activity in Humans, Revealing Species-Specific Differences in UCP-1 Regulation', *Cell Metabolism*, 24(1), pp. 130–141. doi: 10.1016/j.cmet.2016.06.011.

Rask, E. *et al.* (2001) 'Tissue-Specific Dysregulation of Cortisol Metabolism in Human Obesity', *The Journal of Clinical Endocrinology & Metabolism*, 86(3), pp. 1418–1421. doi: 10.1210/jcem.86.3.7453.

Rask, E. *et al.* (2002) 'Tissue-Specific Changes in Peripheral Cortisol Metabolism in Obese Women: Increased Adipose 11β-Hydroxysteroid Dehydrogenase Type 1 Activity', *The Journal of Clinical Endocrinology & Metabolism*, 87(7), pp. 3330–3336. doi: 10.1210/jcem.87.7.8661.

Rauch, A. *et al.* (2010) 'Glucocorticoids suppress bone formation by attenuating osteoblast differentiation via the monomeric glucocorticoid receptor', *Cell Metabolism*, 11(6), pp. 517–531. doi: 10.1016/j.cmet.2010.05.005.

Reddy, T. E. *et al.* (2012) 'The Hypersensitive Glucocorticoid Response Specifically Regulates Period 1 and Expression of Circadian Genes', *Molecular and Cellular Biology*, 32(18), pp. 3756–3767. doi: 10.1128/MCB.00062-12.

Redman, L. M. *et al.* (2007) 'Effect of Calorie Restriction with or without Exercise on Body Composition and Fat Distribution', *The Journal of Clinical Endocrinology & Metabolism*, 92(3), pp. 865–872. doi: 10.1210/jc.2006-2184.

Reynolds, R. M. *et al.* (2005) 'Cortisol Secretion and Rate of Bone Loss in a Population-Based Cohort of Elderly Men and Women', *Calcified Tissue International*, 77(3), pp. 134–138. doi: 10.1007/s00223-004-0270-2.

Rharass and Lucas (2018) 'MECHANISMS IN ENDOCRINOLOGY: Bone marrow adiposity and bone, a bad romance?', *European Journal of Endocrinology*, 179(4), pp. R165–R182. doi: 10.1530/EJE-18-0182.

Rivier, C. and Vale, W. (1983) 'Modulation of stress-induced ACTH release by corticotropin-releasing factor, catecholamines and vasopressin', *Nature*, pp. 325–327. doi: 10.1038/305325a0.

Rodriguez-Cuenca, S. *et al.* (2005) 'Depot differences in steroid receptor expression in adipose tissue: possible role of the local steroid milieu', *American Journal of Physiology-Endocrinology and Metabolism*, 288(1), pp. E200–E207. doi: 10.1152/ajpendo.00270.2004.

Roldan-Valadez, E. *et al.* (2013) 'Gender and age groups interactions in the quantification of bone marrow fat content in lumbar spine using 3T MR spectroscopy: A multivariate analysis of covariance (Mancova)', *European Journal of Radiology*, 82(11), pp. e697–e702. doi: 10.1016/j.ejrad.2013.07.012.

Ronchetti, S., Migliorati, G. and Riccardi, C. (2015) 'GILZ as a Mediator of the Anti-Inflammatory Effects of Glucocorticoids', *Frontiers in Endocrinology*, 6(NOV), pp. 1–6. doi: 10.3389/fendo.2015.00170.

Rosen, E. D. and Spiegelman, B. M. (2014) 'What We Talk About When We Talk About Fat', *Cell*, 156(1–2), pp. 20–44. doi: 10.1016/j.cell.2013.12.012.

Rosenstock, J. *et al.* (2010) 'The 11- beta -Hydroxysteroid Dehydrogenase Type 1 Inhibitor INCB13739 Improves Hyperglycemia in Patients With Type 2 Diabetes Inadequately Controlled by Metformin Monotherapy', *Diabetes Care*, 33(7), pp. 1516–1522. doi: 10.2337/dc09-2315.

von Ruesten, A. *et al.* (2011) 'Trend in Obesity Prevalence in European Adult Cohort Populations during Follow-up since 1996 and Their Predictions to 2015', *PLoS ONE*, 6(11), p. e27455. doi: 10.1371/journal.pone.0027455.

Russell, P. K. *et al.* (2018) 'The androgen receptor in bone marrow progenitor cells negatively regulates fat mass', *Journal of Endocrinology*, 237(1), pp. 15–27. doi: 10.1530/JOE-17-0656.

Sabatino, F. *et al.* (1991) 'Assessment of the role of the glucocorticoid system in aging processes and in the action of food restriction', *Journals of Gerontology*, 46(5), pp. 171–179. doi: 10.1093/geronj/46.5.B171.

Sabin, F. R. *et al.* (1936) 'Changes in the bone marrow and blood cells of developing rabbits', *The Journal of experimental medicine*, 64(1), pp. 97–120. doi: 10.1084/jem.64.1.97.

Scheller, E. L. *et al.* (2015) 'Region-specific variation in the properties of skeletal adipocytes reveals regulated and constitutive marrow adipose tissues', *Nature Communications*, 6(1), p. 7808. doi: 10.1038/ncomms8808.

Scheller, E. L. *et al.* (2016) 'Marrow Adipose Tissue: Trimming the Fat', *Trends in Endocrinology & Metabolism*, 27(6), pp. 392–403. doi: 10.1016/j.tem.2016.03.016.

Scheller, E. L. *et al.* (2019) 'Bone marrow adipocytes resist lipolysis and remodeling

in response to β-adrenergic stimulation', *Bone*, 118, pp. 32–41. doi: 10.1016/j.bone.2018.01.016.

Scheller, E. L. and Rosen, C. J. (2014) 'What's the matter with MAT? Marrow adipose tissue, metabolism, and skeletal health', *Annals of the New York Academy of Sciences*, 1311(1), pp. 14–30. doi: 10.1111/nyas.12327.

Schellinger, D. *et al.* (2001) 'Potential value of vertebral proton MR spectroscopy in determining bone weakness.', *American Journal of Neuroradiology*, 22(8), pp. 1620–7.

Schellinger, D. *et al.* (2004) 'Bone Marrow Fat and Bone Mineral Density on Proton MR Spectroscopy and Dual-Energy X-Ray Absorptiometry: Their Ratio as a New Indicator of Bone Weakening', *American Journal of Roentgenology*, 183(6), pp. 1761–1765. doi: 10.2214/ajr.183.6.01831761.

Scherer, P. E. *et al.* (1995) 'A Novel Serum Protein Similar to C1q, Produced Exclusively in Adipocytes', *Journal of Biological Chemistry*, 270(45), pp. 26746–26749. doi: 10.1074/jbc.270.45.26746.

Schubring, C. *et al.* (1998) 'Longitudinal analysis of maternal serum leptin levels during pregnancy, at birth and up to six weeks after birth: Relation to body mass index, skinfolds, sex steroids and umbilical cord blood leptin levels', *Hormone Research*, 50(5), pp. 276–283. doi: 10.1159/000023290.

Schwartz, A. V. *et al.* (2013) 'Vertebral bone marrow fat associated with lower trabecular BMD and prevalent vertebral fracture in older adults', *Journal of Clinical Endocrinology and Metabolism*, 98(6), pp. 2294–2300. doi: 10.1210/jc.2012-3949.

Schwartz, A. V. and Sellmeyer, D. E. (2007) 'Thiazolidinediones: New Evidence of Bone Loss', *The Journal of Clinical Endocrinology & Metabolism*, 92(4), pp. 1232–1234. doi: 10.1210/jc.2007-0328.

Seifert-Klauss, V. *et al.* (2012) 'Progesterone and bone: a closer link than previously realized', *Climacteric*, 15(1), pp. 26–31. doi: 10.3109/13697137.2012.669530.

Seifert-Klauss, V. and Prior, J. C. (2010) 'Progesterone and Bone: Actions Promoting Bone Health in Women', *Journal of Osteoporosis*, 2010, pp. 1–18. doi: 10.4061/2010/845180.

Seimon, R. V. *et al.* (2013) 'Effects of energy restriction on activity of the hypothalamo-pituitary-adrenal axis in obese humans and rodents: implications for diet-induced changes in body composition', *Hormone Molecular Biology and Clinical Investigation*, 15(2), pp. 71–80. doi: 10.1515/hmbci-2013-0038.

Semjonous, N. M. *et al.* (2011) 'Hexose-6-Phosphate Dehydrogenase Contributes to

Skeletal Muscle Homeostasis Independent of 11β-Hydroxysteroid Dehydrogenase Type 1', *Endocrinology*, 152(1), pp. 93–102. doi: 10.1210/en.2010-0957.

Sergio, G. (2008) 'Exploring the complex relations between inflammation and aging (inflamm-aging): anti-inflamm-aging remodelling of inflamm- aging, from robustness to frailty', *Inflammation Research*, 57(12), pp. 558–563. doi: 10.1007/s00011-008-7243-2.

Shabalina, I. G. *et al.* (2013) 'UCP1 in Brite/Beige Adipose Tissue Mitochondria Is Functionally Thermogenic', *Cell Reports*, 5(5), pp. 1196–1203. doi: 10.1016/j.celrep.2013.10.044.

Shan, T. *et al.* (2013) 'Distinct populations of adipogenic and myogenic Myf5-lineage progenitors in white adipose tissues', *Journal of Lipid Research*, 54(8), pp. 2214–2224. doi: 10.1194/jlr.M038711.

Shapses, S. A. *et al.* (2013) 'Vitamin D supplementation and calcium absorption during caloric restriction: a randomized double-blind trial', *The American Journal of Clinical Nutrition*, 97(3), pp. 637–645. doi: 10.3945/ajcn.112.044909.

Shen, W. *et al.* (2007) 'MRI-measured bone marrow adipose tissue is inversely related to DXA-measured bone mineral in Caucasian women', *Osteoporosis International*, 18(5), pp. 641–647. doi: 10.1007/s00198-006-0285-9.

Shen, W. *et al.* (2012) 'Relationship between MRI-measured bone marrow adipose tissue and hip and spine bone mineral density in African-American and Caucasian participants: The CARDIA study', *Journal of Clinical Endocrinology and Metabolism*, 97(4), pp. 1337–1346. doi: 10.1210/jc.2011-2605.

Shen, W. *et al.* (2014) 'Comparison of the Relationship Between Bone Marrow Adipose Tissue and Volumetric Bone Mineral Density in Children and Adults', *Journal of Clinical Densitometry*, 17(1), pp. 163–169. doi: 10.1016/j.jocd.2013.02.009.

Sheng, H. *et al.* (2013) 'Pathomorphological changes of bone marrow adipocytes in process of steroid-associated osteonecrosis.', *International journal of clinical and experimental pathology*, 6(6), pp. 1046–50.

Sher, L. B. *et al.* (2004) 'Transgenic Expression of 11β-Hydroxysteroid Dehydrogenase Type 2 in Osteoblasts Reveals an Anabolic Role for Endogenous Glucocorticoids in Bone', *Endocrinology*, 145(2), pp. 922–929. doi: 10.1210/en.2003-0655.

Shetty, S. *et al.* (2016) 'Bone turnover markers: Emerging tool in the management of osteoporosis', *Indian Journal of Endocrinology and Metabolism*, 20(6), p. 846. doi: 10.4103/2230-8210.192914.

Sheu, Y. *et al.* (2017) 'Vertebral bone marrow fat, bone mineral density and diabetes: The Osteoporotic Fractures in Men (MrOS) study', *Bone*, 97, pp. 299–305. doi: 10.1016/j.bone.2017.02.001.

Shinoda, Y. *et al.* (2006) 'Regulation of bone formation by adiponectin through autocrine/paracrine and endocrine pathways', *Journal of Cellular Biochemistry*, 99(1), pp. 196–208. doi: 10.1002/jcb.20890.

Simpson, E. R. and Waterman, M. R. (1988) 'Regulation of the synthesis of steroidogenic enzymes in adrenal cortical cells by ACTH', *Annual Reviews Physiology*, 50, pp. 427–440.

Singhal, V. *et al.* (2018) 'Impaired bone strength estimates at the distal tibia and its determinants in adolescents with anorexia nervosa.', *Bone*, 106, pp. 61–68. doi: 10.1016/j.bone.2017.07.009.

Slade, J. M. *et al.* (2012) 'Human bone marrow adiposity is linked with serum lipid levels not T1-diabetes', *Journal of Diabetes and its Complications*, 26(1), pp. 1–9. doi: 10.1016/j.jdiacomp.2011.11.001.

Slyfield, C. R. *et al.* (2012) 'Three-dimensional dynamic bone histomorphometry', *Journal of Bone and Mineral Research*, 27(2), pp. 486–495. doi: 10.1002/jbmr.553.

Snijder, M. B., Dekker, J. M., Visser, M., Bouter, L. M., *et al.* (2003) 'Associations of hip and thigh circumferences independent of waist circumference with the incidence of type 2 diabetes: the Hoorn Study', *The American Journal of Clinical Nutrition*, 77(5), pp. 1192–1197. doi: 10.1093/ajcn/77.5.1192.

Snijder, M. B., Dekker, J. M., Visser, M., Yudkin, J. S., *et al.* (2003) 'Larger Thigh and Hip Circumferences Are Associated with Better Glucose Tolerance: The Hoorn Study', *Obesity Research*, 11(1), pp. 104–111. doi: 10.1038/oby.2003.18.

So, A. Y.-L. *et al.* (2009) 'Glucocorticoid regulation of the circadian clock modulates glucose homeostasis', *Proceedings of the National Academy of Sciences*, 106(41), pp. 17582–17587. doi: 10.1073/pnas.0909733106.

Sooy, K. *et al.* (2010) 'Partial Deficiency or Short-Term Inhibition of 11 -Hydroxysteroid Dehydrogenase Type 1 Improves Cognitive Function in Aging Mice', *Journal of Neuroscience*, 30(41), pp. 13867–13872. doi: 10.1523/JNEUROSCI.2783-10.2010.

Sottile, V., Seuwen, K. and Kneissel, M. (2004) 'Enhanced Marrow Adipogenesis and Bone Resorption in Estrogen-Deprived Rats Treated with the PPARgamma Agonist BRL49653 (Rosiglitazone)', *Calcified Tissue International*, 75(4), pp. 329–337. doi: 10.1007/s00223-004-0224-8.

Souverein, P. C. (2004) ‘Use of oral glucocorticoids and risk of cardiovascular and cerebrovascular disease in a population based case-control study’, *Heart*, 90(8), pp. 859–865. doi: 10.1136/hrt.2003.020180.

Spaanderman, D. C. E. *et al.* (2019) ‘Androgens modulate glucocorticoid receptor activity in adipose tissue and liver’, *Journal of Endocrinology*, 240(1), pp. 51–63. doi: 10.1530/JOE-18-0503.

Speakman, J. R. and Mitchell, S. E. (2011) ‘Caloric restriction’, *Molecular Aspects of Medicine*, 32(3), pp. 159–221. doi: 10.1016/j.mam.2011.07.001.

Spencer, R. L. and Deak, T. (2017) ‘A users guide to HPA axis research’, *Physiology and Behavior*, pp. 43–65. doi: 10.1016/j.physbeh.2016.11.014.

Spiess, J. *et al.* (1981) ‘Primary structure of corticotropin-releasing factor from ovine hypothalamus.’, *Proceedings of the National Academy of Sciences*, 78(10), pp. 6517–6521. doi: 10.1073/pnas.78.10.6517.

Spychala, M. S. *et al.* (2018) ‘Age-related changes in the gut microbiota influence systemic inflammation and stroke outcome’, *Annals of Neurology*, 84(1), pp. 23–36. doi: 10.1002/ana.25250.

Van Staa, T. P. *et al.* (2000) ‘Use of Oral Corticosteroids and Risk of Fractures’, *Journal of Bone and Mineral Research*, 15(6), pp. 993–1000. doi: 10.1359/jbmr.2000.15.6.993.

Steppan, C. M. *et al.* (2000) ‘Leptin is a potent stimulator of bone growth in ob/ob mice’, *Regulatory Peptides*, 92(1–3), pp. 73–78. doi: 10.1016/S0167-0115(00)00152-X.

Stewart, J. *et al.* (1988) ‘The Effects of Acute and Life-Long Food Restriction on Basal and Stress-Induced Serum Corticosterone Levels in Young and Aged Rats*’, *Endocrinology*, 123(4), pp. 1934–1941. doi: 10.1210/endo-123-4-1934.

Stimson, R. H. *et al.* (2017) ‘Acute physiological effects of glucocorticoids on fuel metabolism in humans are permissive but not direct’, *Diabetes, Obesity and Metabolism*, 19(6), pp. 883–891. doi: 10.1111/dom.12899.

Straub, L. G. and Scherer, P. E. (2019) ‘Metabolic Messengers: adiponectin’, *Nature Metabolism*, 1(3), pp. 334–339. doi: 10.1038/s42255-019-0041-z.

Sukumar, D., Shapses, S. A. and Schneider, S. H. (2015) ‘Vitamin D supplementation during short-term caloric restriction in healthy overweight/obese older women: Effect on glycemic indices and serum osteocalcin levels’, *Molecular and Cellular Endocrinology*, 410(1), pp. 73–77. doi: 10.1016/j.mce.2015.01.002.

Sulston, R. J. *et al.* (2016) ‘Increased Circulating Adiponectin in Response to

Thiazolidinediones: Investigating the Role of Bone Marrow Adipose Tissue', *Frontiers in endocrinology*, 7(21), pp. 1–17. doi: 10.3389/fendo.2016.00128.

Swanson, C. *et al.* (2006) 'Glucocorticoid Regulation of Osteoclast Differentiation and Expression of Receptor Activator of Nuclear Factor-κB (NF-κB) Ligand, Osteoprotegerin, and Receptor Activator of NF-κB in Mouse Calvarial Bones', *Endocrinology*, 147(7), pp. 3613–3622. doi: 10.1210/en.2005-0717.

Syed, F. A. *et al.* (2008) 'Effects of estrogen therapy on bone marrow adipocytes in postmenopausal osteoporotic women', *Osteoporosis International*, 19(9), pp. 1323–1330. doi: 10.1007/s00198-008-0574-6.

Syed, F. A. *et al.* (2010) 'Effects of chronic estrogen treatment on modulating age-related bone loss in female mice', *Journal of Bone and Mineral Research*, 25(11), pp. 2438–2446. doi: 10.1002/jbmr.129.

Tagami, T. *et al.* (2004) 'Adiponectin in anorexia nervosa and bulimia nervosa', *Journal of Clinical Endocrinology and Metabolism*, 89(4), pp. 1833–1837. doi: 10.1210/jc.2003-031260.

Tamm, K. *et al.* (2009) 'Genes targeted by the estrogen and progesterone receptors in the human endometrial cell lines HEC1A and RL95-2', *Reproductive Biology and Endocrinology*, 7(1), p. 150. doi: 10.1186/1477-7827-7-150.

Tamura, N. *et al.* (2005) 'Effects of testosterone on cancellous bone, marrow adipocytes, and ovarian phenotype in a young female rat model of polycystic ovary syndrome', *Fertility and Sterility*, 84(2), pp. 1277–1284. doi: 10.1016/j.fertnstert.2005.06.017.

Tang, G. Y. *et al.* (2010) 'Evaluation of MR spectroscopy and diffusion-weighted MRI in detecting bone marrow changes in postmenopausal women with osteoporosis', *Clinical Radiology*, 65(5), pp. 377–381. doi: 10.1016/j.crad.2009.12.011.

Tavassoli, M. (1976) 'Ultrastructural development of bone marrow adipose cell', *Cells Tissues Organs*, 94(1), pp. 65–77. doi: 10.1159/000144545.

Templeton, Z. S. *et al.* (2015) 'Breast Cancer Cell Colonization of the Human Bone Marrow Adipose Tissue Niche', *Neoplasia*, 17(12), pp. 849–861. doi: 10.1016/j.neo.2015.11.005.

Tencerova, M. *et al.* (2018) 'High-Fat Diet-Induced Obesity Promotes Expansion of Bone Marrow Adipose Tissue and Impairs Skeletal Stem Cell Functions in Mice', *Journal of Bone and Mineral Research*, 33(6), pp. 1154–1165. doi: 10.1002/jbmr.3408.

Tencerova, M. and Kassem, M. (2016) 'The Bone Marrow-Derived Stromal Cells:

Commitment and Regulation of Adipogenesis', *Frontiers in Endocrinology*, 7(SEP). doi: 10.3389/fendo.2016.00127.

Thompson, N. M. *et al.* (2004) 'Ghrelin and des-octanoyl ghrelin promote adipogenesis directlyin vivo by a mechanism independent of GHS-R1a', *Endocrinology*, 145(1), pp. 234–242. doi: 10.1210/en.2003-0899.

Tobiansky, D. J. *et al.* (2018) 'Testosterone and Corticosterone in the Mesocorticolimbic System of Male Rats: Effects of Gonadectomy and Caloric Restriction', *Endocrinology*, 159(1), pp. 450–464. doi: 10.1210/en.2017-00704.

Tomiyama, A. J. *et al.* (2010) 'Low Calorie Dieting Increases Cortisol', *Psychosomatic Medicine*, 72(4), pp. 357–364. doi: 10.1097/PSY.0b013e3181d9523c.

Tomlinson, J. W., Draper, N., *et al.* (2002) 'Absence of Cushingoid phenotype in a patient with Cushing's disease due to defective cortisone to cortisol conversion.', *The Journal of Clinical Endocrinology and Metabolism*, 87(1), pp. 57–62. doi: 10.1210/jcem.87.1.8189.

Tomlinson, J. W., Sinha, B., *et al.* (2002) 'Expression of 11β-hydroxysteroid dehydrogenase type 1 in adipose tissue is not increased in human obesity', *Journal of Clinical Endocrinology and Metabolism*, 87(12), pp. 5630–5635. doi: 10.1210/jc.2002-020687.

Tomlinson, J. W. *et al.* (2004) '11β-Hydroxysteroid Dehydrogenase Type 1: A Tissue-Specific Regulator of Glucocorticoid Response', *Endocrine Reviews*, 25(5), pp. 831–866. doi: 10.1210/er.2003-0031.

Tomlinson, J. W. *et al.* (2008) 'Reduced Glucocorticoid Production Rate, Decreased 5 -Reductase Activity, and Adipose Tissue Insulin Sensitization After Weight Loss', *Diabetes*, 57(6), pp. 1536–1543. doi: 10.2337/db08-0094.

Trotter, T. N. *et al.* (2016) 'Adipocyte-Lineage Cells Support Growth and Dissemination of Multiple Myeloma in Bone', *The American Journal of Pathology*, 186(11), pp. 3054–3063. doi: 10.1016/j.ajpath.2016.07.012.

Tuljapurkar, S. R. *et al.* (2011) 'Changes in human bone marrow fat content associated with changes in hematopoietic stem cell numbers and cytokine levels with aging', *Journal of Anatomy*, 219(5), pp. 574–581. doi: 10.1111/j.1469-7580.2011.01423.x.

Vande Berg, B. C. *et al.* (1999) 'Fat conversion of femoral marrow in glucocorticoid-treated patients: A cross-sectional and longitudinal study with magnetic resonance imaging', *Arthritis & Rheumatism*, 42(7), pp. 1405–1411. doi: 10.1002/1529-0131(199907)42:7<1405::AID-ANR14>3.0.CO;2-W.

Vandermosten, L. *et al.* (2017) '11β-hydroxysteroid dehydrogenase type 1 has no effect on survival during experimental malaria but affects parasitemia in a parasite strain-specific manner', *Scientific Reports*, 7(1), p. 13835. doi: 10.1038/s41598-017-14288-x.

Vanderschueren, D. *et al.* (1990) 'Sex- and age-related changes in bone and serum osteocalcin', *Calcified Tissue International*, 46(3), pp. 179–182. doi: 10.1007/BF02555041.

Vasikaran, S. *et al.* (2011) 'Markers of bone turnover for the prediction of fracture risk and monitoring of osteoporosis treatment: a need for international reference standards', *Osteoporosis International*, 22(2), pp. 391–420. doi: 10.1007/s00198-010-1501-1.

Veilleux, A. *et al.* (2010) 'Expression of genes related to glucocorticoid action in human subcutaneous and omental adipose tissue', *The Journal of Steroid Biochemistry and Molecular Biology*, 122(1–3), pp. 28–34. doi: 10.1016/j.jsbmb.2010.02.024.

Veldhuis-Vlug, A. G. and Rosen, C. J. (2017) 'Mechanisms of marrow adiposity and its implications for skeletal health', *Metabolism*, 67(1), pp. 106–114. doi: 10.1016/j.metabol.2016.11.013.

Veldhuis-Vlug, A. G. and Rosen, C. J. (2018) 'Clinical implications of bone marrow adiposity', *Journal of Internal Medicine*, 283(2), pp. 121–139. doi: 10.1111/joim.12718.

Velez-delValle, C. *et al.* (2013) 'Glucocorticoid Paradoxically Recruits Adipose Progenitors and Impairs Lipid Homeostasis and Glucose Transport in Mature Adipocytes', *Scientific Reports*, 3(1). doi: 10.1038/srep02573.

Verhaar, H. J. J. *et al.* (1994) 'A comparison of the action of progestins and estrogen on the growth and differentiation of normal adult human osteoblast-like cells in vitro', *Bone*, 15(3), pp. 307–311. doi: 10.1016/8756-3282(94)90293-3.

Verma, M. *et al.* (2018) '11β-hydroxysteroid dehydrogenase-1 deficiency alters brain energy metabolism in acute systemic inflammation.', *Brain, Behavior, and Immunity*, 69, pp. 223–234. doi: 10.1016/j.bbi.2017.11.015.

Verma, S. (2002) 'Adipocytic proportion of bone marrow is inversely related to bone formation in osteoporosis', *Journal of Clinical Pathology*, 55(9), pp. 693–698. doi: 10.1136/jcp.55.9.693.

Vilà, R. *et al.* (2001) 'Urinary free cortisol excretion pattern in morbid obese women', *Endocrine Research*, 27(1–2), pp. 261–268. doi: 10.1081/ERC-100107186.

Villareal, D. T. *et al.* (2006) ‘Bone mineral density response to caloric restriction-induced weight loss or exercise-induced weight loss: a randomized controlled trial.’, *Archives of Internal Medicine*, 166(22), pp. 2502–10. doi: 10.1001/archinte.166.22.2502.

Villareal, D. T. *et al.* (2016) ‘Effect of Two-Year Caloric Restriction on Bone Metabolism and Bone Mineral Density in Non-Obese Younger Adults: A Randomized Clinical Trial’, *Journal of Bone and Mineral Research*, 31(1), pp. 40–51. doi: 10.1002/jbmr.2701.

de Vries, F. *et al.* (2007) ‘Use of inhaled and oral glucocorticoids, severity of inflammatory disease and risk of hip/femur fracture: a population-based case-control study.’, *Journal of internal medicine*, 261(2), pp. 170–7. doi: 10.1111/j.1365-2796.2006.01754.x.

Wabitsch, M. *et al.* (2001) ‘Serum Leptin, Gonadotropin, and Testosterone Concentrations in Male Patients with Anorexia Nervosa during Weight Gain’, *The Journal of Clinical Endocrinology & Metabolism*, 86(7), pp. 2982–2988. doi: 10.1210/jcem.86.7.7685.

Wagner, E. R. *et al.* (2010) ‘Therapeutic Implications of PPARγ in Human Osteosarcoma’, *PPAR Research*, 2010(2), pp. 1–16. doi: 10.1155/2010/956427.

Wahrenberg, H., Lönnqvist, F. and Arner, P. (1989) ‘Mechanisms underlying regional differences in lipolysis in human adipose tissue.’, *Journal of Clinical Investigation*, 84(2), pp. 458–467. doi: 10.1172/JCI114187.

Wake, D. J. *et al.* (2003) ‘Local and systemic impact of transcriptional up-regulation of 11β-hydroxysteroid dehydrogenase type 1 in adipose tissue in human obesity’, *Journal of Clinical Endocrinology and Metabolism*, 88(8), pp. 3983–3988. doi: 10.1210/jc.2003-030286.

Walsh, T. B. *et al.* (1978) ‘Adrenal Activity in Anorexia Nervosa’, *Psychosomatic Medicine*, 40(6), pp. 499–506. doi: 10.1097/00006842-197810000-00005.

Wamil, M. *et al.* (2011) ‘Novel fat depot-specific mechanisms underlie resistance to visceral obesity and inflammation in 11B-hydroxysteroid dehydrogenase type 1-deficient mice’, *Diabetes*, 60(4), pp. 1158–1167. doi: 10.2337/db10-0830.

Wan, Y. and Nordeen, S. K. (2002) ‘Overlapping but Distinct Gene Regulation Profiles by Glucocorticoids and Progestins in Human Breast Cancer Cells’, *Molecular Endocrinology*, 16(6), pp. 1204–1214. doi: 10.1210/mend.16.6.0848.

Wang, H. H. *et al.* (2017) ‘Removal of mouse ovary fat pad affects sex hormones, folliculogenesis and fertility’, *Journal of Endocrinology*, 232(2), pp. 155–164. doi:

10.1530/JOE-16-0174.

Wang, K. *et al.* (2018) 'MRI Study on the Changes of Bone Marrow Microvascular Permeability and Fat Content after Total-Body X-Ray Irradiation', *Radiation Research*, 189(2), pp. 205–212. doi: 10.1667/RR14865.1.

Wang, L., Mishina, Y. and Liu, F. (2015) 'Osterix-Cre Transgene Causes Craniofacial Bone Development Defect', *Calcified Tissue International*, 96(2), pp. 129–137. doi: 10.1007/s00223-014-9945-5.

Wang, X. *et al.* (2015) 'Addition of Exercise Increases Plasma Adiponectin and Release from Adipose Tissue.', *Medicine and science in sports and exercise*, 47(11), pp. 2450–5. doi: 10.1249/MSS.0000000000000670.

Wáng, Y. X. J. *et al.* (2015) 'Rapid increase in marrow fat content and decrease in marrow perfusion in lumbar vertebra following bilateral oophorectomy: An mr imaging-based prospective longitudinal study', *Korean Journal of Radiology*, 16(1), pp. 154–159. doi: 10.3348/kjr.2015.16.1.154.

Wehrli, F. W. *et al.* (2000) 'Cross-sectional Study of Osteopenia with Quantitative MR Imaging and Bone Densitometry', *Radiology*, 217(2), pp. 527–538. doi: 10.1148/radiology.217.2.r00nv20527.

Wei, L. L. *et al.* (1993) 'Evidence for Progesterone Receptors in Human Osteoblast-like Cells', *Biochemical and Biophysical Research Communications*, 195(2), pp. 525–532. doi: 10.1006/bbrc.1993.2077.

Weinstein, R. S. *et al.* (2010) 'Endogenous glucocorticoids decrease skeletal angiogenesis, vascularity, hydration, and strength in aged mice', *Aging Cell*, 9(2), pp. 147–161. doi: 10.1111/j.1474-9726.2009.00545.x.

Weiss, L. P. and Wislocki, G. B. (1956) 'Seasonal variations in hematopoiesis in the dermal bones of the nine-banded armadillo', *The Anatomical Record*, 126(2), pp. 143–163. doi: 10.1002/ar.1091260203.

White, U. A. and Tchoukalova, Y. D. (2014) 'Sex dimorphism and depot differences in adipose tissue function', *Biochimica et Biophysica Acta (BBA) - Molecular Basis of Disease*, 1842(3), pp. 377–392. doi: 10.1016/j.bbadis.2013.05.006.

Whorwood, C. B. *et al.* (2001) 'Regulation of Glucocorticoid Receptor α and β Isoforms and Type I 11β-Hydroxysteroid Dehydrogenase Expression in Human Skeletal Muscle Cells: A Key Role in the Pathogenesis of Insulin Resistance?', *The Journal of Clinical Endocrinology & Metabolism*, 86(5), pp. 2296–2308. doi: 10.1210/jcem.86.5.7503.

Wiesenborn, D. S. *et al.* (2014) 'The effect of calorie restriction on insulin signaling in

skeletal muscle and adipose tissue of Ames dwarf mice', *Aging*, 6(10), pp. 900–912. doi: 10.18632/aging.100700.

Wood, C. L. *et al.* (2018) 'Animal models to explore the effects of glucocorticoids on skeletal growth and structure', *Journal of Endocrinology*, 236(1), pp. R69–R91. doi: 10.1530/JOE-17-0361.

Woods, G. N. *et al.* (2018) 'Chronic Kidney Disease Is Associated With Greater Bone Marrow Adiposity', *Journal of Bone and Mineral Research*, 33(12), pp. 2158–2164. doi: 10.1002/jbmr.3562.

Woods, G. N. *et al.* (2019) 'Greater Bone Marrow Adiposity Predicts Bone Loss in Older Women', *Journal of Bone and Mineral Research*, p. jbmr.3895. doi: 10.1002/jbmr.3895.

Woolf, A. D. (2003) 'Preventing fractures in elderly people', *BMJ*, 327(7406), pp. 89–95. doi: 10.1136/bmj.327.7406.89.

Wu, H. *et al.* (2019) 'Advantages of Single-Nucleus over Single-Cell RNA Sequencing of Adult Kidney: Rare Cell Types and Novel Cell States Revealed in Fibrosis', *Journal of the American Society of Nephrology*, 30(1), pp. 23–32. doi: 10.1681/ASN.2018090912.

Wu, J. *et al.* (2012) 'Beige Adipocytes Are a Distinct Type of Thermogenic Fat Cell in Mouse and Human', *Cell*, 150(2), pp. 366–376. doi: 10.1016/j.cell.2012.05.016.

Wu, L. *et al.* (2013) '11β-Hydroxysteroid dehydrogenase type 1 selective inhibitor BVT.2733 protects osteoblasts against endogenous glucocorticoid induced dysfunction.', *Endocrine journal*, 60(9), pp. 1047–58. doi: 10.1210/jc.2003-022025.

Wu, T. *et al.* (2018) 'Chronic glucocorticoid treatment induced circadian clock disorder leads to lipid metabolism and gut microbiota alterations in rats', *Life Sciences*, 192(6), pp. 173–182. doi: 10.1016/j.lfs.2017.11.049.

Xu, C. *et al.* (2009) 'Direct Effect of Glucocorticoids on Lipolysis in Adipocytes', *Molecular Endocrinology*, 23(8), pp. 1161–1170. doi: 10.1210/me.2008-0464.

Xu, X., Hoebeke, J. and Björntorp, P. (1990) 'Progestin binds to the glucocorticoid receptor and mediates antiglucocorticoid effect in rat adipose precursor cells', *Journal of Steroid Biochemistry*, 36(5), pp. 465–471. doi: 10.1016/0022-4731(90)90089-B.

Yang, F. (2010) *The role and regulation of 11β-hydroxysteroid dehydrogenase in lung inflammation*. University of Edinburgh.

Yau, J. L. W. *et al.* (2001) 'Lack of tissue glucocorticoid reactivation in 11 -hydroxysteroid dehydrogenase type 1 knockout mice ameliorates age-related learning impairments', *Proceedings of the National Academy of Sciences*, 98(8), pp.

4716–4721. doi: 10.1073/pnas.071562698.

Yau, Joyce L. W. *et al.* (2015) 'Diurnal and stress-induced intra-hippocampal corticosterone rise attenuated in 11β-HSD1-deficient mice: a microdialysis study in young and aged mice', *European Journal of Neuroscience*, 41(6), pp. 787–792. doi: 10.1111/ejn.12836.

Yau, Joyce L.W. *et al.* (2015) 'Intrahippocampal glucocorticoids generated by 11β-HSD1 affect memory in aged mice', *Neurobiology of Aging*, 36(1), pp. 334–343. doi: 10.1016/j.neurobiolaging.2014.07.007.

Yeung, D. K. W. *et al.* (2005) 'Osteoporosis is associated with increased marrow fat content and decreased marrow fat unsaturation: A proton MR spectroscopy study', *Journal of Magnetic Resonance Imaging*, 22(2), pp. 279–285. doi: 10.1002/jmri.20367.

Yin, L., Li, Y. and Wang, Y. (2006) 'Dexamethasone-induced adipogenesis in primary marrow stromal cell cultures: mechanism of steroid-induced osteonecrosis.', *Chinese medical journal*, 119(7), pp. 581–8. doi: 10.1097/00029330-200604010-00012.

Yu, E. W. *et al.* (2017) 'Marrow adipose tissue composition in adults with morbid obesity', *Bone*, 97, pp. 38–42. doi: 10.1016/j.bone.2016.12.018.

Zannas, A. S. *et al.* (2016) 'Gene–Stress–Epigenetic Regulation of FKBP5: Clinical and Translational Implications', *Neuropsychopharmacology*, 41(1), pp. 261–274. doi: 10.1038/npp.2015.235.

Zgheib, S. *et al.* (2014) 'Long-Term physiological alterations and recovery in a mouse model of separation associated with time-restricted feeding: A tool to study anorexia nervosa related consequences', *PLoS ONE*, 9(8), pp. 1–13. doi: 10.1371/journal.pone.0103775.

Zhang, J. (2006) 'Differential interaction of RU486 with the progesterone and glucocorticoid receptors', *Journal of Molecular Endocrinology*, 37(1), pp. 163–173. doi: 10.1677/jme.1.02089.

Zhang, Y. *et al.* (1994) 'Positional cloning of the mouse obese gene and its human homologue', *Nature*, 372, pp. 425–432.

Zhang, Z. *et al.* (2017) 'Macrophage 11β-HSD-1 deficiency promotes inflammatory angiogenesis', *Journal of Endocrinology*, 234(3), pp. 291–299. doi: 10.1530/JOE-17-0223.

Zhao, Q. *et al.* (2016) 'The clock gene *PER1* plays an important role in regulating the clock gene network in human oral squamous cell carcinoma cells', *Oncotarget*, 7(43), pp. 70290–70302. doi: 10.18632/oncotarget.11844.

Zhou, B. O. *et al.* (2017) ‘Bone marrow adipocytes promote the regeneration of stem cells and haematopoiesis by secreting SCF’, *Nature Cell Biology*, 19(8), pp. 891–903. doi: 10.1038/ncb3570.

Zhou, H., Cooper, M. S. and Seibel, M. J. (2013) ‘Endogenous Glucocorticoids and Bone’, *Bone Research*, 1(2), pp. 107–119. doi: 10.4248/BR201302001.

Zhu, M. *et al.* (2004) ‘Circulating adiponectin levels increase in rats on caloric restriction: the potential for insulin sensitization’, *Experimental Gerontology*, 39(7), pp. 1049–1059. doi: 10.1016/j.exger.2004.03.024.

Zoch, M. L., Clemens, T. L. and Riddle, R. C. (2016) ‘New insights into the biology of osteocalcin’, *Bone*, 82, pp. 42–49. doi: 10.1016/j.bone.2015.05.046.